

**The reduction, refinement and replacement of animals in
anti-filarial drug research**

Thesis submitted in accordance with the requirements of
the University of Liverpool for the degree of Doctor of Philosophy

by

Amy Elizabeth Marriott

September 2019

DECLARATION

Declaration

This thesis is the result of my own work and effort. This research was conducted at the Liverpool School of Tropical Medicine and the University of Liverpool, under the supervision of Dr Joseph Turner. The material contained in this thesis has not been presented, nor is currently being presented, either wholly or in part, for any other degree or qualification.

.....

Abstract

Filarial helminths are vector-borne, tissue-dwelling parasitic worms that cause the neglected tropical diseases: lymphatic filariasis, onchocerciasis, loiasis and mansonellosis in humans, and dirofilariasis in cats and dogs. Drugs that are deployed through mass drug administration programs (human filariasis) or prophylactic treatments (dirofilariasis), target only the transmissible (microfilariae; mf), or early larval (L3-L4) stages of disease. They exert little effect on adult worms, which can survive and reproduce for >10 years. There is also a risk of severe adverse events to standard anti-filarial drugs and resistance has been reported in both humans and animals. There is, therefore, an urgent, unmet need for drugs able to safely target adult stage parasites (macrofilaricides). For macrofilaricide candidates to be tested, there is a heavy reliance on *in vivo* models due to technical difficulties in maintaining target human/animal filarial viability *in vitro*. Substantial animal use is currently required due to intra-group variability and single end-point analysis.

The work conducted in this thesis presents the development of alternative drug models to refine, reduce and replace animal usage for anti-filarial drug testing. Specific culture media conditions and co-cultures with mammalian cell lines were assessed to support the *in vitro* development of *Brugia malayi* or *Dirofilaria immitis* larvae from infective stages derived from *Aedes aegypti* mosquitoes for up to five weeks. Inbred immunodeficient mouse strains were evaluated as a superior *in vivo* model compared with outbred *Meriones* gerbils for the long-term (>25 week) maintenance of *B. malayi* adult infections. Three week *in vitro* co-cultures, using human lymphatic endothelial cell primary cell bilayers, have been evaluated to maintain *B. malayi* parasite survival and intra-nematode *Wolbachia* symbiont titres comparable to those *in vivo*. This *in vitro* system has been validated to screen anti-*Wolbachia* and direct nematocidal drugs over a two-week time course. Novel *in vivo* bio-imaging technologies: ultrasonography (USG) and fluorescent intravital bioimaging have been

ABSTRACT

scrutinized for the ability to track accurate filarial infection biomass and treatment responses. USG has been validated as a minimally-invasive procedure to diagnose active adult infections, estimate adult parasite burdens and track macrofilaricidal drug activity longitudinally. Considering overall animal use, adoption of these innovations may reduce animal use by >50% in testing macrofilaricidal drugs and simultaneously refine *in vivo* procedures by obviating the use of surgical implantations of adult parasites.

Acknowledgements

Firstly, I would like to thank my primary supervisor, Dr Joseph Turner, without whom this project would not have been possible. I would like to thank him for his help and guidance, for sharing his expert wisdom and knowledge, and for his continual positivity and enthusiasm which have helped to make this PhD such an enjoyable experience. In addition, I offer my thanks to my secondary supervisor, Professor Mark Taylor, for his support and stimulating scientific discussion. I am also grateful to my progress assessment panel members, Professor Giancarlo Biagini and Professor Harish Poptani, for offering support and useful discussion during our annual meetings.

Thank you to the National Centre for the Reduction, Refinement and Replacement of animals in scientific research, who provided the funding for this project, and also provided numerous training events which were of invaluable help.

All members of the lab (both past and present) deserve recognition for their support and training; most notably Dr Hanna Sjoberg – who spent a lot of time and effort training me in a variety of *in vivo* techniques in the early days, and Andy Steven and John Archer - whose help has been indispensable, particularly on ‘dissection days’! Thanks also go to Julio Furlong-Silva, Anfal Yousef, Shannon Quek and Rachel Clare for ‘riding out’ the PhD journey alongside me and, have become great friends along the way.

On a more personal note, I am forever indebted to my family, particularly my parents Wendy and Chris, who have continually encouraged me to pursue my dreams. I would also like to express my gratitude to my best friends Jess and Grace; thank you for appreciating I have had to put my social life on hold for the last however long, and for the constant motivational ‘pep-talks’, (and not repeatedly asking ‘have you not finished your thesis yet?’ – world’s most

ACKNOWLEDGEMENTS

annoying question!). Thanks also go to Shaun, for his genius I.T. and formatting skills, and of course support. I am incredibly lucky to have you all.

Thank you

Publications, Presentations and Prizes

Peer-reviewed publications

Publications arising through the course of the PhD:

Marriott, A.E., Sjoberg, H., Tyrer, H. *et al.* Validation of ultrasound bioimaging to predict worm burden and treatment efficacy in preclinical filariasis drug screening models. *Sci Rep* **8**, 5910 (2018). <https://doi.org/10.1038/s41598-018-24294-2>

Oral presentations

- **November 2018 - Laboratory Animal Science Association, Birmingham, UK**

Title: 'The reduction, refinement and replacement of animals in anti-filarial drug research'

- **June 2018 – Annual 'Centre for pre-clinical imaging' Symposium, University of Liverpool, UK**

Title: 'Non-invasive bioimaging to track parasitic helminths and determine drug effects *in vivo*'

- **March 2018 – British Society for Parasitology, Aberystwyth, UK**

Title: 'Development of a long-term *Brugia malayi* lymphatic endothelial cell co-culture system and its validation as an alternative to *in vivo* screening for anti-*Wolbachia* drug assessment'

Poster presentations

- **September 2017 – Molecular and Cellular Biology of Helminth Parasites, Hydra, Greece**

Title: 'Long-term *in vitro* culture of adult *Brugia malayi* parasites to evaluate drug response and host-parasite interactions'

- **March 2017 - British Society for Parasitology, Dundee, UK**

Title: 'Near infra-red optical imaging to track fluorescently labelled filarial parasites *in vivo*'

Title: 'Long-term *in vitro* culture of adult *Brugia malayi* parasites'

- **November 2016 – American Society of Hygiene and Tropical Medicine, Atlanta, USA**

Title: 'Application of Ultrasonography to detect peritoneal filarial dance sign in preclinical *rodent Brugia malayi* macrofilaricidal drug screening models'

- **March 2016 – British Society for Parasitology, London, UK**

Title: 'Application of ultrasonography to detect peritoneal filarial dance sign in preclinical *Brugia malayi* drug screening models'

Prizes

- **PLOS NTD Top 5 Posters**

British Society for Parasitology, Dundee, UK

Table of Contents

Declaration.....	i
Abstract.....	ii
Acknowledgements.....	iv
Publications, Presentations and Prizes	vi
Table of Figures.....	xiii
Table of Tables	xvi
Abbreviations.....	xvii
Chapter 1: General Introduction.....	21
1.1. Helminths as a neglected tropical disease.....	22
1.2. Filarial nematode parasites.....	22
1.3. General Filarial Life Cycle	23
1.4. Lymphatic Filariasis	26
1.5. Lymphatic filariasis specific life cycle.....	27
1.6. Lymphatic filariasis disease.....	29
1.7. Onchocerciasis	30
1.8. Onchocerciasis specific life cycle	31
1.9. Onchocerciasis disease	33
1.10. Dirofilariasis.....	34
1.11. Dirofilariasis specific life-cycle	36
1.12. Dirofilariasis disease.....	37
1.13. <i>Wolbachia</i> endosymbionts of filariae	38
1.14. Registered anti-filarial drugs.....	41
1.14.1. Piperazines.....	43
1.14.2. Benzimidazoles	44
1.14.3. Melarsomine	45
1.15. Doxycycline	46
1.16. Human Filariasis control and elimination strategies.....	47
1.17. Mass Drug Administration regimens.....	49
1.18. Research and development of new anti-filarial drugs.....	49
1.19. Novel short-course macrofilaricides	50
1.20. Direct-acting macrofilaricides	51
1.21. Novel anti- <i>Wolbachia</i> drugs.....	51
1.22. <i>In vitro</i> filariasis culture systems and their use in drug screening.....	53
1.23. <i>In vivo</i> models of filariasis for drug screening.....	57
1.24. The 3Rs principles applied to anti-filarial drug discovery	61

TABLE OF CONTENTS

1.25. Thesis aims	63
Chapter 2: Development of a larval filarial growth culture system.....	65
2.1. Abstract	66
2.2. Introduction	67
2.3. Scientific and 3Rs Aims	69
2.4. Materials and Methods.....	70
2.4.1. Animals.....	70
2.4.2. <i>Brugia malayi</i> parasite maintenance	70
2.4.3. <i>In vitro</i> culture of <i>BmL3</i> stage parasites	71
2.4.4. Cell culture	71
2.4.5. Parallel <i>in vivo</i> experiments	72
2.4.6. Motility and survival analyses.....	73
2.4.7. Length measurement analysis	73
2.4.8. MTT viability assessments	73
2.4.9. DNA extractions	74
2.4.10. Gene cloning and qPCR to determine <i>Wolbachia</i> titres	74
2.4.11. <i>Dirofilariae immitis</i> larval <i>in vitro</i> culture	75
2.4.12. Statistical analysis	76
2.5. Results.....	77
2.5.1. Initial primary feeder cell vs cell-free L3 cultures.....	77
2.5.2. Evaluation of different cell and media types on the survival and motility of <i>in vitro</i> cultured <i>BmL3</i>	79
2.5.3. Evaluation of different cell and media types on the growth of <i>in vitro</i> cultured <i>BmL3</i>	81
2.5.4. Evaluation of <i>Wolbachia</i> titres in <i>BmL3</i> cultured on different cell and media types	84
2.5.5. Evaluation of metabolic activity of <i>BmL3</i> cultured on different cell and media types	87
2.5.6. Initial <i>Dirofilariae immitis in vitro</i> cultures	89
2.6. Discussion.....	91
Chapter 3: Development and initial validation of a long-term adult female <i>Brugia malayi</i> culture system for screening macrofilaricidal candidates	96
3.1. Abstract	97
3.2. Introduction	98
3.3. Scientific and 3Rs aims.....	102
3.4. Materials and Methods.....	103
3.4.1. Animals.....	103
3.4.2. <i>Brugia malayi</i> parasite maintenance	103
3.4.3. <i>B. malayi</i> Experimental Infections	103

TABLE OF CONTENTS

3.4.4.	Adult <i>B. malayi</i> Implantation Surgeries	103
3.4.5.	Cell cultures.....	104
3.4.6.	Macrophage co-culture.....	105
3.4.7.	<i>In vitro</i> culture of parasites.....	105
3.4.8.	Motility scoring and survival analyses	106
3.4.9.	MTT viability assessments	106
3.4.10.	DNA extractions	106
3.4.11.	Gene cloning and qPCR.....	107
3.4.12.	Microfilariae and embryo release profiles.....	107
3.4.13.	Anti- <i>Wolbachia</i> Drug Screen Validation	107
3.4.14.	Direct-acting Macrofilaricide Drug Screen Validation	108
3.4.15.	Statistics	108
3.1.	Results.....	109
3.1.1.	Comparison of gerbil, CB.17 SCID and selective cytokine knockout infection models in the propagation and long-term maintenance of <i>B. malayi</i> adults.....	109
3.1.2.	Comparison of gerbil, CB.17 SCID and selective cytokine knockout infection models in the propagation of <i>B. malayi</i> microfilariae	115
3.1.3.	Initial optimisation of an adult <i>B. malayi</i> culture system	117
3.1.4.	Evaluation of microfilariae release during culture period of female or female+male <i>B. malayi</i>	125
3.1.5.	Evaluation of a trans-well co-culture system to improve the adult female <i>B. malayi</i> culture period.....	126
3.1.6.	<i>In vitro</i> uterine release over a 21 day culture period	131
3.1.7.	<i>Wolbachia</i> titres in female <i>B. malayi</i> post culture	133
3.1.8.	Validation of culture system to screen anti- <i>Wolbachia</i> drugs.....	137
3.1.9.	Validation of culture system as to screen anti-nematodicidal drugs	141
3.1.	Discussion.....	144
Chapter 4: Development and validation of pre-clinical ultrasound to predict worm burden and treatment efficacy in animal models of filariasis.....		154
4.1.	Abstract	155
4.2.	Introduction	156
4.3.	Scientific and 3Rs Aims	158
4.4.	Materials and Methods.....	159
4.4.1.	Animals.....	159
4.4.2.	<i>Brugia malayi</i> parasite production	159
4.4.3.	Experimental Infections	159
4.4.4.	Surgical implantation of Adult <i>Brugia malayi</i> parasites	159
4.4.5.	Preclinical Ultrasonography.....	160
4.4.6.	Drug treatments.....	161

TABLE OF CONTENTS

4.4.7.	Endpoint Parasitological assessments	161
4.4.8.	Statistics	162
4.5.	Results	163
4.5.1.	Optimization and characterization of intra-peritoneal FDS detection	163
4.5.2.	Sensitivity and specificity of <i>B. malayi</i> adult parasite loads by USG in operator-blinded studies.....	165
4.5.3.	Validation of USG to predict macrofilaricidal activity in preclinical drug screening.....	167
4.5.4.	Application of USG to semi-quantify <i>B. malayi</i> adult parasite loads <i>in vivo</i>	170
4.5.5.	Evaluation of estimated reductions in animal use for drug screening post-implementation of USG assessment.....	172
4.6.	Discussion.....	174
Chapter 5: Development of intra-vital optical bio-imaging of fluorescently-labelled filariae to measure treatment efficacy in mouse models of filariasis.....		178
5.1.	Abstract	179
5.2.	Introduction	180
5.3.	Scientific and 3Rs aims.....	182
5.4.	Materials and Methods.....	183
5.4.1.	Animals.....	183
5.4.2.	<i>Brugia malayi</i> parasite production	183
5.4.3.	<i>in vitro</i> fluorescent staining optimisation	183
5.4.4.	<i>In vitro</i> imaging	184
5.4.5.	IVIS image acquisition	184
5.4.6.	<i>in vivo</i> fluorescent microfilariae infusion.....	185
5.4.7.	IVIS fluorescent imaging of stained microfilariae <i>in vivo</i>	186
5.4.8.	Endpoint cardiac puncture and dissections.....	186
5.4.9.	Mf Giemsa staining and enumeration	186
5.4.10.	<i>In vivo</i> ivermectin drug response imaging study	186
5.4.11.	Surgical implantation of fluorescently labelled adult <i>B. malayi</i>	187
5.4.12.	<i>In vivo</i> IVIS imaging of adult stage parasites.....	187
5.4.13.	<i>In vivo</i> Flubendazole drug response imaging study	188
5.4.14.	Parasitology analysis	188
5.4.15.	Adult MTT assay.....	188
5.4.16.	Intraperitoneal mf quantification	188
5.4.17.	Statistics	189
5.5.	Results.....	190
5.5.1.	<i>In vitro</i> microfilariae staining and imaging	190
5.5.2.	<i>In vivo</i> imaging optimisation	192

TABLE OF CONTENTS

5.5.3. <i>B. malayi</i> microfilaraemic CB.17 SCID mouse ivermectin drug response pilot imaging study.....	196
5.5.4. <i>B. malayi</i> microfilaraemic CB.17 SCID mouse ivermectin drug response imaging study B.....	202
5.5.5. CB.17 SCID mouse <i>B. malayi</i> adult implant flubendazole drug treatment imaging experiment.....	206
5.6. Discussion.....	210
Chapter 6: Concluding remarks, uptake and future work	214
7.1. Replacement	215
7.2. Reduction	216
7.3. Refinement.....	217
References	219

Table of Figures

Figure 1.1. Distribution of lymphatic filariasis and status of preventative chemotherapy in endemic countries in 2017.....	27
Figure 1.2. Life-cycle of Lymphatic Filariasis.....	29
Figure 1.3. Distribution of onchocerciasis and status of preventative chemotherapy in endemic countries in 2017.....	31
Figure 1.4. Lifecycle of Onchocerciasis.....	33
Figure 1.5. Incidence of heartworm.....	35
Figure 1.6. Lifecycle of veterinary heartworm.....	37
Figure 2.1. Initial <i>Brugia malayi</i> larval primary feeder cell vs cell free cultures.....	78
Figure 2.2. Survival and motility analysis of <i>BmL3</i> cultured on different cell and media types for 14d.....	80
Figure 2.3. Length measurements of <i>BmL3</i> cultured on different cell and media types.....	83
Figure 2.4. <i>Wolbachia</i> expansions of <i>in vitro</i> reared parasites compared with baseline <i>BmL3</i> and equivalent <i>in vivo</i> time-point titres.....	87
Figure 2.5. Assessment of metabolic activity of cultured <i>Bm</i> larvae at day 14 in comparison to parasites reared <i>in vivo</i>	88
Figure 2.6. Initial <i>in vitro</i> <i>Dirofilariae immitis</i> larval cultures.....	90
Figure 3.1. Meta-analysis comparison of filarial adult parasitological yields 12-52 week age-infections in gerbils, CB.17 SCID or BALB/c IL-4R $\alpha^{-/-}$ IL-5 $^{-/-}$ mice.....	111
Figure 3.2. Meta-analysis comparison of filarial adult parasitological yields in separated 12-25 week and >25 week age infections in gerbils, CB.17 SCID or BALB/c IL-4R $\alpha^{-/-}$ IL-5 $^{-/-}$ mice 2.....	114
Figure 3.3. Meta-analysis comparison of the propagation of microfilariae of 12-52 week age-infections in gerbils, CB.17 SCID or BALB/c IL-4R $\alpha^{-/-}$ IL-5 $^{-/-}$ mice.....	116

TABLE OF FIGURES

Figure 3.4. Initial optimisation of female <i>B. malayi</i> cultures for 28 days with and without specific human cell monolayers.....	121
Figure 3.5. Initial optimisation of male <i>B. malayi</i> cultures for 28 days with and without specific human cell monolayers.....	124
Figure 3.6. mf release per female <i>B. malayi</i> over 10 day mixed sex and single sex cultures	126
Figure 3.7. 21 day trans-well adult <i>Bm</i> female co-culture system with macrophages or LEC bilayers.....	130
Figure 3.8. 21 day uterine release profiles from cultured female <i>Bm</i>	132
Figure 3.9. Comparison of <i>Wolbachia</i> titres over culture period in relation to <i>in vivo</i> recovered parasites.....	133
Figure 3.10. Comparison of metabolic activity and <i>Wolbachia</i> titres between mixed sex vs single sex implants and cultured females.....	136
Figure 3.11. Validation of culture system as an A-WOL drug model.....	140
Figure 3.12. Validation of culture model as a direct-acting macrofilaricide drug model	143
Figure 4.1. USG identification of rodent intraperitoneal filarial dance sign.....	164
Figure 4.2. Semi-quantification of <i>B. malayi</i> worm burden by USG in SCID mouse (A) and gerbil (B) drug screening models	171
Figure 5.1. <i>In vitro</i> microfilariae (mf) fluorescent staining optimisation.....	191
Figure 5.2 <i>In vivo</i> IVIS imaging optimisation with high yield parasitaemia (250,000 mf infused/mouse).....	193
Figure 5.3. <i>In vivo</i> IVIS imaging optimisation with low yield parasitaemia (100,000 mf infused/mouse).....	195
Figure 5.4. Pilot IVM drug challenge	198
Figure 5.5. CB.17 SCID mouse IVM drug response imaging study A.....	201
Figure 5.6a CB.17 SCID IVM treatment response imaging experiment B.....	204

TABLE OF FIGURES

Figure 5.6b CB.17 SCID IVM treatment response imaging experiment B – <i>ex vivo</i> imaging	205
Figure 5.7. CB.17 SCID mouse <i>B. malayi</i> adult implant flubendazole drug challenge	209

Table of Tables

Table 1.1 Definitive and intermediate vector hosts of medically and veterinary-important filarial species including rodent filariae used in research.....	25
Table 1.2. <i>Wolbachia</i> distributions and clades across filarial species.	41
Adapted from (Lefoulon et al., 2016, Lefoulon et al., 2015, Bouchery et al., 2013)	41
Table 3.1. Summary of parasitology between gerbils, CB.17 SCID mice and IL-4R α -/-IL-5-/- mice.....	117
Table 3.2. Comparison of metabolic activity and <i>Wolbachia</i> loads between cultured <i>B. malayi</i> female worms and single sex <i>in vivo</i> controls	134
Table 4.1. Optimisation of intra-peritoneal FDS detection by ultrasound in anaesthetised mice or gerbils.....	164
Table 4.2. Sensitivity and specificity of USG in determining adult motile <i>B. malayi</i>	166
Table 4.3. USG ipFDS detection compared with adult <i>B. malayi</i> parasitological readouts in experimental macrofilaricide drug screens	169
Table 4.4. Meta-analysis of <i>B. malayi</i> worm burden variation, statistical power and hypothetical animal use for preclinical drug screening pre- and post-implementation of USG imaging assessment	173

ABBREVIATIONS

Abbreviations

ABZ	Albendazole
ABZ-SOX	Albendazole Sulfoxide
ADLA	Acute Dermatolymphangioadenitis
APOC	African Programme for Onchocerciasis Control
AWOL	Anti-Wolbachia Drug Consortium
BEI	Biodefense and Emerging Infections Research Resources Repository
Bm	<i>Brugia malayi</i>
BmL3	<i>B. malayi</i> Larvae
BSU	Biomedical Services Unit
BZ	Benzimidazole
CCD	Charge-Coupled Device
CDTI	Community Directed Treatment with Ivermectin
DALYs	Disability-Adjusted Life Years
DEC	Diethylcarbamazine
DHB	Dihydroxybenzoic
DMEM	Dulbecco's Modified Eagle's Media
DMSO	Dimethyl Sulfoxide
DNA	Deoxyribonucleic Acid
DOX	Doxycycline
EBM-2	Endothelial Basal Media
EDTA	Ethyldiaminetetraacetic Acid
EOMA	Mouse Hemangioendothelioma Endothelial Cells
EGM-2 MV	Endothelial Growth Media-2 Modified Version
EMEM	Essential Modified Eagle's Media

ABBREVIATIONS

FBS	Foetal Bovine Serum
FBZ	Flubendazole
FDS	Filarial Dance Sign
FMT	Fluorescence Molecular Tomography
FR3	Filariasis Reagent Resource Centre
GABA	Gamma-Aminobutyric Acid
GPELF	Global Programme to Eliminate Lymphatic Filariasis
HEK	Human Embryonic Kidney
HI FBS	Heat Inactivated Foetal Bovine Serum
IFN	Interferon
IL	Interleukin
iL	Infective Larvae
IP	Intraperitoneal
IV	Intravenous
IVIS	<i>In Vivo</i> Imaging System
IVM	Ivermectin
LEC	Lymphatic Endothelial Cell
LF	Lymphatic Filariasis
LLCMK2	Lilly Laboratories Cell Monkey Kidney 2
LSTM	Liverpool School of Tropical Medicine
MDA	Mass Drug Administration
MDCK	Madin-Darby Canine Kidney
MEM	Minimum Essential Media
mf	Microfilariae
ML	Macrocyclic Lactone
MOX	Moxidectin

ABBREVIATIONS

MRI	Magnetic Resonance Imaging
MTT	3-(4,5-dimethylthiazol-2-yl)-2,5-diphenyl tetrazolium bromide
n	Number
NC3Rs	National Centre for The Reduction, Refinement and Replacement of Animals in Scientific Research
NCTC	National Cancer Institute's Tissue Culture Section
NIR	Near Infra-Red
ns	Non-significant
NTD	Neglected Tropical Disease
OCP	Onchocerciasis Control Programme
OD	Optical Density
OEAP	Onchocerciasis Elimination Programme for the Americas
P	Probability
PAI	Photoacoustic Imaging
PBMCs	Peripheral Blood Mononuclear Cell
PBS	Phosphate Buffered Saline
PCT	Preventative Chemotherapy
PET	Positron Electron Tomography
PK-PD	Pharmacokinetic-Pharmacodynamic
PMA	12-O-Tetradecanoylphorbol-13-Acetate
qPCR	Quantitative Polymerase Chain Reaction
R	Receptor
RDT	Rapid Diagnostic Tests
ROI	Region of Interest
RPM	Revolutions Per Minute
RPMI	Roswell Park Memorial Institute

ABBREVIATIONS

SAE	Severe Adverse Event
SC	Subcutaneous
SCID	Severe-Combined Immunodeficient
SHO	Severe Combined Immunodeficient Hairless Outbred
STH	Soil-Transmitted Helminths
SPECT	Single-Photon Emission Computed Tomography
SPF	Specific Pathogen-Free
SSV	Standard Suspension Vehicle
SUR	Suramin
TB	Tuberculosis
TCP	Target Candidate Profile
THP-1	Tohoku Hospital Pediatrics-1
TRE	Total Radiant Efficiency
WHO	World Health Organisation
WSP	<i>Wolbachia</i> Surface Protein
USG	Ultrasonography

Chapter 1: General Introduction

1.1. Helminths as a neglected tropical disease

Neglected tropical diseases (NTDs) are a group of 20 disabling conditions amongst the world's poorest populations (Hotez, 2007b), termed so to highlight the severe lack of funding received in contrast to 'the big three'; tuberculosis, HIV/AIDs and malaria (Molyneux, 2004). Helminth (worm) infections constitute a part of this NTD list, primarily in the form of soil-transmitted helminths (STH), consisting of *Ascaris lumbricoides*, *Trichuris trichiura* and hookworm roundworm species (*Ancylostoma duodenale* and *Necator americanus*), in which an estimated 24% of the world's population are infected; schistosomiasis, caused by the genus, *Schistosoma*, a flatworm species which infect over 200 million people; food-borne trematodes, including Chinese liver-flukes, lung flukes and liver-flukes; cestodes, which are flat tapeworms often causing disease upon ingestion of eggs; guinea-worm, which causes infection upon ingestion of water containing infected water fleas; and finally, filarial nematodes, which are mosquito-borne and responsible for lymphatic filariasis (LF), onchocerciasis and loiasis, infecting over 120 million individuals with 856 million people at risk (WHO report, 2018).

Neglected tropical diseases account for approximately 26.06 million disability-adjusted life years (DALYs) globally (James et al., 2018). In addition to clinical disease, NTDs further impact the poorer populations of the world, with individuals of the 'bottom billion', the 1.4 billion people who live below the poverty level defined by the World Bank (Hotez, 2011), predicted to have at least one NTD, further inducing poverty through detriment to worker productivity and child development (Hotez, 2007a, Perera et al., 2007, Molyneux et al., 2018, Litt et al., 2012).

1.2. Filarial nematode parasites

The Filariae, (family Onchoceridae; ONC) are a taxonomic grouping within the phylum, Nematoda (roundworms). According to recent detailed molecular taxonomic analysis, the

onchocercidae family is comprised of five distinct ‘clades’ (ONC1-5) which are parasitic in a diverse range of definitive hosts including amphibians, birds, mammals and reptiles (Lefoulon et al., 2015). Of medical importance are the lymphatic filariae: *Brugia malayi*, *B. timori* and *Wuchereria bancrofti*, the subcutaneous dwelling *Loa loa*, *Mansonella ozzardi*, *M. streptocerca* and *Onchocerca volvulus* and the intra-peritoneal parasite, *M. perstans*. In addition, *Dirofilaria immitis* and *D. repens*, which are filarial parasites of veterinary importance in cats and dogs, can also cause arrested zoonotic human infections and pathology. Although not of medical/veterinary importance, the rodent filariae, *Acanthocheilonema viteae* and *Litomosoides sigmodontis*, as well as the cat filaria, *B. pahangi*, are often used in research as representative surrogate species that can be maintained in the laboratory. In addition, due to the historical lack of suitable laboratory models of *Onchocerca*, natural cattle infections of the closely related ONC 3 clade parasites: *Onchocerca gutturosa*, *O. lienalis* and *O. ochengi* are often used in research.

A feature common to all filariae is the requirement of an obligate period of larval development in an arthropod intermediate host. These arthropods, including blood feeding flies, mites, midges, mosquitoes and ticks, act as transmission vectors by transferring infections between definitive hosts. As such, filariases are considered as ‘vector-borne’ diseases and competent vector species ecology and habitat dictate the epidemiological patterns of each individual filarial parasitic infection. Table 1.1 summarises the vector and definitive hosts of filariae of medical and veterinary importance, including species used in medical research.

1.3. General Filarial Life Cycle

Filarial nematodes have a complex, biphasic life cycle involving both a blood feeding arthropod vector and a mammalian definitive host (Table 1.1). Female vector species becomes infected upon taking a blood meal from an infected definitive host and ingesting

microscopic microfilariae (mf), typically 200 μM in length and 5 μM in diameter. For certain filariae, mf are encased within a remnant nematode egg shell, known as a 'sheath'. During the initial penetration out of the arthropod midgut, mf 'ex-sheath' to form the first-stage "L1" larvae. L1 initiate a migration route through various tissues and body cavities of the vector, the route and timings of which are specific to each filarial-vector relationship. During this period, vector-stage filarial larvae undergo two moults whereby the outer cuticle is shed to allow a period of growth within the vector, from L1-L2 and from L2 to infective larvae (iL3). The iL3 (0.5-1mm in length) are positioned in the head and mouthparts, poised to infect a definitive host when parous vectors take a second blood meal. The rate of development within the vector is dependent on temperature, known as the 'extrinsic incubation period' and usually requires average temperatures to remain at or above 14-20 degrees centigrade for iL3 development to be achievable over a period of 2-3 weeks, coincident with the vector's feeding interval. Upon initial infection through the bite site, it is thought that all filarial L3, independent of species, initially parasitise the lymphatic system to migrate and evade immune-dependent destruction in the skin. Lymphatic filariae remain resident within the lymphatics, whilst subcutaneous filariae emerge to infect sub-cutaneous tissues. Larvae undergo two further moults and develop through the L4 (initially 1.5-2mm) and L5 (immature adult stage, 1-2cm approx.) within these niches. A further pre-patent incubation period is necessary before adults are sexually mature. This coincides with a sustained period of growth from the micro- to macroscopic where adult females attain lengths of between 5-20 cm. Adult males are typically shorter and more slender, reflecting the fact that females contain pairs of uteri extending almost the full length of their bodies. Adult worms can reside in the lymphatics or subcutaneous tissues for >12 years. When the adult worms mate they produce mf, their microscopic progeny, to disseminate either in the circulation or skin. Thus, the infection is transmitted and the life cycle is completed when a competent blood feeding vector takes a blood meal.

Table 1.1 Definitive and intermediate vector hosts of medically and veterinary-important filarial species including rodent filariae used in research

Filarial Species (Clade)	Vector	Major host	Other hosts	Laboratory life cycle host
<i>Acanthocheilonema viteae</i> (ONC 4)	<i>Ornithodoros</i> ticks	Rodents	-	Gerbils
<i>Brugia malayi</i> (ONC 5)	<i>Anopheles</i> , <i>Mansonia</i> mosquitoes	Humans	Civet cats, Domestic cats, Dogs, Leaf monkey	Gerbils Mice (immunodeficient)
<i>Brugia timori</i> (ONC 5)	<i>Anopheles</i> , <i>Mansonia</i> mosquitoes	Humans	-	none
<i>Brugia pahangi</i> (ONC 5)	<i>Mansonia</i> mosquitoes		Civet cats, Domestic cats, Dogs	Ferrets, Gerbils, Mice, Rats
<i>Dirofilaria immitis</i> (ONC 3)	<i>Aedes</i> <i>Anopheles</i> <i>Culex</i> mosquitoes	Dogs	Cats, Ferrets, Foxes & other wild canids Humans (arrested)	none
<i>Dirofilaria repens</i> (ONC 3)	<i>Aedes</i> <i>Anopheles</i> <i>Culex</i> mosquitoes	Dogs	Cats, Foxes & other wild canids Humans (arrested)	none
<i>Onchocerca gutturosa</i> (ONC 3)	<i>Simulium</i> blackflies	Cows	-	none
<i>Onchocerca lienalis</i> (ONC 3)	<i>Simulium</i> blackflies	Cows	-	none
<i>Onchocerca ochengi</i> (ONC 3)	<i>Simulium</i> blackflies	Cows	-	none
<i>Onchocerca volvulus</i> (ONC 3)	<i>Simulium</i> blackflies	Humans	-	Chimpanzees
<i>Loa loa</i> (ONC 5)	<i>Chrysops</i> tabinid flies	Humans	Drills	Baboons (splenectomised) Mice (immunodeficient)
<i>Litomosoides sigmodontis</i> (ONC 4)	<i>Ornithonyssus</i> mites	Cotton rats	-	Gerbils, Mice
<i>Mansonella ozzardi</i> (ONC 5)	<i>Culicoides</i> midges	Humans	Monkeys	none
<i>Mansonella perstans</i> (ONC 5)	<i>Culicoides</i> midges	Humans	Monkeys	none
<i>Mansonella streptocerca</i> (ONC 5)	<i>Culicoides</i> midges	Humans	Chimpanzees	none
<i>Wuchereria bancrofti</i> (ONC 5)	<i>Aedes</i> , <i>Anopheles</i> , <i>Culex</i> , mosquitoes	Humans	-	none

Adapted from (Nanduri and Kazura, 1989, Philipp et al., 1984)

1.4. Lymphatic Filariasis

Lymphatic filariasis (LF) is distributed in South America, Africa, Southeast Asia and The Pacific (Taylor et al., 2010b, Molyneux et al., 2003) (Figure 1.1). When assessed in 2000, an estimated 120 million individuals in 73 endemic countries were infected, with a total population of 1.3 billion at risk of acquiring infection (<https://www.who.int/lymphatic-filariasis/global-progress/en/>). Due to elimination programmes, in 2014, the number of estimated cases had reduced to 63 million (Ramaiah and Ottesen, 2014). *W. bancrofti* is the main etiological agent of lymphatic filariasis (LF), responsible for approximately 90% of cases. *W. bancrofti* has the widest distribution of all LF parasites due to the broad range of mosquito vectors that can transmit infection. It has high prevalence in Sub-Saharan Africa, south and southwest Asia, and was introduced to countries in the Caribbean and Latin America with the slave trade (Michael and Bundy, 1997). *Brugia malayi* and *B. timori*, transmitted predominantly by *Mansonia* mosquitoes, constitutes a further 10% of cases in tropical regions of South and Southeast Asia and co-infection with *W. bancrofti* prevails in southern India (Michael and Bundy, 1997). *B. timori*, constitutes the remainder of LF cases and has the most restricted geographic range of all filarial species, with prevalence only in Indonesia and Timor-Leste (McNulty et al., 2013).

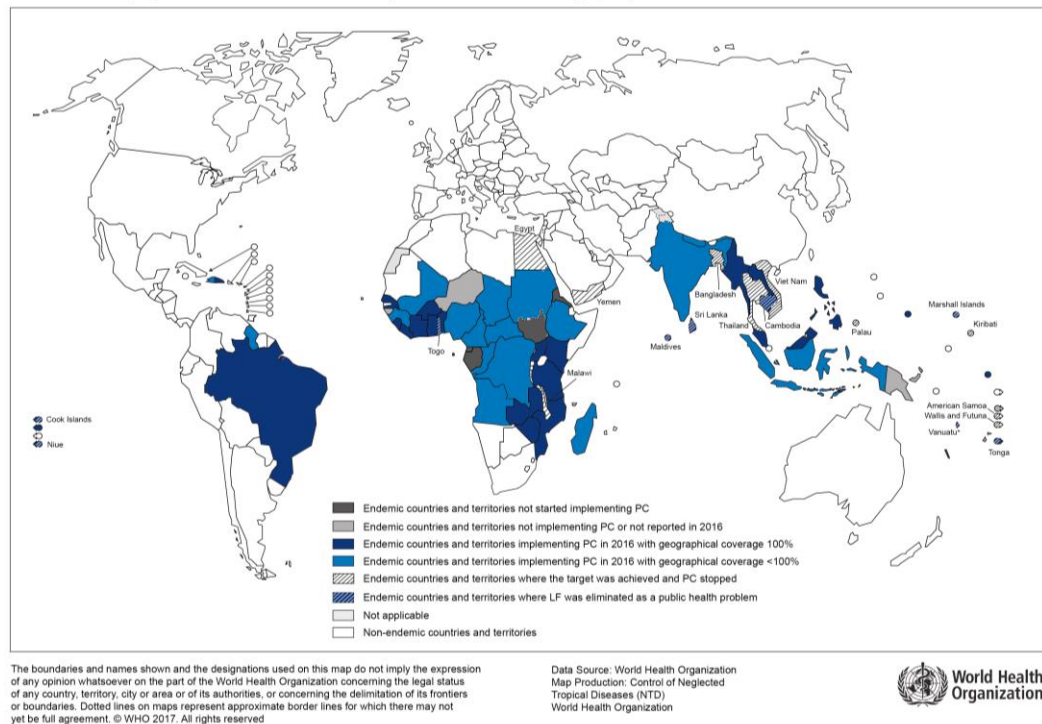


Figure 1.1. Distribution of lymphatic filariasis and status of preventative chemotherapy in endemic countries in 2017

Image from: http://apps.who.int/neglected_diseases/ntddata/lf/lf.html The PCT/MDA status for each country (indicated by the colour key), is a simplification of the overall country status of lymphatic filariasis highlighting endemic regions and where preventative chemotherapy is conducted, however this does not represent the heterogeneity in the focal distribution of the disease within the country.

1.5. Lymphatic filariasis specific life cycle

Both *Brugia spp.* and *W. bancrofti* are transmitted by female mosquitoes and, in optimum temperature conditions, iL3 can develop 13 days after blood feeding (Figure 1.2). LF species are some of the more rapid growing filarial species, attaining sexual maturity in the lymphatic system as little as twelve weeks following initial infection (Ash and Riley, 1970, Ash, 1973). In experimental models, the *B. malayi* L3-L4 moult occurs at 7-9 days and the L4-L5 moult at 28-35 days after initial infection (Ash and Riley). Adult *B. malayi* are approximately 3-5 cm in length whilst *W. bancrofti* are typically larger, reaching 7-10 cm. Adults demonstrate a proclivity for the limb and groin lymphatics, including the supra-testicular lymphatics in the

case of *W. bancrofti* infections of male patients. Adults reside within 'worm nests'; zones of grossly dilated lymphangions (lymphatic collecting vessels adjoined by lymphatic valves). The reproductive life-span of *W. bancrofti* is estimated at 5 years (Dreyer et al., 2005). Mating worms can produce >1000 sheathed mf per day. Mf migrate with lymph traffic to enter the blood stream via the thoracic duct. Mature mf can persist in the blood for 100-200 days. Most lymphatic filarial mf of *B. malayi* and *W. bancrofti* display an oscillatory nocturnal periodicity in peripheral blood, peaking at 9pm-12am. Nocturnal periodic mf sequester in deeper cardiopulmonary vasculature during day light hours. This periodicity is aligned to the peak biting times of local mosquito vectors and thus certain strains of *W. bancrofti* in Polynesia display an inverted diurnal periodicity which is aligned to the local *Aedes* vector. Sub-periodic 'zoophilic' strains of *B. malayi* also exist which display a less pronounced nocturnal periodicity. Upon blood feeding, mf rapidly invade the peritrophic matrix and exsheath to escape the bloodmeal within the mid-gut. The L1 stage forms a 'sausage' morphology within flight muscles before developing to L2 which then migrate to the head and proboscis undergoing a final moult to L3.

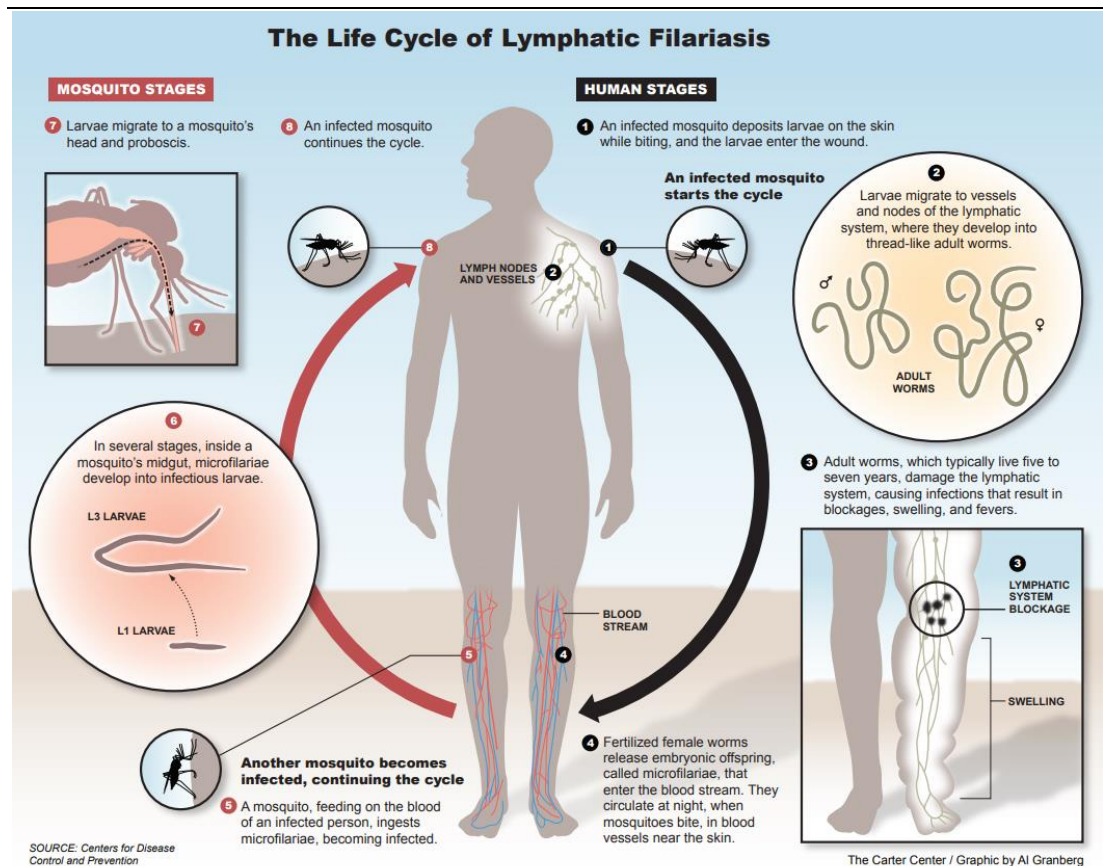


Figure 1.2. Life-cycle of Lymphatic Filariasis

Image from: <https://mectizan.org/news-resources/life-cycle-lymphatic-filariasis/> As a mosquito takes a blood meal, it deposits larvae onto the skin which then migrate through the bite wound. Larvae then migrate to the lymphatics where they continue to develop to adult worms, releasing microfilariae into the circulation. These microfilariae are then ingested by the mosquito when a blood meal is taken, develop through to larvae inside the mosquito which continues the life cycle when the mosquito takes another bloodmeal.

1.6. Lymphatic filariasis disease

The main disease symptoms of LF are forms of secondary lymphoedema: hydrocele and elephantiasis (Pfarr et al., 2009, Nutman, 2013) which combined, affect 40 million individuals worldwide, making LF a major cause of global disability. Hydrocele occurs in an estimated 25 million male bancroftian filariasis patients (brugian filariasis does not induce this disease manifestation) and is due to impaired lymphatic drainage by parasitized supra-testicular lymphatics leading to fluid accumulation within the scrotum. Elephantiasis is a chronic

progressive form of limb lymphoedema affecting an estimated 15 million patients, mostly women. Developing larvae and adult filarial parasites induce lymphatic disease after infection of the lymphatic system. A main driver of pathology is the death of filariae *in situ* within lymphatics, either naturally or due to host non-permissive immune responses. Dreyer et al. (Dreyer et al., 2000) proposes multiple co-factors also contribute to the development of limb lymphoedema including secondary microbial infections of the skin. These secondary opportunistic infections can drive episodes of acute dermatolymphangioadenitis (ADLA) causing further inflammatory damage to the skin and superficial lymphatics.

1.7. Onchocerciasis

Onchocerca volvulus, infects an estimated 37 million individuals, primarily in sub-Saharan Africa (James et al., 2018), although foci of infections still exist in Latin America and Yemen. Latin American foci are now limited to the Brazilian/Venezuelan Amazonian rainforest due to successful elimination programmes in Columbia, Ecuador, Guatemala and Mexico (World Health Organisation, 2018) (Figure 1.3).

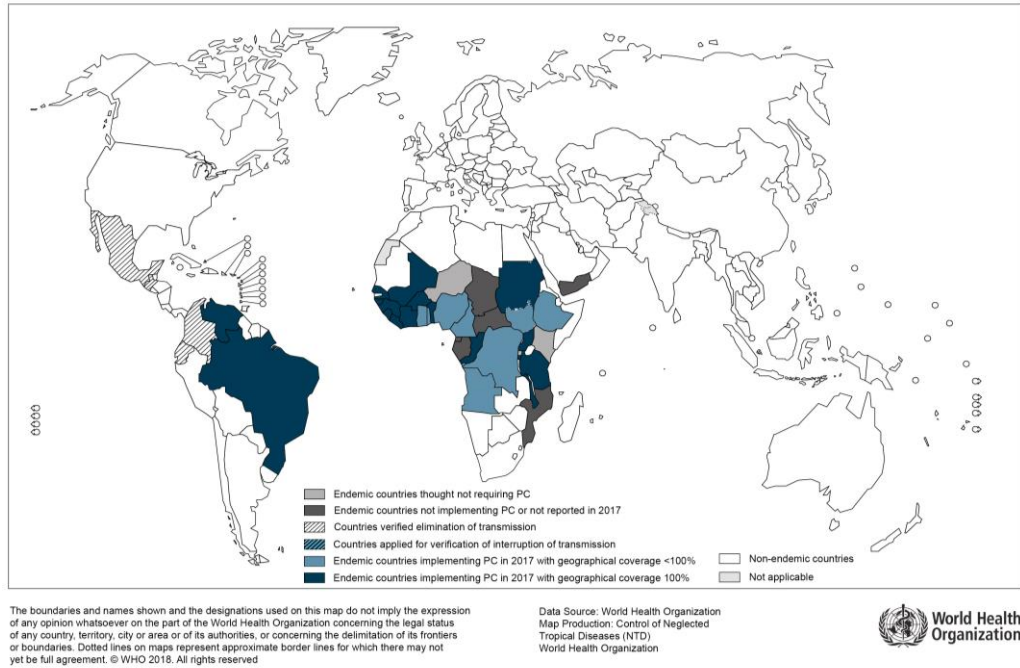


Figure 1.3. Distribution of onchocerciasis and status of preventative chemotherapy in endemic countries in 2017

Image from: http://apps.who.int/neglected_diseases/ntddata/lf/lf.html The PCT/MDA status for each country (indicated by the colour key), is a simplification of the overall country status for onchocerciasis, however this does not represent the heterogeneity in the focal distribution of the disease within the country.

1.8. Onchocerciasis specific life cycle

Blackfly of the genus, *Simulium*, transmit *O. volvulus* as well as other cattle *Onchocerca* parasites. Most of the *Onchocerca* life cycle biology in the definitive host has been ascertained from either *in vitro* cultures of larval *O. volvulus*, experimental infections of chimpanzees or using the related *O. ochengi* as a model via experimental infections of cattle (Abraham et al., 1993, Trees et al., 2000, Eberhard et al., 1995, Voronin et al., 2019, Duke, 1980). Infectious stage (i)L3 (0.5 mm in length) penetrate the bite site and initially infect and migrate within lymphatics to emerge in the subcutaneous tissues where adult parasitism eventually establishes (Figure 1.4). The L3-L4 moult initiates rapidly, as little as 3 days post-infection and is usually completed by day 7. From this point, *O. volvulus* are comparatively

slow growing, compared with lymphatic (ONC 5) parasites. The L4-L5 moult proceeds at approximately 2 months. It takes a further 280-532 days for adults to become patent and this coincides with a tremendous growth phase from <1 cm at the early L5 stage to 33 – 50 cm mature female worms. Adult male worms measure 19-42 cm and are slenderer. Adult parasites form bundles which may reside in deeper subcutaneous tissues or in more superficial nodules (onchocercomata) which are vascularised collagen containing capsules rich in immune cell infiltrates. These often form adjacent to bony protrusions under the skin and are readily palpable as a clinical diagnostic feature. Adult parasites can live for an average of 8-10 years. Whilst female worms are sluggishly motile within these nodules, male worms are migratory and can move between onchocercomata to mate with different female worms. Mating produces 1000-3000 unsheathed mf per day. *O. volvulus* mf migrate into the skin and typically form gradient densities in the skin of the trunk, head or limbs related to distance from onchocercomata/adult worm bundles. The microfilarial stage can survive for upwards of one year in the skin. Blackfly acquire mf infection due to abrading skin to create a blood pool to feed upon. *Onchocerca* mf migrate from the midgut to flight muscles, form the sausage stage L1 and undergo two moults with migration to the proboscis in approximately 9 days. The IL3 burst out of the mouth parts during feeding to infect the next host.

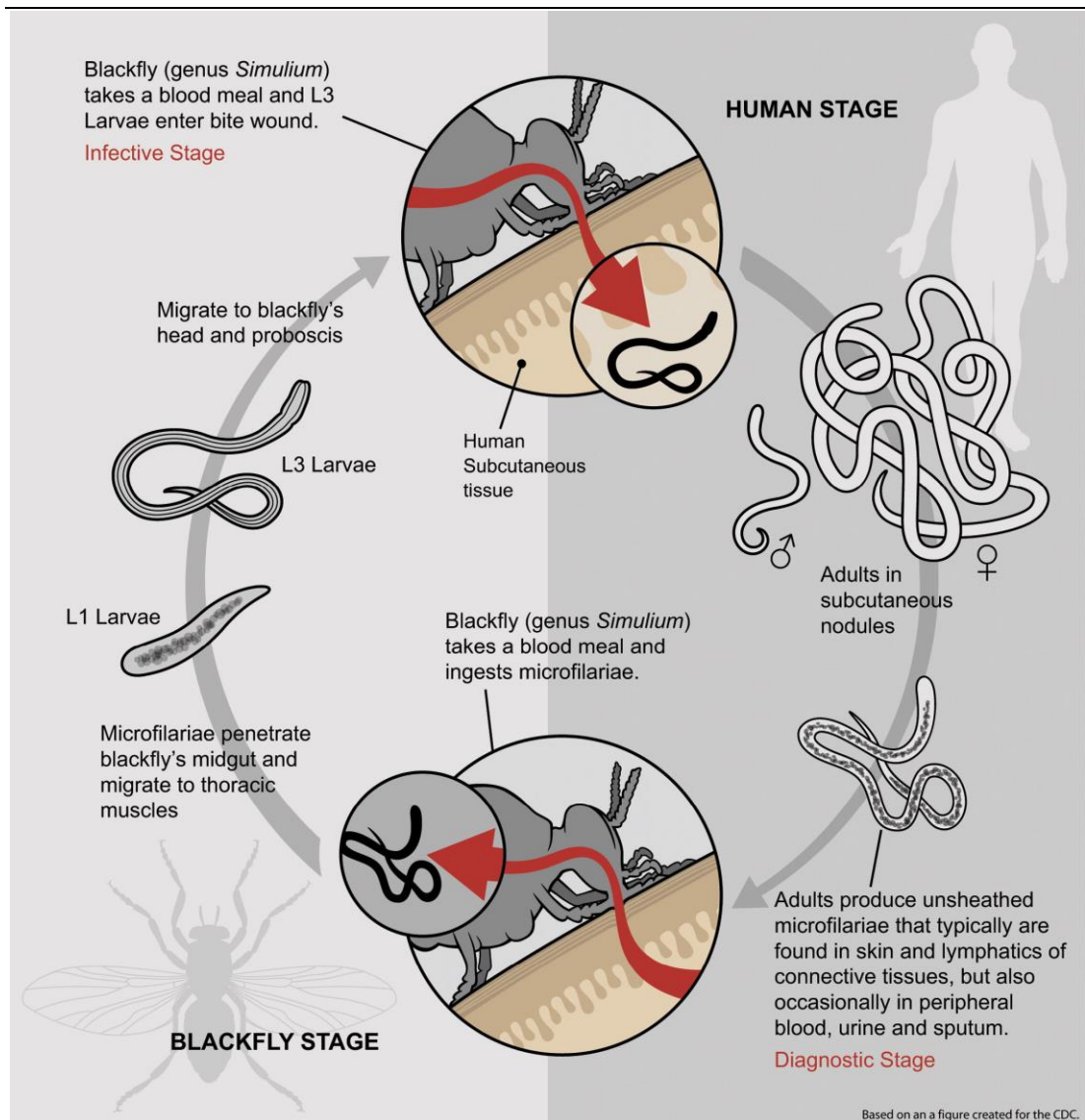


Figure 1.4. Lifecycle of Onchocerciasis

Figure from: <http://blogs.biomedcentral.com/bugbitten/2015/09/11/good-news-mexico-river-blindness-eradication-confirmed/> Blackfly takes a blood meal and L3 larvae enter the wound, develop through subcutaneous tissues to form adults in subcutaneous nodules, these adults produce unsheathed mf which can be found in the peripheral circulation, where they can be picked up by blackflies to continue the cycle.

1.9. Onchocerciasis disease

Onchocerciasis is a spectrum of dermal and ocular diseases. All disease manifestations are induced by death of aged mf in the skin which induces inflammatory reactions to antigenic contents released as mf deteriorate. These reactions are typically allergic-type in nature

(including recruitment of eosinophil granulocytes and mast cell activation). Immune-mediated inflammatory reactions cause 'troublesome itching' (Murdoch, 2018, Murdoch, 2010). The incidence of troublesome itching precedes or co-occurs with the development of skin rashes known as acute and chronic papular onchodermatitis. More chronic exposure to mf infections in the skin give rise to other pathologies including lichenified onchodermatitis involving premature atrophy and fibrosis of the skin (lizard skin), hanging groin (a form of lymphoedema) and skin depigmentation (leopard skin). An estimated 6.5 million infected individuals suffer skin complaints (Murdoch, 2018). The most severe form of onchocerciasis is ocular keratitis (river blindness). Around 800,000 people are estimated to be blind or visually impaired due to ocular onchocerciasis, ranking river blindness the second leading cause of infection-induced blindness worldwide. As with dermal disease, ocular pathology is a result of entrapped disintegrating mf, mainly in the corneal tissue of the anterior ocular chamber. Dead mf can trigger granulocyte influx and degranulation causes collateral damage manifest as a punctate then sclerosing keratitis. *Onchocerca volvulus* mf can also occasionally migrate to the posterior segment of the eye. The presence of mf in this site occurs more frequently when skin infections are high. Death of mf at this anatomical location is particularly pathogenic as it can induce vascular leakiness and optic nerve damage (Pearlman, 1997, Pearlman and Hall, 2000, Hall and Pearlman, 1999).

1.10. Dirofilariasis

Dirofilariasis is caused by two veterinary filarial parasites; *Dirofilaria immitis*, the causative agent of heartworm disease in dogs and pulmonary dirofilariasis in cats, and *D. repens*, which causes a subcutaneous infection in cats and dogs (Simon et al., 2012). Both species can be transmitted to humans to cause zoonotic pathologies (Pampiglione et al., 1995, Jelinek et al., 1996, Reddy, 2013). *Dirofilaria immitis* is distributed in the tropics and sub-tropics throughout the world whilst *D. repens* is absent from The Americas. Data is scant on

estimates of global prevalence or burden of disease in either companion animals or humans. Data are limited to areas of the world where dirofilariasis is highly prevalent and been recognised as both a veterinary and public health problem. As more epidemiological surveys have been carried out longitudinally, there is evidence that veterinary dirofilariasis is increasing in prevalence and distribution to erstwhile more temperate zones of USA and Northern Europe (Morchón et al., 2012) (Figure 1.5). This is speculated to be due to the effects of climate change providing extended habitats for local mosquito vector species and the potential for *Dirofilaria* larval development, at least during summer months. In the USA, the most intensively monitored country, prevalence of *D. immitis* ranges between 1-12% of surveyed dogs in mainland states. Regarding zoonotic human dirofilariasis, case study collections have documented a reported 1782 confirmed infections of which 372 are pulmonary and 1410 are subcutaneous/ocular (Simon et al., 2005, Simon et al., 2012).

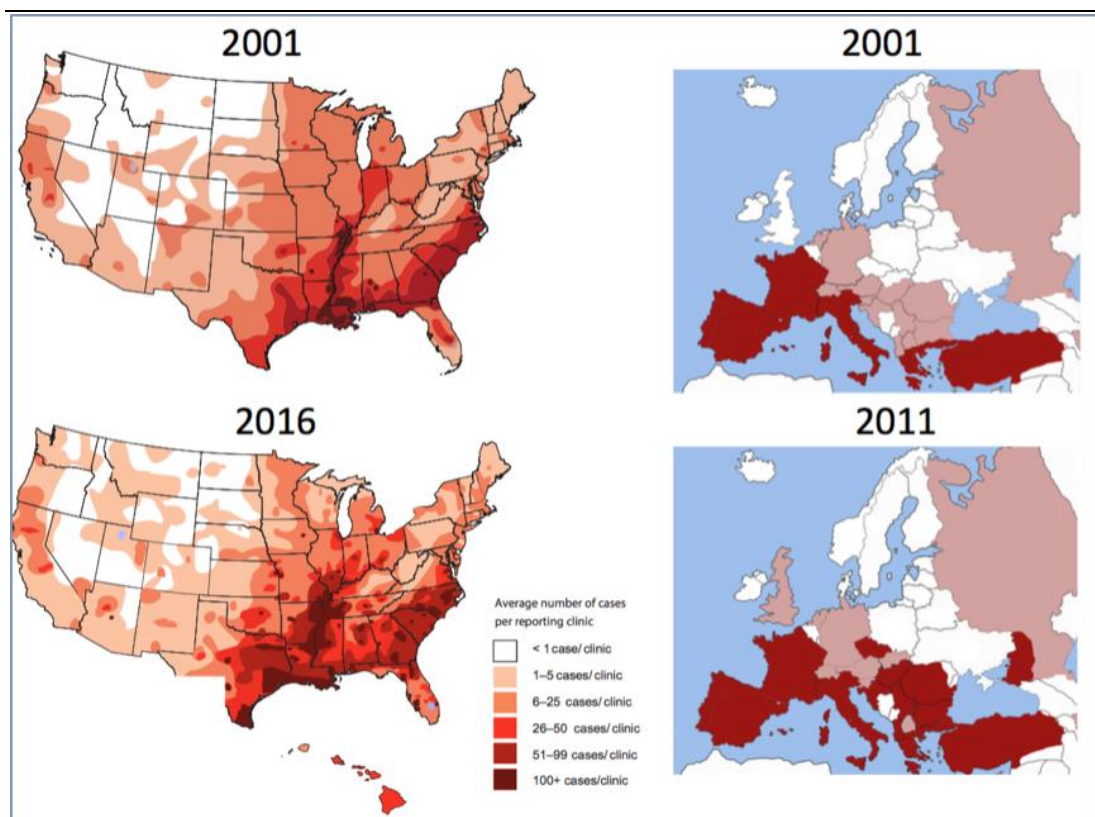


Figure 1.5. Incidence of heartworm

Figure from: <https://www.heartwormsociety.org/veterinary-resources/incidence-maps> Incidence of heartworm in the USA between 2001 and 2016., marking the number of cases/clinic.

1.11. Dirofilariasis specific life-cycle

The major vector species of *D. immitis* in the USA is *Aedes aegypti*, although multiple species of *Aedes*, *Anopheles*, and *Culex* are competent vectors of *D. immitis* and *D. repens*. As with other filariae, an initial infection route via the skin lymphatics is suggested for *Dirofilaria spp.* Similar to other ONC 3 *Onchocerca* parasites, *Dirofilaria* initially establish in the subcutaneous tissues and initiate moulting rapidly after 3-4 days. *D. immitis* continue to migrate from the subcutaneous tissues into striated muscle whereas *D. repens* remain in the subcutaneous zone and form collagenous nodules, similar to *Onchocerca spp.* The L4-L5 moult proceeds at approximately two months. For *D. immitis*, the juvenile L5 stage migrates from muscle to invade the vasculature and establish in the pulmonary artery and right ventricle between 70-85 days post-infection. At this stage, the juvenile adults are 25-33mm in length (Figure 1.6). Upon infection of cardiopulmonary tissues a rapid growth phase is initiated whereby female worm length increases ~10-fold by the point of sexual maturity and mf production at ~6 months (slightly delayed in cats) whereby adult female worms can measure 25-30 cm. Adult infections can persist for >5 years. Circulating, unsheathed mf acquire densities >1000/ml of peripheral blood, can persist in circulation for as long as two years and are transmitted to mosquitoes via blood feeding. Cats are rarely microfilaraemic for *D. immitis* but *D. repens* microfilaraemias do proceed in cats, making it a reservoir for transmission. Upon ingestion, mf penetrate the peritrophic membrane and migrate to the Malpighian tubules within 24 h. Moulting to L2 occurs within the Malpighian tubules at 8-10 days and the L2-L3 moult occurs around 11-13 days, dependent on environmental temperature. L3 migrate to the head and mouthparts to complete the life cycle (Otto, 1969).

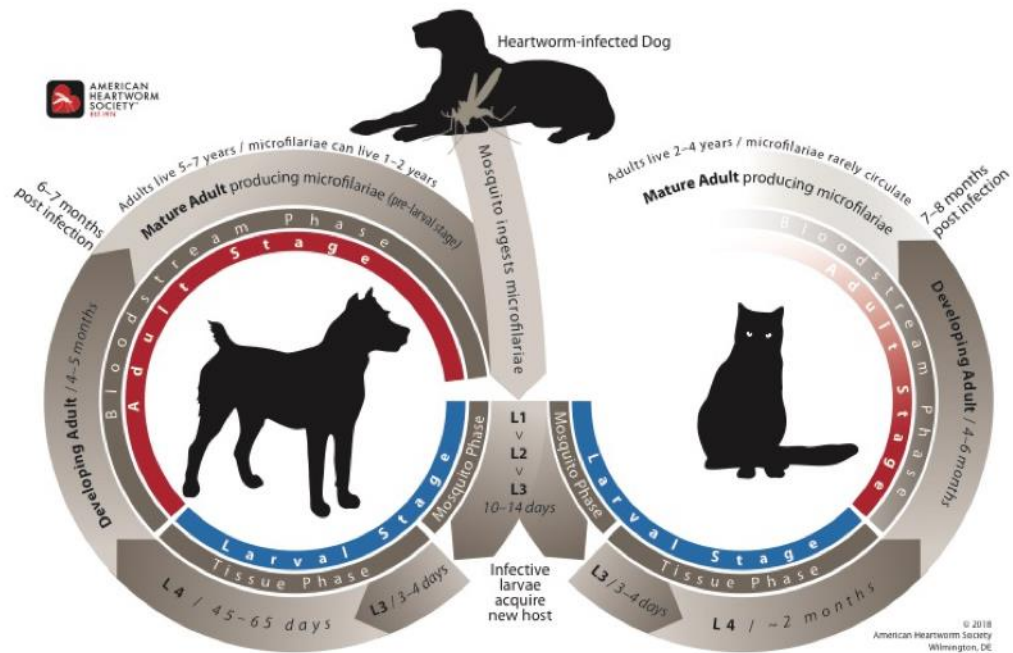


Figure 1.6. Lifecycle of veterinary heartworm

Figure from: <https://www.heartwormsociety.org/pet-owner-resources/2014-03-24-22-40-20> Infective larvae transfer to host via mosquito bite, these larvae then migrate through the subcutaneous tissues, eventually reaching the heart at the adult stage. These adults then begin to produce microfilariae, which are picked up when mosquitoes take a bloodmeal, develop through to larvae within the mosquito, which can then enter another host when the mosquito bites again.

1.12. Dirofilariasis disease

Dirofilaria immitis adult infections of the heart are the cause of canine cardiopulmonary dirofilariasis (heartworm disease). In 2012, a recorded 48,000 dogs tested positive for heartworm disease in the USA (www.heartwormsociety.org). The presence of live adult worms in the pulmonary artery provokes a host pathological response triggering an enlargement and proliferation of the endothelial lining with collagen deposition. This leads to a narrowing of the artery (endarteritis) and along with chronic parasitism and high worm burdens can lead to hypertension and chronic congestive heart failure. Additionally, death

of adult worms and bolus release of antigens into the lung can induce inflammatory thromboembolisms. Both conditions are potentially fatal. Cats are less permissive to chronic infections than dogs. This means that disease manifestations are typically acute and pulmonary in nature, coincident with the arrival of adults within the heart and with a high incidence of fatality. Humans are non-permissive hosts to *D. immitis* although microfilaraemias can establish in *D. repens* infections. Pathology is induced by migration and death of immature adult parasites in the lungs, for *D. immitis*, forming characteristic 'coin-shaped' lesions which can be visualised by lung X-ray. For *D. repens*, sub-cutaneous or ocular inflammatory lesions are manifest (Jelinek et al., 1996).

1.13. *Wolbachia* endosymbionts of filariae

In the 1970s, an intracellular bacteria of filarial nematodes was discovered via electron microscopy (Kozek and Marroquin, 1977, Kozek, 1977). Researchers subsequently genetically characterised these obligate intracellular bacteria as the genus, *Wolbachia*, prior characterised to infect numerous insects and arachnids. *Wolbachia* are members of the Rickettsiales order of α -proteobacteria, closest related to *Ehrlichia* and *Anaplasma* species (Bandi et al., 1998).

Wolbachia occurs in the medically- and veterinary-important filarial species: *B. malayi/timori*, *D. immitis/repens*, *M. ozzardi/perstans*, *O. volvulus* and *W. bancrofti*. Not all filariae possess *Wolbachia* and of note, the medically important *L. loa* is devoid of symbiosis (Büttner et al., 2003). Whilst all but *O. flexuosa* of the ONC3 clade thus far studied possess *Wolbachia* symbiosis, the proportion of aposymbiotic species in the ONC4 and ONC5 clades are higher, including the common filarial laboratory model organism, *Acanthocheilonema viteae*. Further, whilst *Wolbachia* has been observed in all wild isolates sampled of *B. malayi*, *O. volvulus* and *W. bancrofti*, a more inconsistent distribution may be apparent for *M. perstans*, with isolates identified with no evidence of *Wolbachia* infection (Casiraghi et al.,

2001, Keiser et al., 2008, Coulibaly et al., 2009, Grobusch et al., 2003, McGarry et al., 2003) see Table 1.2. These patterns of *Wolbachia* presence and absence may represent a 'secondary loss' of symbiosis. Certainly for *A. viteae*, *L. loa* and *O. flexuosa*, presence of *Wolbachia* insertions into filarial genomes is evidence of secondary loss events (Wu et al., 2013).

Molecular phylogenetic and whole genome analysis of *Wolbachia* in arthropods and nematodes demonstrates that *Wolbachia* comprise as many as eight distinct clades (Lefoulon et al., 2016). The arthropod *Wolbachia* clades A and B are more heterogeneous with more complex genomes and evidence of mobile genetic elements, whereas nematode *Wolbachia* clades C,D and F have smaller genomes and lack mobile DNA (Foster et al., 2005). Whilst it might be presumed that parasitic filariae acquired *Wolbachia* from their arthropod vectors, a recent hypothesis suggests clade C *Wolbachia* of ONC3 filariae, which demonstrates a high degree of co-evolution, may be the root ancestral source of original infection with *Wolbachia* which then latterly transferred to arthropods (Lefoulon et al., 2016).

Wolbachia is found within all life cycle stages of filariae, infecting the hypodermal cells of the lateral chords of both male and female worms as well as the female germline. *Wolbachia* are thus transmitted vertically from female filariae. An invasion event from somatic hypodermal tissues into the distal tip ovaries and germline cells occurs during L4 larval development (Landmann et al., 2012).

From data derived from *B. malayi*, *Wolbachia* (clade D) undergo an exponential growth expansion during the early stages of mammalian infection. Infectious L3 stage harbour between 10^2 - 10^3 *Wolbachia*, determined by quantification of genomic DNA copies of the single copy *Wolbachia* gene, *Wolbachia surface 39protein (wsp)*. This rapidly expands to $>10^5$ *Wolbachia* in mid-L4 stages and $>10^6$ in juvenile adults. *Wolbachia* titres attain $>10^7$ in mature

adult female *B. malayi*. Titres are lower in males, reflecting both the smaller size of males vs females and *Wolbachia* invasion into the female germline.

By tetracycline-mediated clearance of *Wolbachia* in experimental systems it has been shown that *Wolbachia* is required for both filarial larval development and embryogenesis. Thus, treatment of gerbils infected with *Litomosoides sigmodontis* or *Brugia spp.* with tetracyclines stunts L4 growth, prevents L4-L5 moulting and blocks adult filarial development (Bosshardt et al., 1993). Treatment at the pre-patent adult stage of infection in rodents effectively blocks embryogenesis and mf release (Halliday et al., 2014) whilst treatment at the patent-stage similarly blocks embryogenesis causing a gradual and complete loss of mf from the circulation (Hoerauf et al., 1999). Research into the nature of the symbiosis identifies that *Wolbachia* produce an excess of nucleotides and therefore may provide a source of nucleotides during rapid filarial cell division (Foster et al., 2005). Examination of biosynthetic pathway enzymes absent or incomplete from *B. malayi* but functional in *Wolbachia*, implicate haem and vitamin B2 (riboflavin) as products that endosymbionts may provide in more abundance than filariae can scavenge from their parasitic niche, especially at times of high growth demand (Li and Carlow, 2012).

Table 1.2. *Wolbachia* distributions and clades across filarial species.

Adapted from (Lefoulon et al., 2016, Lefoulon et al., 2015, Bouchery et al., 2013)

Filarial Species (Clade)	<i>Wolbachia</i> presence/absence	<i>Wolbachia</i> clade
<i>Acanthocheilonema viteae</i> (ONC 4)	absent	-
<i>Brugia malayi</i> (ONC 5)	present	Clade D
<i>Brugia timori</i> (ONC 5)	Present	Clade D
<i>Brugia pahangi</i> (ONC 5)	Present	Clade D
<i>Dirofilaria immitis</i> (ONC 3)	Present	Clade C
<i>Dirofilaria repens</i> (ONC 3)	Present	Clade C
<i>Onchocerca gutterosa</i> (ONC 3)	Present	Clade C
<i>Onchocerca lienalis</i> (ONC 3)	Present	Clade C
<i>Onchocerca ochengi</i> (ONC 3)	Present	Clade C
<i>Onchocerca volvulus</i> (ONC 3)	Present	Clade C
<i>Loa loa</i> (ONC 5)	Absent	-
<i>Litomosoides sigmodontis</i> (ONC 4)	Present	Clade D
<i>Mansonella ozzardi</i> (ONC 5)	Present	Clade F
<i>Mansonella perstans</i> (ONC 5)	Present	Clade F
<i>Mansonella streptocerca</i> (ONC 5)	Currently unknown. No published data on the presence of <i>Wolbachia</i>	Currently unknown. No published data on the presence of <i>Wolbachia</i>
<i>Wuchereria bancrofti</i> (ONC 5)	Present	Clade D

1.14. Registered anti-filarial drugs

- **Macrocyclic lactones**

The macrocyclic lactones (ML: avermectins and milbemycins) are derivatives of natural fermentation products of soil bacteria, *Streptomyces* such as *S. avermitilis*. Examples of avermectins are ivermectin and selamectin whilst milbemycin oxime and moxidectin are common milbemycins. Whilst originally developed for veterinary indications against gut nematodes, ML drugs have a range of activities against filarial parasites (Campbell, 1982, Wolstenholme et al., 2016, Nolan and Lok, 2012). Ivermectin (IVM; mectizan) has been used extensively in control and elimination mass drug administration (MDA) for both LF and onchocerciasis and was first introduced for human use in 1981. At the standard dose used of

single dose of 150-200 µg/kg, IVM exerts a 'microfilaricidal' effect via agonistic targeting of the nematode glutamate-gated chloride channel (GluCl), and also gamma-aminobutyric acid (GABA) channels, inducing paralysis, loss from either the circulation of skin and subsequent destruction of mf via the lymphatics (Taylor et al., 2010b, Basanez et al., 2008, Brown et al., 2000). IVM also affects late-stage, inter-uterine mf within adult female worms. This promotes a 'long-tail' of microfilaricidal activity whereby resumption of circulating or skin mf is absent for as long as six-months post-treatment. However, at this dose, there is no significant impact on adult worms, even following repetitive treatments. Whilst there are some treatment-associated side-effects caused by death of mf causing inflammatory reactions (known as Mazzotti reactions in the case of onchocerciasis) (Guderian et al., 1991, Basanez et al., 2008), these are generally well-tolerated and most pronounced in IVM-naïve populations where mf parasite loads are high. Because filarial mf tolerate IVM at doses in the physiological range *in vitro* without phenotypic changes, it has been suggested that part of mode-of-action requires a host immunological component. One hypothesis proposes that via impeding excretory/secretory apparatus within mf, reduced immunomodulatory molecule release allows for immune cell-dependent clearance (Moreno et al., 2010). However, IVM works with high efficacy in both immune intact and severe-combined immunodeficient mice (lacking adaptive immunity) which may implicate innate immune responses in the augmented activity of the drug *in vivo* (Halliday et al., 2014).

Selective toxicity against IVM stems from a lack of GluCl channels in mammals and exclusion from the central nervous system by p-glycoprotein efflux pumps. With billions of treatments being administered in control and elimination campaigns, IVM is proven to be a safe microfilaricide in areas for LF or onchocerciasis. However, in areas co-endemic for loiasis, cases of severe adverse drug events (SAEs) have been reported (Gardon et al., 1997, Boussinesq et al., 2003). Severe adverse events are typified by neurological pathology, coma and in some instances, death. The severity of SAEs are positively correlated with increasing

microfilarial density, with patients at a parasitaemia of 30,000 mf/ml having a greatly increased risk. Severe adverse events are due to the rapid death of microfilariae occluding the microvasculature in the brain exacerbated by inflammatory immune responses to the dying mf and mf invasion into the brain due to a damaged blood brain barrier (Gardon et al., 1997), although the specific underlying mechanisms are not yet fully elucidated. Estimates between 2001 and 2002 reported 207 SAEs of which 65 were probable *L. loa* encephalopathy temporally related to IVM treatment (Boussinesq et al., 2003). IVM treatment of loa co-infected individuals with lower mf parasitaemias between 8,000 – 20,000 mf/ml remain at risk of non-neurological symptoms in response to rapidly dying mf, which can be temporarily debilitating (Mackenzie et al., 2003, Aziz et al., 1982).

Moxidectin (MOX), has recently shown superiority to IVM in phase III clinical trials. Compared to IVM, MOX sustains an absence of detectable mf from the skin of onchocerciasis patients for 12 months compared to 6 months (Awadzi et al., 2014, Opoku et al., 2018). Superiority stems from the drug's increased lipophilicity creating a long-lasting depot in sub-cutaneous tissues. MOX was approved by the FDA in 2018 as new recommended treatment for onchocerciasis. Because the mode of action and kinetics of mf depletion are similar for MOX and IVM, the drug cannot be used as an alternative to IVM to treat *L. loa* co-infected patients.

Both IVM and MOX, as well as other ML, are marketed prophylactic 'preventatives' for heartworm in client-owned cats and dogs. ML are efficacious in killing infectious L3 and developing L4 larvae and thus preventing the establishment of adult heartworm infections. IVM is given as a single monthly oral chewable tablet whereas MOX can be administered topically once every 3 months or as a slow-release injection once every 6 months.

1.14.1. Piperizines

The piperazine derivative, diethylcarbamazine citrate (DEC), was first introduced as an anti-filarial agent in 1947. It is primarily a microfilaricide although it does also have some

macrofilaricidal activity, mainly against juvenile developing adults. The mode-of-action and molecular target of DEC remains rather obscure. DEC is not active against mf *in vitro* pointing toward a host-directed mechanism. DEC modifies the metabolism of arachidonic acid and production of eicosanoids such as prostanoids and leukotrienes both secreted by *B. malayi* mf and mammalian host cells, including endothelium. Therefore, one theory proposes that DEC may induce vasoconstriction and immobilise bloodborne mf for immune-mediated targeting. This theory does not particularly address the potent microfilaricidal activity of DEC against skin-or ocular dwelling *O. volvulus* mf (Maizels and Denham, 1992).

DEC was used as a front-line treatment for onchocerciasis until the early 1980s. At this point it was contra-indicated following an accumulation of case reports indicating the drug caused severe Mazzotti reactions, including irreversible ocular adverse reactions (Bird et al., 1979, Bird et al., 1980). Similarly, it can cause SAE in *L. loa* patients, similar to IVM, and is only suggested to be used as a treatment under careful clinical monitoring. DEC is used for the treatment of LF outside of Africa in MDA programmes.

1.14.2. Benzimidazoles

Several benzimidazoles (BZ) are registered for human use and one, albendazole (ABZ), is frequently used as part of annual combination therapy for the treatment of LF with DEC and/or IVM at a single dose of 400 mg. ABZ acts as a pro-drug to the active metabolite, albendazole sulfoxide (ABZ-SOX). This metabolite then binds to the colchine sensitive site of β -tubulin inhibiting microtubule assembly (Kwarteng et al., 2016). This perturbs cell division and cell transport such as glucose uptake, resulting in cell death due to the depletion of glycogen. ABZ-SOX therefore targets rapidly dividing cells with high energy demands. Whilst even multiple dose 400 mg ABZ is ineffective at killing adult filarial parasites, ABZ transiently blocks embryogenesis, leading to a gradual decline in mf. Selective toxicity stems from an amino acid substitution in mammalian tubulin rendering ~ 10 -fold decreased binding of ABZ-

SOX. Further, gut absorption of ABZ is low (approximately 10%), limiting systemic exposure of the drug. ABZ has also been used as a monotherapy for the treatment of loiasis, whereby 21-day treatment with 400 mg can partially reduce circulating mf. Further, ABZ twice yearly MDA has been used as an alternative approach to IVM for the elimination of bancroftian filariasis where loiasis is co-endemic (Pion et al., 2017).

Flubendazole (FBZ), is related BZ anthelmintic approved for the treatment of gastrointestinal helminths of human and veterinary importance in 1980 and is given to treat human gut worms via oral tablet (Geary et al., 2019). It was trialled for use as an anti-filarial drug against onchocerciasis in a clinical trial in Mexico in 1986 (Mackenzie and Geary, 2011). In this trial, FBZ demonstrated significant and selective macrofilaricidal activity (skin mf were not affected). However, FBZ was administered by injection to increase systemic exposure and caused severe adverse reactions at the injection site stopping the re-purposing of this drug via parenteral delivery.

Mebendazole (MBZ), also within the BZ class, is an effective treatment against pinworms, roundworms, whipworms and hookworms through distribution in community-wide eradication programmes. Mebendazole exerts its action by preventing glucose absorption which are required for worm survival. Studies have been conducted to evaluate the efficacy of MBZ against filarial worms, for which it has shown efficacy against loa and mansonella microfilariae (Van Hoegaerden et al., 1987). Trials have also been carried out to examine its efficacy in bancroftian filariasis, however due to its poor enteric absorption high doses are required to be efficacious against microfilarial stages which induces gastrointestinal side effects (Sarma et al., 1988).

1.14.3. Melarsomine

Melarsomine hydrochloride (immiticide), an aromatic organic arsenical, is the only approved treatment cure for adult dirofilariasis. It is given as an intramuscular injection. The mode of

action is not known. Melarsomine has low selective toxicity and induces adverse reactions around the injection site. Further, there is risk of severe treatment adverse reactions following drug-mediated death of parasites causing potentially fatal thromboembolisms. For these reasons melarsomine is delivered as split dose over an interval of 30 days. Further, prior to treatment initiation, dogs have to undergo a rigorous pre-assessment and high worm burdens (assessed by radiography or echo-cardiogram) may preclude treatment. Dogs need to be restricted from exercise over the course of treatment. Corticosteroid treatments may be administered to reduce inflammation during death of adult worms. Because of increased risk of thromboembolisms, melarsomine is not recommended for the treatment of feline dirofilariasis.

1.15. Doxycycline

Doxycycline (DOX) targeting *Wolbachia* leads to a range of anti-filarial outcomes assessed in phase II and III community trials. A 4-6 week, 100-200 mg/day treatment regimen has been confirmed to effectively and sustainably deplete *Wolbachia* (>90% depletion level) from filarial tissues in bancroftian filariasis, brugian filariasis and onchocerciasis patients (Taylor et al., 2005b, Debrah et al., 2007, Wanji et al., 2009). A putative bacteriostatic mode-of-action is assumed via targeting the *Wolbachia* 30S ribosomal sub-unit, preventing protein synthesis. Effective *Wolbachia* depletions by long-course doxycycline leads to gradual waning of mf in blood and skin, long-term transmission - blocking sterility of adult worms and eventual significant macrofilaricidal activity (typically >70% macrofilaricidal 18-24 months post treatment) (Walker et al., 2014). Further, DOX can improve lymphoedematous pathology in elephantiasis LF patients in a mode-of-action distinct to anti-*Wolbachia* or general antibiotic activities (Mand et al., 2012). Because DOX treatment is not directly microfilaricidal and also because *L. loa* lacks the symbiosis, DOX is safe to treat onchocerciasis or LF in *L. loa* co-infections (Turner et al., 2010a, Tamarozzi et al., 2011, Boussinesq et al.,

2003). It has been approved by the WHO as an alternative strategy to IVM for the treatment of onchocerciasis. One drawback of DOX is the long treatment timeframe required to deplete *Wolbachia* levels to a level where they will not rebound. DOX is also not appropriate for use in children under the age of 8 years or pregnant women, due to its action as a calcium-chelator which can hinder bone development during pregnancy and in young children (Jick et al., 1981, Czeizel and Rockenbauer, 2000, Cohan et al., 1963) . For both these reasons, DOX is unsuitable for MDA but is proposed as a treatment option in specific test and treat elimination scenarios. Additionally, there is the concern that the use of broad-spectrum antibiotics may contribute to overall risk of antimicrobial resistance development (Sanprasert et al., 2010).

DOX treatment has further proved to be effective in treating heartworm in infected dogs in combination with IVM (Bazzocchi et al., 2008). It is currently recommended to be used as an adjunct treatment for canine dirofilariasis to deplete *Wolbachia* and uterine contents prior to melarsomine treatment (Kramer et al., 2018).

1.16. Human Filariasis control and elimination strategies

Current strategies to control and eliminate human filarial disease focus on the blockade of the transmissible (mf) stage, as no safe, effective macrofilaricidal treatment deployable at scale is currently available. Elimination and disease control, in the case of onchocerciasis, is delivered through preventative chemotherapy (PCT) with the goal of reducing the circulating parasite density in the blood or skin of infected individuals, and thus the intensity of infection in communities to levels where transmission is no longer sustainable by the vector (Ottesen, 1998). MDA functions on the basis that all at risk populations are treated with PCT regardless of infection state (Hooper et al., 2014). Prior to MDA, patients only received treatment on a 'test and treat' basis, usually in response to symptoms (Boussinesq et al., 2018). Thus,

asymptomatic individuals persisted as a reservoir for disease and treatment was not delivered for long enough to be effective in reducing transmission.

In 1974, the WHO launched the Onchocerciasis Control Program (OCP) in West Africa. As onchocerciasis prevalence is strongly correlated with the proximity of riverine breeding sites of the blackfly vector (Taylor et al., 2010b), the OCP exclusively employed vector control through the treatment of breeding sites with larvicides, in efforts to combat disease transmission (Boatin, 2008). The OCP incorporated MDA into their approach following the free donation of ivermectin by Merck in 1987 (Taylor et al., 2010a). Combined, the transmission cycle was interrupted 14 years after the initiation of the OCP (WHO, 2019). By the end of the OCP in 2002, 600,000 cases of blindness had been prevented and 18 million children were born free from the risk of disease or blindness resulting from onchocerciasis (WHO, 2018). Meanwhile, with some countries remaining endemic for onchocerciasis, the African Programme for Onchocerciasis Control (APOC) was launched in 1995 to cover areas in sub-Saharan Africa, which pioneered the use of community directed treatment with ivermectin (CDTI) (Boatin, 2008). The Onchocerciasis Elimination Program for the Americas (OEAP) was later implemented in 1993 to target Latin America, with strategic bi-annual delivery of ivermectin to cover 85% of affected communities (Kim et al., 2015).

The WHO committed to the elimination of LF through the launch of the Global Programme to Eliminate Lymphatic Filariasis (GPELF) in 2000, following the declaration of LF as eradicable/potentially eradicable in 1997 (WHO 2014, 2015, 2018). This is the largest drug-based elimination program ever attempted, with an estimated 4.4 billion treatments distributed across 56 endemic countries, to target elimination by 2020 (WHO 2014, 2015, 2018). The programme owes its success to the donation of anthelmintic drugs from pharmaceutical companies, and the use of rapid diagnostic tests (RDT) to simplify LF detection to establish regions requiring MDA intervention (Ottesen, 1998). 3 phases

constitute the GPELF; the mapping of regions with active LF transmission, the blockade of transmission with annual rounds of MDA, and the verification that disease transmission does not recur. The program has proven success, with a 46% reduction in the number of people at risk of infection between 2000 and 2012. By the end of 2012, 46 countries had entered the post-MDA surveillance phase and to date, 15 countries have declared LF elimination (WHO, 2019).

1.17. Mass Drug Administration regimens

Due to the longevity of fecund adult worms, MDA is required annually or bi-annually for 5-6 years (LF) or twelve years (onchocerciasis) with effective geographic coverage to ensure transmission is blocked, and microfilarial reservoirs do not rebound (Ottesen, 1998, Verver et al., 2018).

Three drugs are used throughout the MDA programmes: IVM, donated by Merck; DEC, donated by Eisai; and ABZ, donated by GlaxoSmithKline (Tisch et al., 2005). IVM is the sole drug used in onchocerciasis programmes, whereas DEC or IVM in combination with ABZ are deployed through the LF programmes, dependent on areas of co-infection with onchocerciasis and/or loiasis.

1.18. Research and development of new anti-filarial drugs

There is renewed investment from major philanthropic agencies (e.g. Bill and Melinda Gates Foundation, Department for International Development) to support the development and implementation of new tools, including macrofilaricidal drugs, to target LF and onchocerciasis for elimination as a public health problem in line with the 2030 Sustainable Development Goals. New tools, including new drugs, are thought to be necessary to achieve global elimination of human filarial disease. Many specific, multi-factoral issues and caveats to achieving elimination with existing microfilaricide MDA include: development of IVM drug resistance (evidenced in onchocerciasis), loiasis SAE and the associated repercussions of

reduced community acceptability to MDA, 'treatment fatigue' to protracted MDA, especially after additional health benefits are no longer experienced, the breakdown of community drug distribution strategies, civil unrest, cross border issues and hard-to-reach communities (for instance, Yanomami Amazonian nomadic tribes) (Botto et al., 2016).

For veterinary dirofilariasis, the emergence of ML resistance jeopardises the standard approach of ML-based prophylaxis (Wolstenholme et al., 2015, Bourguinat et al., 2017). Further, the side-effects associated with melarsomine and the lack of any indicated cure of feline heartworm disease means that new approaches are also urgently required in the control and treatment of dirofilariasis.

1.19. Novel short-course macrofilaricides

Strategies to develop new macrofilaricides generally falls into one of two approaches: 1) candidates that are directly toxic to filarial nematodes via targeting of filarial macromolecules and pathways or 2) candidates that target *Wolbachia*-specific essential gene products, emulating the sterilising activity of DOX. For both approaches, to be a solution to accelerating global elimination of LF and onchocerciasis, candidates need to fulfil a strict set of guidelines known as the macrofilaricide target candidate profile (TCP). Most criteria are, as with the development of any new chemical entity drug, related to safety toxicology, drug metabolism and pharmacokinetics. The macrofilaricide TCP also considers specific requirements for suitable deployment to achieve filarial elimination in resource poor settings. These include: oral (temperature stable) formulation, efficacy after ≤ 7 days treatment administration, a high $>70\%$ macrofilaricidal activity, avoidance of treatment-associated inflammatory side effects and appropriate safety to administer in children and pregnant women (Bakowski and McNamara, 2019).

1.20. Direct-acting macrofilaricides

The pharmacopeia of registered human drugs and specific veterinary anthelmintics have been evaluated pre-clinically. Potential 'low-hanging fruits' of drugs with pre-existing safety pharmacology data with activity against filariae *in vivo* and/or *in vitro* currently include: an oral reformulation of FBZ, oxfendazole, a veterinary BZ, which is the active metabolite of fenbendazole, auranofin, a rheumatoid arthritis drug, emodepside, a veterinary ion channel antagonist anthelmintic and imatinib (Glivec) an anti-cancer drug (Bulman et al., 2015, Fischer et al., 2019, Sjoberg et al., 2019, O'Connell et al., 2015). The oral formulation of FBZ has recently been discontinued due to poor efficacy and selective toxicity, whilst emodepside, oxfendazole and imatinib are currently entering phase II proof-of-concept trials as filarial indications.

1.21. Novel anti-*Wolbachia* drugs

The Anti-*Wolbachia* drug consortium (A-WOL) was launched at the Liverpool School of Tropical Medicine in 2007, with the objective of developing an oral short-course drug specifically targeting *Wolbachia*. Formed as a consequence of the barriers encountered with doxycycline, the AWOL drug discovery programme aimed to find, or develop, drugs that specifically target *Wolbachia*, to initiate a slow, safe death of adult worms or permanent sterilisation, after one 7-day oral treatment regimen. Any potential candidates had to retain a high safety profile with onchocerciasis and *L. loa* co-infected individuals, in addition to being amenable in resource limited settings (Bakowski and McNamara, 2019). Over 2 million compounds from pharmaceutical diversity compound libraries have been screened against insect *Wolbachia* using high throughput technologies. For this, *Aedes albopictus* C6/36 cells naturally devoid of *Wolbachia*, were artificially infected with *A. albopictus* *Wolbachia* (wAIB) and exposed to chemical libraries for 9 days, before being qPCR processing to assess activity

against *Wolbachia* (Johnston et al., 2014). Despite screening the complete human pharmacopoeia, the process was time consuming, labour intensive and lacked throughput.

To increase the screening throughput and capacity, the Operetta high-content automated imaging system was developed for use as screening platform (Clare et al., 2015). Here, *Wolbachia* infected C6/36 cells were incubated with compounds and SYTO11 viability dye for 7 days and imaged using the Operetta to calculate the percentage reduction of *Wolbachia* infected cells. This allowed for potential hits to be identified using a ‘traffic light system’, whereby compounds reducing the number of *Wolbachia* infected cells by >90% were classified as potent hits (green), those reducing numbers by 50-90% considered moderate hits (amber) and those with no activity, or exhibiting toxicity, could be screened out (red). The throughput was further industrialised and automated in collaboration with Astra Zeneca, whereby whole 384 culture well plates could be scanned for *Wolbachia* specific fluorescence, simultaneously.

At this point, promising candidates were then triaged for activity against nematode *Wolbachia*. Due to the lack of a robust *in vitro* model of the appropriate adult stage, studies were instead carried out on the more accessible mf stages, which are easier to maintain in culture. This allowed for candidates that could not penetrate the nematode cuticle to be blocked from further progression. Successful candidates at this stage were then progressed directly into *in vivo* pre-clinical proof-of-concept testing.

As a result of A-WOL screening, several compounds have been identified with significant activity against *Wolbachia*. Some of these have been re-purposed antibiotics, for example minocycline, a derivative of doxycycline, which has shown superior activity at equivalent doses to doxycycline (Sharma et al., 2016) Rifampicin, an approved antibiotic in the treatment of tuberculosis (TB) has also been evaluated to have significant activity against *Wolbachia*, however only at high doses to achieve ideal drug exposure as determined

through pharmacokinetic-pharmacodynamic (PKPD) modelling studies (Aljayoussi et al., 2017), to achieve the necessary *Wolbachia* depletion over 7 days. Others have been developed through a rational medicinal chemistry approach starting from ‘hit’ clusters of related molecules identified in cell-based phenotypic screening (Johnston et al., 2017). Of these, AWZ1066S, based on an azaquinazoline scaffold, has been shown to achieve superior *Wolbachia* reductions in days of *in vivo* dosing (Hong et al., 2019). AWZ1066 has now entered formal preclinical development with first-in-human phase I testing scheduled for 2020. The most advanced discovery output from the AWOL programme has been the development of ABBV-4083 (‘TylAMac’). This is an analogue of the veterinary antibiotic drug Tylosin A, in which the chemical structure has been altered to improve oral bioavailability. TylAMac exhibits superior anti-*Wolbachia* activity in comparison to DOX and can reduce *Wolbachia* by between 90-99.9% based on 7-14 day dose regimens. TylAMac has been further successful in drug safety trials and is now currently in phase II clinical trials (Taylor et al., 2019, Hübner et al., 2019, von Geldern et al., 2019).

The success of these compounds into the clinic necessitates scrutiny in phase I-III clinical trials. Due to this, several early-stage hits identified from screening are still undergoing early pre-clinical development to act as ‘back-ups’ and alternative treatments in the bid to eliminate filarial disease. Some of these back-ups may also be appropriate as veterinary *Dirofilaria* indications.

1.22. *In vitro* filariasis culture systems and their use in drug screening

Filarial *in vitro* cultures can be categorised as: 1. Growth cultures of filarial mammalian stage larvae, 2. adult filarial cultures and 3. mf-specific cultures. *B. malayi*, *L. loa*, *M. perstans*, *O. volvulus* and *D. immitis* can be cultured from the vector-stage L3 to undergo L3-L4 moulting with relatively high success (over 50% moulting rate) in relatively simple, serum

supplemented media (Lok et al., 1984b, Falcone et al., 1996, Abraham et al., 1987, Devaney, 1985, Lok et al., 1984a, Zofou et al., 2018). The relative ease with which L3 can be cultured to grow and moult into L4 *in vitro* has been exploited in direct-acting nematocidal drug screening studies (Gloeckner et al., 2010, Evans et al., 2013). Whilst applying drug testing to the L3-L4 stage is relevant for heartworm preventative drug discovery, they are less useful in discerning macrofilaricidal activities without necessary corroboration against adult stage parasites.

Addition of mammalian cell lines into larval cultures (so called 'feeder cell' layers) can further support the onward development of L4 larvae, with records of successful development reported through to adult stages of *B. malayi*, *M. perstans* and *O. volvulus*. A variety of mammalian cell lines have been assessed including lines derived from kidney cells, fibroblasts, skeletal muscle cells, endothelial cells and leukocytes. However, the reproducibility of L3-adult filarial *in vitro* culture systems is debatable. Considering *B. malayi*, some of the first published studies in this area, (Riberu et al., 1990) used culture vessels with 10% human serum in attempts to achieve the L3-L4 moult. It was concluded that by using this system, 85% of L3 larvae could reach the fecund adult stage. However, this has never been reproduced, presumably due to the variability and complexity of human serum which could provide different signals to initiate the moults depending on the donor. The donor source was never declared, speculating whether the serum was recovered from an infected individual, which could have significantly improved the developmental success due the genetic propensity amongst other factors. In 1994, different medium supplements were evaluated to enhance the moulting process (Smillie et al., 1994). L3 stage parasites were initially cultured in simple media (NCTC-135 + Iscove's Dulbecco's medium) with 10-15% of one of the following: Bovine Albumin Fraction, Foetal Bovine Serum, pooled human serum from hospital patients and finally, Human Serum collected from a single individual. The results suggested larvae cultured in human serum from a single individual, human serum

from hospital patients and FBS attempted the moult to L4 stage, however only cultures with serum from a single individual attempted a further moult. The study further showed that up to 28 days of culture, the larvae were comparable to that observed in jirds, however after this stage their development was incomparable. Furthermore, this study suggested that optimal growth and development of the parasites *in vitro* may be dependent on certain, unidentified components of human serum, similar to the Riberu study. In contrast to the work carried out by Riberu and Smillie, one group attempted co-culture with Human Dermal Fibroblasts and T-cell lines appeared to achieve a successful moult (69%) to the L4 stage with a further 2.6% progressing to the young adult stage (Falcone *et al*, 1995), suggesting cells of lymphoid origin – enriched where the parasites naturally reside – are beneficial in the moulting process. This is further evident in studies with *O. volvulus* (Voronin *et al.*, 2019), whereby L3 moult to L4 with 30-60% success in the presence of peripheral blood mononuclear cell (PBMC) co-cultures.

The most reliable *in vitro* systems applied in drug screening use isolated mf or adult parasites from either naturally or experimentally infected animal hosts. For macrofilaricidal drug development, testing against freshly derived *ex vivo* adult stages is most relevant, although large differences exist in the longevity of adults in culture, which may limit the ability to accurately assess potential macrofilaricidal effects of *Wolbachia* depleting agents and/or slow-acting drugs. One of the most successful examples of *in vitro* filarial culture is that of the bovine onchocerca parasite, *Onchocerca gutturosa*. Here, male *O. gutturosa* can survive for up to 6 months on a monkey kidney cell feeder layer. This male adult *Onchocerca* culture system has been used to screen drugs, albeit with low throughput (Townson *et al.*, 1987, Townson, 1988, Townson *et al.*, 1986).

Culture of female stage parasites has the advantage of examining embryotoxic treatment effects on the reproductive system. However, unlike male worms retrieved from cattle

Onchocerca, the culture of female stages is mainly limited to short-term experiments of 5 days or less due to an inability to maintain female worms for long periods of time. In terms of brugian filariasis, the majority of adult cultures have focused on media-only systems, predominantly using RPMI with FBS, in which parasites are cultured between 24 and 120 hours in order to evaluate the effects of rapid direct-acting macrofilaricides, nanoparticle formulations or gene expression (Marcellino et al., 2012, O'Neill et al., 2016, Ballesteros et al., 2016). Although these efforts have been seemingly effective, parameters evaluating 'in vitro' parasite fitness have centred around motility and survival assessments, which are often subjective to the investigator. In efforts to combat this subjectivity and to also increase the throughput of drug screens, imaging platforms and computer applications have been developed to automate this process and increase the reliability of scoring (Buckingham et al., 2014, Partridge et al., 2018, Marcellino et al., 2012, Storey et al., 2014).

To further incorporate quantitative assessments into analyses, some studies have employed biochemical readouts, such as the MTT 3-(4,5-dimethylthiazol-2-yl)-2,5-diphenyltetrazolium bromide (MTT assay) to assess parasite metabolic activity as an output of viability. This assay is dependent on the concept that in viable cells NAD(P)H-dependant cellular reductase enzymes are able to reduce the yellow tetrazolium MTT 3-(4,5-dimethylthiazol-2-yl)-2-5-diphenyltetrazolium dye to a purple formazan product, which can then be quantified using colorimetric plate readers, and can thus evaluate direct-acting drug activity (Comley et al., 1989).

Lacking from current *in vitro* systems, both adult and larval, is the evaluation into the stability of endosymbiont *Wolbachia* populations in cultured parasites. Additionally, in all systems scrutinised, comparison with an appropriate *in vivo* control has not been documented, raising uncertainties of the utility in drug screening experiments. For instance, current *in vitro* systems may be prone to a higher than desirable 'false hit' rate because viability of parasites and stress responses induced *ex vivo* may influence sensitivity to test compounds. For

example, Geary et al (Ballesteros et al., 2016) described the dysregulation of several genes encoding stress indicators after retrieval from jirds, which remained over 5 days of *in vitro* culture. Furthermore, an induction of autophagy due to physiological stress may increase sensitivity to *Wolbachia* depletion, as filarial *Wolbachia* populations are known to be regulated by autophagic processes (Voronin et al., 2012). Combined, these phenomena can result in parasites that do not accurately replicate the physiological conditions at the infection site in a host and consequently, drug screening ‘hits’ identified through these *in vitro* systems may lead to failure of translation in *in vivo* studies due to artefactual sensitivities both to direct acting and anti-*Wolbachia* compounds *in vitro*.

1.23. *In vivo* models of filariasis for drug screening

Because there is currently no reliable culture system to generate adult filariae from infectious stage larvae at scale *in vitro*, animal models are heavily relied upon for drug efficacy testing. Such animal models are laborious, time consuming and slow the overall translation of preclinical candidates.

Despite constituting only 10% of filarial infection cases, *B. malayi* is the most studied causative nematode of LF due to its ability to be maintained under laboratory conditions. Related filarial species naturally infecting animals; *B. pahangi* infecting cats, *L. sigmodontis* infecting cotton rats, and *A. viteae* infecting rodents, are also studied *in vivo* and serve as models to inform and predict human filariae research.

Successful transmission of sub-periodic *B. malayi* and *B. pahangi* were initially confined exclusively to cats, a natural host, as well as dogs and three species of monkey; *Macaca irus*, *M. nemestrina* and *M. rhesus* (Denham and Fletcher, 1987, Edeson et al., 1960). These models however, were difficult to manage within a laboratory setting and unsuitable to maintain in large numbers for experimentation. As an alternative, filariae naturally permissive in rodents; *L. sigmodontis*, infecting cotton rats (Schneider et al., 1968), and *A.*

vitae, infecting gerbils, have been used as general filariae models to study the disease in a more facile manner. Additionally, the use of small rodents to establish human filariae have been explored, albeit with limited success. Initial models were developed to mimic a human infection, whereby parasites were injected into animals subcutaneously in attempts to reach the lymphatics. Although a larger rodent, *B. malayi* infection in ferrets (*mustela putorius furo*) have been determined to closely mirror that of humans, whereby adults are located primarily in the lymphatics, in addition to lower numbers in the heart and skin 5-8 months post-subcutaneous infection (Crandall et al., 1987, Crandall et al., 1982, Jackson-Thompson et al., 2018). Ferrets also develop pathologies, for example lymphangiectasia, lymphadenopathy and lymphatic obstruction, as observed in humans, and can hence serve as a suitable model to evaluate these in further detail. Experimentation into small rodent models was initially undertaken by Edenson and Warton in white mice and guinea pigs. However, infections failed to establish in all animals (Edeson et al., 1960). Rabbits also failed to establish *Brugia* infections in studies carried out by Ahmed et al, 1967 (Ahmed, 1967). Further attempts were conducted across an array of rodent species. Of these, golden hamsters developed patent infections with a 50% success rate (Malone and Thompson, 1975), although only very low numbers of parasites were yielded from the heart alone. Infections of limited success were also observed in cotton rats, whereby earlier larval stages were retrieved from the skin and subcutaneous tissues, before migrating to the heart and pulmonary arteries in the latter stages of infection. Here, parasites were also evident in the lymph glands and testes, although failed to develop patency (Ramachandran and Pacheco, 1965). *Mastomys*, multimammate rodents, represent a more successful model for *Brugia* infections. In *M. coucha* and *M. natalensis*, parasite tropism follows the same trajectory as previously described, with L3-L4 migrating through the subcutaneous tissue, before reaching the heart, lungs and testes at adult stage. On average, 11-21% of the initial inoculum develop are able to survive for up to 442 days post-infection, with up to 90% of this population

developing a stable patency (Sänger et al., 1981), however the persistence of this patency is highly variable. The best rodent model, and now the most widely accepted model of *Brugia* infection, is the *Meriones unguilatus* model, more commonly referred to as the Mongolian jird. In this model, adult parasites, of which up to 70% develop extended patency (Ash and Riley, 1970), primarily inhabit the lymphatic vasculature and spermatic cords, as well as residing in the heart and lungs. Infection is more profound in males than females, and thus this sex has been selected for the model.

Despite being the best rodent model for lymphatic dwelling filariae infection, a prominent drawback prevails regarding parasite excision. Due to the subsequent residence of parasites in multiple tissues and organs, parasite retrieval proves challenging, particularly for efficacy testing, in which a high yield of parasites is required. To combat this issue, and thus increase the development of pre-clinical *in vivo* testing, intraperitoneal (IP) infections were conducted to confine parasites for more accurate, and facile recoveries in large numbers (McCall et al., 1973, Mutafchiev et al., 2014). Intraperitoneal (ip) infections were trialled in both jirds and *Mastomys* species, with jirds retaining similar parasitaemias to that of subcutaneous (sc) infections, whereas ip infections failed in *Mastomys*.

Another deficiency of the jird model is that reagents required for the identification of immunoglobins and other immune cell subsets are not readily available, as is also observed in the ferret model. Instead, these components are generally tailored to murine models. However filarial infections in immunocompetent mice have very limited success, and do not develop microfilariaemias (Nelson et al., 1991b). As an alternative, the severe-combined immunodeficient (SCID) mouse model was evaluated, following published research confirming brugian infection can be established in T-lymphocyte immunodeficient mutant nude mice. It was thus determined that the SCID mouse, lacking functional B- and T-lymphocytes, allowed for the development of fully patent adults from L3 stage, both in

subcutaneous and intraperitoneal infections. This SCID model has since been validated for use as a pre-clinical model for *in vivo* drug efficacy studies (Halliday et al., 2014) with the goal to find a novel drug to treat the adult stage to accelerate filariasis elimination targets.

The SCID mouse model has also proved successful in the subcutaneous implantation of the cattle *Onchocerca*, *O. ochengi*, for pre-clinical screening (Halliday et al., 2014). This was established due to a lack of facile models, and concerns over the translation of results conducted in the jird with *Brugia* to human clinical trials targeting *O. volvulus*. This was primarily due to differences in the parasite biology, which has hindered the development of macrofilaricides (Mackenzie and Geary, 2011, Awadzi, 2003). Prior to this, attempts of developing small rodent models of onchocerciasis were limited to larval stage implantations, whereby L3 stages were implanted under the skin within micro-chambers to achieve the moult to L4 stage, under the brief exposure of screening compounds (Taylor et al., 1994). The only other models supporting the full life cycle were in higher mammals, primarily in cattle and non-human primates (Eberhard et al., 1995, Morris et al., 2013, Trees et al., 2000).

Higher mammals have also been heavily relied upon for *L. loa* parasite production and pre-clinical studies. The naturally infected drill, *Mandrillus leucophaeus*, and splenectomised baboons as a surrogate, are the typical models of *L. loa* (Duke, 1980, Orihel and Eberhard, 1985, Wanji et al., 2015, Wanji et al., 2017), although they carry a very low throughput and are difficult to maintain within a laboratory. Recently, a murine model has been developed using compound immunodeficient, lymphogenic mice lacking the common gamma-chain (γ c). Here, parasites develop into fecund adult infections from the subcutaneous infection of larval stages (Pionnier et al., 2019). Using the same model, researchers were also able to optimise and validate, using a reference microfilaricide, as a stage-specific (mf) system to screen any potential filarial candidates with having no activity against the *L. loa* mf stage, so as not to risk the induction of SADEs.

In terms of veterinary dirofilariasis, there are currently no rodent, or validated *in vitro* models, available and so experimentation is confined exclusively to laboratory infected cats and dogs. Experiments are therefore timely, highly expensive, and very low throughput. Welfare issues with experimentally infected dogs are also common, as parasite burdens in these laboratory maintained animals are usually >10-fold higher than those observed in naturally infected dogs (Chiara Lucchetti, personal communication, University of Parma, Italy).

In conclusion, present development of new drugs targeting adult stages very heavily relies on the use of animals to determine drug effects at an early stage of the drug development process. Such animal models are laborious, time consuming and slow the overall translation of preclinical candidates. In the case of LF, a variety of small rodent models exist supporting adult development and long-term survival. In the case of onchocerciasis, only relatively short-term implantations of life cycle stages into rodents are routinely used in drug screening. For both onchocerciasis and loiasis, screening of novel therapeutics has traditionally relied on higher mammals.

1.24. The 3Rs principles applied to anti-filarial drug discovery

The National Centre for the Reduction, Refinement and Replacement of animals in scientific research (NC3Rs) focuses on performing more humane animal research by using methods which avoid or replace animal usage, minimise the numbers of animals used per experiment, and utilising approaches which minimise animal suffering and improve welfare.

Many issues prevail concerning animal usage within anti-filarial drug screening. As discussed, the life-cycle is fully reliant on animal models; jirds for the life cycle maintenance for mf production for *in vitro* assays and mosquito feeds and jirds to generate adults for *in vivo* pre-clinical screens.

Although the current screening pipeline utilises mf to determine drug activity against a whole nematode as opposed to an insect cell line alone, discrepancies in the translation to *in vivo* outcomes are apparent. Whilst testing compounds against mf or adult males is currently the only reliable means of scrutinising long-term drug effects against filariae *in vitro*, and good for the prioritisation of candidates, they are not necessarily the most appropriate. *Wolbachia* titres are considerably lower, and more stable, in mf and male stages than in the female target, thus making them more susceptible to drug treatments. Furthermore, differences in bioaccumulation of drugs in mf and adult males may vary compared to females. *Wolbachia* also reside in reproductive tissues within the female, presenting another compartment which may present a challenge in terms of drug permeability. As a result, compounds providing encouraging data in current *in vitro* systems can be prematurely progressed to the pre-clinical stage and fail, resulting in the use of large numbers of animals, which could be reduced with a more appropriate, robust *in vitro* model.

There are currently no consistent means of determining *in vivo* drug efficacy until the end of study, therefore requiring animal sacrifice. The only method which can be used is the invasive sampling of mf within the peritoneal cavity to determine if drugs have been effective in blocking embryogenesis and inducing sterility in female worms. However, this also requires animals to be anaesthetised. As efficacy cannot be determined longitudinally, multiple animal groups are required to assess different treatment and washout regimes. This slows the progression of candidates and adds further costs to *in vivo* studies.

To summarise, there are several areas within the field of anti-filarial drug screening in which the 3Rs principles can be incorporated to improve experimental outcomes, whilst refining, reducing, and potentially replacing the use of animals for this purpose.

1.25. Thesis aims

- **Reduction**

With the overall aim of reducing the number of animals used in filarial drug development, chapter 2 will aim to develop a larval *in vitro* model able to support parasite development to enable drug testing against these larval stages to reduce animal testing. Chapter 3 will define whether using immunodeficient mouse models can offer any significant benefit for long-term *B. malayi* infections in comparison to gerbils, to reduce the number of rodents initially required for infection. Chapter 3 will also focus on the development of stage-specific *in vitro* adult cultures, and assessing whether the addition of different feeder cell layers can enhance parasite survival. These *in vitro* cultured parasites will be robustly assessed using an array of metabolic and molecular techniques to accurately compare against parasites excised from parallel *in vivo* experiments. This *in vitro* system will then be initially validated for use as a drug model, utilising reference 'gold-standard' anti-*Wolbachia* and direct-acting compounds, before evaluating the efficacy of novel therapeutics, to reduce the number of animals utilised for pre-clinical testing against adult stage parasites without prior *in vitro* testing against this life-cycle stage.

- **Refinement**

Chapters 4 and 5 will focus on the optimisation of longitudinal, non-invasive bio-imaging tools for use as prognostic indicators of drug efficacy *in vivo* to refine animal usage during pre-clinical drug development stages. More specifically, chapter 4 will evaluate the use of ultrasonography to visualise adult stage *B. malayi* to discern whether animals can be grouped based on infection intensity prior to drug testing, and whether ultrasonography can be used to predict direct-acting treatment efficacy against adult stage parasites. Chapter 5 will

optimise the fluorescent staining *B. malayi* microfilariae life cycle stages, and evaluate the persistence of fluorescent signals using the Perkin Elmer *in vivo* imaging system (IVIS), before drug challenge studies begin to determine whether drug efficacy can be evaluated using these tools.

- **Replacement**

Different *in vitro* systems, using an array of cell types and media, will be evaluated in chapter 2 in attempts to support the development of *B. malayi* larvae from mosquitoes through to adults capable of releasing microfilariae, negating the need for a rodent host. *In vitro* reared parasites will be compared against parallel *in vivo* parasites and evaluated using molecular and cellular techniques. A similar system will also be optimised to support the initial development of *Dirofilariae immitis*.

Chapter 2: Development of a larval filarial growth culture
system

2.1. Abstract

The heavy reliance on animal models within filarial drug development is primarily due to the lack of an *in vitro* system capable of supporting the development from larval stages through to fecund adults. Although some attempts have been made to culture larval stages, reproducibility is very low and parasites have not been robustly analysed to ensure *in vivo* likeness. This chapter evaluates the suitability of different feeder cell and cell-free cultures to support the development of L3 *Brugia malayi*, using multiple molecular analyses to confirm *in vitro* 'fitness' against tandem *in vivo* infections. Similar systems were also set-up to evaluate the *in vitro* development of the veterinary filariae, *Dirofilaria immitis*, with the over-arching aim of reducing, and potentially replacing, the need for animals in maintaining the filarial life cycles, and for larval drug screening purposes. It was found that feeder cells offered improvements in the culture longevity of both *B. malayi* and *D. immitis*, compared to cell-free systems. Cultured *B. malayi* were comparable to those extracted from mice for up to 8 days, however beyond this point parasite health deteriorated across all culture conditions and were no longer comparable to those *in vivo* of the same time-frame. More encouragingly, cell cultures were able to support the development of *D. immitis* larvae *in vitro* for upwards of 38 days with a 30% survival rate. These data conclude that whilst it remains unattainable to achieve the whole life-cycle from larval mosquito stages to fecund adults *in vitro*, there is potential to conduct *in vitro* larval stage drug testing, which would significantly reduce the number of animals for this purpose.

2.2. Introduction

The inability to generate the filarial life-cycle *in vitro* results in the heavy reliance on rodent models, such as mice and gerbils, to produce different life-cycle stages for experimental purposes and pre-clinical drug screening (Halliday et al., 2014). Furthermore, the lack of a functional larval-specific *in vitro* model hinders the progression of potential prophylactic treatments, particularly in the context of the veterinary filariae, *Dirofilariae immitis*. The development of an *in vitro* model suitable to sustain the development to fecund adults, or at least for up to 28 days to ensure robust analysis of any potential anti-*Wolbachia* drug candidates, could potentially obviate the need for such animal models.

Several researchers have attempted to re-create the first moulting stage (L3-L4) *in vitro*, some of which have been successful enough to support development to adults, which were capable of releasing mf (Riberu et al., 1990). One significant issue prevails however, in that experiments cannot be repeated with equivocal success rates. The predominant reason for this is due to the use of human serum, often used in high concentrations, which contains a multitude of factors which may support parasite development, and can significantly differ between batch, individual, infection status, and medical history. This was further exemplified in a study conducted by Smillie et al, which defined significantly different success rates between commercially obtained serum, pooled serum from hospital patients, serum isolated from a single individual (Smillie et al., 1994).

Cell feeder layers have been well documented in the support of parasite development in other filarial species, for example in the maintenance and development of *Onchocerca* (Townson, 1988, Voronin et al., 2019), and more recently, *Mansonella* (Njouendou et al., 2017) and *Loa loa* (Zofou et al., 2018) larval stages. This has rendered monkey kidney cells (LLCMK2) as the 'gold standard' in supporting parasite development *in vitro*. Other cell types

have also been utilised in the context of *Brugian* cultures, including human dermal fibroblasts and Jurkat T cell leukemia cell lines, monkey kidney cells (Falcone et al., 1995, Falcone et al., 1996), and peripheral blood mononuclear cells. However, despite promoting moulting, all cell systems required serum supplementation, often from a human source, again creating issues surrounding the reproducibility of these cultures.

Although culture attempts are less documented with *Dirofilariae*, feeder cells have also been employed to promote moulting, for example co-culture with dog sarcoma cell lines (Devaney, 1985, Abraham et al., 1987).

Appropriate tandem *in vivo* controls are lacking from the majority of reported cultured systems for *Brugia* and *Dirofilariae* species, thus highlighting whether these systems are translational to an *in vivo* setting. Furthermore, the parameters evaluating moulting efficiency are often subject to the investigator, for example the counting of cast cuticles in culture, or do not robustly analyse parasite 'fitness' by means of biochemical analyses or assessing *Wolbachia* loads, known to be essential for the development and survival of these parasites (McGarry et al., 2004b, Taylor et al., 2010b). Additionally, none of the systems described have been applied, or adequately validated for downstream applications as an *in vitro* drug model have not been successful in supporting the full life-cycle of filariae *in vitro*. Thus, animal models are still heavily relied upon for the generation of all life cycle stages and for larval drug screening purposes, highlighting the urgency for a robust *in vitro* model that allows for animal usage to be significantly reduced, or replaced.

2.3. Scientific and 3Rs Aims

- The development of an *in vitro* system to generate adult worms (at least 28 days old) from mosquito stage L3 parasites to replace the need for rodent models to generate adult stage parasites.
- Development of an *in vitro* larval growth model system suitable for assessing direct and anti-*Wolbachia* prophylactic drug candidates for veterinary indications (heartworm), reducing and replacing the need for animals as larval drug screening models.

2.4. Materials and Methods

2.4.1. Animals

Interleukin four receptor alpha (IL-4R α)^{-/-}IL-5^{-/-} BALB/c breeding pairs were a gift from Achim Hoerauf, University Hospital, Bonn. Male CB.17 Severe-Combined Immuno Deficient (SCID) mice were purchased from Charles River, UK. *Meriones unguiculatus* (Mongolian gerbils; jirds) breeding pairs were purchased from Charles River, Europe. Animal stocks were maintained under specific pathogen-free (SPF) conditions at the biomedical services unit (BSU), University of Liverpool, Liverpool, UK. Male IL-4R α ^{-/-}IL-5^{-/-} BALB/c mice were 6-8 weeks old and weighed 18-24 g at start of experiments. Male gerbils were 4–6 months old and weighed 80–100 g at start of experiments. All experiments were approved by the ethical committees of the University of Liverpool and Liverpool School of Tropical Medicine (LSTM) and conducted under Home Office Animals (Scientific Procedures) Act 1986 (UK) requirements.

2.4.2. *Brugia malayi* parasite maintenance

The life cycle of *B. malayi* was maintained in mosquitoes and Mongolian gerbils. For *B. malayi* larvae (*BmL3*) generation, microfilariae (mf) were collected from infected gerbils via catheterisation. For this, Mongolian gerbils were anaesthetized with isoflurane and subjected to peritoneal washes with RPMI 1640 media (ThermoFisher Scientific) to harvest mf. Mf were then purified using PD10 column size exclusion chromatography (Amersham), enumerated by microscopy and mixed with human blood to a final concentration of 15–20,000 mf/ml. Mf were then fed to female *Aedes aegypti* mosquitoes through an artificial membrane feeder (Hemotek). Blood fed mosquitoes were reared for 14 days with daily sugar-water feeding to allow development to *BmL3* stage. At day 14, *BmL3* were collected from infected mosquitoes by crushing and concentration using a Baermann's apparatus and Roswell Park Memorial Institute (RPMI) media (Sigma).

2.4.3. *In vitro* culture of BmL3 stage parasites

The fraction from the crush containing L3 parasites was then transferred into a petri-dish. Highly motile L3 were then picked using a pipette and transferred into a 15ml falcon tube containing fresh, pre-warmed RPMI media with penicillin-streptomycin to remove any remaining mosquito debris. Tubes were then incubated in a water bath set to 37°C and parasites were left for 20 minutes to allow gravitation to the bottom of the tube. Once parasites had settled, they were removed and placed into a tube with fresh RPMI media and the process was repeated twice to thoroughly wash parasites. Following the wash stages, parasites were plated into 12 well plates containing 3ml RPMI media + 10% Heat inactivated Foetal Bovine Serum (HI FBS; Sigma) at a density of ≤ 50 parasites/well. Plates were incubated overnight at 37 °C with 5% CO₂. Following overnight incubation, parasites that had died or deteriorated over night were removed and discarded. Those that remained highly motile were selected for culture and plated at a density of 20 L3/well onto each culture condition (n=20/well). Media was changed every 3 days. Cultured parasites were taken for analysis at day 8, after the L3-L4 should have been completed, and day 14 as a final endpoint.

2.4.4. Cell culture

Human Embryonic Kidney (HEK) 293 cell line: HEK cells were purchased from Lonza and cultured at 37°C with 5% CO₂ in Dulbecco's Modified Eagle Medium (DMEM) supplemented with 2mM L-glutamine, 10% heat-inactivated FBS (Sigma), 100 U/ml penicillin, 100 µg/ml streptomycin (Pen/Strep, Gibco), and 1 mM Pyruvate. Cells were seeded at a density of 3000-5000 cells/cm² in 75 cm² (T-75) cell culture treated flasks.

Lilly Laboratories Cell Monkey Kidney 2 (LLCMK2) cell line: The rhesus monkey kidney cell lines were a kind gift from Dr Simon Townson and maintained in Minimum Essential Media (MEM) with 10% HI FBS, 100 U/ml penicillin and 100 µg/ml streptomycin. Cells were seeded

at a density of $2-4 \times 10^4$ cells/cm² in T-75 cell culture treated flasks and were split at 70-80% confluency.

Lymphatic Endothelial Cell (HMVEC-dLyAd; LEC) line: LECs, a primary cell line derived from adult human dermal lymphatic microvascular endothelial cells, were purchased from Lonza and cultured at 37°C with 5% CO₂ in Microvascular Endothelial Cell Growth Medium-2 (EGM-2 MV) media. Media was composed of Endothelial Basal Media (EBM-2) supplemented with the EGM-2 MV SingleQuotes bullet kit (Lonza), to make up EGM-2 MV full media.

Madin-Darby Canine Kidney (MDCK) cell line: MDCKs, derived from the kidney tubule of adult Cocker Spaniels, were purchased from The European Collection of Authenticated Cell Cultures (ECACC) of Public Health England. Cells were cultured at 37°C with 5% CO₂ in Minimum Essential Eagle Media (MEM) with 10% HI FBS, 100 U/ml penicillin and 100 µg/ml streptomycin. Cells were seeded at a density of 3000-5000 cells/cm² in 75 cm² (T-75) cell culture treated flasks.

For passaging, all cell types were washed with sterile Phosphate Buffered Saline (Sigma), to ensure removal of any dead cells, and incubated for ≤5 minutes with 0.25% (w/v) trypsin-ethyldiaminetetraacetic acid (EDTA). Trypsin activity was neutralised by the addition of the equivalent volume of media, containing FBS. Cells were further detached mechanically, using a cell scraper (purchased), and centrifuged at 1500 x rpm for 10 minutes. The clear supernatant was removed and the cell-containing pellet was re-suspended in corresponding culture media, and counted with 0.4% trypan blue using a TC10 automated cell counter (Bio-Rad).

2.4.5. Parallel *in vivo* experiments

To ensure an appropriate *in vivo* control, male IL4Rα^{-/-}IL-5^{-/-} mice were infected via the intraperitoneal route with 150 L3 of the same batch used for *in vitro* culture. At the specific

time-points when *in vitro* cultured larvae were taken for analysis, mice were dissected to retrieve the same stage larvae for *in vivo* controls against cultured larvae for all analyses.

2.4.6. Motility and survival analyses

Parasites were examined for motility daily using a 4-score scale, based on a system originally devised by Rao and Well (Rao and Well, 2002). Those scoring 0 were considered immotile; those with a score of 1 displayed twitching motions of the head or tail; a score of 2 indicated slow sigmoidal motility; a score of 3 equated to moderate sigmoidal motility and finally, a score of 4 indicated rapid sigmoidal motility, as observed when freshly isolated from *in vivo*.

2.4.7. Length measurement analysis

To determine growth, an indicator of progression to the next life cycle stage, 6-10 larvae per condition were removed from the culture. Larvae were then transferred into fresh PBS and cooled at 4°C for 20 minutes to reduce motility, in order to improve accuracy of length assessments. Individual larvae were then imaged using a Zeiss LSM880 confocal microscope using transmitted light. Images were then processed in ImageJ to calculate length.

2.4.8. MTT viability assessments

To assess parasite viability quantitatively at the day 14 end-point, the colorimetric 3-(4,5-dimethylthiazol-2-yl)-2,5-diphenyl tetrazolium bromide (MTT) assay was employed. The MTT assay is based on the concept that cellular NADPH-dependent oxidoreductase enzymes in living tissues reduce the MTT yellow dye to the insoluble purple formazan product, which can then be quantified using a plate reader, to reflect the number of living cells. For this, parasites were removed from culture and washed in pre-warmed PBS. Parasites were grouped in numbers of 10 then transferred into separate wells of a 96 well plate and incubated with 5 mg/ml MTT (Sigma) in PBS for 2 hours at 37°C. Following incubation, parasites were washed in PBS and incubated for 1 hour with 100% Dimethyl Sulfoxide

(DMSO; Sigma) to solubilise the purple formazan product. The plate was then analysed using a fluorescent plate reader set at 450nm, including a primary shake step. Data were expressed as a percentage change in optical density readings from the *in vivo* control median.

2.4.9. DNA extractions

DNA extraction was performed on individual parasites using a Qiagen QIAmp DNA mini kit. Worms were transferred into Eppendorf tubes and incubated overnight at 56°C with ATL buffer and proteinase K to allow initial protein digestion. After incubation, ethanol (100%) was added to tubes and samples were subjected to two wash buffer stages with subsequent centrifugation steps at 13x100 rpm. DNA was then eluted with 50µl elution buffer and transferred to 96 well plates to be frozen for qPCR analysis.

2.4.10. Gene cloning and qPCR to determine *Wolbachia* titres

Plasmids, containing the inserts of amplified *B. malayi Wolbachia* (wBm) surface protein, were prepared and stored in glycerol stocks at -20°C for use as qPCR standards. For this, DNA was isolated from a single adult female worm using the QIAmp DNA mini kit loosely based on the 'tissue' protocol provided by Qiagen. Extracted DNA was then amplified with qPCR using the following primers:

- WSP-BamHI (5' GGA TXX GCT TCT TCA ATA GTG CT 3')
- WSP-HindIII (5' AAG CTT CGC TTG CAG TAC AAT AGT GE 3')

The PCR reaction mixture consisted of 1 µl of primers at a concentration of 300 nM, 12.5 µl Taq polymerase, 7 µl RNase free ultra-pure water and 1 µl extracted DNA. The PCR product was then ligated into the PCR 2.1 vector and cloned into TOP10 cells, using a standard TOPO TA cloning kit (Invitrogen). Sample plasmid DNA was then extracted from the cells using a QIAprep Spin Miniprep kit (Qiagen) and quantified using a Nanodrop. 10-fold dilutions were

then prepared between 100 pg/ml and 0.1 fg/ml (equivalent to approximately 2×10^7 to 2×10^1 copies) and stored at -20°C in glycerol until use.

For the quantitative PCR (qPCR), standards were diluted in a 7-fold series (from 1×10^7 to 10 copies/ μl). The following degenerate primers, designed to be internal to the cloned sequence, were used:

- WSP 420 (5' TGT TGG T(AG)T TGG T(GC)T TGG TG 3')
- WSP 583 (5' AAC CAA A(AG)T AGC GAG C(CT)C CA 3')

The PCR master reaction mix was constituted of 1x QuantiTect SYBR green PCR Master Mix, 3.0 mM MgCl_2 and 0.2 μM of each primer, made up to 14 μl ultra-pure water. 2 μl of standard/sample of DNA was added in duplicate to each tube. Samples were denatured for 15 minutes at 95°C , before amplification for 40 cycles at 94°C for 15 seconds and annealing at 60°C for 30 seconds, followed by an increase to 72°C for 30 seconds. Fluorescence data were collected during each cycle at 72°C . Melting curve analysis ranged between 60 and 95°C to confirm the presence of specific gene products and the absence of non-specific products. The thermocycler software generated a standard curve and the copy numbers in the starting templates were calculated by reference to this standard curve. Copy numbers were determined in duplicate and a mean taken of the results.

For data analysis, *Bm wsp* copy numbers were averaged and multiplied by the elution volume and divided by the volume of DNA sample added to the reaction mixture (2 μl). Data were represented graphically as \log_{10} of *Wolbachia* load per L3.

2.4.11. *Dirofilariae immitis* larval *in vitro* culture

L3 stages of the canine filariae, *Dirofilariae immitis*, were imported from the Filariasis Reagent Resource Centre (FR3) laboratories (Georgia, USA) via the Biodefense and Emerging Infections Research Resources Repository (BEI). Upon arrival, *DiL3* were warmed in a water

bath set to 37°C for approximately 30 minutes to allow parasites to regain motility. After this time, highly motile L3 were picked using a 1000 µl pipette and placed at a density of 10-20 / well into 12-well plates containing either an MDCK monolayer with 4 ml of EMEM, an LLCMK2 monolayer with 4 ml EMEM, or 4 ml EMEM alone. Survival and motility were scored daily and experiments were stopped when survival reached 50% for cell-free cultures (EMEM) and 30% for Di maintained on the MDCK and LLCMK2 feeder layers. 5-10 parasites were taken at baseline L3, 7 days, 12 days, 21 days and 39 days for length measurements.

2.4.12. Statistical analysis

Data were tested for normal distribution using D'Agostino & Pearson omnibus normality tests. Data that passed normality tests were analyzed by one-way ANOVA with Tukey's multiple comparisons tests. Data significantly different from a normal distribution were analyzed using Kruskal-Wallis with Dunn's multiple comparisons tests. Significance was defined at alpha <0.05 and analyzed using GraphPad Prism v6.0h.

2.5. Results

2.5.1. Initial primary feeder cell vs cell-free L3 cultures

Based on the success of larval growth co-cultures of *M. perstans* and *L. loa* (Njouendou et al., 2017, Zofou et al., 2018) as well as protracted maintenance of *Onchocerca* adult male worms (Townson, 1988), LLCMK2 cells were trialed to assess support of larval growth and survival of *B. malayi* (Figure 2.1). On the LLCMK2 cell layer, *B. malayi* L3 stages remained highly motile for 4 days into culture (Figure.2.1.B). After this point, L3 cultured on LLCMK2 cells declined in motility, reaching a score of 3 by day 6. LLCMK2 cells supported 100% survival for up to 7 days (the *in vivo* L3-L4 moult point). Survival drastically declined from 90% at day 6 to 0 by day 9 (Figure 2.1.A). *B. malayi* L3 cultured without a cell feeder layer (MEM) survived for longer, with 10% of parasites alive by the 14 day end-point, (Mantel-Cox log rank test; P=0.0015), however motility steadily declined throughout the period with surviving parasites displaying an average score of 1.

The MTT assay was used to determine the viability of cultured parasites in comparison to those freshly isolated from IL-4R α ^{-/-}IL-5^{-/-} mice at the 14 day end-point (Figure 2.1.C). As survival was determined as 0 at the end of study in the LLCMK2 group, parasites were taken to confirm a lack of viability which was determined with the absence of MTT reductase activity. Parasites cultured without cells (MEM) exhibited a lower MTT reductase OD reading than the *in vivo* control (median = 0.0033, range = 0.001-0.0035 O.D. vs median 0.008 O.D, range = 0.0006-0.01; Mann-Whitney test, P<0.01), indicating a reduction in viability in comparison to the *in vivo* reared parasites. Due to the limited success of this study, *Wolbachia* titre and length analyses were not conducted.

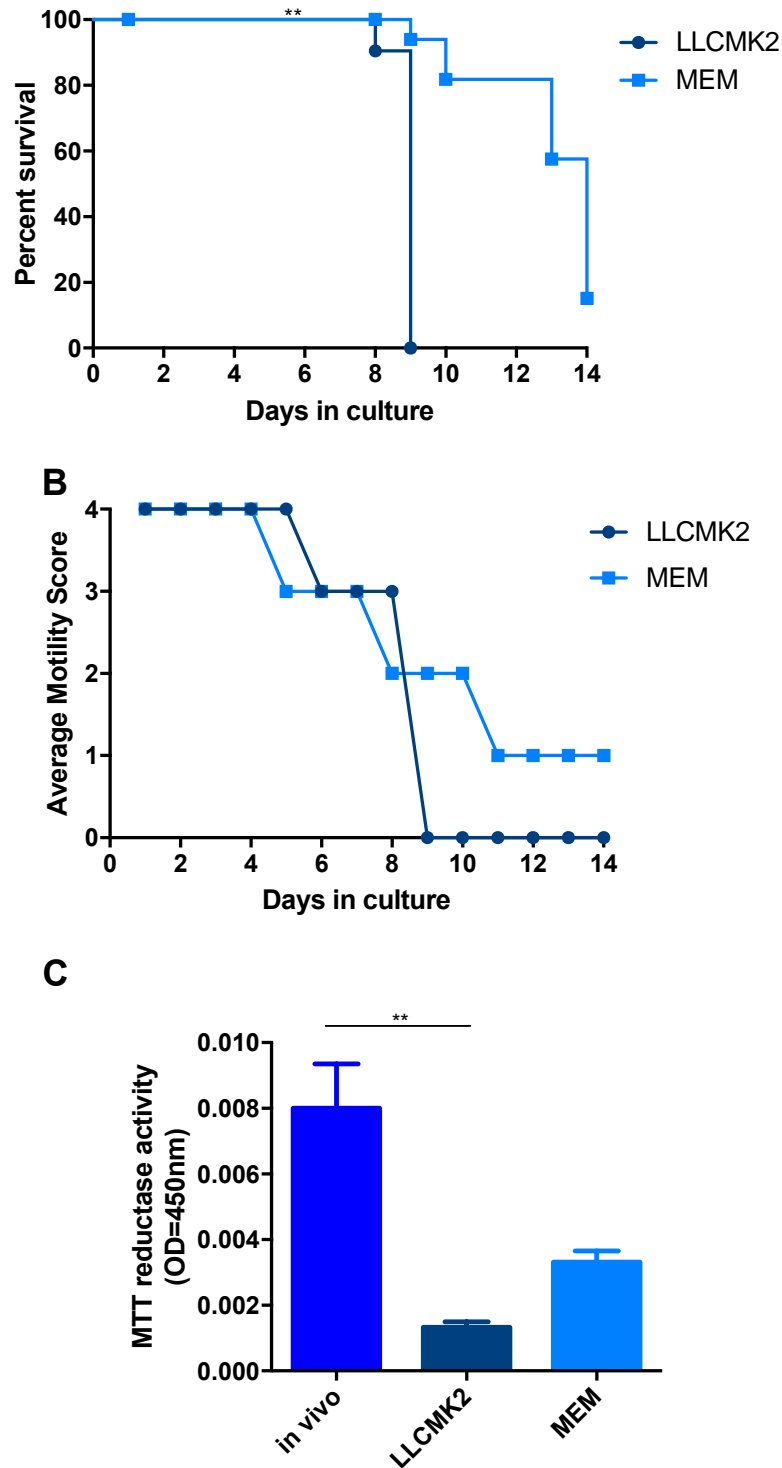


Figure 2.1. Initial *Brugia malayi* larval primary feeder cell vs cell free cultures.

Kaplein-meyer survival curves of *Brugia malayi* L3 cultured with monkey kidney cells (LLCMK2) vs cell-free (MEM) cultures over 14d in 12-well plates (10-20/well, 37°C, 5% CO₂) (A). Average motility scores of cultured *Bm*L3 on cell (LLCMK2) vs cell-free (MEM) culture conditions over 14d (B). MTT reductase activity (viability) of parasites cultured under cell (LLCMK2) and cell-free (MEM) conditions in comparison to parasites retrieved from mice at 14d (C). Data is derived from groups of 50 larvae in total/group (A-C). Data in C is median O.D. measures ± interquartile range per individual larvae. Significance is indicated **P<0.01

2.5.2. Evaluation of different cell and media types on the survival and motility of *in vitro* cultured *BmL3*

Following on from the limited success utilising the LLCMK2 cell line, two further mammalian cell lines were trialled; HEK and LECs, alongside a variety of different cell-free, media-only conditions. By the day 8 time-point, all cell types supported similar, high levels of larval survival (average HEK survival = 87.2%; LEC monolayer = 95.5%; LEC + insert = 92.7%) (Figure 2.2.A). After this point, parasites across all cell conditions showed a gradual decline in survival to day 14 (average HEK survival = 30.9%; LEC monolayer = 27.3%; LEC + insert = 39.0%). Full motility was retained in all surviving parasites across all cell types for 8-10 days. After these time-points, motility scores of surviving larvae decreased, reaching a score of 2 by days 12 and 14 in the LEC monolayer and insert conditions, respectively, whilst parasites maintained in the HEK group had declined to a score of 1 by day 12 (figure 2.2.B).

The survival of parasites maintained under cell-free conditions generally declined more quickly than those maintained on cell layers (Figure 2.2.C). Over the course of the experiment, survival was significantly greater in parasites maintained in DMEM (Mantel-Cox log rank test, $P=0.0014$). At the day 8 time-point, 100% of parasites were alive in the DMEM group, whereas survival had declined across all other cell-free systems (average RPMI 10% FBS survival = 65.5%; RPMI 5% FBS survival = 67.9%; RPMI 10% FBS High Glucose = 62.1%; RPMI 5% FBS High Glucose = 65.9%; DMEM = 100%; EMEM = 60.4%; EGM2-MV = 72.9%) Survival then continued to decrease until day 14, of which a greater proportion of parasites survived in the DMEM group (average RPMI 10% FBS survival = 8.5%; RPMI 5% FBS = 9.8%; RPMI 10% FBS High Glucose = 8.6%; RPMI 5% FBS High Glucose = 9.9%; DMEM = 19.4%; EMEM = 5.4%; EGM-2 MV = 10.2%,). At day 8, parasites in all groups aside from EMEM retained full motility (Figure 2.2.D). After this point, motility decreased for the duration of

the study whereby all surviving parasites across all groups had a motility score of 1 by day 14 (Figure 2.2).

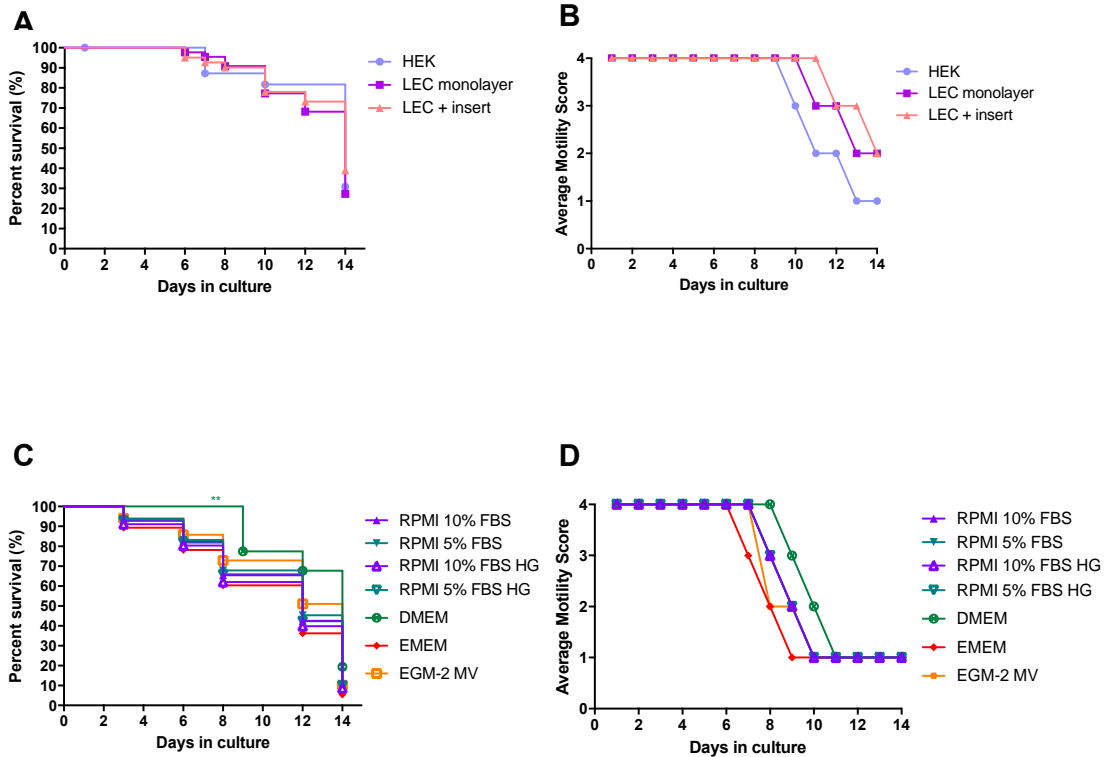


Figure 2.2. Survival and motility analysis of *BmL3* cultured on different cell and media types for 14d

Kaplein-meyer survival curve of *BmL3* cultured on different endothelial cell types (human endothelial kidney, lymphatic endothelial) (A) over 14d in 12-well plates (cultured at a density of 10-20/well, 37°C, 5% CO₂) Average motility scores of *BmL3* cultured on different cell types (B). Kaplein-meyer survival curve of *BmL3* cultured on different cell-free media types (RPMI with 5% or 10% FBS with and without high glucose concentrations, DMEM, EMEM, EGM-2 MV) (C). Average motility scores of *BmL3* cultured on different cell-free media types (D). Data is derived from groups of 80-100 larvae, cultured at 10-20 *BmL3*/well for 14d at 37°C at 5% CO₂ in 12-well plates. Significant difference in survival is indicated *P<0.05, **P<0.01.

2.5.3. Evaluation of different cell and media types on the growth of *in vitro* cultured *BmL3*

Length measurements at day 8 confirmed a significant increase in the length of parasites recovered from mice (*in vivo*) in comparison to L3 retrieved directly from mosquitoes (L3 median = 1.147 mm, range = 0.755-1.423; *in vivo* median = 1.78, range = 0.896-1.929 mm \pm 0.05; Kruskal-Wallis statistic = 47.42, Dunn's multiple comparisons test P=0.0008). Whilst increases in length were observed across all the RPMI media variations (RPMI 10% FBS median = 1.579 mm, range = 1.513-2.152 mm \pm 0.115; RPMI 5% FBS average = 1.553 mm, range = 0.822-2.149; RPMI 10% FBS High Glucose median = 1.652 mm, range = 0.999-1.894; RPMI 5% FBS High Glucose median = 1.522 mm, range = 0.825-1.980), only parasites maintained in DMEM were significantly longer than mosquito-derived L3 stages (median = 1.745 mm, range = 1.443-2.206; Dunn's multiple comparisons test, P=0.0332). Parasites maintained in EGM-2 MV and EMEM did not exhibit any growth (EGM-2 MV median = 0.905 mm, range = 0.762-1.124; EMEM median = 0.945 mm, range = 0.770-1.189) and were significantly shorter than those recovered from *in vivo* (Dunn's multiple comparisons test, P<0.0001) (Figure 2.3.A).

Parasites cultured in the presence of cells also displayed an increase in length at day 8, with those maintained on HEK cells significantly longer than the L3 mosquito stage (median = 1.743, range = 0.858-2.190; Kruskal-Wallis statistic = 20.91; Dunn's multiple comparisons test P=0.0224) and the longest of all culture conditions at day 8. Parasites maintained on LEC monolayers grew to a median of 1.707 mm, range = 0.864-1.908, a length which was intermediate between L3 stages and *in vivo* growth. The LEC + insert condition supported the growth of parasites to a median of 1.540 mm (range = 0.690-2.000), which was significantly less than the recorded *in vivo* growth (P=0.0228) (Figure 2.3.B).

CHAPTER 2

By day 14, parasites underwent a further growth increase *in vivo* (median = 2.216 mm, range = 1.685–4.058, P=0.0028, Mann-Whitney test). Whilst parasites maintained under cell-free conditions exhibited slight length increases in comparison to day 8 (RPMI 10 % FBS median = 1.847 mm, range = 1.341-2.324; RPMI 5% FBS median = 1.923 mm, range = 1.695–2.282; RPMI 10% FBS High Glucose median = 1.814 mm, range = 0.999–1.973; RPMI 5% FBS High Glucose median = 1.92, range = 1.678-2.158; EMEM median = 0.945, range = 0.770-1.337; EGM-2 MV median = 1.046, range = 0.776-1.424), all culture conditions were sub-optimal compared to *in vivo* growth (Kruskal-Wallis, Dunn’s multiple comparisons test, versus *in vivo* d14) (Figure 2.3.C). Similarly, all larvae maintained on cell layers demonstrated significantly impaired growth compared to *in vivo* controls (HEK median = 1.737, range = 1.341-2.856; LEC median = 1.728, range = 1.373-2.00; LEC + insert median = 1.779, range = 1.599-2.098) (Figure 2.3.D).

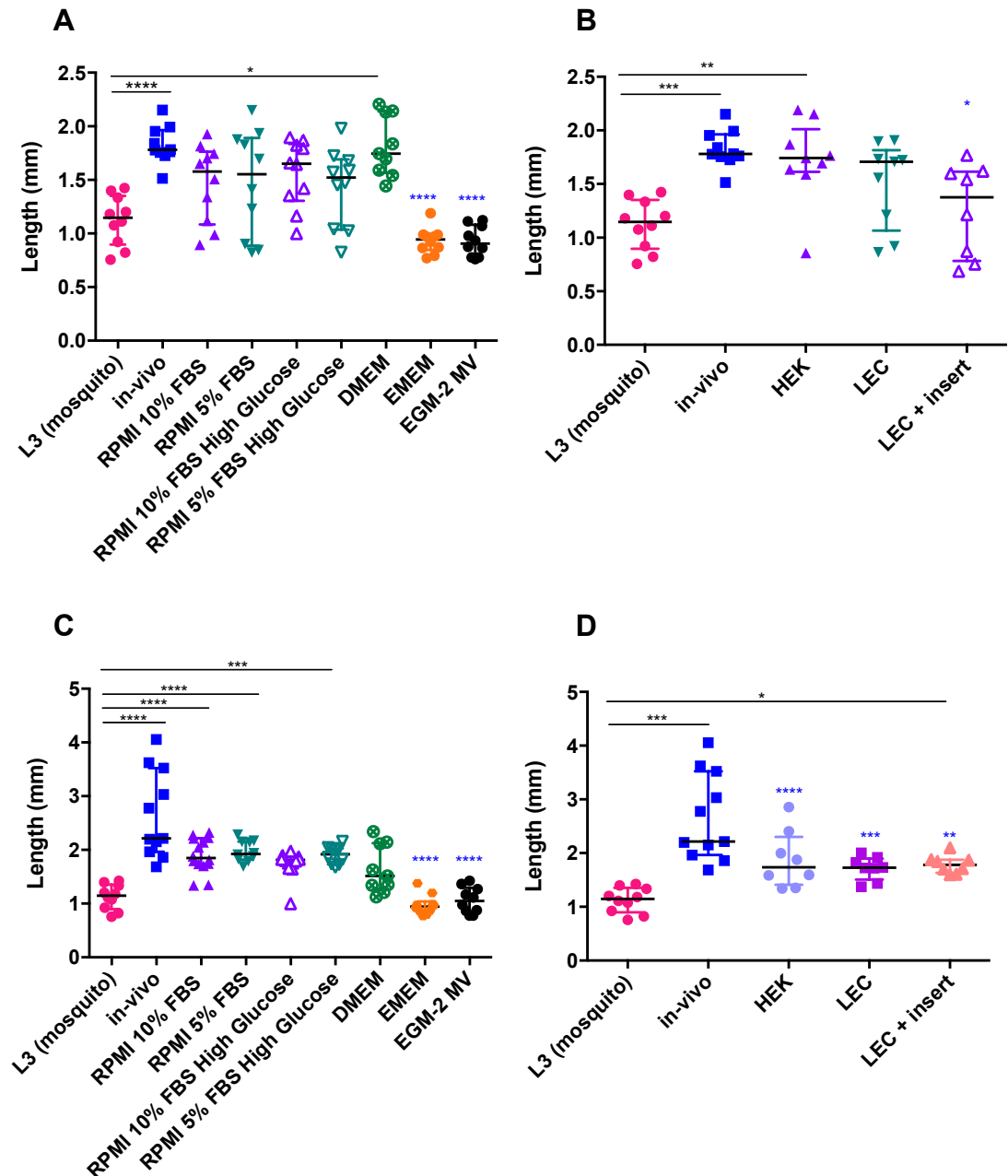


Figure 2.3. Length measurements of *BmL3* cultured on different cell and media types

Median length measurements of *BmL3* cultured on different cell-free media types after 8 days in culture (10-20/well in 12-well plates with RPMI 10% FBS, RPMI 5% FBS with and without high glucose concentrations, DMEM, EMEM, EGM-2 MV) (A). Median length measurements of *BmL3* cultured on different cell types (human endothelial kidney, lymphatic endothelial) after 8 days in culture (B). Median length measurements of *BmL3* cultured on different cell-free media types after 14 days in culture (C). Median length measurements of *BmL3* cultured on different cell types after 14 days in culture (B). All length measurements were compared against *BmL3* freshly dissected from mosquitoes at the start of study, 'L3 (mosquito) <pink> and parasites recovered from *in vivo* at the corresponding time point, 'in-vivo' <blue>. Horizontal bars represent the median. Error bars represent interquartile range. Data is derived from groups of 8-14 larvae/group taken from cultures set up at 10-20/well in 12-well plates at 37°C, 5% CO₂. Significance is indicated *P<0.05, ***P<0.001, ****P<0.0001.

2.5.4. Evaluation of *Wolbachia* titres in *Bm*L3 cultured on different cell and media types

Quantitative (q)PCR analysis carried out on *in vivo* recovered parasites at day 8 indicated a significant expansion of *Wolbachia* (median = 1.7×10^5 , range = 2.3×10^4 – 2.94×10^5) through the L3-L4 moult within the host, in comparison to the L3 mosquito stages (median = 1.39×10^4 , range = 193 - 6.78×10^4) (Figure 2.4.A).

Of all the cultured parasites, only the HEK feeder layer (Figure 2.4.B) and DMEM cell-free conditions (Figure 2.4.A) supported *Wolbachia* expansions which were significantly higher than L3 stages and comparable to those *in vivo* (HEK median = 4.69×10^4 , range = 648 – 5.5×10^5 ; DMEM median = 1.47×10^5 , range = 6.13×10^4 – 2.14×10^5 ; Kruskal-Wallis statistic = 22.11, both $P < 0.0001$ versus mosquito L3, Dunn's multiple comparisons test). *Wolbachia* titres failed to expand within LEC and LEC-insert maintained parasites, were significantly lower than those *in vivo*, and comparable to titres in mosquito L3 stages (LEC median = 1.72×10^4 , range = 950 – 2.5×10^5 ; LEC + insert median = 9615, range = 653 – 2.14×10^4 both $P < 0.0001$ versus d14 *in vivo* L4 larvae, Dunn's multiple comparisons test). This trend was also apparent with the remainder of the cell-free conditions (RPMI 10% FBS median = 2.07×10^4 , range = 7.3×10^3 – 4.86×10^4 ; RPMI 5% FBS median = 2.37×10^4 , range = 1.2×10^4 – 4.94×10^4 ; RPMI 10% FBS High Glucose median = 1.12×10^4 , range = 2.83×10^3 – 6.22×10^4 ; RPMI 5% FBS High Glucose median = 1.4×10^4 , range = 9.46×10^3 – 6.22×10^4 ; EMEM median = 7.35×10^3 , range = 2.1×10^3 – 5.0×10^4 ; EGM-2 MV median = 10025, range = 1.62×10^3 – 3.97×10^4 all $P < 0.0001$ versus d14 *in vivo* L4 larvae, Dunn's multiple comparisons test) (Figure 4).

By day 14, a further expected expansion was confirmed in *in vivo* recovered parasites (median = 6.395×10^6 , range = 1.53×10^5 – 1.64×10^7 , versus d8 *in vivo* recovered L4, $P < 0.0001$, Mann-Whitney test. No significant expansions were observed in any of the parasites

CHAPTER 2

maintained *in vitro* between d8 and d14 except larvae cultured on HEK feeder layers (P=0.0061, Mann-Whitney test) (Figure 2.4.C+D).

All conditions however, failed to emulate *in vivo* expansion of *Wolbachia* at 14 days post-infection (HEK median = 2.54×10^5 , range = $5.51 \times 10^4 - 7.04 \times 10^5$; LEC median = 1.81×10^4 , range = $3.44 \times 10^3 - 3.65 \times 10^4$; LEC + insert median = 1.34×10^4 , range = $6.23 \times 10^3 - 2.5 \times 10^4$; RPMI 10% FBS median = 2.05×10^4 , range = $1.54 \times 10^3 - 7.39 \times 10^4$; RPMI 5% FBS median = 2.5×10^4 , range = $6.5 \times 10^3 - 7.0 \times 10^4$; RPMI 10% FBS High Glucose median = 2.44×10^4 , range = $6.93 \times 10^3 - 7.34 \times 10^4$; RPMI 5% FBS High Glucose median = 4.0×10^4 , range = $5.9 \times 10^3 - 8.3 \times 10^4$; DMEM median = 2.49×10^5 , range = $5.51 \times 10^4 - 7.04 \times 10^5$; EMEM median = 8005, range = $1.81 \times 10^3 - 4.89 \times 10^4$; EGM-2 MV median = 2.38×10^4 , range = $1.73 \times 10^3 - 6.0 \times 10^4$ all $P < 0.0001$ versus d14 *in vivo* control).

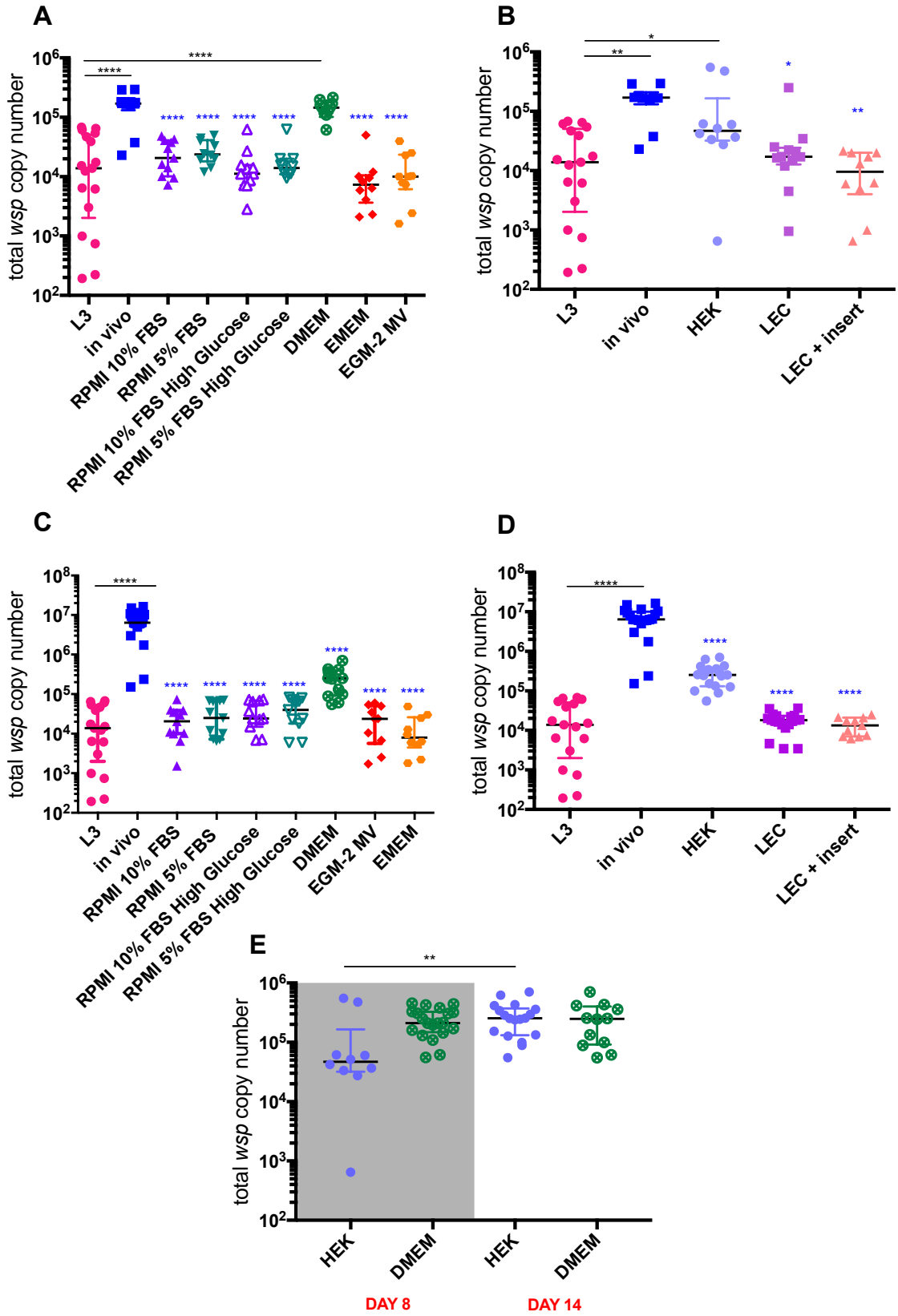


Figure 2.4. *Wolbachia* expansions of *in vitro* reared parasites compared with baseline *BmL3* and equivalent *in vivo* time-point titres

qPCR *Wolbachia* load analysis of parasites cultured in different media types (cell-free; RPMI 10% FBS, RPMI 5% FBS – both with and without high glucose concentrations, DMEM, EGM-2 MV, EMEM) after 8d in culture (A). qPCR *Wolbachia* load analysis of parasites cultured on different endothelial cell types (human kidney, lymphatic endothelial) after 8d in culture (B). qPCR *Wolbachia* load analysis of parasites cultured in different media types (cell-free) after 14d in culture (C). qPCR *Wolbachia* load analysis of parasites cultured on different cell types after 14d in culture (D). Cross-comparison of *Wolbachia* titres between the most successful cell-free (DMEM) and cell (HEK) cultures between 8 and 14 days in culture (E). All cultures were conducted at 37°C, 5% CO₂. Data plotted is derived from groups of 10-20 larvae. Horizontal bars represent the median. Error bars represent interquartile range. Significance is indicated *P<0.05, **P<0.01, ****P<0.0001 using a one-way anova comparing culture conditions to both L3 from mosquitos and *in vivo* recovered parasites of the equivalent time-point. Black asterisks indicate statistical difference from L3 (mosquito), blue asterisks indicate statistical difference from *in vivo* derived larvae.

2.5.5. Evaluation of metabolic activity of *BmL3* cultured on different cell and media types

Metabolically active parasites possess MTT reductase enzymes which reduce the tetrazolium salt, MTT, to formazan, which can then be quantified as a marker of viability. 14 day end-point viability assessments confirmed *in vivo* recovered *B. malayi* larvae had a median O.D. (MTT reductase activity) reading of 0.115 (read at 450nm, range = 0.066 – 0.196) (Figure 2.5.A+B). In comparison, all larvae, cultured either with or without feeder cells, exhibited a significantly reduced MTT reductase activity in comparison to *in vivo* recovered parasites (HEK median = 0.067 OD, range = 0.055 – 0.08; LEC median = 0.042 OD, range = 0.02-0.067; LEC + insert median = 0.040 OD, range = 0.005 – 0.065; RPMI 10% FBS median = 0.065 OD, range = 0.056 – 0.071; RPMI 5% FBS median = 0.054 OD, range = 0.034 – 0.063; RPMI 10% FBS High Glucose median = 0.069 OD, range = 0.054 – 0.114; RPMI 5% FBS High Glucose median = 0.080 OD, range = 0.054 – 0.114; DMEM median = 0.0605 OD, range = 0.040 – 0.100; EMEM median = 0.043OD, range = 0.025 – 0.064; EGM-2 MV median = 0.0345 OD,

range = 0.02 – 0.063 all $P < 0.0001$ versus d14 *in vivo* larvae except 5% FBS high glucose, $P < 0.01$, Kruskal Wallis with Dunn's multiple comparisons test).

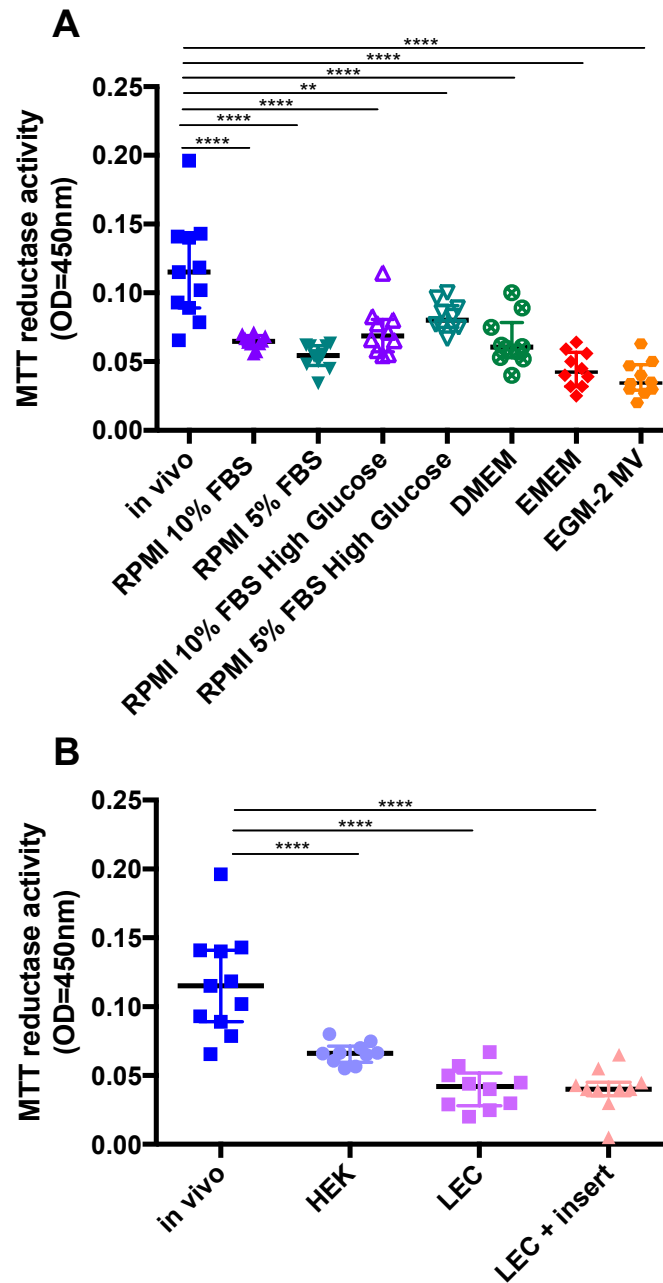


Figure 2.5. Assessment of metabolic activity of cultured *Bm* larvae at day 14 in comparison to parasites reared *in vivo*

MTT reductase activity of *Bm* larvae cultured in different media types after 14 days (cell-free; RPMI 10% FBS, RPMI 5% FBS both with and without high glucose concentrations, DMEM, EGM-2 MV, EMEM) (A). MTT reductase activity of *Bm* larvae cultured on different endothelial cell types (human endothelial kidney, lymphatic endothelial) after 14 days (cells) (B). Cultures were conducted at 37°C, 5% CO₂ in 12-well plates at 10-20 L3/well. Horizontal bars represent the median. Error bars represent interquartile range. Data is derived from 10-11 larvae per group. Significance is indicated ** $P < 0.01$, **** $P < 0.0001$.

2.5.6. Initial *Dirofilariae immitis in vitro* cultures

Initial *in vitro* cultures of the veterinary / zoonotic filarial nematode, *Dirofilaria immitis*, demonstrated improved survival with the presence of an MDCK feeder cell layer ($P < 0.0001$, Mantel-Cox log rank test), with 38% parasites surviving after 38 days in culture, on average (Figure 2.6.A). *D. immitis* larvae cultured without the presence of cells exhibited a decrease in survival earlier into cultures, by around day 20. Parasite survival continued to decline until day 28 when no parasites were considered motile (alive) at this point. Parasites cultured on LLCMK2 cell layers survived better than with media alone, with approximately 20% of parasites surviving up to 38 days in culture (Figure 2.6.B).

The motility of cultured *D. immitis* larvae remained high at a score of 4 for 5, 9 and 10 days into culture for those maintained on LLCMK2 feeder layers, cell-free conditions (EMEM) and MDCK cell layers, respectively (Figure 2.6.C). Parasites maintained without cells retained a score of 3 for the duration of the study, until all parasites had perished. *D. immitis* larvae maintained on the MDCK feeder layer displayed a reduced motility for approximately 15 days, before regaining motility until the end of the study. Parasites maintained on the LLCMK2 feeder layer also displayed a reduced motility for approximately 25 days in culture, before displaying an increased motility from day 30 until the study end-point.

Length measurements were taken in a repeat study using only MDCK cells vs cell-free (EMEM) conditions at multiple time points throughout the culture (Figure 2.6.D). Measurements indicated an initial slow growth up until day 39 in parasites maintained on the MDCK feeder layer, which were significantly longer than L3 stage *D. immitis* larvae at the start of the study. No differences in length were observed between *D. immitis* larvae maintained with or without cells at earlier time-points (d7 and 12).

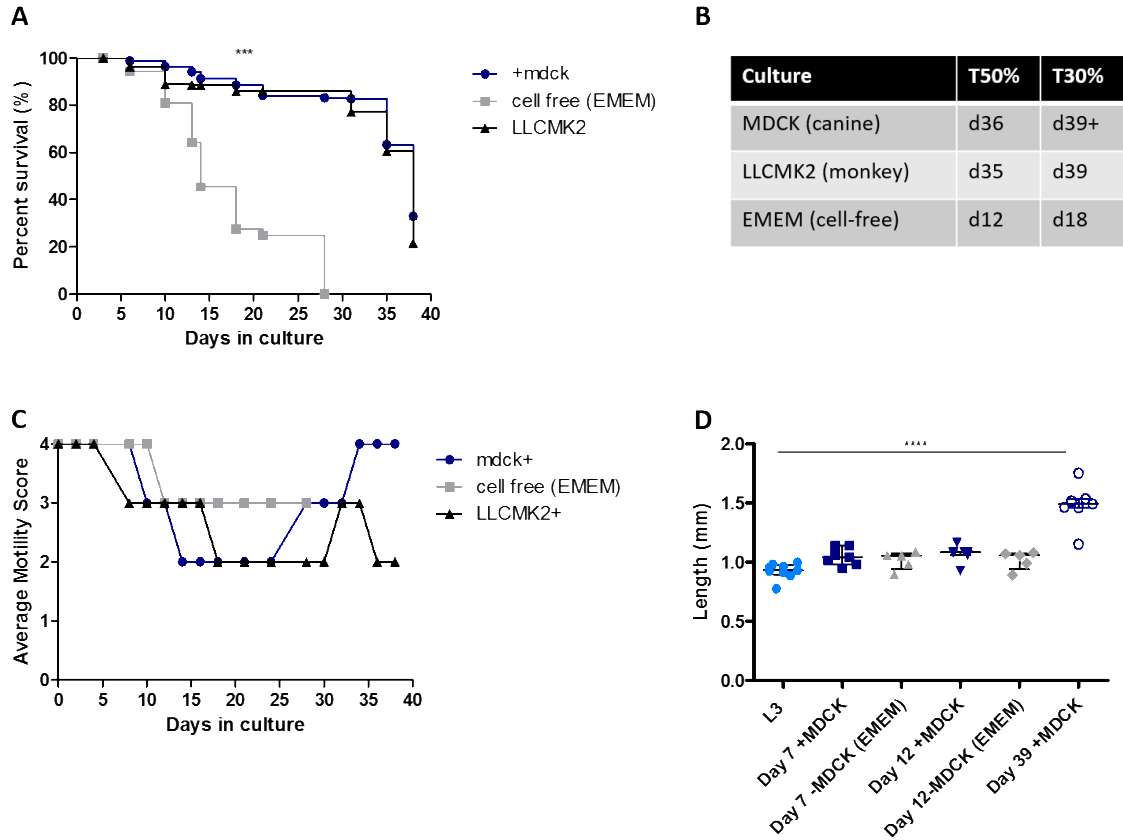


Figure 2.6. Initial *in vitro* *Dirofilaria immitis* larval cultures

Kaplein-meyer survival curve of *Di* larvae maintained in cultures over 39 days with MDCK cells or EMEM media (cell free) (A), table summarizing survival between MDCK, LLCMK2 and EMEM cultures at 50% and 30% survival (B), average motility scores of *Di* larvae over the course of the culture period on MDCK, LLCMK2 cells or EMEM media (C), length measurements of cultured *Di* at days 7, 12 and 39 (D). Bars represent median \pm interquartile range. Larvae were plated at a density of 10 L3/well with cultures conducted at 37°C, 5% CO₂ in 12-well plates. Data is derived from 10 larvae per group (A-C), data is derived from 5-7 larvae (D). Significance is indicated ***P<0.001, ****P<0.0001.

2.6. Discussion

Previous attempts to culture larval stages of *B. malayi* have been difficult to reproduce due to the use of variable lots of human serum in high concentrations.

Although the benefit of adding cells to parasite cultures is well documented in *Onchocerca*, *Mansonella* and *Loa loa* cultures, it is difficult to draw conclusions from *Brugian* co-cultures due to the continual addition of human sera (Falcone et al., 1995, Riberu et al., 1990, Smillie et al., 1994, Tippawangkosol et al., 2002, Mak et al., 1983). Difficulties in reproducibility have hindered the development of these platforms into systems suitable for assessing drug efficacy, and an alternative model to produce adult stage parasites, thereby reducing animal usage.

To minimise issues with reproducibility, commercially available FBS was used across all cultures in this chapter, at concentrations relevant to the physiological setting (5-10%). Although previous literature has suggested the benefit of adding 75 μ M ascorbic acid to cultures, the supplement kit added to make up the EGM-2 MV media already contained ascorbic acid, which is well within the physiological range, and thus no further ascorbic acid was added. Other researchers also using this media described the benefit of adding 75 μ M ascorbic acid to EGM-2 MV (Lu et al., 2018), however did not make it clear whether this was added to the existing concentration, or instead of, questioning the validity of these data. No clear benefit of adding ascorbic acid to the culture media was concluded from the cultures conducted in this chapter, and thus was not experimented across any other media or feeder cell layer.

Non-standardised metrics have commonly been used to determine culture success. Moulting rate is one such method however the techniques to establish this are variable; either by counting the number of cuticles shed into the culture well, or morphological analysis which may be subjective to the investigator. Attempts were made to quantify the number of shed

cuticles across all culture types tested, however this was determined to be unreliable due to cuticles adhering to cell feeder layers which made them difficult to visualise.

Full survival and motility analyses have rarely been reported in previous literature, presumably due to the low percentage of parasites surviving to further life-cycle stages. Survival analyses from this study highlighted an improvement with the addition of feeder cells for up to 8 days into culture. Beyond this point, larval health declined both with and without the presence of cells, however the survival was greater overall with the addition of cells. No cell type; lymphatic specific (LEC) or general mammalian endothelial cell type (LLCMK2, HEK), were significantly better than another in terms of survival. This might suggest the addition of cells provided more of a physical effect, whereby parasites may use the cells to aid ex-sheathment, rather than the secretion of tissue and/or species -specific paracrine molecules to promote moulting and growth. Alternatively, factors secreted universally by all cell types may be responsible in temporarily supporting the early development of *B. malayi* larvae. Separation of larvae from co-cultures in trans-well inserts would help to resolve which of these hypotheses are correct.

Length measurements have been reported in some previous culture studies, although only very few have an *in vivo* comparator. Here, measurements at day 8 confirmed growth, and hence development of *B. malayi*, in comparison to L3 stages fresh from mosquitoes. Length was only significantly greater, and comparable to *in vivo* retrieved *B. malayi*, in larvae maintained on the HEK feeder layer or the cell-free DMEM. By day 14, *in vitro* reared parasites had not grown to the same extent as those *in vivo* and thus were no longer representative of *in vivo* development. Similar phenomena have been observed in previous studies whereby cultured parasites were comparable in length to data recorded for jirds after 8 days (Falcone et al., 1995, Ash and Riley, 1970), however after this point were also no longer comparable. Within the same study, the length of parasites cultured in 10% human

serum were sub-optimal in comparison to equivalent time points in *in vivo* data sets collected in this chapter.

To further evaluate whether *in vitro* cultured parasites were comparable to those *in vivo*, *Wolbachia* titres were evaluated. This was also important for potential future use of *B. malayi* cultured larvae in anti-*Wolbachia* drug screening. It is well versed that filarial worms undergo an extensive *Wolbachia* expansion upon entry into to mammalian host, as early as 8 days (McGarry et al., 2004a, Fischer et al., 2011), and is essential for the survival and development of the parasite, as documented by the inability to develop to adult stage upon elimination of *Wolbachia* with tetracyclines in early larval infections in jirds (Bosshardt et al., 1993). Although *Wolbachia* populations had increased in comparison to L3, only those maintained on HEK monolayers, or DMEM, had titres statistically comparable to those recovered *in vivo*. However, despite expanding further between day 8 and the study endpoint, *Wolbachia* expansions were sub-optimal compared to those *in vivo*. Failure to expand *Wolbachia* populations coincided with the decrease in survival, suggesting that sub-optimal *Wolbachia* populations might be the critical factor for loss of viability during the L4 growth phase (Veneti et al., 2003, Ferree and Sullivan, 2006, Clark et al., 2003). These culture conditions therefore may be useful in the future to determine intrinsic *Wolbachia*-products aiding growth of larval *B. malayi* via addition of specific *Wolbachia* derived macromolecules into the co-cultures. For instance, *Wolbachia* haem biosynthesis has been demonstrated to be important in the symbiosis, with *B. malayi* lacking specific haem biosynthetic enzymes (Gill PLoS NTD 2014). It is possible therefore that titrations of exogenous haem might overcome the demise of L4 in *in vitro* co-culture systems. Further, introduction of functional *Wolbachia* haem biosynthetic enzymes in culture may elucidate the filarial-*Wolbachia* symbiosis at this point in the life cycle.

This is the first time *Wolbachia* has been analysed within the context of cultured *B. malayi* parasites. The fact that parasites cultured under certain conditions (ie HEK co-cultures) are able to grow and expand for up to 8 days suggests parasites are representative of the *in vivo* situation at this point. The evidence that parasites in some groups display lengths comparable to those *in vivo*, despite having sub-optimal *Wolbachia* loads, leads to the hypothesis that the L3-L4 stage may not be as highly dependent on *Wolbachia* and instead, is more crucial in the preparation and process of the L4-L5 (immature adult) moult.

It is thus evident, through previous studies and work described here, that a component is lacking from both systems which is not released from the cell types trialled. Falcone et al utilised a two-cell system; human dermal fibroblasts and a human jurkat leukemia T cell line, albeit still using human sera; however only a very small percentage (2.6%) were able to survive to the young adult stage. In earlier studies, parasites that were initially primed in rodent hosts were then able to survive *in vitro*, suggesting a 'priming' effect, potentially from the immune system. The role of immune cells potentially elongating parasite culture is evident in work by Turner et al, whereby the addition of alternatively activated macrophages appear to enhance the survival of L3 over 7 days (Turner et al., 2018). Immune cells have also been found to elongate *Onchocerca* cultures, where after transfer onto PBMCs after initial culture on LLCMK2 cells, parasites are able to develop further and can be utilised in drug screens (Voronin et al., 2019). These outcomes thus may indicate that a more complex cell system would aid *Brugia* survival *in vitro*. Matrigels with multiple cell types were considered – however these were not feasible as they would not allow for the retrieval of live parasites for confirmatory analyses.

In conclusion, the systems evaluated were not able to offer a replacement for animal models. Instead, a *B. malayi* culture system using HEKs may be appropriate for a short-term (7 days)

CHAPTER 2

drug assay to assess anti-*Wolbachia* or direct-acting drug candidates, as within this time-frame *in vitro* cultured parasites are comparable to those *in vivo*.

Alternatively, there is greater optimism for a *D. immitis in vitro* culture system that may replace the use of experimentally infected dogs. Initial experiments have indicated parasites are able to survive much longer in culture than *Brugia*, potentially due to being of a different clade of filariae which is more related to *Onchocera*, which also survive in culture for much longer periods than *Brugia*. Instead, client owned dogs which are naturally infected with *D. immitis* could be a source of microfilariae to feed mosquitoes to produce L3 for drug screening purposes and the development of further life-cycle stages. However, with a lack of a rodent *in vivo* model to provide an appropriate *in vivo* comparator, further evaluation of the culture system would need to be conducted, for example analyses of *Wolbachia* titres.

Chapter 3: Development and initial validation of a long-term adult female *Brugia malayi* culture system for screening macrofilaricidal candidates

3.1. Abstract

The development of new drugs targeting adult stage filarial parasites is significantly hindered by the lack of a robust *in vitro* model. Instead, the testing of potential direct-acting and anti-*Wolbachia* therapeutic candidates heavily relies on pre-clinical mouse or gerbil models. To develop new *in vitro* systems, adult worms need to be harvested from these infection models, of which the worm burden is often highly variable. To compensate for this, additional animals are required for infection. This chapter evaluates parasite burden data collated over 10 years from immune-deficient mouse strains and outbred Mongolian gerbils, to establish the optimal species and strain to generate a high level of parasites with low variation, to reduce the number of animals initially required for infection. Adult worms extracted from this selected model were then tested under different feeder cell and cell-free conditions to optimise and validate a long-term *in vitro* model. To ensure the model successfully translates to pre-clinical testing, cultured parasites were compared against those freshly isolated from *in vivo* using biochemical and molecular analyses. IL-4R α ^{-/-}IL-5^{-/-} BALB/c selective immunodeficient mice were superior to both CB.17 SCID mice and Mongolian gerbils in generating high yields of adult worms with less variation. Adult females retrieved from these mice could be successfully cultured for up to 21 days in the presence of a lymphatic endothelial cell co-culture system with comparable motility, metabolic activity and *Wolbachia* titres to those maintained *in vivo* for identical time-frames. Drug validation studies, using both reference and novel direct-acting and anti-*Wolbachia* therapeutics, confirmed efficacy which could be discerned between compounds. This confirms the utility of the *in vitro* model in informing, and providing an alternative to immediate pre-clinical screening, thus reducing the number of animals used for this purpose.

3.2. Introduction

Identification of novel macrofilaricidal drugs is hampered due to both low throughput and short life-span of adult filarial parasites *in vitro*. The majority of anti-filarial or anti-*Wolbachia* *in vitro* drug screens utilise more accessible and/or abundant life cycle stages; namely the mf or infectious L3 stage (Clare et al., 2019, Hong et al., 2019, Storey et al., 2014, Voronin et al., 2019, Townson et al., 1987, Abraham et al., 1987). A major caveat to these screening systems is that anthelmintic or anti-*Wolbachia* activities may not translate to the target adult stages of the parasite due to stage-specific expression of drug targets or relative yields and cell division rates of *Wolbachia* symbionts.

Although some *in vitro* adult filarial drug screening models exist, they are generally limited to short-term experiments of 7 days or less due to the unreliability of maintaining viable adult filariae for more extended periods of time. A notable exception to this has been the development of a monkey kidney cell co-culture drug screening system of male filariae of the bovine onchocerca parasite, *Onchocerca gutturosa*, a surrogate for *O. volvulus*, whereby adult parasites can be maintained for upwards of 4 months (Townson et al., 1986).

In terms of human lymphatic filariasis drug screening platforms, elongation of the culture period to maintain viable adult parasites has been less successful. The majority of cultures have focused on media-only systems, predominantly using RPMI with FBS, in which parasites are cultured between 24 and 120 hours in order to evaluate the effects of rapid direct-acting macrofilaricides, nanoparticle formulations or gene expression (Marcellino et al., 2012, O'Neill et al., 2016, Ballesteros et al., 2016). The longest culture period reported used endothelial basal media supplemented with 20% calf serum, however worm survival deteriorated by day 13 (Lu et al., 2018).

More recently, feeder cell co-cultures have been assessed for the rodent parasite *Litomosoides sigmodontis*. Adult female culture can be extended from 5 to 40 days, with a

50% survival rate, due to the co-culture of a murine endothelial cell line (EOMA). Contrastingly, a study using *B. malayi* female worms showed no additional benefit of culturing in the presence of human primary lymphatic endothelial cells compared with serum supplemented medium, with reductions in survival at 13 days (Evans et al., 2016).

Parameters evaluating *in vitro* parasite fitness have centred around motility and survival assessments, which are often subjective to the investigator. In efforts to combat this subjectivity and to also increase the throughput of drug screens, imaging platforms and computer applications have been developed to automate this process and increase the reliability of scoring (Partridge et al., 2018, Buckingham et al., 2014, Storey et al., 2014).

To incorporate quantitative assessments of viability into analyses, some studies have employed the MTT assay, as previously described in Chapter 2.

No studies thus far have evaluated the stability of endosymbiont *Wolbachia* populations in cultured parasites. Additionally, in all systems scrutinised, comparison with an appropriate *in vivo* control has not been documented, raising uncertainties of the quality of cultured worms and utility in drug screening experiments. For instance, current *in vitro* systems may be prone to a higher than desirable 'false hit' rate because viability of parasites and stress responses induced *ex vivo* may influence sensitivity to test compounds. For example, Geary et al described the dysregulation of several genes encoding stress indicators after retrieval from jirds, which remained over 5 days of *in vitro* culture (Ballesteros et al., 2016). Furthermore, an induction of autophagy due to physiological stress may increase sensitivity to *Wolbachia* depletion, as filarial *Wolbachia* populations are known to be regulated by autophagic processes (Voronin et al., 2012). Combined, these phenomena can result in parasites that do not accurately replicate the physiological conditions at the infection site in a host and consequently, drug screening 'hits' identified through these *in vitro* systems may

lead to failure of translation in *in vivo* studies due to artefactual sensitivities both to direct acting and anti-*Wolbachia* compounds *in vitro*.

As discussed briefly in the introduction chapter, there is no robust, reproducible *in vitro* system to propagate adult stage filarial parasites from infectious stage larvae, and certainly no system which produces mature fecund female parasites. Therefore, adult stage drug screening relies on the use of animals to propagate numbers of adult stages required for *in vitro* screening experiments. Such animal models are expensive, time consuming and sometimes logistically challenging to use for the generation of adult-stage parasites. Whilst the gerbil model is a useful laboratory model for generation of *Litomosoides* or *Brugia*, the productivity in terms of numbers of adults and mf produced is highly variable, declines with age of infection and is generally low yielding, especially for the human parasite *B. malayi*. For drug testing this reduces the throughput and overall translation of preclinical candidates.

More recently, immunodeficient mice have been appraised as long term susceptible hosts for *Brugia*, *Lito* and *loa loa* (Halliday et al., 2014, Nelson et al., 1991a, Pionnier et al., 2019) and have been validated as a functional drug model for microfilaricides, macrofilaricides and anti-*Wolbachia* candidates (Pionnier et al., 2019, Halliday et al., 2014) models provide an alternative *in vivo* system and also alleviate some of the issues with parasite variation.

From a 3Rs perspective, lack of validation regarding *in vitro* cultured adult filarial fitness, including *Wolbachia* stability compared to the *in vivo* condition, is of concern. 'False-hits' caused by artefacts of *in vitro* culture may lead to incorrect transition into *in vivo* pre-clinical testing, which increases the number of animals used for *in vivo* screening purposes. The high variability of parasite loads from jirds and decrease in infection levels with age, requires more animals to be initially infected to compensate for this. Inbred immunodeficient mice may provide higher yielding infection models as substitutes for gerbils, reducing overall animal use.

CHAPTER 3

The inability to generate the filarial life-cycle *in vitro* results in the heavy reliance on rodent models, such as mice and gerbils, to produce different life-cycle stages for experimental purposes and pre-clinical drug screening (Halliday et al., 2014).

3.3. Scientific and 3Rs aims

- Assess whether an IL-4R α ^{-/-}IL-5^{-/-} BALB/c selective immunodeficient mouse infection model is a comparable or superior alternative to gerbils or CB.17 SCID mice for the propagation and long term laboratory *in vivo* maintenance of *B. malayi* adults and mf, to reduce the number of animals for life cycle maintenance and parasite generation.
- Optimise a long-term *in vitro* female *Brugia malayi* culture system, using different feeder cell layers and media types, suitable for testing pharmacodynamics of anti-*Wolbachia* or nematocidal compounds.
- Evaluate the *in vitro* 'fitness' of cultured worms using motility, survival, metabolic activity assays and qPCR readouts to quantify parasite viability and endosymbiont *Wolbachia* titres, against matching duration *in vivo* comparators.
- Validate the culture system using the reference anti-*Wolbachia* or direct acting macrofilaricidal reference drugs: doxycycline and flubendazole to assess whether this *in vitro* model can be a reliable indicator of drug translation in *in vivo* testing (reduction in overall animal use).

3.4. Materials and Methods

3.4.1. Animals

Interleukin four receptor alpha (IL-4R α)^{-/-}IL-5^{-/-} BALB/c breeding pairs were a gift from Achim Hoerauf, University Hospital, Bonn. Male CB.17 SCID mice were purchased from Charles River, UK. *Meriones unguiculatus* (Mongolian gerbils; jirds) breeding pairs were purchased from Charles River, Europe. Animal stocks were maintained under specific pathogen-free (SPF) conditions at the biomedical services unit (BSU), University of Liverpool, Liverpool, UK. Male IL-4R α ^{-/-}IL-5^{-/-} BALB/c mice were 6-8 weeks old and weighed 18-24 g at start of experiments. Male gerbils were 4–6 months old and weighed 80–100 g at start of experiments. All experiments were approved by the ethical committees of the University of Liverpool and Liverpool School of Tropical Medicine (LSTM) and conducted under Home Office Animals (Scientific Procedures) Act 1986 (UK) requirements.

3.4.2. *Brugia malayi* parasite maintenance

The life cycle of *B. malayi* was maintained as previously described in Chapter 2.

3.4.3. *B. malayi* Experimental Infections

For *BmL3* infection, male Mongolian gerbils, aged 4–6 weeks, were injected via the intraperitoneal route, with 400 highly motile *BmL3* for life cycle maintenance. Alternatively, male IL-4R α ^{-/-}IL-5^{-/-} mice or male CB.17 SCID mice, both aged 6-8 weeks, were injected with 150 *BmL3* for adult worm stocks. Animals were left for between 12 and 25 weeks post-infection to allow infections to proceed to the chronic adult stage.

3.4.4. Adult *B. malayi* Implantation Surgeries

B. malayi adults were collected from infected donor CB.17 SCID or IL-4R α ^{-/-}IL-5^{-/-} BALB/c mice via peritoneal lavage post-mortem. Parasites were then separated into male and female, washed with pre-heated phosphate buffered saline (PBS, Merck) and collected into

groups of 10 female and 5 male, or 10 female parasites ready for implantation (total n=6-8). Mice were then placed under surgical anaesthesia using isoflurane and received a subcutaneous injection of buprenorphine prior to implantation of the above parasite groups into the peritoneal cavity. Implantation was achieved by making a small incision into the skin and abdominal cavity in the upper right quadrant and inserting parasites into the lower abdominal quadrant using a glass pipette to ensure all parasites were maintained in the cavity. The incisions were then re-sutured after implant and animals were re-housed as before and monitored closely.

3.4.5. Cell cultures

The lymphatic endothelial cell (LEC) line used exclusively throughout this study was Lymphatic human microvascular endothelial cells derived from human dermis (HMVEC_{dh}; Lonza). LEC and human embryonic kidney cells, (HEK293; ECACC) were cultured in T-175 flasks in Endothelial Basal Media (EGM-2 MV; Lonza) and Dulbecco's Modified Eagle Media (DMEM; Sigma), respectively, in a 5% CO₂ incubator set at 37°C. Media was supplemented with 5% foetal bovine serum (FBS; Sigma), 10ml penicillin/streptomycin (Sigma) and 10ml amphotericin B (Sigma) and allowed to reach confluence. Cells for use in cultures were passaged and plated between a passage number of 2-3. For passaging, cells were washed with PBS prior to trypsin-Ethyldiaminetetraacetic acid (EDTA; Sigma) treatment to detach cells. After detachment had been confirmed by microscopy, the trypsin solution was neutralised with an equal volume of corresponding cell media and the cell suspension was centrifuged at 1500rpm for 10 minutes. The supernatant was then discarded and the pellet was re-suspended in cell media before plating onto either 6-well plates, or 6-well transwell plates (Corning) to reach a confluent monolayer.

3.4.6. Macrophage co-culture

To determine whether addition of macrophages to the culture system enhanced parasite survival further, a monocyte-derived cell lines, Tohoku Hospital Pediatrics-1 (THP1), derived from an acute monocytic leukemia patient (gifted by Professor Giancarlo Biagini, Liverpool School of Tropical Medicine), were grown in suspension in a T-75 culture flask with Roswell Park Memorial Institute media (RPMI/RPMI 1640; Sigma). To differentiate the THP1s, a protocol was adapted from <https://bio-protocol.org/e1638>. For this, 2 ml of cell suspension was transferred into inserts of a 6-well transwell plate, at a concentration of 2×10^5 cells/insert. Cells were immediately treated with 10 ng/ml of 12-O-tetradecanoylphorbol-13-acetate (PMA; Peprotek) for 24 hours, to permanently differentiated into an M0-like phenotype. The PMA-containing media was then gently aspirated from the inserts and fresh media was replaced. Cells were then allowed to settle prior to further stimulation. For this, cells were treated with either 50 ng/ml interferon gamma (IFN- γ), or 25 ng/ml of interleukin 4 (IL-4) and interleukin 13 (IL-13), respectively, for M1- and M2-like differentiation. All cytokines were purchased from Peprotek. Terminally differentiated (PMA treated only; M0) cells were left untreated in inserts during this period. 48 hours post M ϕ (IFN- γ) and M ϕ (IL-4/IL-13) stimulation, cells were washed 3 times in fresh media and inserts were added to fresh monolayers of LECs in a 6well plate. 6 ml EGM-2 MV media was then added, as described previously, ready for the addition of parasites.

3.4.7. *In vitro* culture of parasites

Adult parasites were isolated from the peritoneal cavities of IL4R α /IL5 $^{-/-}$ and CB.17 SCID mice via peritoneal lavage post-mortem. Parasites were then washed with pre-warmed, sterile RPMI and separated into males and females. Female parasites of high motility and similar lengths were selected for culture. Initial culture studies evaluated the survival of female *Bm* on different cell monolayers and cell-free conditions to determine optimum culture

conditions and longevity of culture systems. Further optimisation evaluated specific time points (2, 3 and 4 week) using survival, motility, viability (MTT) and *Wolbachia* titres (qPCR) as readouts for *in vitro* fitness. Following this, mixed sex and single sex cultures were set up for 10 days using the optimised cell system to evaluate mf release *in vitro*. All cultured parasites were compared against parasites of the same age, freshly isolated from mice, to ensure cultured parasites were compared against an appropriate *in vivo* control. Culture media was replenished every 3 days, motility was analysed every day and parasites were taken for MTT and qPCR analysis at the time points indicated.

3.4.8. Motility scoring and survival analyses

Parasites were examined for motility daily using a 4-score scale, as described in Chapter 2, based on a scoring system devised by Rao and Weil (Rao et al., 2002).

3.4.9. MTT viability assessments

To assess parasite viability quantitatively at end points, the MTT assay was employed. For this, parasites were removed from culture and washed in pre-warmed PBS. Parasites were then transferred into separate wells of a 96 well plate and incubated with 0.5 mg/ml MTT (Sigma) for 2 hours at 37°C. Following incubation, parasites were washed in PBS, as previous, and incubated for 1 further hour with 100% Dimethyl Sulfoxide (DMSO; Sigma) to solubilise the blue formazan product. The plate was then analysed using a fluorescent plate reader set at 450nm, including a primary shake step. Data were expressed as a percentage change in optical density readings from the *in vivo* control median.

3.4.10. DNA extractions

DNA extraction was performed on individual parasites using a Qiagen QIAmp DNA mini kit. In brief, worms were transferred into Eppendorf tubes and incubated overnight at 56°C with ATL buffer and proteinase K to allow initial protein digestion. Following this, ethanol (100%)

was added to tubes and samples were subjected to two wash buffer stages with subsequent centrifugation steps. In final, DNA was eluted 100 µl elution buffer and transferred to 96 well plates to be frozen for qPCR analysis.

3.4.11. Gene cloning and qPCR

Plasmids, containing the inserts of amplified *B malayi Wolbachia* (wBm) surface protein, were prepared and stored in glycerol stocks at -20°C for use as qPCR standards as described in Chapter 2.

For data analysis, *Bm wsp* copy numbers were averaged and multiplied by the elution volume and divided by the volume of DNA sample added to the reaction mixture (1µl). Data were represented graphically as log₁₀ of *Wolbachia* load per adult female.

3.4.12. Microfilariae and embryo release profiles

Microfilariae and embryo release were evaluated at every media change (every 3 days), throughout the culture period. To prepare contents for counting, spent media from individual wells was centrifuged at 1200rpm for 10 minutes. Supernatants were then discarded and the pellets, containing released uterine products, were re-suspended in a known volume of PBS. Uterine release products, consisting of mf, early morulae, late morulae and embryos, were then evaluated by light microscopy. Data were expressed as the number of stage specific embryo products released per female worm.

3.4.13. Anti-*Wolbachia* Drug Screen Validation

To assess the *in vitro* culture system's ability to evaluate anti-*Wolbachia* drug activity, a drug challenge was carried out using the 'gold-standard' reference drug, doxycycline. ABBV-4083 (TylAMac, a gift from Dale Kempf, AbbVie), a novel macrolide compound proven to have anti-*Wolbachia* activity (Taylor et al., 2019) was also assessed in comparison to doxycycline. For this, parasites were isolated and cultured using the optimised LEC trans-well system.

Doxycycline was prepared in ddH₂O at a concentration of 5µM, whilst the same concentration of TylAMac was prepared in 100% DMSO. Drugs were replenished at each media change. An equivalent percentage of DMSO used in the drug groups was added to vehicle control groups. Parasites were scored daily for motility and survival, with treatment end points at 7 and 14 days. An additional wash-out group, which entailed drug treatment for 7 days followed by a 7 day washout period was included in the study to evaluate any *Wolbachia* recrudescence. QPCR analysis, as previous, was employed at endpoints to evaluate *Wolbachia* reductions in response to treatment.

3.4.14. Direct-acting Macrofilaricide Drug Screen Validation

To evaluate the system's functionality in determining direct acting macrofilaricide activity, Flubendazole (FBZ) and Suramin (SUR) (both Sigma) were used as reference drugs whilst evaluating the activity of two novel Dihydroxybenzoic (DHB) compounds; OX2083 and OX3153 (a gift from Professor David Satelle, University College London). In this study, female worms were cultured as previous, before the addition of the compounds made up to a concentration of 10 µM in DMSO. The equivalent DMSO concentration was added to control wells. Parasites were maintained for 14 days in culture with daily motility scoring and an endpoint MTT readout.

3.4.15. Statistics

Data were tested for normal distribution using D'Agostino & Pearson omnibus normality tests. Data that passed normality tests were analyzed by one-way ANOVA with Tukey's multiple comparisons tests. Data significantly different from a normal distribution were analyzed using Kruskal-Wallis with Dunn's multiple comparisons tests. Significance was defined at alpha <0.05 and analyzed using GraphPad Prism v6.0h.

Survival curves were compared using Mantel-Cox log-rank tests.

3.1. Results

3.1.1. Comparison of gerbil, CB.17 SCID and selective cytokine knockout infection models in the propagation and long-term maintenance of *B. malayi* adults

Parasitological readout data from *Meriones gerbil* (jird), CB.17 SCID and BALB/c IL4R α ^{-/-}/IL5^{-/-} mouse *B. malayi* intra-peritoneal infections were collated from 32 independent experiments, spanning between 2012-2018. Length of experimental infections ranged between 12-52 weeks Adult worm recoveries were expressed as a percentage of the initial *BmL3* inoculation into animals, to allow for comparisons across species and strains. The mf yields in the peritoneum were normalised to number of female *B. malayi* worms present, to allow accurate comparisons of mf production in different infection models.

One-way ANOVA and Kruskal-Wallis analyses (with post-hoc pairwise testing) were applied to determine significant differences in the parasite recoveries between the above species and strains. In terms of total percentage of *B. malayi* adults recovered, gerbils yielded a median 4% of initial inoculate (range = 0-46%) whilst CB.17 SCID and BALB/c IL4R α ^{-/-}/IL5^{-/-} infected mice produced 13% (range = 0-49%) or 12% (range = 0-59%) of initial infectious inoculate, respectively (Figure 3.1.A). This equated to a ≥ 3 -fold increase in adult filarial yields (Kruskal-Wallis statistic = 32.82, $P < 0.0001$ gerbils vs CB.17 SCID or IL4R α ^{-/-}/IL5^{-/-} mice, Dunn's multiple comparisons test). Yields between CB.17 SCID and IL4R α ^{-/-}/IL5^{-/-} mice were not significantly different. When comparing yields of female *B. malayi*, gerbils yielded a median 2% (range = 0-35.5%) of initial inoculate whilst CB.17 SCID and BALB/c IL4R α ^{-/-}/IL5^{-/-} infected mice produced 9% (range = 0-42%) and 10% (range = 0-48.7%) of initial infectious inoculate, respectively (Figure 3.1.B). This equated to a 4 or 5-fold increase in adult female yields (Kruskal-Wallis statistic = 40.83, $P < 0.0001$ gerbils vs CB.17 SCID or IL4R α ^{-/-}/IL5^{-/-} mice, Dunn's multiple comparisons tests). Male *B. malayi* yields were 1.5% (range = 0-26%) of initial

CHAPTER 3

inoculate for gerbils and 3% (range = 0-14%) and 2.3% (range = 0-18%) of initial infectious inoculate, respectively for CB.17 SCID and BALB/c $IL4R\alpha^{-/-}/IL5^{-/-}$ mice (Figure 3.1.C). This equated to a 2 or 1.3-fold increase in adult male adult burdens (Kruskal-Wallis statistic = 15.35, $P < 0.001$ gerbils vs CB.17 SCID or $IL4R\alpha^{-/-}/IL5^{-/-}$ mice, Dunn's multiple comparisons test).

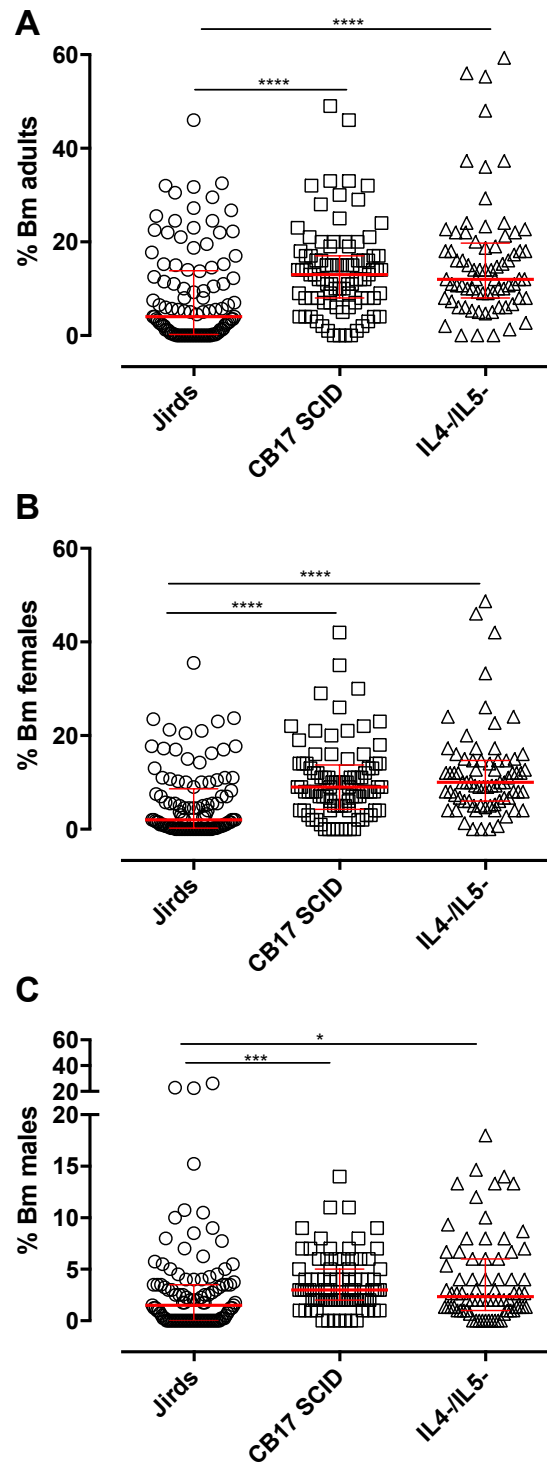


Figure 3.1. Meta-analysis comparison of filarial adult parasitological yields 12-52 week age-infections in gerbils, CB.17 SCID or BALB/c IL-4 $\alpha^{-/-}$ /IL-5 $^{-/-}$ mice

Parasites recovered per strain/species of mice and jirds as (A) total % of *Bm*, (B) % of female *Bm* parasites recovered, (C) % of male *Bm* parasites recovered at 12-52 week infections. Each point represents the amount of parasites recovered from a single animal. Horizontal lines represent mean values. Error bars represent standard error of the mean. Significance is indicated as **** $P \leq 0.0001$, *** $P \leq 0.001$, ** $P \leq 0.01$, * $P \leq 0.05$.

These pooled data were then grouped into different age-of-infection time points (12-25 weeks and >25 weeks) for further analyses to scrutinise whether differences between yields in gerbils and immunodeficient mice varied with chronicity of patent infection.

In the 12-25 week age of infection, the total percentage of *B. malayi* adults recovered from gerbils yielded a median 5.9% of initial inoculate (range = 0-46%) whilst CB.17 SCID and BALB/c IL4R $\alpha^{-/-}$ /IL5 $^{-/-}$ infected mice produced 13% (range = 0-46%) or 14.7% (range = 0-56%) of initial infectious inoculate, respectively (Figure 3.2.A). This equated to a >2-fold increase in adult filarial yields (Kruskal-Wallis statistic = 12.43, $P < 0.0020$ gerbils vs SCID or IL4R $\alpha^{-/-}$ /IL5 $^{-/-}$ mice, Dunn's multiple comparisons test). Yields between CB.17 SCID and IL4R $\alpha^{-/-}$ /IL5 $^{-/-}$ mice were not significantly different. When comparing yields of female *B. malayi*, gerbils yielded a median 3.9% (range = 0-35.5%) of initial inoculate, whilst CB.17 SCID and BALB/c IL4R $\alpha^{-/-}$ /IL5 $^{-/-}$ infected mice produced 8% (range = 0-42%) and 11% (range = 0-42%) of initial infectious inoculate, respectively (Figure 3.2.B). This equated to a >2-fold increase in adult female yields (Kruskal-Wallis statistic = 17.81, $P < 0.0001$ gerbils vs SCID or IL4R $\alpha^{-/-}$ /IL5 $^{-/-}$ mice, Dunn's multiple comparisons test). Male *B. malayi* yields were 2.3% (range = 0-26%) of initial inoculate for gerbils and 3% (range = 0-11%) and 2.7% (range = 0-18%) of initial infectious inoculate, respectively, for CB.17 SCID and BALB/c IL4R $\alpha^{-/-}$ /IL5 $^{-/-}$ mice (Figure 3.2.C). This equated to a >1-fold increase in adult male *B. malayi* burdens (Kruskal-Wallis statistic = 19.58, $P < 0.0001$ gerbils vs SCID or IL4R $\alpha^{-/-}$ /IL5 $^{-/-}$ mice, Dunn's multiple comparisons test).

In the later age of infection (>25 weeks) the total percentage of *B. malayi* adults recovered from mice were again markedly increased in the mouse strains compared to gerbils. More specifically, gerbils yielded a median 0.5% of initial inoculation (range = 0-29.5%), whereas CB.17 SCID and BALB/c IL4R $\alpha^{-/-}$ /IL5 $^{-/-}$ infected mice produced 13% (range = 0-49%) and 10% (range = 0-59%) of initial inoculates, respectively (Figure 3.2.D). This equated to a >20-fold increase in adult filarial yields (Kruskal-Wallis statistic = 18.98, $P < 0.0001$ gerbils vs SCID or

IL4R $\alpha^{-/-}$ /IL5 $^{-/-}$ mice, Dunn's multiple comparisons test). Yields between the two mouse strains were not significantly different. Upon analysis of female *B. malayi*, gerbils yielded a median 0.3% (range = 0-23.8%) of initial inoculate, whilst CB.17 SCID and BALB/c IL4R $\alpha^{-/-}$ /IL5 $^{-/-}$ infected mice produced 9% (range = 0-35%) and 8.5% (range = 0-48.7%), respectively (Figure 3.2.E). This equated to an >28-fold increase in adult female burdens (Kruskal-Wallis statistic = 18.98, P<0.0001 gerbils vs CB.17 SCID or IL4R $\alpha^{-/-}$ /IL5 $^{-/-}$ mice, Dunn's multiple comparisons test) (Figure 3.2.F). A similar pattern ensued when adult male recoveries were evaluated. Male *B. malayi* yields were 0.1% (range = 0-5.8) of initial inoculate for gerbils, and 3% (range = 0-14%) and 2.3% (range = 0-13.3%) for CB.17 SCID and BALB/c IL4R $\alpha^{-/-}$ /IL5 $^{-/-}$ mice, respectively. This equated to a 3-fold increase in adult male *B. malayi* burdens (Kruskal-Wallis statistic = 19.58, P<0.0001 gerbils vs CB.17 SCID or IL4R $\alpha^{-/-}$ /IL5 $^{-/-}$ mice, Dunn's multiple comparisons test).

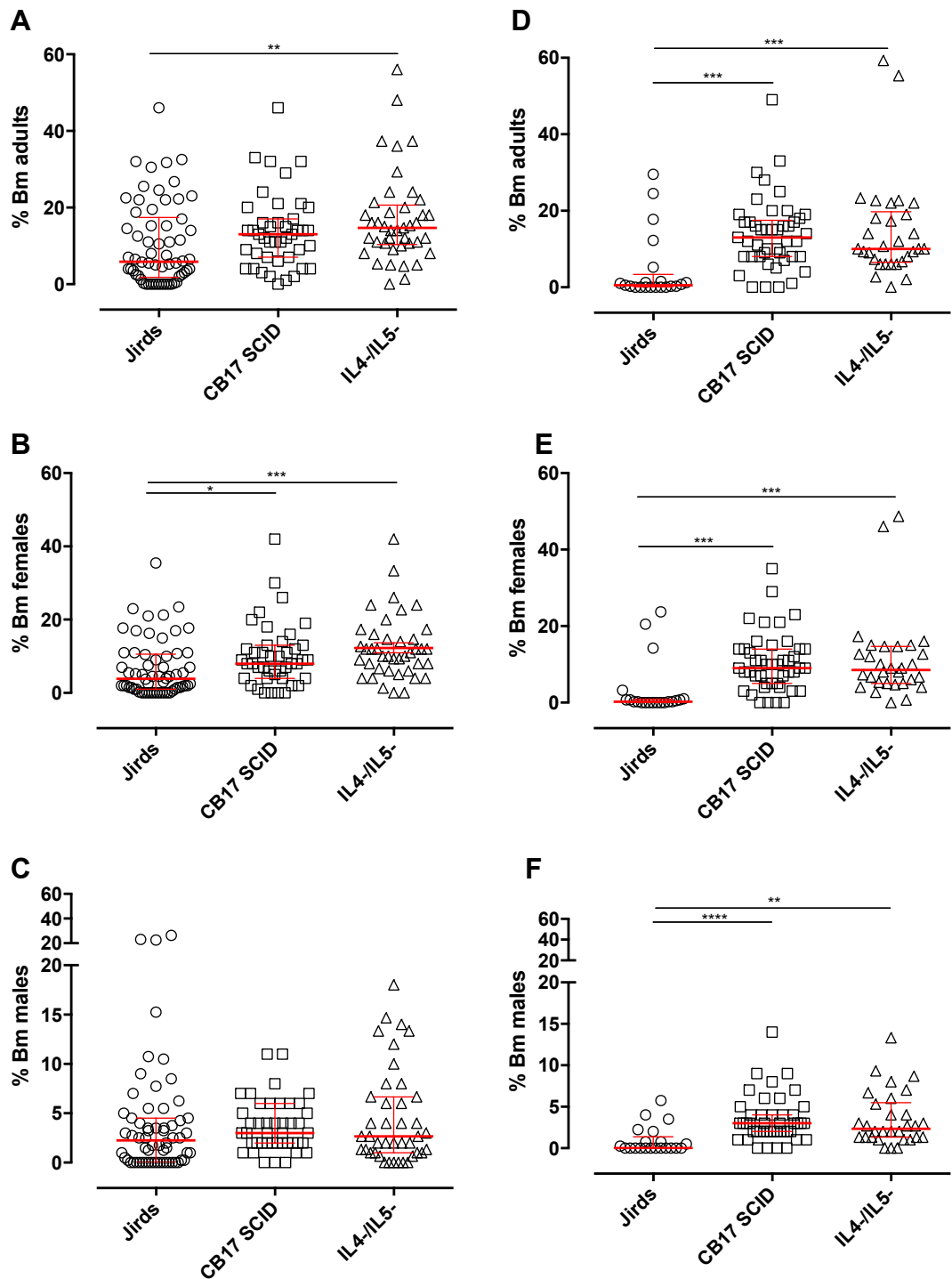


Figure 3.2. Meta-analysis comparison of filarial adult parasitological yields in separated 12-25 week and >25 week age infections in gerbils, CB.17 SCID or BALB/c IL-4R α ^{-/-}IL-5^{-/-} mice 2

Total parasite recoveries per strain/species of mice and jirds as (A) total % of *Bm* in 12-25wk infections (B), % of female *Bm* parasites recovered in 12-25wk infections (C), % of male *Bm* parasites recovered in 12-25wk infections (D), total % of *Bm* in >25wk infections (E), % of female *Bm* parasites recovered in >25wk infections (F), % of male *Bm* parasites recovered in >25wk infections. Each point represents amount of parasites recovered from an individual animal. Horizontal lines represent mean values. Error bars represent standard error of the mean. ***P \leq 0.001, **P \leq 0.01, *P \leq 0.05.

3.1.2. Comparison of gerbil, CB.17 SCID and selective cytokine knockout infection models in the propagation of *B. malayi* microfilariae

In addition to evaluating adult parasite recoveries, the numbers of mf released per female worm were evaluated to determine whether any differences in yield across species and strain occurred, and if these differed with chronicity of infection (Figure 3.3.).

Overall, the number of mf released per female worm in gerbils was a median of 7.4×10^4 (range = 1.7×10^3 - 2.6×10^5), whilst the number of mf released/female in CB.17 SCID and BALB/c IL4R $\alpha^{-/-}$ /IL5 $^{-/-}$ infected mice was approximately 5-fold and 20-fold lower, with median mf releases of 1.5×10^4 (range = 17.3 - 6.4×10^5) and 3.5×10^3 (range = 45.18 – 9.4×10^4), respectively, per female worm (Kruskal-Wallis statistic = 22.27, $P < 0.0001$ gerbils vs CB.17 SCID or IL4R $\alpha^{-/-}$ /IL5 $^{-/-}$ mice, Dunn's multiple comparisons test) (Figure 3.3.A).

In 12-25 week infections, gerbils yielded a median of 7.4×10^4 (range = 3.0×10^4 - 2.6×10^5) mf/female, whilst CB.17 SCID and BALB/c IL4R $\alpha^{-/-}$ /IL5 $^{-/-}$ infected mice produced median yields of 1.5×10^4 (range = 17.3 - 6.34×10^5) and 4.5×10^3 (range = 45.18 - 9.4×10^4), respectively (Figure 3.3.B). This equated to a 5-fold and 16-fold decrease in the number of mf released/female in CB.17 SCID and IL4R $\alpha^{-/-}$ /IL5 $^{-/-}$ infected mice, respectively, in comparison to infected gerbils (Kruskal-Wallis statistic = 23.89, $P < 0.0001$ Dunn's multiple comparisons test).

In >25 week age infections, female *B. malayi* were continuing to release mf across the two mouse strains and gerbils, with no significant differences in mf release between strains or species (Figure 3.3.C). Gerbils yielded a median of 1.7×10^4 (range = 0 - 4.2×10^5) mf/female, whereas CB.17 SCID and BALB/c IL4R $\alpha^{-/-}$ /IL5 $^{-/-}$ infected mice produced yields of 5.1×10^4 (range = 1.5×10^4 - 2.3×10^5) and 1.0×10^4 (range = 2.7×10^3 - 9.4×10^4) mf/female, respectively. This

equated to a >0.4-fold decrease in the number of mf released/female in CB.17 SCID and IL4R α ^{-/-}/IL5^{-/-} infected mice, respectively, in comparison to infected gerbils.

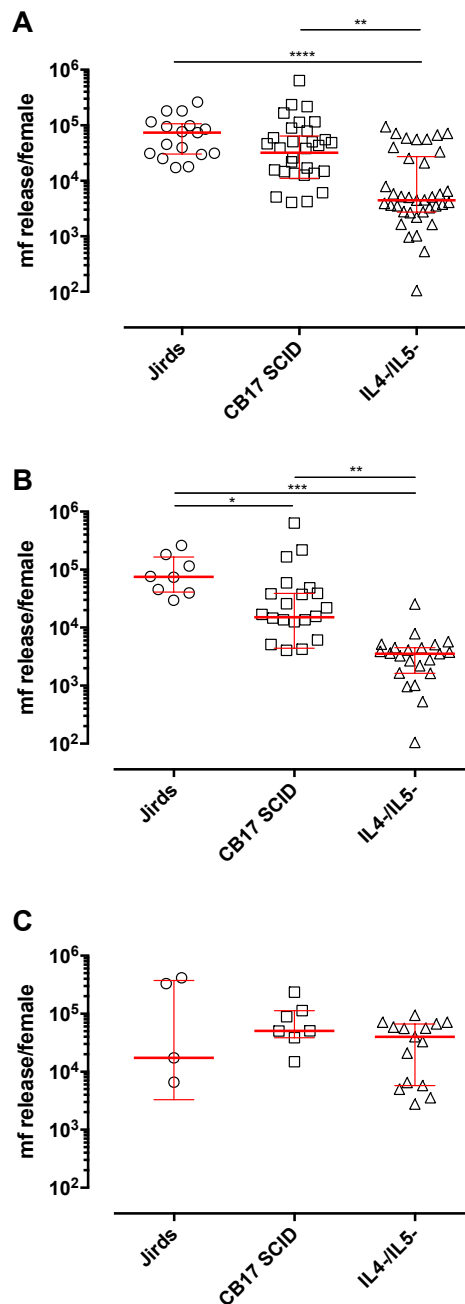


Figure 3.3. Meta-analysis comparison of the propagation of microfilariae of 12-52 week age-infections in gerbils, CB.17 SCID or BALB/c IL-4R α ^{-/-}/IL-5^{-/-} mice

Total number of microfilariae recovered per female *B. malayi* in gerbils, CB.17 SCID or BALB/c IL-4R α ^{-/-}/IL-5^{-/-} mice across all ages of infection (12-52 week) (A), number of microfilariae recovered per female *B. malayi* in 12-25 week infections (B), number of microfilariae recovered per female *B. malayi* in >25 week age infections (C). Each point represents an individual animal. Bars represent median \pm interquartile range. Significance is indicated as ****P \leq 0.0001, ***P \leq 0.001, **P \leq 0.01, *P \leq 0.05.

Table 3.1. Summary of parasitology between gerbils, CB.17 SCID mice and IL-4R α ^{-/-}/IL-5^{-/-} mice

Strain	Total median recoveries (%) (range, total n)	Total average recoveries (%) (range, total n)	% infections not producing males (total n)	% infection failure rate (total n)
Jird	4 (0-32.5, 105)	8.3 (0-32, 105)	34 (105)	19.2 (105)
CB.17 SCID	13 (0-49, 88)	13.8 (0-49, 88)	7.9 (88)	4.5 (88)
IL4R α ^{-/-} /IL-5 ^{-/-}	12 (0-59.3, 72)	15.8 (0-59, 72)	12.5 (72)	4.1 (72)

3.1.3. Initial optimisation of an adult *B. malayi* culture system

Initial experimentation was conducted to determine the average lifespan of male and female *B. malayi* (*Bm*) adult parasites in culture following isolations from IL-4R α ^{-/-}/IL-5^{-/-} mice and which, if any, mammalian cell type promoted survival. Metabolic activity post-culture was compared to parasites freshly isolated from mice as a reference positive control.

Female or male *B. malayi* parasites, isolated from IL4R α ^{-/-}/IL-5^{-/-} mice at between 12-25 weeks post-infection, were cultured into 6 well plates at a density of 2 parasites/well onto either a human adult dermal lymphatic microvascular endothelial cell monolayer (LEC); a human kidney epithelial cell monolayer (HEK294), or their subsequent cell media, EGM-2 MV or DMEM, respectively. Motility and survival were assessed daily and quantitative viability readouts (MTT) were taken at 14 and 28 day time-points (Figure 3.4.A).

Although survival over the 28 day culture period was not determined to be significantly different between culture conditions, by day 21 survival was highest in female *B. malayi* maintained on the LEC monolayer, whereby 95% survived (46/48 females) (Figure 3.4.B). This compared with a survival of 78% for female *B. malayi* maintained on HEK monolayers (38/48 females) 74% (36/48 females) for female *B. malayi* maintained on cell-free DMEM 5% FCS

culture medium and 68% (32/48 females) for female worms maintained on cell-free EGM-2 MV culture medium (Mantel-Cox log-rank test, $P=0.3875$).

By the end of the culture period on day 28, survival had declined across all culture conditions. Female *B. malayi* maintained on the LEC monolayer had the highest survival, with 29% of parasites surviving (8/24 females). Comparatively, 6% of female *B. malayi* survived on HEK monolayers (2/24 females) whilst *B. malayi* maintained in equivalent cell-free culture medium had declined to 5% survival (1/24 females) or 0% survival (0/24 females) for DMEM and EGM-2 MV 5% FCS, respectively (Mantel-Cox log-rank test, $P=0.3875$).

Regarding motility assessments, surviving female *B. malayi* cultured on LEC monolayers retained on average, a full motility score emulating *in vivo* isolated filariae, up until day 16 (Figure 3.4.C). Comparatively, average motility of surviving female *B. malayi* began to decline in other culture conditions from day 12. By statistical analysis of individual female filaria motility scores at day 14, it was confirmed that female *B. malayi* maintained on LEC monolayers were significantly higher than those maintained on HEK monolayers, DMEM 5%FCS and EGM-2 MV 5% FCS culture groups (Kruskal-Wallis statistic = 17.47, $P=0.0006$ with Dunn's multiple comparisons test) (Figure 3.4.D).

By the end of the culture period, by day 28, the minority of surviving female *B. malayi* all exhibited a similar decline in motility in all culture conditions, whereby all female parasites exhibited a twitching phenotype (Figure 3.4.E).

In terms of quantitative MTT viability assessments, at 14 days post-culture, female *B. malayi* parasites cultured on the LEC monolayer displayed similar metabolic activity compared to freshly isolated *in vivo* worms, with on average, a non-significant, 15% reduction in MTT reductase activity compared to median *in vivo* control female filariae (median control optical density = 0.48) (Figure 3.4.F). In comparison, metabolic activity of female parasites cultured on HEK monolayers, DMEM 5%FCS or EGM-2 MV 5% FCS were reduced by 83%, 75% and

CHAPTER 3

58%, respectively. The decline in metabolic activity in HEK monolayers versus LEC monolayers was significant (Kruskal-Wallis statistic = 11.4, $P=0.0098$, Dunn's multiple comparisons test). By day 28 of the culture period, viability had diminished by $\geq 90\%$ in all groups compared with freshly isolated adult female filariae (Figure 3.4.G).

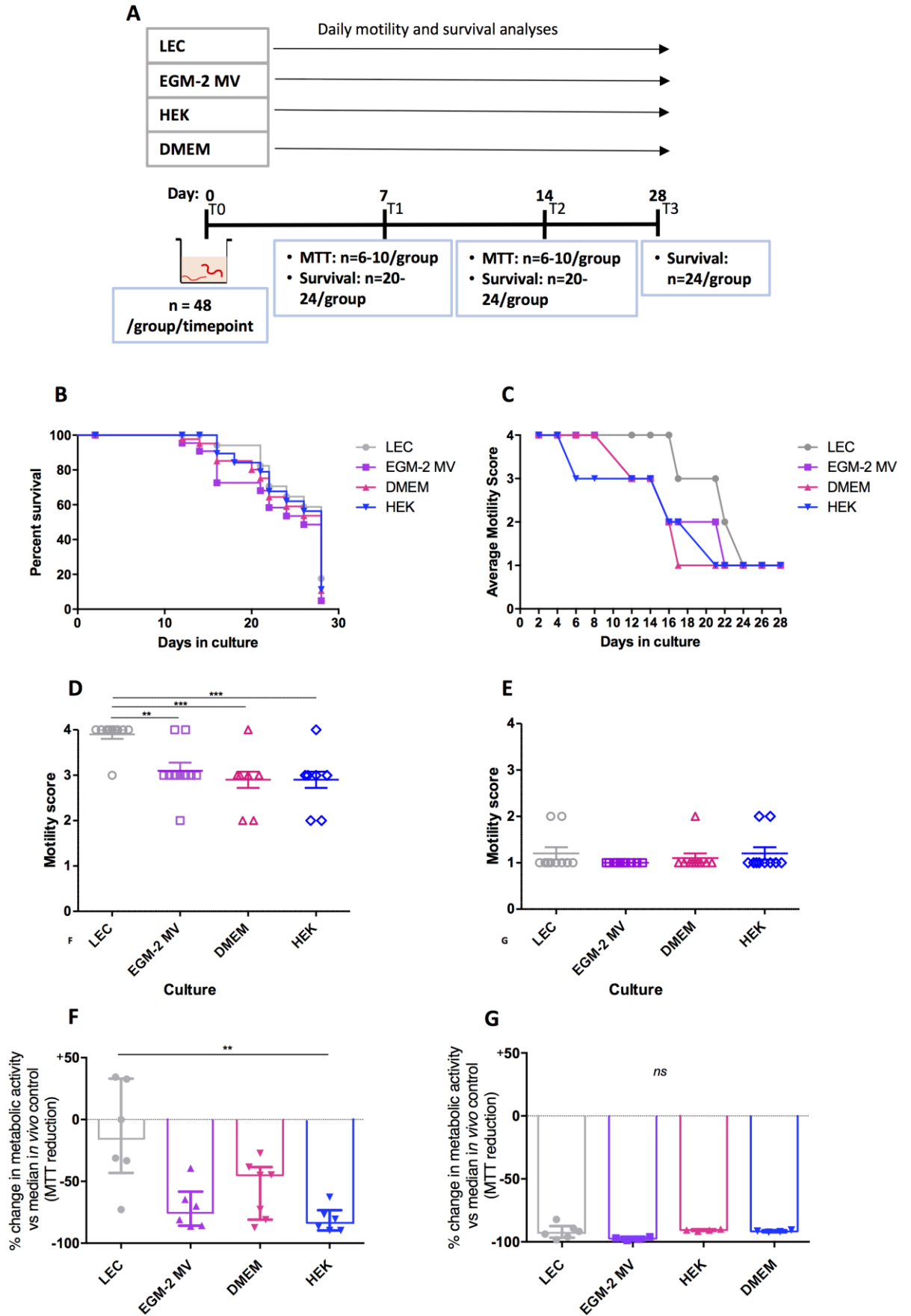


Figure 3.4. Initial optimisation of female *B. malayi* cultures for 28 days with and without specific human cell monolayers

Experimental set-up schematic; adult female *Bm* cultured at 37°C, 5% CO₂ for 28 days (2/well in 6-well plates) with and without the presence of cells with daily survival/motility monitoring and MTT reductase activity taken at day 14 and day 28 end-point (A) Kaplein-Meier survival curves across 28 day culture (B), average motility scores of surviving worms over 28 days (C), motility score assessments of individual worms at 14 (D), and 28 days (E), MTT viability assessments at 14 days (F) and 28 days expressed as percentage change in MTT reductase activity from *in vivo* control median level. Each point represents a measure from an individual adult *B. malayi* female. Horizontal bars represent either the mean (D-E) or median (F-G). Error bars represent either standard error of the mean (D-E) or interquartile range (F-G). ***P≤0.001, **P≤0.01,

Compared to females, male *B. malayi* parasites cultured under the same conditions deteriorated more rapidly during the culture period (Figure 3.5.C). By day 14, survival had declined with only 50% (24/48) of males surviving on LEC monolayers. 40% (19/48) survival was observed with males cultured on HEK monolayers, whilst 46% (22/48) had survived in DMEM 5% FCS and 42% (20/48) survived in EGM-2 MV. By the end of the culture period at day 28, 0% survival was apparent in *male B. malayi*, irrespective of culture condition. No differences were apparent across the different conditions when tested with Mantel-Cox log rank tests.

In terms of motility assessments, all culture conditions, with the exception of the LEC monolayer, induced a decline in parasite motility early into culture (Figure 3.5.B). By day 14, male *B. malayi* maintained on the LEC monolayer displayed a significantly higher motility in comparison to the other culture conditions tested (Kruskal-Wallis statistic = 38.48, P<0.0001, with Dunn's multiple comparisons test) (Figure 3.5.D). Motility continued to decline across all cultures until the 28 day end-point, where at this point all males had perished (Figure 3.5.E).

In terms of quantitative viability assessments at days 14 and 28, *B. malayi* males across all culture conditions had reduced MTT reductase activity of a median of 100% in comparison

CHAPTER 3

to the median control group (median control optical density = 0.32) (Figure 3.5.F+G). This confirmed parasite death as opposed to merely a periodic loss of motility.

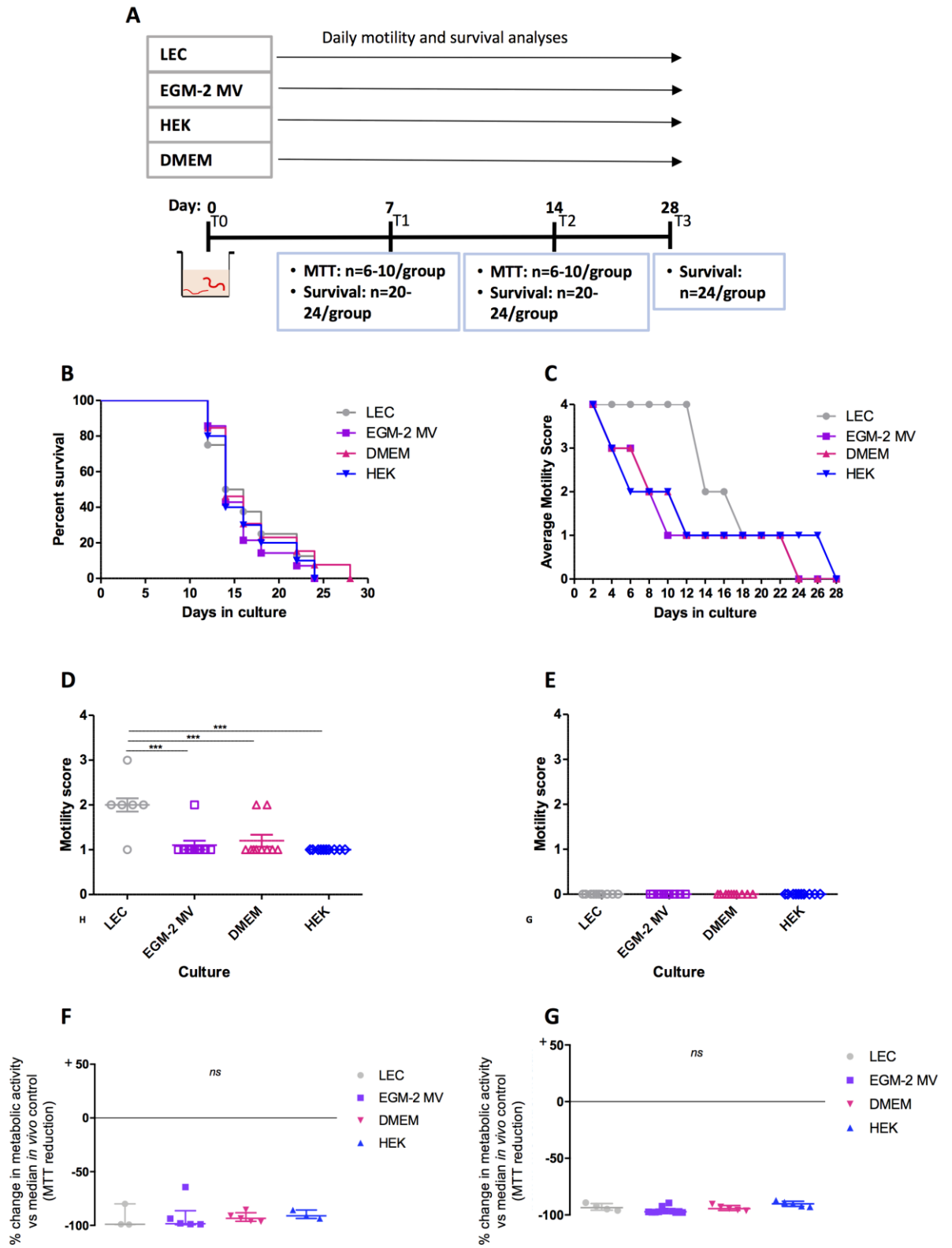


Figure 3.5. Initial optimisation of male *B. malayi* cultures for 28 days with and without specific human cell monolayers

Experimental set-up schematic; adult male *Bm* cultured at 37°C, 5% CO₂ for 28 days (2/well in 6-well plates) with and without the presence of cells with daily survival/motility monitoring and MTT reductase activity taken at day 14 and day 28 end-point (A) Kaplein-Meier survival curves (B), average motility scores (C), individual 14 day motility scores (D), individual 28 day motility scores (E), 14 day MTT viability assay (F), 28 day MTT viability assay, expressed as percentage change in MTT reductase activity (viability) from *in vivo* control median level (G). Each point represents a measurement from an individual adult *B. malayi* male. Horizontal bars represent either the mean (D-E) or median (F-G). Error bars represent either standard error of the mean (D-E) or interquartile range (F-G). ***P<0.001, **P<0.01.

3.1.4. Evaluation of microfilariae release during culture period of female or female+male *B. malayi*

In order to scrutinise mf release over the culture period, and evaluate whether mixed sex cultures extended mf release, two *B. malayi* females, or two females and two males were placed into individual culture wells on either LEC monolayers or corresponding cell free EGM-2 MV media. Due to the rapid deterioration of male *B. malayi* viability *in vitro*, cultures were limited to 10 days. At each time point, released mf derived from cultures were pooled to generate an average mf count which was then adjusted for number of female worms (Figure 3.6).

Mf release peaked at day 4 in culture except for mixed sex LEC cultures, which peaked on day 5. At peak mf production, levels of mf were: 3125 mf/female for female only LEC cultures, 2200 mf/female for female + male LEC cultures, 2225 mf/female for female only EGM-2 MV cultures and 1387 mf/female for female + male EGM-2 MV cultures. When cultured on LEC feeder cells, female only cultures were 29% and mixed sex cultures were 37% higher than corresponding peak mf production in cell free medium. Post 5 days in culture, mf release began to decline in each condition. The cease in mf production occurred more rapidly in females cultured in EGM-2 MV, whereby production ceased at day 8 in female only cultures, and day 6 in mixed sex cultures. Females cultured on the LEC monolayer exhibited a more gradual decline in mf release, with low numbers of mf still being released after 10 days in culture (LEC female culture average release 250 mf/female; LEC mixed sex cultures average release 150 mf/female).

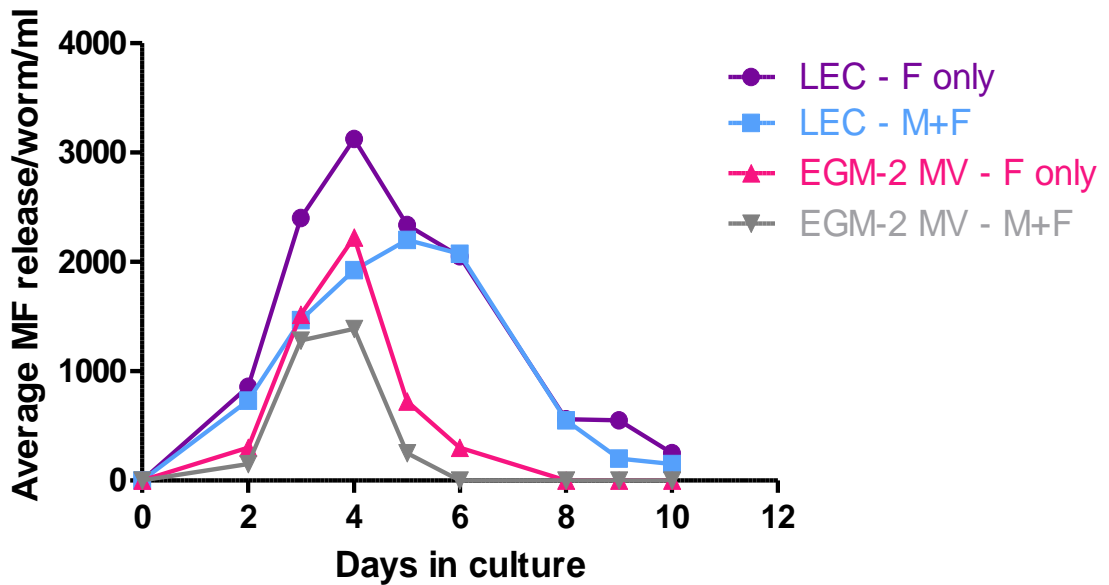


Figure 3.6. mf release per female *B. malayi* over 10 day mixed sex and single sex cultures

Average number of microfilariae released per adult female into culture per culture condition; female only LEC cultures, mixed sex LEC cultures, female only EGM-2 MV (cell-free) cultures, mixed sex EGM-2 MV (cell-free) cultures, every 2 days. Females cultured at 2/well, mixed-sex cultured were 2 females and 2 males/well, both in 6-well plates maintained at 37°C, 5% CO₂ in an incubator.

3.1.5. Evaluation of a trans-well co-culture system to improve the adult female *B. malayi* culture period

After primary experiments to evaluate culture length and optimal cell monolayer were completed, the use of a co-culture trans-well system was tested for improvements to culture longevity sustaining *B. malayi* female parasite viability (Figure 3.7.A). LECs were used, as previously evaluated to be the optimal cell type for culture, sustaining viability and motility comparable to *in vivo* isolates for a period >14<28 days. LEC monolayers were prepared, as previous, and THP-1 human monocyte-derived macrophages, either in a non-polarised state or polarised with recombinant (r)IFN- γ or rIL-4/r13, termed M ϕ (naïve), M ϕ (IFN- γ) or M ϕ (IL-4/13), or an additional monolayer of LECs, were added on top of this layer within a trans-well insert (Figure 3.7.B). Parasites were placed between the monolayer and the insert, with end-

point readouts at day 21. Female *B. malayi* cultured LEC monolayers were used as comparative controls.

Control LEC cultures (LEC monolayers) supported 100% survival for >16 days in culture (Figure 3.7.C). Beyond this point survival decreased slightly, with 88% of female *B. malayi* surviving by the 21 day end-point. In the presence of LEC + M ϕ (naïve) cells, parasite survival was significantly greater, whereby 100% survival was maintained throughout the study (Mantel-Cox log-rank test, P=0.0027). 100% survival was maintained for 15 days in the presence of LEC + M ϕ (IFN- γ) cells, however survival then began to deteriorate, reaching 67% survival by the end-point – significantly lower than the other culture conditions. Female *B. malayi* maintained on LEC + M ϕ (IL-4/13) cells retained 100% survival for >16 days in culture before declining to 96% at day 18 and ending with 80% survival at day 21. 100% survival was achieved throughout the 21 day culture in parasites maintained on the LEC+LEC condition – significantly greater along with the LEC + M ϕ (naïve) condition.

LEC monolayers supported full *B. malayi* motility <8 days although an average motility score of 3 was maintained until d21 (Figure 3.7.D). In contrast, female *B. malayi* cultured in the presence of LEC + M ϕ (naïve) retained full motility for the duration of the study. *B. malayi* cultured in the LEC + M ϕ (IFN- γ) group showed the most marked decline in motility, reaching an average score of 3 by day 8 of the study which further depleted to a score of 2 on the final day. Female worms cultured on LEC + M ϕ (IL-4/13) and LEC + LEC insert exhibited identical motility patterns, whereby full motility was achieved for 16 days, followed by a decrease to an average score of 3 until the end of study at d21. Analysis at endpoint indicated LEC+M ϕ (naïve) and LEC+LEC cultures supported superior motility compared with all other groups (Kruskal-Wallis statistic = 36.27, P<0.0001, with Dunn's multiple comparisons test) (Figure 3.7.E).

After assessing viability (MTT reductase activity) using the MTT assay at end-point, *B. malayi* female parasites cultured on control LEC monolayers exhibited an 80% median reduction in MTT reductase (metabolic) activity in comparison to the *in vivo* control, which was set at 0 (Figure 3.7.F). In the presence of LEC+M ϕ (naïve) cells, parasites displayed significantly increased metabolic activity compared with the control LEC monolayer group, with a 22% median reduction in comparison to the *in vivo* control. *B. malayi* females cultured in the presence of LEC+M ϕ (IFN γ) cells exhibited a more pronounced reduction in metabolic activity, with a median reduction of 69% when compared to those *in vivo*. Female *B. malayi* cultured in the presence of LEC+ M ϕ (IL-4/13) and LEC+LEC displayed median reductions of 26% and 24%, respectively, compared to *in vivo* (Kruskal-Wallis statistic = 12.63, P=0.0132, with Dunn's multiple comparisons test).

CHAPTER 3

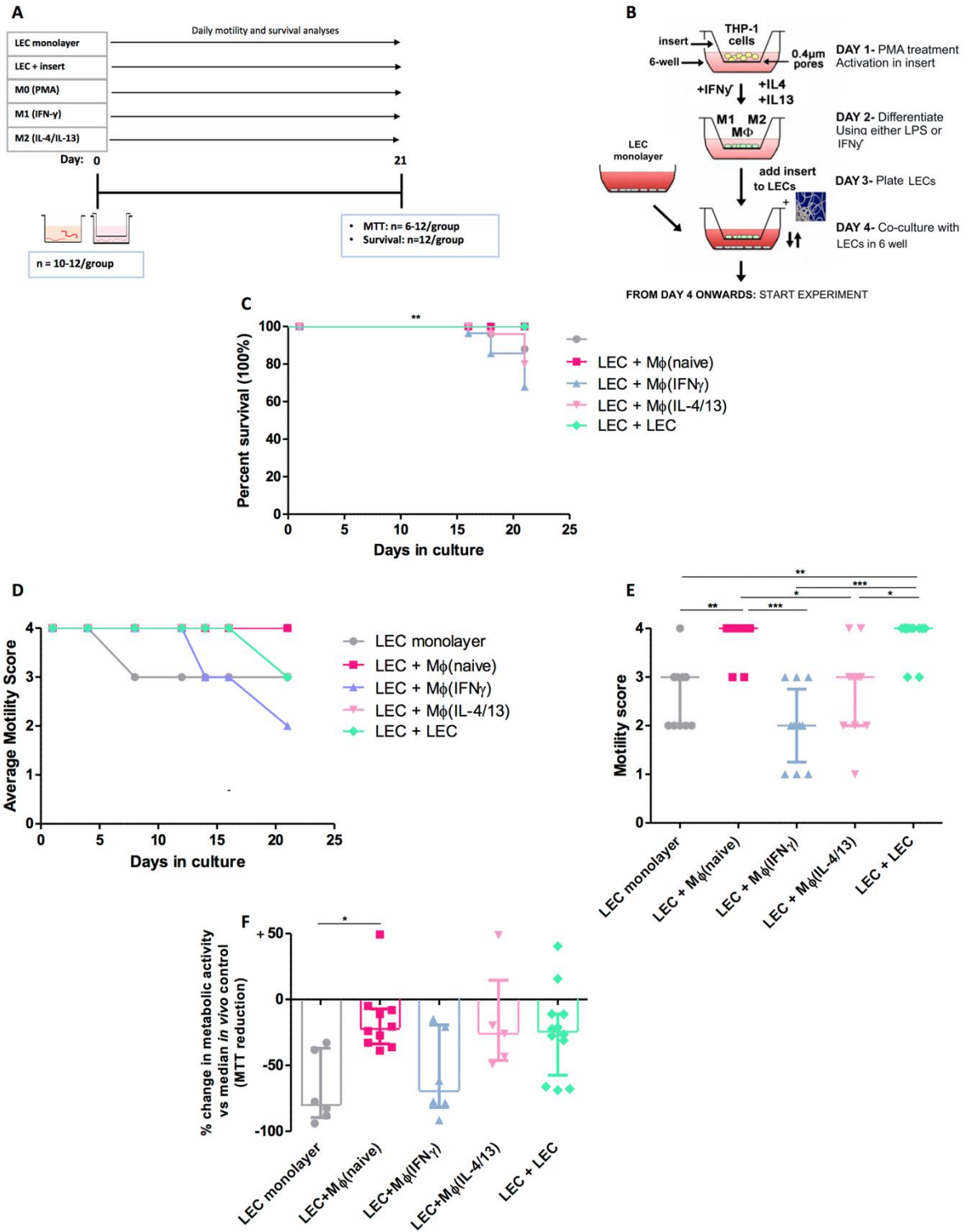


Figure 3.7. 21 day trans-well adult *Bm* female co-culture system with macrophages or LEC bilayers

Experimental set-up schematic; adult female *Bm* cultured at 2F/well in 6-well plates at 37°C, 5% CO₂ for 21 days with daily motility/survival analyses, and end-point MTT reductase activity analysis (A), Macrophage differentiation and co-culture set-up schematic, adapted from <https://bio-protocol.org/e1638> (B), Kaplein-Meyer survival curves across the 21 day culture (C), average motility across the 21d culture (D), individual motility scores at d21 (E,) 21 day MTT reductase viability assay, expressed as percentage change in MTT reductase activity (viability) from *in vivo* control median. Each point represents an average value of 10-12 worms (D) or an individual adult female *B. malayi* (E-F). Horizontal bars represent median values, error bars represent interquartile range. ****P≤0.0001, **P≤0.01, *P≤0.05.

3.1.6. *In vitro* uterine release over a 21 day culture period

Based on initial analysis of mf release in culture, a full analysis of uterine release contents (mf, early morulae 'pre-pretzel', late morulae 'pretzel' and embryos) from female *B. malayi* cultured on LEC monolayers or LEC co-cultures compared with EGM-2 MV cell-free controls were undertaken to evaluate whether culture condition influenced sustained embryogenesis (Figure 3.8). Mature mf release peaked after 3 days in culture, significantly higher than late morulae stages, for all groups (average: EGM-2 MV;9410, LEC monolayer; 9250, LEC co-culture; 4500 /female) (one-way ANOVA $P < 0.0001$ with Tukey's multiple comparisons test), however was not significantly different between culture conditions (Figure 3.7.A). By day 7, mf release had significantly reduced across all culture conditions (Figure 3.7.B) (average: EGM-2 MV, 400; LEC monolayer; 608; LEC co-culture, 204). This trend continued until the end of the study (day 21) (Figure 3.7.C), whereby mf released ceased in the LEC co-culture group and had reduced to an average of 8/female/ml for the EGM-2 MV and LEC monolayer groups. The release of embryos was significantly higher than other embryonic species across all groups at day 7 (Figure 3.7.B) (one-way ANOVA $P < 0.0001$ with Tukey's multiple comparisons test) with an 84% and 96% increase from day 3 analysis for EGM-2 MV (average: 2940/female/ml) and LEC monolayer (average: 5150/female/ml), respectively, and only a 25% increase for the LEC co-culture group (average:1308/female/ml). There was also an increase in the number of pre-pretzel/early morulae stages released from worms in the LEC monolayer group (average: 1000/female/ml) which was significantly higher than the same stage release from the LEC co-culture group (average: 258/female/ml) ($P \leq 0.001$, Kruskal-Wallis post-test). This increase was followed by a slight decrease at day 21, in which the number of embryos released decreased by 6%, 2% and 8% for EGM-2 MV (average: 1475/female/ml), LEC monolayer (average: 825/female/ml) and LEC co-culture (average:

983/female/ml), respectively. The number of embryos released remained significantly higher than mf and pretzel stages from day 7 to day 21. A very low proportion of pretzel/late morulae stages were released over the course of the culture. The only recorded values were those at day 7, in which an average of 66 and 50 /female/ml were released in the LEC monolayer and LEC co-culture groups, respectively.

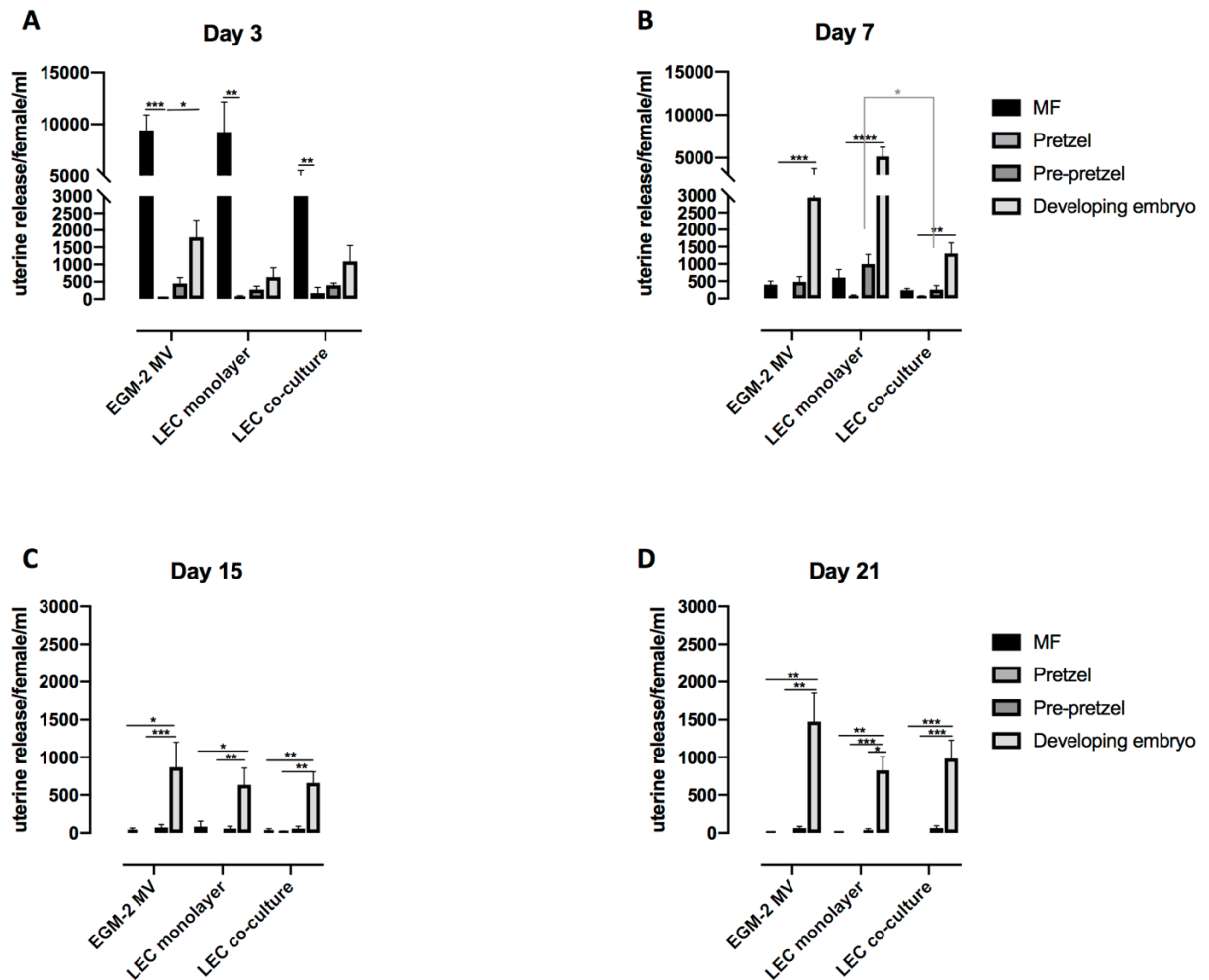


Figure 3.8. 21 day uterine release profiles from cultured female *Bm*

Mf, pretzel/late morulae, pre-pretzel/early morulae and embryo release expressed per female at day 3 (A), day 7 (B), day 15 (C) and day 21 (D) into culture, after collection of media and enumeration by light microscopy. Error bars represent SEM.

**** $P \leq 0.0001$, *** $P \leq 0.001$, ** $P \leq 0.01$, * $P \leq 0.05$. One-way ANOVA, Kruskal-Wallis post-hoc test (intra- and inter-groups).

3.1.7. *Wolbachia* titres in female *B. malayi* post culture

The *Wolbachia* yields within female *B. malayi* after 7, 14 or 21 day culture were compared with levels from parasites immediately retrieved from IL-4R α ^{-/-}IL-5 mice. After one to two weeks in culture, *Wolbachia* loads had declined by on average 55% of *in vivo* controls. By three weeks, levels had declined by 74.4% (Figure 3.9. and Table 3.2.).

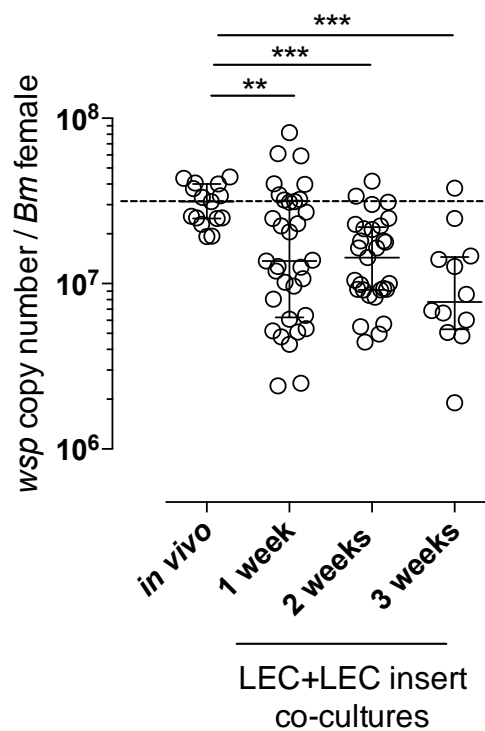


Figure 3.9. Comparison of *Wolbachia* titres over culture period in relation to *in vivo* recovered parasites

Comparisons of *Wolbachia* titres from adult *Bm* females maintained on LEC+LEC co-cultures at 2F/well in 6-well plates maintained at 37°C, 5% CO₂ at 1 week, 2 week and 3 week time-points, compared against those reared *in vivo*. Data is *wsp* copy number estimated by QPCR from individual female *B. malayi* freshly excised from IL-4R α ^{-/-}IL-5^{-/-} mice or following 1-3 weeks in LEC+LEC insert co-cultures. Median and interquartile range values are indicated. Significant differences determined by Kruskal-Wallis one-way ANOVA with Dunn's post hoc tests are indicated **P<0.01 and ***P<0.001.

Table 3.2. Comparison of metabolic activity and *Wolbachia* loads between cultured *B. malayi* female worms and single sex *in vivo* controls

Condition	Median <i>wsp</i> copy number per adult female <i>B. malayi</i> ($\times 10^7$) (range)	Median % change from <i>in vivo</i> control
<i>In vivo</i> isolation	3.13 (1.9-4.4)	-
1 week co-culture	1.4 (0.24-8.2)	55.3%
2 weeks co-culture	1.4 (0.44-4.2)	55.3%
3 weeks co-culture	0.8 (0.19-3.8)	74.4%

Thus far, a 21 day culture period with a trans-well, LEC co-culture 'bi-layer' had been defined as sufficient to maintain female *Bm* survival at $\geq 80\%$ and full motility. However, metabolic activity, whilst not significantly different from *in vivo* isolated females was reduced on average by 25% and *Wolbachia* content declined by between 55-74%. Because mf production was not sustained *in vitro*, the cessation of embryogenesis may have impacted on overall metabolic activity and *Wolbachia* content, compared with freshly isolated, gravid female worms. To more accurately interpret whether quantitative measures of metabolic activity and *Wolbachia* post-culture reflected a real decline in viability of somatic tissues with impact on *Wolbachia* titres or merely reflected reduced embryogenesis and *Wolbachia* replication in developing embryos, female-only *in vivo* implants were utilised as controls.

Eight mice were implanted with either 10 female and 5 male (positive control), or 10 female parasites each and culled for parasite retrieval 14 days later. LEC + LEC insert cultures (n=12), were set up in parallel and removed from culture for analyses at the end-point (Figure 3.10.A).

CHAPTER 3

In terms of metabolic activity, no significant differences were determined between mixed sex vs female only implantations, or cultured females (Figure 3.10.B). Female only implants had an MTT reductase reading 17% lower than those of the mixed sex implants (mixed sex average = 0.66 ± 0.07 ; female only average = 0.55 ± 0.05), whilst the cultured parasites were 24% lower (average = 0.50 ± 0.07).

Insufficient numbers of females were retrieved from male + female implants, therefore female worms from L3 inoculations were recovered to act as the positive 'comparator'. *Wolbachia* titres in female only implants were significantly lower (37%) (2.01×10^7 , range = 2.6×10^5 - 3.62×10^7) than those recovered from mixed sex inoculations (median = 3.27×10^7 , range = 1.93×10^7 - 4.41×10^7) (Kruskal-Wallis statistic = 0.0320, $P < 0.05$). A reduction of 32% was observed in the cultured females (median = 2.2×10^7 , range = 5.68×10^6 - 4.17×10^7), however this was not deemed significant (Figure 3.10.C).

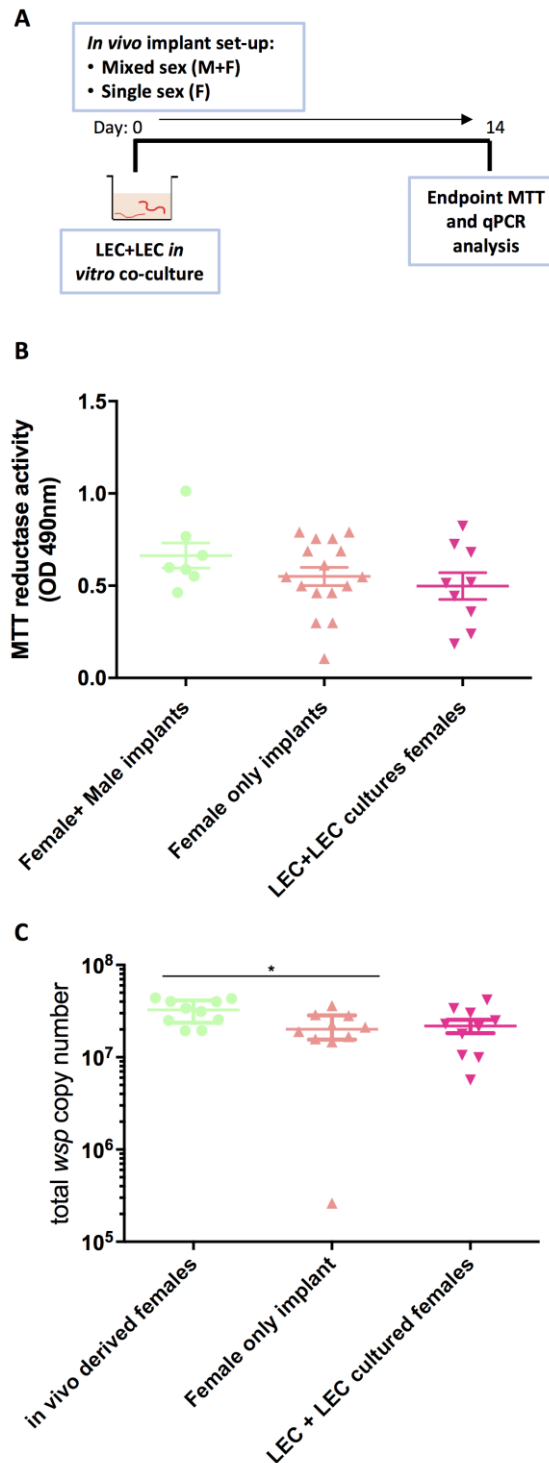


Figure 3.10. Comparison of metabolic activity and *Wolbachia* titres between mixed sex vs single sex implants and cultured females

Experimental set-up schematic; mice surgically implanted with female only or male and female adult *Bm* whilst female *Bm* set up into LEC+LEC trans-well cultures for 14 days with endpoint MTT reductase activity and qPCR *Wolbachia* titre analyses (A), MTT reductase activity of F+M implants, F-only implants and cultured females (B), total *wsp* copy number of F+M implants, F-only implants and cultured females (C). Each point represents an individual female *Bm*. Horizontal bars represent median values, error bars represent interquartile range. *** $P \leq 0.001$, ** $P \leq 0.01$, * $P \leq 0.05$.

3.1.8. Validation of culture system to screen anti-*Wolbachia* drugs

To evaluate the functionality of the optimised LEC + LEC insert culture system as a drug model for assessing anti-*Wolbachia* candidates, the reference drug doxycycline was trialled. Doxycycline (DOX) was added to cultures at a physiologically relevant (peak plasma equivalent) concentration of 5 μM , as previously determined from in-house PK-PD studies. ABBV-4083, a novel orally bioavailable tylosin analogue (“TylAMac”) with proven superior anti-*Wolbachia* activity *in vivo* compared to DOX against adult *B. malayi*, was used at 5 μM to discern whether the co-culture system was of use to determine variation in anti-*Wolbachia* activities between classes of drug. Parasites were dosed for either 7 day, 14 day or 7 day plus a 7 day washout period (n=12/group). Vehicle control groups were set up in parallel for 7d and 14d. Parasites were recovered at the indicated time points to assess *Wolbachia* loads using qPCR (Figure 3.11.A).

Parasite survival was unaffected throughout the study (Figure 3.11.B). Only slight changes were observed in motility, with those in the TylAMac group reducing to a score of 2 by day 14 (Figure 3.11.C).

The median *Wolbachia* load at the end of the 7 day DOX group (median = 5.26×10^6 , range = 1.21×10^6 - 3.46×10^7) displayed a significant decrease in comparison to the vehicle control group (median = 2.3×10^7 , range = 5.10×10^6 - 8.19×10^7 , as did the TylAMac group (median = 3.47×10^6 , range = 2.32×10^6 - 9.76×10^6) (Kruskal-Wallis statistic=22.34, $P < 0.0001$) (Figure 3.11.D). Of the 7 day doxycycline group, a median reduction of 77% was observed, with 26% of parasites reaching the desirable depletion of >90% (Figure 3.11.D). In the case of TylAMac, After 14 days of dosing with DOX, there was again a significant decrease in *Wolbachia* load in comparison to the vehicle control group (Figure 3.11.E) (vehicle control median = 1.44×10^7 , range = 4.43×10^6 - 4.17×10^7 ; 14d DOX median = 3.89×10^6 , range = 1.11×10^6 - 4.33×10^7) (Kruskal-Wallis statistic=22.19, $P < 0.0001$). Here, the median *Wolbachia* depletion was 73%, with 37%

CHAPTER 3

reaching a depletion more than 90% - a greater percentage than those dosed for 7 days. Those dosed for 7 days with DOX followed by a 7 day washout period, exhibited a recrudescence in *Wolbachia* populations (median = 6.17×10^6 , range = 6.76×10^5 - 1.06×10^8). Here, the median *Wolbachia* depletion decreased to 57%. Of that population, only 17% achieved the >90% depletion level. Contrarily, in the TylAMac washout group, the *Wolbachia* recrudescence was not as marked, with median *Wolbachia* reductions of 79% in comparison to the vehicle control (median = 3.02×10^6 , range = 9.89×10^5 - 2.00×10^7) (Figure 3.11.F).

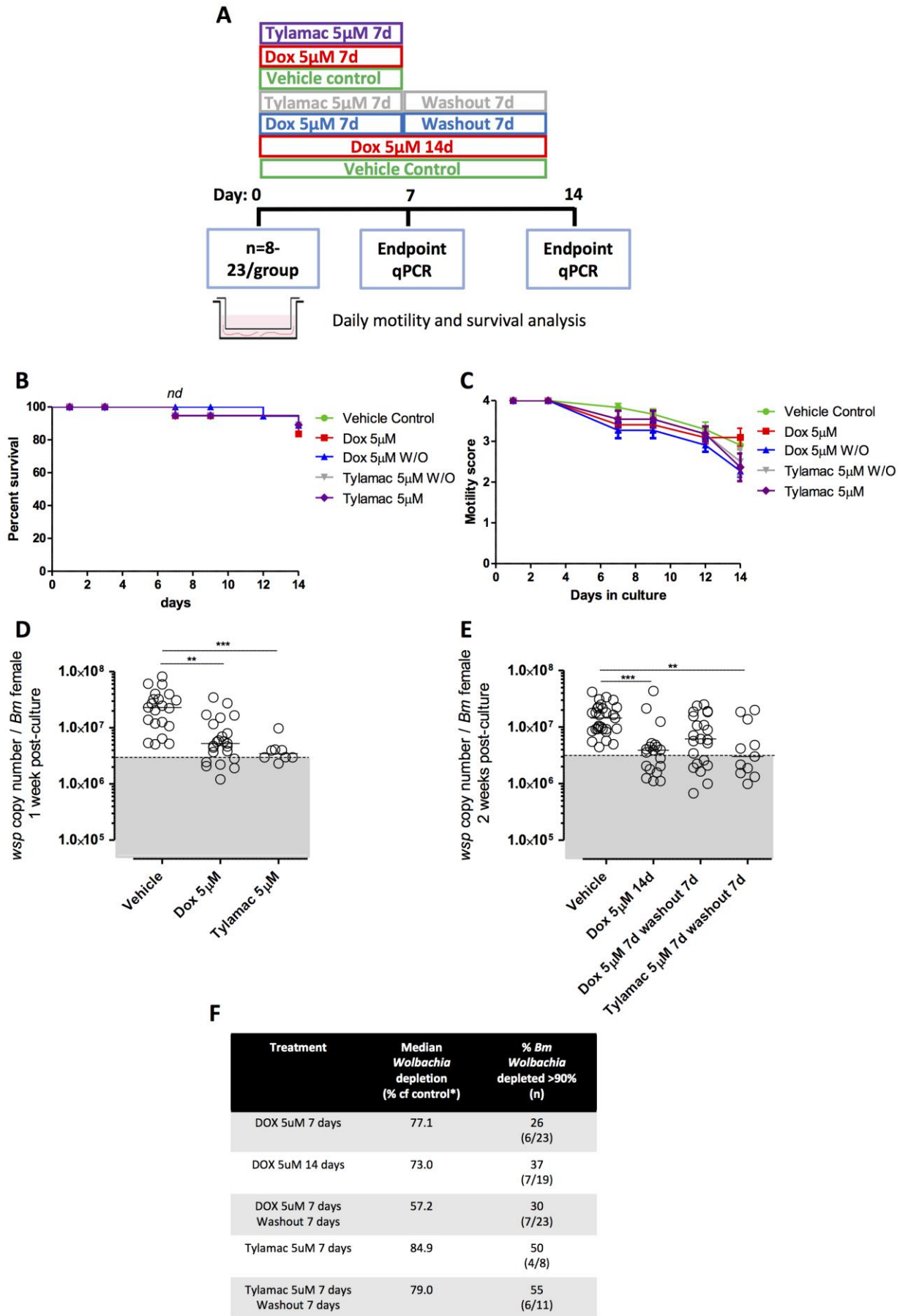


Figure 3.11. Validation of culture system as an A-WOL drug model

Experimental set-up schematic; adult female *Bm* cultured at 2F/well in LEC+LEC 6-well trans-well plates with drug for 7 or 14d with daily motility/survival analysis and endpoint qPCR *Wolbachia* readouts (A), kaplein-meyer survival curves across 14 day timepoint (B), average motility scores over the course of the drug study (C), 7 day *Wolbachia* titre readouts (D), 14 day *Wolbachia* titre readouts (E), *Wolbachia* depreciation summary table (F). Each point represents an average value of 10-12 worms (C). Each point represents an individual adult female *Bm* (D-E). Horizontal bars represent median values, error bars represent interquartile range. ****P≤0.0001, **P≤0.01, *P≤0.05.

3.1.9. Validation of culture system as to screen anti-nematocidal drugs

To assess the utility of the system in evaluating direct-acting macrofilaricidal activity, the reference compounds Flubendazole (FBZ) and Suramin (SUR) were evaluated at 10 μ M. 2 novel DHB compounds, OX2983 and OX3153 were also tested at the same concentration, to determine their potency. A DMSO vehicle group was set up in conjunction as a positive control. Parasites were assessed daily for motility and survival with an endpoint MTT readout to assess metabolic activity as a function of nematocidal drug activity (Figure 3.12.A).

Parasites cultured in the vehicle control group retained 100% survival throughout the course of the study, as was the case with the OX3153 test compound (Figure 3.12.B). After 12 days of drug treatment, parasite survival in the FBZ and SUR groups decreased to 83% and 77%, respectively. Survival further decreased to 50% by day 13 with the FBZ, yet remained unchanged in the SUR group. Day 13 was also the first day a survival decline was observed in the OX2983 group, whereby a decrease to 60% was observed. By the 14 day endpoint, all parasites in the FBZ group had perished, whilst 12% and 20% of parasites survived in the SUR and OX2983 groups, respectively.

Regarding motility, parasites treated with FBZ and SUR exhibited the quickest decline, decreasing by one motility score every two days, before reducing to an average score of 1 by day 6 or 7, respectively (Figure 3.12.C). The DHB test compounds reduced parasite motility slower than the reference drugs, with OX3153 reducing parasite motility to an average score of 1 at day 14. The OX2983 test compound failed to decrease motility any further than an average score of 2, which was observed at day 14. The DMSO control had no effect on motility throughout the study. Due to this, motility curves were compared against this group. Both FBZ and SUR proved to be statistically significant against the DMSO control, whereas

CHAPTER 3

no significance was observed with either of the test compounds (Kruskal-Wallis statistic=19.60, $P=0.0006$).

Further analysis of the endpoint motility assessments determined all test groups to exhibit a significantly lower score than those in the vehicle control group (Figure 3.12.D) (Kruskal-Wallis statistic=26.36, $P<0.0001$).

Following quantitative metabolic activity assessment using the MTT assay, parasites in the DMSO control group displayed the highest MTT reductase activity (Figure 3.12.E) (average OD reading = 0.43). Those treated with FBZ exhibited significantly lower activity, indicating a decrease in viability by 71.8% in comparison to the control group (Kruskal-Wallis statistic=33.14, $P<0.0001$; average OD reading = 0.12). SUR treated parasites displayed a reduction in activity by 28.1%, significantly higher than that of the FBZ treated parasites (average OD reading = 0.31). DHB test compounds OX2983 and OX3153 displayed reductions in activity of 40.8% and 32.2%, respectively, neither of which were deemed significantly different from the control. (OX2983 average OD reading = 0.25; OX3153 average OD reading = 0.43).

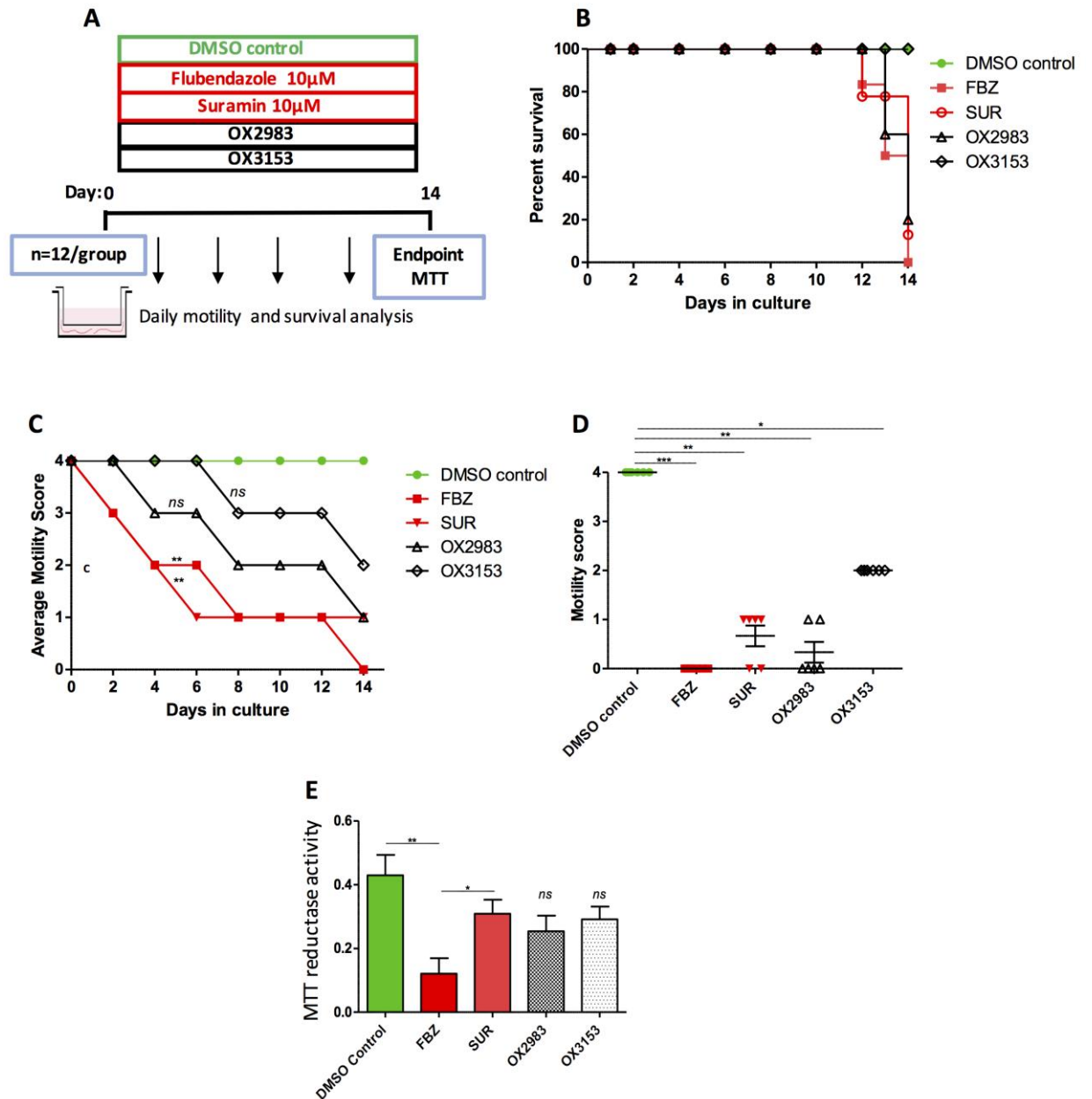


Figure 3.12. Validation of culture model as a direct-acting macrofilaricide drug model

Experimental set-up schematic; adult female *Bm* cultured at 2F/well in LEC+LEC 6-well trans-well plates with drug for 14d with daily motility/survival analysis and endpoint MTT reductase activity analysis (A), Kaplan-Meier survival curves across drug study (B), average motility scores over the course of the drug study (C), day 14 individual motility scores (D), MTT reductase activity of drug treated and DMSO control adult female *Bm* (E). Each point represents an average value of 10-12 worms (C). Each point represents the average motility score per well (total n=6) (D-E). Horizontal bars represent average values, error bars represent standard error of the mean (D). Error bars represent interquartile range (E). ***P<0.001, **P<0.01, *P<0.05.

3.1. Discussion

In vivo models are heavily relied upon for drug efficacy testing of anti-*Wolbachia* drugs in efforts to eliminate filarial disease. Although some *in vitro* drug models exist, they are often not of the correct life cycle stage and focus primarily on direct-acting macrofilaricides. Models existing of the adult stage are only briefly exposed to drugs, and prematurely progressed into *in vivo* screens without extensive assessment. Additionally, most *in vitro* models have not undergone thorough assessment to determine real parasite 'fitness' and have not been validated against *in vivo* models. Combined, these issues heavily impact the outcomes of *in vivo* screens, whereby there are discrepancies in translation from *in vitro* to *in vivo* models, contributing to disappointing success rates, as well as being time consuming, costly, and greatly increasing animal usage.

As there is no system to generate macrofilariae from larval stages *in vitro*, animal models are heavily relied upon to generate parasites. Although Mongolian jirds are an established laboratory model of all filarial life cycle stages (Mutafchiev et al., 2014), variation in parasite load is high and a high incidence of infection failure rate is observed. This thus requires more animals to be infected to compensate. Through an extensive meta-analysis, it was determined that immunodeficient mouse strains serve as an improved model for long term infections, based on parasitological readouts. It was determined that by using either a SCID or BALB/c IL4R α ⁻/IL5⁻ mouse strain, parasite yields could be increased by 66-90% on average and the rate of infection failure was greatly reduced, ultimately reducing the number of animals required for parasite generation. Patent infections were confirmed in all animals of both strains, with the number of males produced per animal higher in mice than jirds. Infection loads remained stable across early and later time points in both mouse strains, further justifying the applicability of these strains for use as an improved model for filariasis and subsequent drug screening. It was however noted that CB.17 SCID mice often

encountered welfare issues post 6 months of infection and occasionally required single housing. Thus, it was determined that the BALB/c IL4R α ⁻/IL5⁻ strain served as a more appropriate model for parasite production, particularly with long-term infections, to reduce and refine animal usage.

In efforts to address the issues with current *in vitro* culture systems, a long-term female *Bm* culture model, capable of supporting worm viability as compared against *in vivo* recovered parasites was developed. Initially, a non-specific human kidney epithelial feeder cell layer (HEK) versus one specific to the parasite's niche habitat (LEC), with their respective cell media were evaluated to determine whether a feeder cell layer aided survival of adult *B. malayi*, and if so, was this due to a specific cell type. The comparative survival durations of male and female worms were also evaluated. At the 14 day time point, LEC monolayers proved superior in aiding female parasite survival and viability, compared to HEK monolayers and both media types. DMEM performed better than both EGM-2 MV and HEKs, despite EGM-2 MV media containing more amino acids and inorganic salts. LECs also appeared to be the superior cell type with male *Bm* culture, although males began to perish earlier into the culture period than females. This was confirmed in both the motility scores and survival curve data. The female *in vitro* model was therefore pursued, which was more informative considering this sex is the ideal drug target, containing higher *Wolbachia* yields and embryonic stages – with the aim of potential drug candidates to reduce *Wolbachia* loads (>90%) and induce sterility in the females.

The interaction between filarial parasites and LECs has been well documented. Studies have recorded effects of LEC specific gene expression and proliferation in response to parasites, which is not apparent with other cell types, during cultures evaluating lymphangiogenesis in filarial infection. The effect on cells has been explored, however the interplay focussing on the parasites is yet to be recorded (Bennuru and Nutman, 2009). The outcomes of this study

suggest longer-term *in vitro* worm survival is dependent on LEC-specific factors, rather than any general feeder cell layer. However, after 4 weeks in culture, parasites from all conditions had perished. This diminishment suggests lymphatic dwelling parasites may potentially have a naturally limited lifespan in culture. Alternatively, the system could be lacking a specific component, or a more complex system involving multiple cell types could be required.

Female parasites sustained mf release for approximately 10 days, when numbers slowly tapered. The potential for *in vitro* mating and fertilisation, to produce progeny in efforts to achieve the life-cycle *in vitro*, was evaluated by conducting mixed sex cultures, however mf release did not persist any further than 10 days. These observations indicate *in vitro* mating and fertilisation is not feasible, however the reasons for this were not explored further. Previous studies on *brugia* and other related helminths have suggested that the downregulation of certain genes and enzymes can impact mf and embryo release and development (Hewitson et al., 2014). However in this *in vitro* model, it is hypothesised that mf release merely ceases due to a lack of re-fertilisation, due to parasites having comparable *Wolbachia* titres and metabolic activity to those recovered *in vivo*, which suggests parasites are otherwise healthy.

In light of these observations, a culture extension to 21 days was attempted. For this, a LEC co-culture system with the addition of macrophages, differentiated from THP1 cell lines was trialled. It was hypothesised that macrophages, and more specifically alternatively -activated type macrophages polarised by IL-4 and IL-13, could provide other secreted survival factors due to their association in filarial infection, whereby their activation status is linked to the secretion of wound healing growth factors, that may be also beneficial for worm survival (Babu and Nutman, 2012, Gause et al., 2013). Further, macrophages and other immune cells, including peripheral blood mononuclear cells (PBMCs), have already been proven to support larval survival in *brugia* and *onchocerca* (Turner et al., 2018, Voronin et al., 2019).

It was found that M ϕ (IL-4/13) co-cultures enhanced parasite survival from 2 to 3 weeks whereas parasites co-cultured with macrophages classically activated with IFN-g, rapidly deteriorated in health, potentially mirroring *in vivo* events. Unpolarised M ϕ co-cultures also extended survival to 3 weeks. This was potentially due to the macrophages being polarised towards an M2-like phenotype, typical of helminth infections, as a result of the cross talk between LECs and/or adult female *B. malayi*. Whilst this was not further explored within the scope of these studies, it does illustrate an onward basic biology application of the human co-culture system to study the complex interplay between multiple host cells and filarial parasite excretory / secretory molecules *in vitro*. Furthermore, LEC co-cultures in the trans-well were found to offer the same survival advantage as the unpolarised M ϕ and M ϕ (IL-4/13) co-culture systems. This may indicate that the physical environmental changes created by an insert and cell bilayer is sufficient to prolong survival. It was noted that the *B. malayi* parasites frequently migrated into the 'lumen' between the vertical plastic surface and insert. For simplicity, therefore, LEC+LEC co-culture system was selected for further validation of the model, as the addition of M2-like, M1-like, or unpolarised M ϕ into the system offered no significant survival advantage in comparison to LEC trans-wells, and were more laborious and costly to set up. It was thus hypothesised that this extended longevity of the system when using LEC co-cultures could be due to an advantageous effect of surface expression molecules on cells, which may be upregulated in response to the parasites, or more simply, the physical contact with worms and the LEC bilayer (Evans et al., 2016). However, further research is required to fully elucidate the specific effect of these upon parasite longevity *in vitro*.

To further evaluate *in vitro* parasite 'fitness', surgical implantation studies were conducted in which parasites recovered from the same cohort of donor mice were cultured or implanted into recipient mice, to allow for cross comparisons *ex vivo*. Female-only implants were also included to ensure a sex relevant *in vivo* control and to account for any discrepancies in

viability due to the cessation of mating, fertilisation and embryogenesis. To crudely compare *in vivo* fertilisation in female-only versus mixed sex implants, intraperitoneal mf loads were also evaluated at endpoint.

Although no statistical difference was concluded from the mixed sex versus female-only mf release post-mortem, a biological trend was observed in that 76% fewer mf/female were released from the female-only implant group. The mf release per mouse was variable, as also observed with the meta-analysis mf data. Microfilariae release is dependent on multiple factors including the time of fertilisation prior to dissection and/or re-implantation the initial male:female ratio, all of which contribute to the wide range and variation observed. The lower mf release observed in the female-only implants was hypothesised to be due to no re-fertilisation of the females and the eventual cease of mf release due to a pause in embryogenesis, although further research into this area is yet to be studied.

No significant changes in viability, as determined via MTT reductase activity, were observed across any culture groups or implantation groups. It was thus determined that re-fertilisation and the subsequent embryogenesis, and the consequent release of uterine products, did not impact the overall adult parasite viability. Furthermore, *Wolbachia* titres were consistent in female-only and female + male implants. This suggests the cessation of mf release is due to the pause in fertilisation and not due to a decrease in *Wolbachia* which would hinder embryogenesis.

At this stage, *Wolbachia* titre analyses were incorporated into the optimisation as a further indicator of *in vitro* fitness, due to the association of *Wolbachia* with parasite health and survival (Taylor et al., 2005a). *Wolbachia* titres across all groups and time points were within 40% of *in vivo* control parasites. High levels of variation in *Wolbachia* load were observed across all groups, including those *in vivo*. This was to be expected, considering the 2-log difference in adult females reported by McGarry et al and various additional *in vivo* vehicle

control drug groups (McGarry et al., 2004a, Hong et al., 2019, Sharma et al., 2016) and the fact that adult females contain four hypodermal cords, which may not necessarily be populated with equal numbers of *Wolbachia*. Despite the variation and percentage difference in load from the *in vivo* control, it is important to note that all *Wolbachia* copy numbers in each group across both time points fell within the published range (McGarry et al., 2004b, McGarry et al., 2004a). Although no significant differences were concluded between any groups in comparison to *in vivo* titres, it was decided that the LEC + LEC co-culture system would be progressed forward for subsequent drug screening due the superior performance in viability and survival, combined with the encouraging *Wolbachia* data.

Prior to drug model validation, uterine release profiles were further analysed in a more detailed manner, incorporating embryonic and morulae stages into analysis. A similar trend was encountered as previous, whereby mf release was observed followed by a steady decline which reflected the pause in fertilisation. In tandem, an increase in embryo release was observed. It is unclear whether this is a natural process as a response to the pause in embryogenesis, or an indication of an embryonic pathway going awry as a result of culture. Currently, there is no existing literature detailing the embryogenesis pathway in full, for example natural developmental failure rates, so no strong conclusion can be drawn as to why this is occurring. As mentioned, stress-related genes have been found to be upregulated post-removal from jirds (Ballesteros et al., 2016) which is then pro-longed throughout culture. An onward application of this system would be to re-implant cultured females into mice with male parasites to confirm whether fertilisation resumes. Whilst the release of embryos could be a result of stress, both viability readouts and *Wolbachia* titres suggest otherwise, which further evidences the need for additional experimentation, for which this system could be applied as a model. Based on these data, the optimised *in vitro* model will be considered unsuitable in determining any effects on uterine release in response to drug treatment.

It was demonstrated that the optimised LEC co-culture system can be successfully utilised as an anti-*Wolbachia* screening platform; using the 'gold standard' reference drug doxycycline, and a novel, more potent compound, TylAMac (Hübner et al., 2019, Taylor et al., 2019).

In an ideal candidate, *Wolbachia* populations should be reduced to 90%, a threshold level prognostic of significant curative efficacy in LF clinical trials (Turner et al., 2006, Mand et al., 2012), ideally within a 7-day dosing period. With doxycycline, data was concomitant with that *in vivo*, whereby the 'desired' level could not be achieved within 7-14-day timeframe. This was encouraging, as parasite health reflected that of an *in vivo* situation and did not result in 'false-positive' data.

After a 7-day washout period following the equivalent time dosing, a recrudescence in *Wolbachia* was observed, as would occur *in vivo* after this treatment time. This was also observed, albeit to a lesser extent, with the TylAMac dosed parasites. Contrarily, the percentage of parasites reaching >90% depletion levels after washout had increased with both drugs, suggesting somewhat further bactericidal activity post dosing, potentially due to autophagy. This autophagic activity in response to drug treatment has been previously described, primarily in the treatment of tuberculosis (TB) (Kim et al., 2012). Drug induced autophagy has also been studied *in vivo* in *Bm* infected jirds (Voronin et al., 2012) and onchocerca infected cattle (Langworthy et al., 2000). Here, *Wolbachia* recrudescence was observed after short treatments, however with prolonged treatments followed by washout periods and the use of autophagy inhibitors/activators, *Wolbachia* depletion continued post-tetracycline treatment due to autophagy activation and could reason why adult worms take 1-2 years to die with doxycycline treatment. This autophagic response to *Wolbachia* has also been studied in insect cell lines *in vitro* (Makepeace et al., 2006). However, data differed to that *in vivo*, whereby *Wolbachia* recrudescence was not noted, yet *Wolbachia* populations continued to decline after brief exposure of drug – a phenomena which does not occur after

brief exposure *in vivo*. Due to the recrudescence of *Wolbachia* within the co-culture *in vitro* model and the speculated activation of autophagy, this model could provide a more 'representative' model for study autophagy than the cell line, and hence use less animals to study this process in the future. Further, as *Wolbachia* recrudescence was less pronounced with TylAMac, and the number of parasites with >90% *Wolbachia* depletion was higher than with doxycycline, it may suggest that TylAMac could be a more effective 'autophagy activator' than doxycycline, although further research is required to fully elucidate this, for which this culture system could be a model for.

The optimised *in vitro* system was also confirmed to be an effective model in determining direct-acting macrofilaricide activity. Despite flubendazole having proven activity after 5 days of dosing *in vivo* (Mackenzie and Geary, 2011, Geary et al., 2019, Zahner and Schares, 1993), parasites were dosed *in vitro* for 2 weeks to fully exploit the longevity of the system and to evaluate efficacious durations of the novel compounds. This was also the longest time the activity of FBZ has been explored *in vitro*, due to the short-comings of previous *in vitro* systems, and hence the full *in vitro* efficacy of FBZ was undetermined prior to this study. FBZ was more effective than SUR in reducing parasite viability in comparison to control treated parasites and thus, the 2 novel compounds were compared against FBZ. Although both novel compounds had published activity against *Trichuris* larval stages *in vitro* (Partridge et al., 2017) to reduce infectivity when then administered to mice, in this *Bm* system, parasites were dosed at concentrations 10 times lower to remain within physiological concentrations, whilst comparable with efficacious doses of FBZ with the future aim to develop into pre-clinical testing, rather than an environmental approach as with *Trichuris*. It was determined the compounds exhibited a slower activity than FBZ. However, this may be beneficial as an alternative direct-acting macrofilaricide and to avoid the risk of severe drug reactions in response to rapid parasite killing. These data therefore illustrate that the LEC co-culture system is capable in evaluating direct-acting drug activity as exhibited using reference drugs

such as FBZ, whilst discerning activity of unknown compounds that may have greater potency than reference drugs. It must be noted however, that the activity of compounds requiring the host immune system may not be highlighted within this model.

With the likeness to *in vivo* parasites confirmed and *in vitro* drug studies mirroring those conducted *in vivo*, there is confidence that this *in vitro* model serves as an accurate predictor of future anti-*Wolbachia* candidate and direct-acting macrofilaricide efficacy, and is thus capable of reducing and refining the number of animals used for this purpose.

The 2 to 3 week longevity of the culture system is more than suitable for the identification and scrutiny of potential candidates able to reach the essential 7 day treatment time frame for A-WOL therapy and assess treatment time frames of potential direct-acting compounds. The regrowth of *Wolbachia* post-treatment within this culture system further emphasises the efficiency of the model in supporting the health of the both the worm and *Wolbachia*, and accurately predicting therapeutic outcomes that translate to *in vivo* studies. The *Wolbachia* recrudescence further exemplifies the downstream applications of the model, for example in evaluating autophagy processes and other biological mechanisms within *B. malayi in vitro*.

This additional step *in vitro* adult step in the drug screening process bridges the gap between identified 'hits' from short term cell and mf screens, to *in vivo* screens targeting adult filariae. The optimised adult model thus provides a stage-relevant platform in which false-hits can be screened out and not progressed into *in vivo* screens – ultimately reducing the number of animals. Furthermore, efficacy dose testing can be conducted against the correct life cycle stage, obviating the need of animals for this purpose.

Further, as the system is built around lymphatic feeder cell layers, there is potential to utilise the model to identify drugs with anti-morbidity properties, whereby cell proliferation can be quantified as a 'first-point' anti-morbidity screen.

CHAPTER 3

In final, the development of this long-term *in vitro* feeder cell system is important both scientifically and from an animal reduction perspective. Potential compounds can now be robustly scrutinised prior to enrolment into *in vivo* studies, reducing the numbers of animals used for this purpose. Initial efficacy testing can now be conducted *in vitro* rather than *in vivo*, further reducing animal usage. Furthermore, the likeness of cultured parasites to those *in vivo* allow for parasite biology studies to take place *in vitro*, which could previously only be conducted *in vivo*.

Chapter 4: Development and validation of pre-clinical ultrasound to predict worm burden and treatment efficacy in animal models of filariasis

4.1. Abstract

Candidate drugs against filarial disease require testing in pre-clinical models of filariasis. The incidence of infection failures and high intra-group variation means that large group sizes, and hence large numbers of animals, are required for drug testing. Further, a lack of accurate, quantitative adult biomarkers results in protracted time-frames or multiple animal groups for endpoint analyses. This chapter evaluates the use of intra-vital ultrasonography (USG) to identify *B. malayi* in the peritonea of gerbils and CB.17 SCID mice, and assess prognostic value in determining drug efficacy. It was concluded that parasites could be detected, using the signature intra-peritoneal filarial dance sign (ipFDS) with 100% specificity and sensitivity, when >5 *B. malayi* worms were present in CB.17 SCID mice. Semi-quantification of ipFDS could predict worm burden >10 with 87-100% accuracy in CB.17 SCID mice or gerbils. USG was predictive of macrofilaricidal activity in randomized, blinded studies comparing flubendazole, albendazole and vehicle-treated CB.17 SCID mice. Combined, these data estimate that pre-assessment of worm burden by USG could reduce intra-group variation, obviate the need for surgical implantations in gerbils to ensure a definite starting quantity of worms, and reduce total CB.17 SCID mouse usage by 40%. Thus, implementation of USG may reduce animal use, refine endpoints and negate invasive sampling techniques for assessing anti-filarial drug efficacy.

4.2. Introduction

In all *in vivo* models of filarial infection, large variation is evident in the adult parasite success rate from a unit inoculate per animal. Variation is comprised of both negative binomial distribution (skewness) and a low occurrence of non-parasitized animals (where inoculates have either failed to establish adult infections or where adult infections have only transiently established). Currently, accurate quantitative biomarkers of present adult infections are lacking and thus rodents cannot be assessed for infection status or parasitic load prior to enrolment in drug screening. Similarly, due to the lack of accurate markers of present adult infection, drug efficacy can only be evaluated at the end-point of the experiment, through dissection. To compensate, current screening protocols have long washout durations to maximize chances of capturing the 'true' efficacy of 'slow-acting' macrofilaricides, with concomitant risk of reduced survival of remaining adult filariae due to host attrition (independent of drug effect) and/or risk of decline in animal welfare. Additionally, multiple animal groups are enrolled into drug screens to assess different treatment regimens and washout periods, as there are currently no ways to determine this longitudinally. These drawbacks result in the requirement for large and multiple experimental group sizes, increased costs of maintenance, high demand on complex parasite production and protracted iterative cycles, in order to provide decision-making efficacy outputs (e.g. to support pharmaceutical lead-optimisation programmes).

Clinical ultrasonography (USG) has been used in tropical medicine to diagnose and assess therapeutic success in numerous diseases (Bélard et al., 2016). USG is particularly amenable in the detection of macroparasitic tissue infections due to the large size of the pathogens, their distinctive motility and/or the frequent formation of a cystic space in the tissues they inhabit e.g. echinococcosis, cysticercosis and filariasis. In LF, Amaral et al first described the

random thrashing movements of adult *W. bancrofti* as the filarial dance sign (FDS) in dilated lymphatic vessels during scrotal USG (Amaral et al., 1994). *W. bancrofti* USG detection of FDS has been used to diagnose suspected and unsuspected cases of scrotal filariasis (Noroes et al., 1996, Faris et al., 1998), and has been an important tool for the evaluation of macrofilaricide and anti-morbidity drugs (Dreyer et al., 1996, Dreyer et al., 1995, Chaubal et al., 2003, Turner et al., 2010b, Debrah et al., 2007). The reproducible success of USG in detecting FDS in bancroftian filariasis has only been reported in the scrotal region in microfilariaemic males, with more inconsistent detection in the lymphatics of other anatomical locations of microfilariaemic female patients (Mand et al., 2003). Similarly, *B. malayi*, which are smaller than *W. bancrofti* worms (4 cm versus 10 cm) and do not form hydrocoele pathology, have failed to be consistently visualized in microfilariaemic patients (Shenoy et al., 2016). *O. volvulus* adult motility within subcutaneous nodules have also been successfully imaged using USG. Nodules have been subjected to USG as a method of diagnosis and assessing drug treatment efficacy by determining changes in nodular structure, as well as imaging the worm motility within cystic spaces inside the nodules (Homeida et al., 1986, Poltera et al., 1987, Poltera et al., 1991, Poltera and Zak, 1988, Darge et al., 1994, Leichsenring et al., 1990, Mand et al., 2003, Turner et al., 2010a). In a pilot study utilizing rodents infected with *L. sigmodontis* or *B. malayi* and pre-determined as positive for circulating microfilaraemia, the detection of FDS by USG has been demonstrable with more reliable detection in the thoracic cavity versus the lymphatic system (Mand et al., 2006). Here, we have fully assessed the sensitivity, specificity and prognostic value of USG to detect FDS of extravascular *B. malayi* adult filariae contained within the peritoneal cavity of SCID mouse and gerbil preclinical drug screening systems. We demonstrate that USG is highly sensitive and specific in the detection of FDS using 'operator-blinded' studies and can be successfully applied to estimate level of adult worm burden and macrofilaricidal efficacy in drug screening experiments.

4.3. Scientific and 3Rs Aims

- **Assess whether USG can predict infection burden in experimentally infected CB.17 SCID mice and Mongolian gerbils, to enrol animals into drug screening protocols; refining animal usage, reducing experimental bias and maximising the experimental outputs of *in vivo* drug studies.**
- **Evaluate the limit of sensitivity of USG in detecting worm burden using CB.17 SCID mice surgically implanted with decreasing numbers of different sex parasites.**
- **Evaluate the impact of using USG as a longitudinal imaging tool to predict treatment efficacy in *Brugian* filariasis mouse models, using a known macrofilaricide and a drug with no macrofilaricidal activity to reduce and refine animal usage in anti-filarial drug research.**

4.4. Materials and Methods

4.4.1. Animals

Male CB.17 Severe Combined ImmunoDeficient (SCID) mice were purchased from Charles River UK. *Meriones unguiculatus* (Mongolian gerbils; jirds) breeding pairs were purchased from Charles River, Europe. Breeding and experimental stocks were maintained under specific pathogen-free (SPF) conditions at the biomedical services unit (BSU), University of Liverpool, Liverpool, UK. Male SCID mice were 6–10 weeks old and weighed 22–26g at start of experiments. Male gerbils were 4–6 months old and weighed 80–100 g at start of experiments. All experiments were approved by the ethical committees of the University of Liverpool and Liverpool School of Tropical Medicine (LSTM) and conducted under Home Office Animals (Scientific Procedures) Act 1986 (UK) requirements.

4.4.2. *Brugia malayi* parasite production

The life cycle of *Brugia malayi* (*Bm*) was maintained in mosquitoes and Mongolian gerbils as described in Chapter 2.

4.4.3. Experimental Infections

For *Bm*L3 infection, male Mongolian gerbils, aged 4–6 months, were injected via the intraperitoneal route, with either 50 or 400 highly motile *Bm*L3. Male CB.17 SCID mice aged 6–10 weeks, were injected with 100 *Bm*L3. Animals were left for between 12 and 25 weeks post-infection to allow infections to proceed to the chronic adult stage.

4.4.4. Surgical implantation of Adult *Brugia malayi* parasites

Bm adults were collected from infected donor CB.17 SCID mice via peritoneal lavage post-mortem. Parasites were then separated into male and female, washed with pre-heated phosphate buffered saline (PBS, Merck) and collected into the following groups: 4x5 males, 4x5 females, 4x2 males, 4x2 females, 4x1 male, 4x1 female, for implantation (n=4/group,

total n=28). Male CB.17 SCID mice were then placed under surgical anaesthesia using isoflurane and received a subcutaneous injection of buprenorphine prior to implantation of the above parasite groups into the peritoneal cavity. Implantation was achieved by making a small incision into the skin and abdominal cavity in the upper right quadrant and inserting parasites into the lower abdominal quadrant using a glass pipette to ensure all parasites were maintained in the cavity. The incisions were then re-sutured after implant and animals were re-housed as before and monitored closely. The number of parasites inserted into each mouse was blinded to the investigator and coded by ear markings for parasite recovery analysis at the experimental end point.

4.4.5. Preclinical Ultrasonography

To initially optimise the USG technique, a cohort of 5 CB.17 SCID mice were surgically implanted with 13 adult *Bm* parasites and imaged before and after the addition of sterile RPMI media to establish a ipFDS signal. Similarly, 8 gerbils infected with varying numbers of *Bm*L3 were imaged before and after 1 and 3 ml of RPMI to optimize the imaging protocol. To further assess the accuracy of USG in detecting *Bm* parasites and to determine limits of sensitivity in CB.17 SCID mice, USG was performed blinded one week post-surgery. For this, mice and gerbils were anaesthetized with gas isoflurane prior to receiving a 1ml or 3 ml, respectively, intra-peritoneal injection of sterile, pre-heated (37 °C) RPMI media (Merck, UK). The abdominal cavity was then gently massaged to distribute the media and dislodge parasites into fluid pockets to enable easier detection with USG. The abdominal region was then shaved and imaged by USG (Sonosite® MTurbo® 8.5 Mz linear probe, 'small parts' pre-set) for 10–15 minutes with thorough investigation of all quadrants for random thrashing movements (ipFDS) to confirm the presence of parasitic worms. Parasite load and location was semi-quantified using a grid scoring method depending on signal strength and number of locations in which parasite masses were detected. Animals were scored as ipFDS- (no FDS

detection), ipFDS+ (a single location with a weak signal), ipFDS++ (a weak signal at >1 locations) or ipFDS+++ (a strong signal at ≥ 1 locations). For the initial validation of ipFDS, the abdomen was firstly imaged using 'M-mode' of USG, the time motion display, to accurately confirm parasite presence and location due to the recording of very rapid movements exhibited by *Bm* FDS, which are not observed with artefacts of respiration, intestinal peristalsis or blood flow. For further validation, the 'Pulse Wave' modality was applied to depict velocity and flow direction both as a waveform. For this, FDS could be confirmed due the random movements and velocity, as opposed to erythrocytes, which instead exhibit a constant flow and velocity. For the Colour Flow Doppler, the same parameters were examined as a colour map superimposed onto the 2D imaged, whereby flow moving away from the probe can be determined in one colour and flow away determined by another. The random FDS of *B. malayi* allows for colours to change more rapidly during video, and more flow observed moving away from the probe.

4.4.6. Drug treatments

Individual mice (unit of replication; n=5/group) were randomized into treatment groups by ear notch ID (001, vehicle, 002 ABZ, 003 FBZ etc.) Mice were dosed with either a known potent macrofilaricidal parenteral regimen of flubendazole (FBZ); 10 mg/kg daily sc \times 5 days, a related BZ drug regimen of albendazole (ABZ) not expected to confer macrofilaricidal activity, at 5 mg/kg twice daily per oral for 7 days or with vehicle matching ABZ for 7 days. USG was carried out by an investigator blinded to treatment to detect presence or absence of ipFDS as a prognostic marker of macrofilaricidal outcome of the drug screen at +6 weeks.

4.4.7. Endpoint Parasitological assessments

At indicated intervals post-USG imaging, animals were humanely culled before adult *B. malayi* were recovered by extensive peritoneal washes with RPMI medium. Parasite numbers were sexed and counted by microscopy. Motility scoring was based on a system

whereby 3=highly vigorous movements. 2=slow movements, 1=twitching, 0=immotile. Metabolic activity of adult *B. malayi* recovered at necropsy were determined by washing in PBS and individually placing in a solution of MTT (3-(4,5-Dimethylthiazol-2-yl)-2,5-Diphenyltetrazolium Bromide) reagent (Merck) in PBS (final concentration 0.5 mg/ml). Worms were incubated for 2 hours at 37 °C with 5% CO₂. After washing in PBS, adult worms were incubated in 100% DMSO for 1 hour at 37 °C with 5% CO₂ to dissolve and release the blue formazan product. The samples were read at OD 490 nm on a 96-well plate reader (Varioskan, Bio-Rad).

4.4.8. Statistics

Raw or log transformed continuous variables were tested for normal distribution using D'Agostino & Pearson omnibus normality tests. Variables that passed normality tests were analyzed by 1 way ANOVA with Holm-Sidak's multiple comparisons tests. Variables significantly different from a normal distribution were analyzed by Kruskal-Wallis with Dunn's multiple comparisons tests. Differences in frequency of categorical variables were assessed by Chi-Square analysis. Significance was defined at alpha <0.05 and analyzed using GraphPad Prism v6.0h. Power analysis was undertaken using sample means and standard deviations of untreated/vehicle control gerbil or SCID mouse worm burdens combined from 2–3 independent infection or implantation experiments. With the assumption of proportional variation, sample size was calculated for drug efficacy effect sizes of 70% or 90% with a statistical power (1-β) of >75 < 90% with alpha set at 0.05 using a two-sample T test (Russ Lenth PiFace Applet):

4.5. Results

4.5.1. Optimization and characterization of intra-peritoneal FDS detection

Initial experimentation was undertaken to optimize the detection of adult *B. malayi* FDS within the peritoneum. *B. malayi* immature adult stages were aseptically isolated from SCID mice +6 weeks following infection with 100 L3 ip. Six weeks after *B. malayi* immature adult stages had been surgically implanted into recipient SCID mice (adult filariae = +12 weeks old), mice were anaesthetized, orientated in a supine position, abdominal hair removed by shaving and abdomen imaged with a Sonosite Mturbo portable USG with 8.5Mz linear probe. After a maximum of 15 minutes imaging, ipFDS detection was verified in 2/5 animals (Table 4.1.). Mice were then injected with 1ml of pre-warmed, sterile RPMI medium ip, the peritoneum was gently massaged before re-imaging for a further 15 minutes. After this intervention, 5/5 animals had detectable ipFDS signal, most frequently observed in the upper right or upper left abdominal quadrants in cystic spaces between the abdominal wall and viscera (Table 1A, Figure 4.1.A-C). Similarly, four Mongolian gerbils, that had chronic adult infections 3 months post-infection with 400 BmL3, received a 1ml injection before imaging, in which no animals scored positively for ipFDS. When a further 2 ml (total of 3 ml) media was injected into the peritoneal cavity, 4/4 gerbils had detectable ipFDS (Table 4.1.).

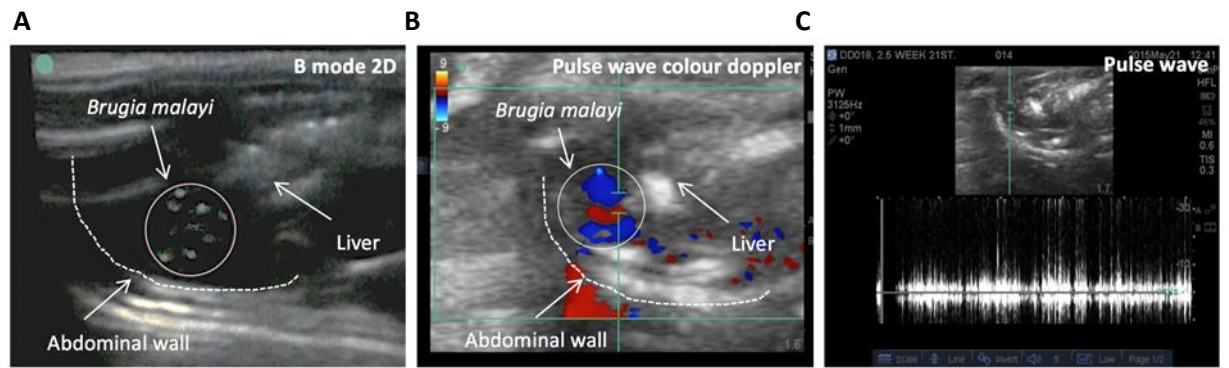


Figure 4.1. USG identification of rodent intraperitoneal filarial dance sign

Presence of *B. malayi* worm clusters with rapid motility detected in B mode within cystic spaces between viscera and abdominal wall of CB.17 SCID mice (A). Irregular *B. malayi* motility (filarial dance sign) captured by pulse wave color doppler (B) and pulse wave (C).

Table 4.1. Optimisation of intra-peritoneal FDS detection by ultrasound in anaesthetised mice or gerbils

ID	ipFDS signal	ipFDS signal (+1ml medium ip)	ipFDS signal (+3ml medium ip)	n adult recovered	<i>Bm</i>
SCID 1	-	+	nd	6	
SCID 2	+	+	nd	6	
SCID 3	+	+	nd	7	
SCID 4	-	+	nd	7	
SCID 5	-	+	nd	4	
Gerbil 1	-	-	+	2	
Gerbil 2	-	-	+	2	
Gerbil 3	-	-	+	12	
Gerbil 4	-	-	+	67	

ipFDS = intra-peritoneal filarial dance sign

*nd = FDS not detected

4.5.2. Sensitivity and specificity of *B. malayi* adult parasite loads by USG in operator-blinded studies

To assess sensitivity and specificity of USG in the detection of ipFDS, including low level worm burdens, CB.17 SCID mice were surgically implanted ip with either 10 female and 5 male (n=16), five female, five male, two female, two male, one female or one male *B. malayi* (all n=5 / group). All *B. malayi* used were +12-13 weeks old sourced from CB.17 SCID donors infected with *BmL3*. A further five SCID mice were submitted to peritoneal surgery and sham implantations. Between one and five weeks post-surgery, animals were imaged by USG for +15 minutes under anaesthesia following introduction of 1 ml pre-warmed medium and peritoneal massage. Mice were imaged in random order, by one of two operators who were blinded to group. The following day post-USG imaging, mice were necropsied and numbers of motile male and female adult *B. malayi* enumerated. Table 4.2. details the sensitivity and specificity of USG in detecting adult *B. malayi* parasites. In total, at necropsy, 42/46 mice had retained one or more motile *B. malayi* adults post-implantation. Therefore, combined with sham implants, a total of 9 mice were confirmed to lack motile *B. malayi*. The USG operators were able to accurately predict the absence of motile *B. malayi* in the peritoneum of all 9 infection negative mice (no false positives; 100% specificity). The operators predicted the presence of motile *B. malayi* in 36/42 mice (6 false negatives; 85.7% sensitivity). When examining the false negative rate according to final worm burden at necropsy, the operators were able to predict with 100% sensitivity the presence of >5 adult, motile *B. malayi*. This sensitivity dropped to 81% when ≤ 5 adult parasites were present in the peritoneum. Comparing the ability of USG to detect low level (≤ 5) female vs male implants, the level of sensitivity was similar (77%, female implants vs 82%, male implants). USG was reproducibly able to detect single motile female (7/9) or male (5/5) *B. malayi* within the peritoneal cavity of mice.

Table 4.2. Sensitivity and specificity of USG in determining adult motile *B. malayi*

Total adult <i>Bm</i> recovered (n)	<i>Bm</i> Females (No./mouse)	<i>Bm</i> males (No./mouse)	Mice n	Mice ipFDS+	Mice ipFDS-
12	9,9	3,3	2	2	0
10	9	1	1	1	0
9	7,7	2,2	2	2	0
8	8,6,5	0,2,3	3	3	0
6	4,4,3	2,2,3	3	3	0
5	3	2	1	1	0
4	2	2	1	1	0
2	1	1	1	1	0
5	5		1	1	0
4	4,4		2	2	0
3	3		1	0	1
2	2,2,2,2		4	3	1
1	1,1,1,1,1,1,1,1,1		9	7	2
5		5,5	2	0	2
4		0	0	0	0
3		3,3	2	2	0
2		2,2	2	2	0
1		1,1,1,1,1	5	5	0
0 (including sham)	0	0	9	0	9
total <i>Bm</i> +			42	36	6
total <i>Bm</i> -			9	0	9
Total			51	36	15
sensitivity				85.7%	
sensitivity >5 adult <i>Bm</i>				100%	
sensitivity ≤5 adult <i>Bm</i>				80.6%	
sensitivity ≤5 female <i>Bm</i>				76.5%	
sensitivity ≤5 male <i>Bm</i>				81.8%	
specificity					100%

In order from left to right columns (rows organised by number of worms collected in mice, row gaps indicate a different study n=3 studies): Total numbers of adult *Bm* recovered per mouse (left hand column), number of females recovered per mouse (number per mouse separated by comma), number of males recovered per mouse (number per mouse separated by comma), total number of mice dissected, number of those mice scoring positive for filarial dance sign, number of those mice scoring positive for filarial dance sign. Bottom rows: sensitivity in detecting/predicting numbers of worms calculated from the numbers of worms recovered corresponding to the filarial dance sign score.

4.5.3. Validation of USG to predict macrofilaricidal activity in preclinical drug screening

A known macrofilaricidal regimen of flubendazole was utilised, compared with a known non-macrofilaricidal anthelmintic regimen of oral albendazole to test whether USG could accurately predict macrofilaricidal activity in live animals during drug screening experiments (Halliday et al., 2014, Joseph D. Turner^{1*}, 2017). In both experiments, individual USG operators were blinded to drug group and imaging assessments of mice occurred in random order. In experiment A, mice were implanted with 10 female and 5 male worms and the USG signal was assessed +6 weeks after start of treatment. Necropsies were performed immediately after USG to determine parasite worm burden. Metabolic activity and motility assessments of surviving female worms were also undertaken (Table 4.3.). Following deblinding, ipFDS signal was determined in 8/8 vehicle control treated mice, 8/8 ABZ treated mice and 3/9 FBZ treated mice. The frequency of ipFDS detection was significantly lower in the FBZ group compared with vehicle or ABZ ($P=0.0009$). The USG findings were then compared with the parasitological readout of the drug screen, at termination (Table 4.3.). In all vehicle and ABZ treated animals, motile adult *B. malayi* were recovered. The frequency of infection in FBZ treated mice was significantly reduced (4/9 mice, $P=0.0039$). Evaluating total worm burden, in the vehicle control group, a median of 7 (range 2-12) motile adult *B. malayi* were recovered per mouse. A similar median recovery was evident in the ABZ group, whereas in the FBZ treatment group, median worm burden was significantly reduced ($P=0.0003$) with the four mice that remained infection positive containing a single female worm. Further, motility assessments *ex vivo* evaluated that the majority of adult female *B. malayi* derived from vehicle and ABZ groups retained vigorous motility whilst the four *B. malayi* surviving in the FBZ group displayed a significantly reduced moribund motile phenotype ($P<0.00001$).

CHAPTER 4

In experiment B, mice were infected with 100 *BmL3* and after adult infections had established (+7 weeks), mice were randomised and treatment commenced. Due to the success of USG to predict profound macrofilaricidal activity of FBZ immediately before end-point, in experiment B USG was performed at +2.5 weeks post-treatment, 3.5 weeks prior to end-point, in order to evaluate the prognostic potential of ipFDS signal detection in predicting macrofilaricidal drug activity. A different USG operator undertook evaluations in experiment B. Following de-blinding of treatment groups, USG undertaken at +2.5 weeks post-dosing detected ipFDS signal in 5/5 vehicle and ABZ treated mice. A significantly reduced frequency of ipFDS, in 1/5 FBZ treated mice, was detected ($P=0.0042$). At the end-point, +6 weeks post-dosing, the frequencies of infection positive mice were similar between treatment groups (5/5, 5/5 and 4/5) for vehicle, ABZ and FBZ, respectively. However, total adult *B. malayi* worm burden was significantly reduced in FBZ treated animals compared with vehicle (median recovery 1 vs 18, $P<0.0001$), whilst worm burdens in the ABZ group remained similar (median worm recovery = 19). In the FBZ group, one mouse had four female worms recovered whilst an additional three mice contained a single female *B. malayi*. Motility assessments of recovered adult female worms determined that the majority of *B. malayi* in vehicle and ABZ treatment groups retained vigorous motility whilst the surviving FBZ-treated *B. malayi* displayed significantly reduced and moribund 'twitching' motility ($P<0.0001$). Metabolic activity of sampled female worms was also significantly reduced in both drug groups vs vehicle but to a more profound extent in the surviving FBZ-treated *B. malayi* vs ABZ-treated worms ($P<0.0001$).

Table 4.3. USG ipFDS detection compared with adult *B. malayi* parasitological readouts in experimental macrofilaricide drug screens

Drug group ⁺	USG ipFDS+/total (weeks post-dosing)	Infection status (weeks post-dosing)	Median <i>B. malayi</i> worm burden (range, total n)	Median Female <i>B. malayi</i> worm burden (range, total n)	Median Male <i>B. malayi</i> worm burden (range, total n)	Mean Female <i>B. malayi</i> metabolic activity (SEM, n worms assessed)	Median Female <i>B. malayi</i> motility score [^] (range, total n worms assessed)
EXPT A (implant drug screen, USG operator 1)							
Vehicle	8/8 (6 weeks)	8/8 (6 weeks)	7 (2-12, 57)	4.5 (1-9, 40)	2 (0-3, 17)	0.40, 39 (0.002)	3 (1-3, 39)
ABZ	8/8 (6 weeks)	8/8 (6 weeks)	7 (2-12, 53)	5 (0-9, 39)	2 (0-3, 14)	0.48, 39 (0.07)	3 (1-3, 39)
FBZ	3/9* (6 weeks)	4/9 ^l (6 weeks)	0 [†] (0-3, 4)	0 (0-3, 4)	0 (0-0)	nd	1 [∞] (1-1, 4)
EXPT B (infection drug screen, USG operator 2)							
Vehicle	5/5 (2.5 weeks)	5/5 (6 weeks)	18 (9-23, 85)	10 (6-15, 53)	7 (3-8, 31)	0.69, 10 (0.08)	3 (2-3, 10)
ABZ	5/5 (2.5 weeks)	5/5 (6 weeks)	19 (14-21, 93)	14 (11-16, 67)	5 (3-6, 24)	0.28 [§] , 10 (0.05)	3 (2-3, 10)
FBZ	1/5 [§] (2.5 weeks)	4/5 (6 weeks)	1 [#] (0-4, 7)	1 (0-4, 7)	0 (0-0, 0)	0.01 [∞] , 7 (0.003)	1 [∞] (1-2, 7)

⁺ ABZ = albendazole 5mg/kg *bid* per oral x 7d, FBZ = flubendazole 10mg/kg *qd sc* x 5d

[^] motility score: 3 = vigorously motile, 2 = sluggishly motile, 1 = partial twitching motility, 0 = immotile

* Chi-square analysis $\chi^2=14.04$, *df*,2 *P*=0.0009

^l Chi-square analysis $\chi^2=11.11$, *df*,2 *P*=0.0039

[†] Kruskal Wallis 1 way ANOVA 16.09, *P*=0.0003 (Dunn's tests: vehicle vs FBZ, *P*<0.01, ABZ vs FBZ, *P*<0.01)

[∞] Kruskal Wallis 1 way ANOVA 18.49, *P*<0.0001 (Dunn's tests: vehicle vs FBZ, *P*<0.0001, ABZ vs FBZ, *P*<0.0001)

[§] Chi-square analysis $\chi^2=10.91$, *df*,2 *P*=0.0042

[#] Kruskal Wallis 1 way ANOVA 40.13, *P*<0.0001 (Dunn's tests: vehicle vs FBZ, *P*<0.0001, ABZ vs FBZ, *P*<0.0001)

[∞] 1 way ANOVA *F*=23.93, *P*<0.0001 (Holm-Sidak's tests: vehicle vs ABZ, *P*<0.001, vehicle vs FBZ, *P*<0.0001, ABZ vs FBZ *P*<0.05)

[∞] Kruskal Wallis 1 way ANOVA 20.47, *P*<0.0001 (Dunn's tests: vehicle vs FBZ, *P*<0.001)

4.5.4. Application of USG to semi-quantify *B. malayi* adult parasite loads *in vivo*

We investigated whether the qualitative signal strength of ipFDS determined by USG could be utilised to semi-quantify variation in *B. malayi* adult worm burden that arises following experimental infection with *BmL3*. Cohorts of CB.17 SCID mice (n=31) or gerbils (n=14) were assessed after experimental infection and at time-points following adult parasite establishment in the peritoneum. Additionally, a group of 4 uninfected gerbils were evaluated (operator blinded to infection status). A semi-quantitative scoring system was devised based on number of discreet ipFDS signals in anatomical locations and also apparent density of ipFDS signal, with a low-intermediate signal (+/++) inferring a low density of parasites in either a single or multiple peritoneal quadrants and a strong signal (+++) inferring a dense mass of parasites in either a single or multiple quadrants. At 40 weeks following infection, 4/31 mice had no detectable ipFDS signal, 12/31 had a low to intermediate signal and 15/31 had a strong ipFDS signal. Total *B. malayi* worm burden was assessed at +41 weeks (Fig. 4.2.A). In 3/4 mice with no ipFDS signal, no adult *B. malayi* were found. A single, motile male *B. malayi* was isolated from the other mouse in this group. In mice categorised with a low-intermediate ipFDS signal, median worm burden was 9.5 (range 3-23) and 50% of the group contained ≥ 10 adult *B. malayi*. In mice categorised with a high ipFDS signal, median worm burden was 19 (range 8-33) and 87% of the group had a worm burden ≥ 10 . The difference in worm burden predicted by USG categorisation was significantly different between all sub-groups (1way ANOVA $F=10.82$, $P=0.0003$, Fig1A). After a period of between 3-6 months post-infection the cohort of gerbils were subjected to USG and scored as the CB.17 SCID study above (Fig. 4.2.B). Of the gerbils examined, 4/4 of the sham infected gerbils had no detectable ipFDS. A further 5 gerbils who had received inoculates of L3 were ipFDS

negative and were determined to be uninfected at necropsy. Six gerbils were ascribed a low/intermediate ipFDS signal and contained a range of 1-2 adult parasites at necropsy. The remaining gerbils scoring a strong ipFDS signal contained a median worm burden of 21 (range 12-68). Therefore, in gerbils characterized with a high ipFDS, 100% of the sub-group had a worm burden ≥ 10 adult *B. malayi*, whereas those characterised with an intermediate signal, 0% of animals in the group had a worm burden ≥ 10 adult *B. malayi*.

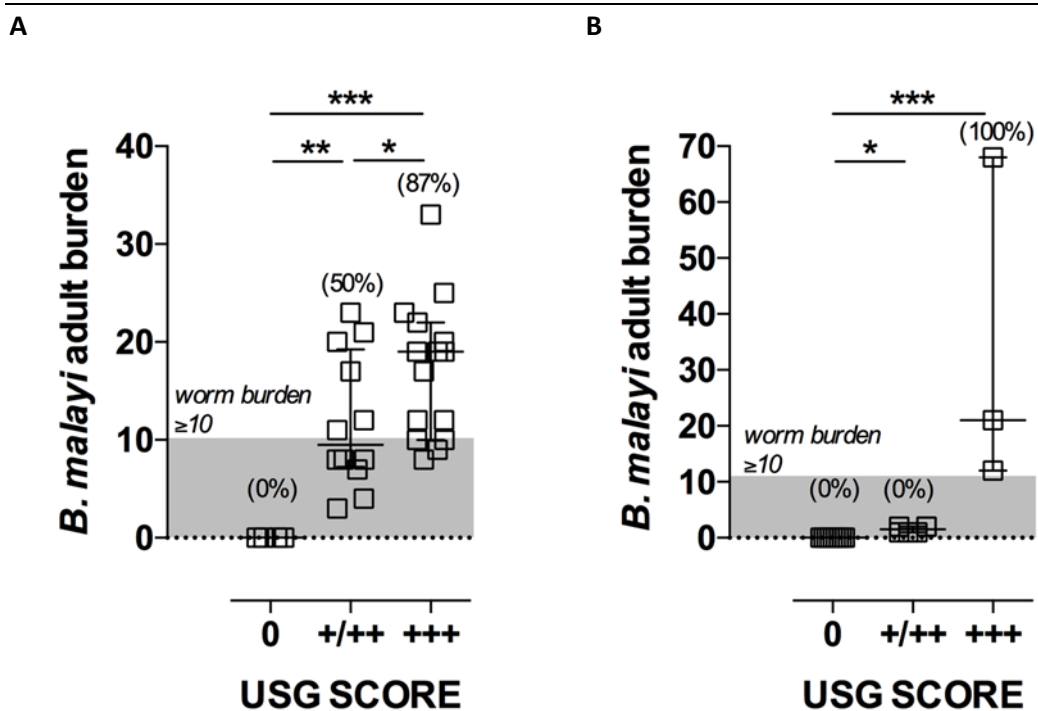


Figure 4.2. Semi-quantification of *B. malayi* worm burden by USG in SCID mouse (A) and gerbil (B)

drug screening models

Positive and negative ipFDS and ipFDS signal strength, semi-quantified in terms of number of anatomical locations and density (+/++ = low-intermediate signal, +++ = strong signal) compared with worm burdens of motile adult *B. malayi* determined at necropsy in 31 parasitized SCID mice (A) or 18 Mongolian gerbils (B). Horizontal bars represent median values and bars represent interquartile range. Percentages in parentheses are numbers of animals in each USG sub-category with a *B. malayi* worm burden ≥ 10 (above shaded area of graph). Significant differences were assessed by 1 way ANOVA with Holm Sidak's multiple comparison's test (A) or Kruskal Wallis with Dunn's multiple comparison's tests (B). Significant differences are indicated * $P < 0.05$, ** $P < 0.01$, *** $P < 0.001$.

4.5.5. Evaluation of estimated reductions in animal use for drug screening post-implementation of USG assessment

Data sets of individual adult *B. malayi* worm burdens derived in multiple preclinical experiments in our laboratory were accumulated to accurately determine sample variation. Data from experimental infections of gerbils and SCID mice, as well as recovery of adults post-surgical implantation in gerbils were assessed (Table 4.4.). From the sample means and standard deviation in adult burdens, minimum group sizes were derived to assess with >75% statistical power a $\geq 70\%$ or $\geq 90\%$ reduction in worm burden of an effective macrofilaricidal drug. The meta-analysis demonstrated that gerbil infections had increased variation in worm burden compared to SCID mice (29.4 ± 33.1 , $n=43$ vs 15.3 ± 8.7 , $n=50$) and higher incidence of infection failures (20% vs 10%). Power calculations determined that nearly 3-fold more animals would be required if assessing $\geq 70\%$ efficacy of a drug candidate in gerbils vs SCID mice (22 vs 8). As prohibitively consuming in terms of gerbil use and cost, the alternative strategy of surgically implanting 20 adult *B. malayi* into gerbil recipients from infected donors was adjudged to markedly reduce variation in resultant adult yields at assay endpoint (9.4 ± 4.4 , $n=11$). Whilst this meant that statistical power of assessing $\geq 70\%$ efficacy was achieved with a group size of seven, when taking into account a 1:1 ratio of donors to recipients, a total gerbil use per drug test of $n=14$ would be necessary. We then evaluated the potential effect of excluding light infections and/or uninfected animals via USG assessment on overall animal use. In gerbils, exclusions of uninfected and low level infections would mean that similar total numbers of animals could be used compared with surgical implantations, whilst obviating the requirement for invasive surgery, as a beneficial refinement to animal welfare (for $\geq 70\%$ efficacy, 14 animals per group). For SCID mice, exclusions of uninfected and low level infections would mean that total animal use per drug group tested could be reduced by between 30-40%, depending on required efficacy level being evaluated.

Table 4.4. Meta-analysis of *B. malayi* worm burden variation, statistical power and hypothetical animal use for preclinical drug screening pre- and post-implementation of USG imaging assessment

	Species / strain	Model	worm burden mean±SD (sample n, expt n)	n animal / drug test (>75%<90% power) [#]		Proportion infections excluded (%)	minimum animal use / drug test [†]	
				≥70% efficacy	≥90% efficacy		≥70% efficacy	≥90% efficacy
Pre-USG assessment	Gerbil	400x <i>Bm</i> L3 infection	29.4±33.1 (43, 3)	22	14	0%	22	14
	Gerbil	20xadult <i>Bm</i> implantation	9.4±4.4 (11, 2)	7	5	-	14	10
	Mouse CB.17 SCID	100x <i>Bm</i> L3 infection	15.3±8.7 (50, 2)	8	6	0%	8	7
ipFDS-excluded	Gerbil	400x <i>Bm</i> L3 infection	37.2±33.1	15	9	20%	18	11
	Mouse CB.17 SCID	100x <i>Bm</i> L3 infection	17.0±7.4	5	4	10%	6	5
ipFDS-/+ /++ excluded (<10 adults)	Gerbil	400x <i>Bm</i> L3 infection	47.4±31.3	9	6	40%	14	9
	Mouse CB.17 SCID	100x <i>Bm</i> L3 infection	19.5±6.0	4	3	25%	5	4

[#]statistical power (1-β, α = 0.05) two sample T test (Russ Lenth Piface Applet)

[†]including donor animals (surgical implantations) or animals used but subsequently excluded due to USG criteri

4.6. Discussion

Intraperitoneal infections of rodents with *Brugia* spp. are convenient small animal models to test activity of candidate filaricidal compounds. However, limitations of the current screening models means large numbers of animals are required to gauge with accuracy the efficacy level of test compounds. Variation in adult parasite worm burden and the occurrence of infection failure in both gerbils and, to a lesser extent, immunodeficient mice, hampers the success of screening systems to delineate the true efficacy level of treatments. To compensate for variation in worm burden, investigators accommodate large group sizes which is costly and increases overall animal use. A second strategy to overcome parasitological variation is the surgical transfer of adult *Brugia* parasites from donor-infected animals prior to drug dosing. Whilst this strategy improves accuracy of drug efficacy evaluation, it requires an invasive procedure and further increases the number of animals, as both recipient and infected donor mice are required. A second limitation of current screening systems is that no accurate quantitative biomarker of active infection is available. Thus, both initial starting adult biomass and endpoints of drug treatment efficacy are difficult to predict. Microfilarial production can be used as a marker of fecund adult infection but is not infallible due to occurrence of single sex infections and because mature mf can persist long term after the death of adult parasites (half-life~100 days). Further, sampling of mf in the peritoneum requires invasive catheter washing under anaesthesia, which can also coincidentally remove adult parasites, particularly male *Brugia*. Ultimately, these drawbacks mean that animals are either maintained for very long durations (up to 8 months post-drug treatment) with the concomitant risk of welfare issues arising, or multiple groups are used to sample different time points after treatment, with yet further increases in overall animal use.

Previously, USG has been used in the field of tropical medicine primarily as a diagnostic tool, and also to assess therapeutic outcomes within the clinical setting. One example is the use of USG to detect pathology caused by certain parasites, such as assessing liver fibrosis and changes in urinary tract structure due to schistosomiasis (King, 2002). USG has also been applied to other diseases, including visceral leishmaniasis and viral haemorrhagic fever, whereby pathological changes in different organs can be used to determine disease state and therapeutic efficacies. In terms of filariasis, USG has been used in the field to detect FDS in hydrocele patients and to determine macrofilaricide and anti-morbidity drug activity (Amaral et al., 1994, Noroes et al., 1996, Dreyer et al., 1996, Dreyer et al., 1998). To date, there has been no literature reported on the use of USG for pre-clinical drug models of *Brugian* filariasis, making this research a novel expansion of the technique to determine efficacy of drug candidates and significantly reduce animal usage in this area. Ultrasonographic detection of adult *Brugia* 'filarial dance sign' was evaluated to determine the efficacy of the tool as a specific adult filarial biomarker to reduce and refine rodent use for *in vivo* filarial drug screening. After optimizing the technique for ipFDS detection in mice and gerbils, multiple operator/operator-blinded studies were conducted, determining that USG was 100% specific in predicting animals who were infection negative, and 86% sensitive in detecting active adult *B. malayi* infection. This increased to 100% sensitivity when >5 adult motile adult parasites were present in the peritoneum. The USG technique could be mastered and transferred from one operator to another with minimal amount of training and practice and without necessary prior experience of USG. Interestingly, sensitivity of ipFDS detection was not significantly different in single sex infections when low numbers of either larger, wider female (4–5 cm × 180–230µM) or smaller, thinner male worms (1–2 cm × 70–80µM) were evaluated *in vivo*. Indeed, single male worms were detectable in 100% of animals tested. This highlights a remarkable sensitivity of USG to detect adult infection and illustrates sensitivity is more related to the rapidity of filarial motility rather than the size of

adult worm per se. Reduction in sensitivity of USG detection reduced from 100% in animals parasitised with >5 adult worms to 81% in animals containing ≤ 5 worms. This probably reflects that with fewer parasite masses in fewer anatomical locations, a positive ipFDS signal is more likely to be missed over the 15 minutes of USG scanning especially if worms are situated in smaller cystic spaces surrounding solid tissues. The results indicate the technique may be able to predictively detect earlier, smaller life-cycle stages such as juvenile adult worms or even fourth-stage larvae, which may have use in determining earlier endpoints of drug or immuno-prophylaxis type preclinical studies. It was demonstrated that USG detection of motile adult *B. malayi* could be successfully applied as an early prognostic measure of effective macrofilaricidal activity. Using flubendazole injection as a reference macrofilaricide, as little as 2.5 weeks after dosing, USG could accurately predict if a rapid-acting macrofilaricidal drug regimen was significantly efficacious in operator-blinded studies. The predictive power of the USG approach was related to both a reduced total adult worm burden but also a severely reduced motility phenotype of surviving worms following effective drug treatment. Thus, we conclude that ipFDS signal is an accurate predictor of whether a drug candidate is likely to deliver significant macrofilaricidal outcome. Implementing USG to screen animals post-treatment would therefore potentially reduce the overall length of washout post-dosing, thus mitigating against reduced welfare of protracted animal experiments and the associated risk of underpowered studies requiring reassessment. When imaging on "B mode", it was possible to infer a semi-quantitative worm burden based on the apparent visual mass of worm movement and also the number of discreet locations where ipFDS was detected. As well as identifying sham infections and infection failures with 100% accuracy, this also enabled USG operators to predict with significant accuracy whether an animal contained a low/moderate or high worm burden, which when compared with yield of parasites at necropsy was between 87–100% accurate at delineating animals with ≥ 10 adult *B. malayi*. We evaluated that if implemented prior to

randomisation into drug screening experiments, with infection negative and light infection animals excluded, this semi-quantitative USG technique would reduce both intra- and inter-group variation and would thus impact on total numbers of animals required for drug screening. For gerbil-specific drug screening experiments, a major benefit of USG evaluation would be to negate the necessity of surgically implanting adult parasites from donors to recipients without increasing overall animal use. For SCID mouse experiments, animal use could be reduced as much as 40%. Further reductions in animal use over and above this would be apparent if experimental designs were altered to reflect the requirement of only a single time point for end-point analysis, after implementing longitudinal USG assessments. In conclusion, USG is a 100% specific and highly sensitive bioimaging technique to detect adult *Brugia* filarial parasites in the peritoneum of infected rodents. The technique can be implemented with minimum training. Implementation of USG would be beneficial in terms of refining animal experiments (negating the requirement for surgery and invasive sampling) and also has the potential to reduce overall animal use by as much as 40% in the context of preclinical anti-filarial drug screening.

Chapter 5: Development of intra-vital optical bio-imaging of fluorescently-labelled filariae to measure treatment efficacy in mouse models of filariasis

5.1. Abstract

Pre-clinical filarial models require multiple animal groups for drug screens due to the limitations of evaluating drug activity against parasites in real time. The only reliable means of determining drug activity against adult stage parasites is by enumeration and subsequent molecular analyses, which can only be retrieved by necropsy, whilst the only means of predicting severe adverse drug reactions due to rapid killing of microfilariae is via multiple invasive sampling; both of which provide only retrospective data. Multiple animals therefore need to be enrolled into drug screens to be able to evaluate different pharmacological regimes. The work outlined in this chapter details the optimisation of fluorescent dyes to stain both microfilarial and adult stage *Brugia malayi*, to track *in vivo* using an *in vivo* imaging system (IVIS). A drug challenge was then carried out using the reference fast-acting microfilaricide, ivermectin, and the reference direct-acting macrofilaricide, flubendazole, to determine whether this optimised fluorescent imaging model would be capable of tracking drug activity longitudinally. Microfilariae retained the VivoTag-750 NHS fluorescent dye for up to 7 days *in vitro* with no toxicity – the maximum culture time, and was therefore used for the staining of adult parasites. Following intravenous infusion, the tropism of fluorescent microfilariae could be tracked for up to 14 days in CB.17 SCID and SCID hairless outbred mice, whilst adult worms could be observed in the peritoneum of mice following surgical implantation. No significant differences could be determined in drug treated mice versus vehicle control mice, in both the microfilariae and adult worm fluorescent imaging models.

5.2. Introduction

Current filarial *in vivo* drug screening models are time consuming and costly, with the majority of models only providing a single time-point readout. In addition, accurate parasite enumeration as a measure of drug efficacy currently requires animals to be culled in the case of adult worm burdens, or invasive techniques (multiple blood withdrawal or peritoneal lavage) in the case of mf enumerations, and provide only retrospective data. There is a paucity of validated pre-clinical prognostic indicators of drug efficacy prior to this end-point. Further, there is no developed non-invasive pre-clinical method to accurately evaluate adverse drug events in response to rapid killing of microfilariae. Thus, such predictions are reliant on recurrent invasive serum sampling to determine immunological profiles and/or multiple experimental groups to collect sufficient tissues for inflammatory profiling at different time points.

Although immunodeficient mouse strains have been employed to increase parasite burden and reduce infection failure rates (Halliday et al., 2014), high numbers of animals are still necessary to evaluate multiple treatment time points and different pharmacological regimes.

By utilising whole animal imaging technologies, animal usage can be significantly reduced as the same cohorts can be studied longitudinally, thus eliminating the need for subsets in multiple time-course studies. Such examples of these technologies include fluorescent and bioluminescent imaging modalities, namely In Vivo Imaging Systems (IVIS); Magnetic Resonance Imaging (MRI); Fluorescence Molecular Tomography (FMT); Positron Electron Tomography (PET); Computed Tomography (CT); Single-Photon Emission Computed Tomography (SPECT); Photoacoustic Imaging (PAI), and have been utilised across an array of research fields ranging from cancer and neurology (Wang and Hu, 2012, Wessels et al., 2007) to infectious diseases (Andreu et al., 2011), to bacterial infections and multi-drug resistant bacteria (Mills et al., 2016).

The majority of bioluminescence and fluorescence imaging modalities are focused around the concept of using genetically encoded fluorescent or bioluminescent reporters to establish a signal. Concepts have further been translated into parasitology, whereby bioluminescent transformed species have been fundamental in determining parasite loads and dissemination *in vivo* in Chagas disease (Hyland et al., 2008), Malaria (Amino et al., 2005, Franke-Fayard et al., 2006), Echinococcosis (Porot et al., 2014) and Leishmaniasis (Lang et al., 2005, Millington et al., 2010). Literature concerning fluorescence imaging are scant, primarily due to the success in which organisms and cells can be labelled, or transformed, with bioluminescence.

Small animal *in vivo* imaging is less advanced within helminth research, and transfection and genetic modification of helminths are very much in their naivety. One successful approach however, has been to exploit the biology of the etiological flatworm of Schistosomiasis. In this example, mice were injected with an imaging agent which was then cleaved via enzymes abundant within the parasite digestive tract, to produce a fluorescent signal (Krautz-Peterson et al., 2009, Salem et al., 2010). However, this cannot be applied to filarial helminths due to the lack of a functional gut.

Via fluorescent labelling, parasites and potentially their response to drugs could be quantified *in vivo*. This imaging could significantly reduce animal usage, whereby animals can be studied longitudinally, drug efficacy can be determined earlier, and aspects of the immune system synergising with therapeutics in parasite killing may be determined without the need for invasive sampling, both reducing and refining animal usage.

5.3. Scientific and 3Rs aims

In this chapter, non-targeted fluorescent labelling and tracking of mf or adult *B. malayi* parasites were attempted *in vitro* and *in vivo*. In addition, changes in fluorescent signals after microfilaricidal or macrofilaricidal drug treatments were evaluated. Specific objectives were to:

- **Determine an optimal fluorescent dye capable of staining mf *in vitro* for prolonged periods.**
- **Optimise a model system to track fluorescently-labelled mf *in vivo* using IVIS technology.**
- **Validate imaging of fluorescently-labelled mf model with reference microfilaricides to establish bioimaging prognostic markers of therapeutic responses *in vivo*, to allow longitudinal imaging to reduce and refine animal usage.**
- **Optimise a model utilising surgically-implanted fluorescent-labelled adult parasites to monitor treatment responses *in vivo* to allow longitudinal imaging to reduce and refine animal usage.**

5.4. Materials and Methods

5.4.1. Animals

Male CB.17 Severe Combined ImmunoDeficient (SCID) mice were purchased from Charles River UK. Severe Combined ImmunoDeficient Hairless Outbred (SHO) mice were purchased from Charles River UK and evaluated for superiority in imaging quality in comparison to the 'hairy' SCID mouse. Breeding pairs were purchased from Charles River, Europe. Breeding and experimental stocks were maintained under specific pathogen-free (SPF) conditions at the biomedical services unit (BSU), University of Liverpool, Liverpool, UK. Male SCID mice were 6–10 weeks old and weighed 22–26 g at start of experiments. Male gerbils were 4–6 months old and weighed 80–100 g at start of experiments. All experiments were approved by the ethical committees of the University of Liverpool and Liverpool School of Tropical Medicine (LSTM) and conducted under Home Office Animals (Scientific Procedures) Act 1986 (UK) requirements.

Microfilariae Model

5.4.2. *Brugia malayi* parasite production

The life cycle of *B. malayi* was maintained in mosquitoes and Mongolian gerbils, as described in Chapter 2. Microfilariae (mf) were collected from infected gerbils via catheterisation and purified using PD10 column size exclusion chromatography (Amersham). Mf were then incubated in phenol red-free RPMI with 1% Pen/Strep and 1% Amp. B at 37°C until use.

5.4.3. *in vitro* fluorescent staining optimisation

To determine the optimum dye and concentration to successfully stain mf, a range of dyes were evaluated with concentrations ranging from 0–300 µM. The dyes and staining details were as following:

- Alexafluor 546 (Thermo-Fisher): Ex= 535 nm Em= 580 nm reconstituted in Dimethylsulfoxide (DMSO)
- Alexafluor 750 (Thermo-Fisher): Ex=745 nm Em=800 nm reconstituted in DMSO
- VivoTag-750 (Perkin-Elmer): Ex=745nm Em=800 nm reconstituted in DMSO

Mf were stained at a density of 10,000 parasites/well in 200 μ l phenol red-free Roswell-Park Memorial Institute (RPMI) media. Stained mf were then cultured in 96 well cell carrier plates with black walls, in order to inhibit the influence of background fluorescence during analysis. Plates were protected from light and incubated at 37°C with 5% CO₂ overnight. After overnight staining, mf were washed thoroughly 3 times with phenol red-free RPMI to ensure removal of any free, or unbound dye. 200 μ l of fresh, pre-warmed phenol red-free RPMI was then added to each well to support mf throughout the 7-day culture period. Motility was scored daily to observe any toxic effects dyes may have had on the parasites. Unstained mf were also set-up as controls in parallel to determine any dye-specific toxicity.

5.4.4. *In vitro* imaging

To determine the fluctuations in fluorescence of the stained mf over time, parasites were imaged every 2 days using both the IVIS and a fluorescent plate reader for cross-comparisons.

5.4.5. IVIS image acquisition

The IVIS system consisted of a cooled charge-coupled device (CCD) camera mounted onto a light-tight specimen chamber. The fluorescent excitation light was provided by a halogen lamp in combination with appropriate excitation filters. Emission filters were placed in front of the camera aperture to allow recording of specific wavelengths of light, depending on the emission spectra of the fluorescent profile examined. Optimal filter sets and exposure times were initially determined using the filter spectrum analysis tool within the Living Image

software. Once optimised, non-specific fluorescence was recorded by using a lower wavelength excitation filter and subtracted from original images by using the Image Math Tool in Living Image software (version 3.2, Caliper Life Sciences). The corrected image was then superimposed onto a greyscale reference photograph taken under low illumination using the Living Image software to aid the determination of the anatomical location of the signal. Fluorescence was quantified on the raw data before non-specific fluorescence was removed, by using the Region of Interest (ROI) tool in the Living Image software, where only light emanating from within a specified area was measured. Images were acquired using the following settings unless otherwise stated: excitation filter 745 nm and emission filter 780 nm background excitation filter 465 nm; f-stop 2; binning 4; exposure time 60s. Fluorescence intensity was displayed on a pseudocolour spectrum (where dark red represents the lowest intensity and yellow the highest) and presented as efficiency, a measurement normalized to the incident excitation intensity ($\text{efficiency} = \frac{\text{radiance of the subject}}{\text{illumination intensity}}$). By displaying fluorescence as efficiency, images taken at different time-points and with different exposure times could be directly compared with each other.

The fluorescence signal for each well was determined by selecting a region of interest (ROI) and quantifying as the Total Radiant Efficiency (TRE, $[\text{photons/sec}]/[\mu\text{W}/\text{cm}^2]$). TRE represents the sums of fluorescent pixels within the ROI.

5.4.6. *in vivo* fluorescent microfilariae infusion

Between 100,000-250,000 mf were stained with VivoTag-750 and infused into the tail vein of male CB.17 SCID mice. SHO mice were also infused to evaluate whether there was any benefit of using hairless mice for imaging. Sham infusions of phenol-red free RPMI were included in the study to account for any background fluorescence. Mice were allowed to recover and imaged at 24h, 168h and 336h time-points to confirm experimental success and

mf distribution. In parallel, 2 x 20 µl tail bleed samples were taken for confirmatory parasitology.

5.4.7. IVIS fluorescent imaging of stained microfilariae *in vivo*

IVIS imaging was conducted at 1h, 24h, 168h, and 336h time-points. For this, mice were anaesthetised using isoflurane. Once fully unconscious, mice were transferred to the IVIS camera chamber and anaesthesia was maintained using isoflurane, administered through individual nose cones.

5.4.8. Endpoint cardiac puncture and dissections

At 336h post-infusion, tail bleeds were taken and imaging was conducting prior to necropsy. 40µl of blood was removed from the heart via cardiac puncture using a 27-gauge needle, and scratched onto a glass microscope slide for parasitological analysis.

5.4.9. Mf Giemsa staining and enumeration

For preparation of slides for mf enumeration, slides were immersed in ddH₂O for 3 minutes 30 seconds, followed by immersion in 100% methanol for 1 minute, before placement into coplin jars with 40% giemsa (Sigma) for 45 minutes (Hira, 1977). Following staining, the backs of slides were gently rinsed under a tap to remove excess dye and allowed to dry overnight. Once dry, slides were examined under a light microscope to identify the now giemsa stained mf.

5.4.10. *In vivo* ivermectin drug response imaging study

Brugia malayi mf were retrieved from jirds, stained, incubated and washed as previously described. Once washed, mf were centrifuged at 300 g for 5 minutes and the pellet re-suspended in 200-400 µl phenol-red free RPMI in individual microcentrifuge tubes at a density of 250,000 mf/microcentrifuge tube. Meanwhile, ivermectin (IVM) was prepared at 1 mg/kg in 1% DMSO and the vehicle control was prepared as 1% DMSO in water. Across a

range of experiments, CB.17 SCID and SHO mice received tail vein infusions of approximately 250,000 mf, sham infusions (phenol-red free RPMI) or received an injection of heat-killed mf. Mice were allowed several hours to fully recover before IVIS imaging, conducted under the parameters previously described to establish baseline signals prior to drug dosing. Mice then received either IVM or a vehicle control via oral administration. Mice were imaged again 48h post-dosing to determine any changes in fluorescence in response to drug treatment. At this point, 20 μ l tail bleed samples were taken for confirmatory parasitology. Mice were imaged and sampled again at the 7-day end-point before necropsy, whereby cardiac punctures were taken and, in some cases, organs were excised for *ex vivo* imaging.

Adult Model

5.4.11. Surgical implantation of fluorescently labelled adult *B. malayi*

Following the successful staining of mf, adult parasites were excised from BALB/c IL-4R α ^{-/-} IL-5^{-/-} IL4/IL5 mice and incubated with 150 μ M VivoTag-750 overnight. Excess dye was removed the following day by washing the parasites in phenol-red free RPMI 3 times. Adults were then separated into 10 females and 3-5 males in preparation for surgical implantation as described in Chapter 4.

5.4.12. *In vivo* IVIS imaging of adult stage parasites

After recovering for 2 hours post-surgery, mice were imaged using IVIS, under the previously described settings, at baseline (day 1, 2-hours post-surgery), day 2 (24-hours post-surgery and first dose), day 6 (24-hours post end-dose, 6 days post-surgery), and day 10 (endpoint, 10 days post-surgery and start of dosing).

5.4.13. *In vivo* Flubendazole drug response imaging study

After a baseline imaging signal had been established, 4 mice received a subcutaneous dose of 10 mg/kg flubendazole, prepared in standard suspension vehicle (SSV; 0.5% sodium carboxymethyl cellulose, 0.5% benzyl alcohol, 0.4% Tween80, 0.9% sodium chloride), in the nape of the neck, whilst the remaining 4 mice received an equivalent volume and percentage of vehicle to constitute the control group. Both vehicle control and treatment groups were dosed once daily for 5 days.

5.4.14. Parasitology analysis

At necropsy, adult parasites were recovered, sexed and enumerated and their motility and viability (MTT assay) assessed to confirm drug efficacy. Mf were also washed out from the peritoneal cavity to determine any drug effects on numbers.

5.4.15. Adult MTT assay

For viability analysis, adults were individually placed into wells of a 96-well plate prior to the addition of 0.5 mg/ml MTT in PBS for 2 hours at 37 °C. After incubation, parasites were removed from the plate and submerged into a petri dish of PBS to wash off any excess MTT solution. Following this, parasites were transferred to a fresh 96-well plate using forceps, and 100% DMSO was added for 1.5 hours to solubilise

5.4.16. Intraperitoneal mf quantification

To quantify the number of mf released by adult females *in vivo*, mf were collected into 15ml falcon tubes during dissections. Tubes were centrifuged at 1200 rpm for 10 minutes and the supernatant discarded. Pellets were re-suspended in a known volume of RPMI, before aliquots were taken for dilutions to enable accurate enumeration using a light microscope. Data were presented as average number of mf released/female.

5.4.17. Statistics

Data were tested for normal distribution using D'Agostino & Pearson omnibus normality tests. Data that passed normality tests were analyzed by one-way ANOVA with Holm-Sidak's multiple comparisons tests. Data significantly different from a normal distribution were analyzed using Kruskal-Wallis with Dunn's multiple comparisons tests. Significance was defined at $\alpha < 0.05$ and analyzed using GraphPad Prism v6.0h.

5.5. Results

5.5.1. *In vitro* microfilariae staining and imaging

To determine an optimal fluorescent stain for mf imaging, Alexafluor-546, Alexafluor-750 and VivoTag-750 dyes were evaluated using both the IVIS system and a fluorescent plate reader (Figure 5.1.A). Alexafluor-546 was selected for optimisation due to previous success in staining both mf and larval stage parasites within the laboratory (J. Turner, personal communication). Mf stained with Alexafluor-546 emitted a peak signal approximately 10-fold higher than that of VivoTag-750, however was discounted due to its predicted unsuitability *in vivo* due to emitting at the same wavelength as the gut, which could potentially interfere with image analysis. The remaining dyes were of a near-infrared wavelength which have previously proven to be optimal for *in vivo* imaging due to increased signal penetration and no background tissue signal overlap. A stronger signal was observed with VivoTag-750 stained mf than those stained with Alexafluor-750, and signal reached a plateau at 150 μ M with no significant decrease in signal throughout the 7 day period. The peak signal with Alexafluor-750 was 33% lower than that of VivoTag-750 and at a higher concentration of 300 μ M. Thus, VivoTag-750 was progressed forward for *in vivo* optimisation.

Although not presented, mf were scored daily for motility to ensure no dose-dependent changes or toxicity were encountered. Mf retained 100% survival with full motility for the full duration across all dye concentrations.

5.5.2. *In vivo* imaging optimisation

In 'proof of concept' experiments, 250,000 stained mf were infused into the tail vein of a CB.17 SCID mouse – a density and strain previously validated for this type of model. SHO mice were also included in this study to determine whether the use of a hairless mouse improved imaging, alongside a non-infected CB.17 SCID control (Figure 5.2.A). At 24 hrs post-infection, a widespread signal was observed in both strains, with a more intense signal in the cardiothoracic and groin regions, potentially indicating a sequestration or potential elimination route (Figure 5.2.B-D). At 7 days post-infection, the widespread signal had diminished and was instead focused solely in the cardiothoracic and groin regions. Cardiothoracic signals had increased by approximately 12% and 6% in the CB.17 SCID and SHO mice, respectively. In contrast, the groin signal had decreased by 50% in SCID mice and 59% in SHO mice. By the 14 day end point, signals in these regions could still be observed, however the cardiothoracic signal intensity had further decreased by 25% and 15% in the CB.17 SCID and SHO line, respectively, whilst groin signals had increased by 4% and 6% for SCID and SHO mice, respectively. End-point peripheral microfilaraemias (Figure 5.2.E) were consistent between both strains, whereas cardiac parasitaemias were 54% higher in SHO mice than SCID mice (Figure 5.2.F), as reflected in the fluorescent signal intensity.

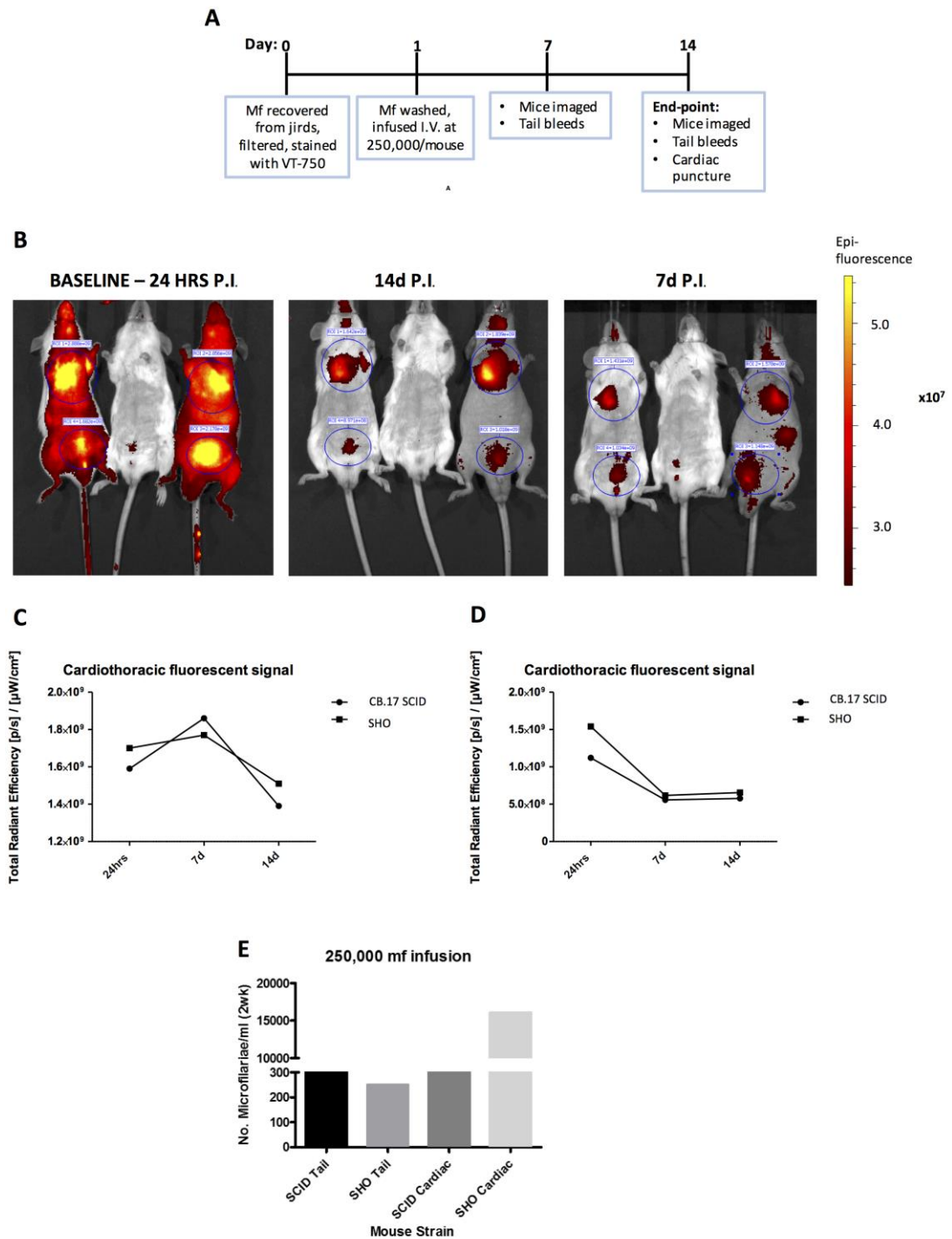


Figure 5.2 *In vivo* IVIS imaging optimisation with high yield parasitaemia (250,000 mf infused/mouse)

Experimental design schematic; mf fluorescently stained *in vitro*, infused i.v. into mice at 250,000/mouse, imaged 24hrs, 7d and 14d later with corresponding blood sampling for mf enumeration (A), fluorescent IVIS images at baseline, d14 and 7d p.i. From left to right = SCID, control, SHO (B), cardiothoracic fluorescent signal (C), groin fluorescent signal (D), cardiac and mf parasitaemias at d14 (E).

Next, lower density parasite infusions of 100,000 mf were trialled to determine whether fluorescent signals could be determined at a lower parasite inoculation and the persistence of signal could be evaluated (Figure 5.3.).

At baseline (24 hours post-infection), no widespread signal was observed in either strains (Figure 5.3.B-D). Signals were primarily focussed in the cardiothoracic and groin region - an earlier time point than observed with the 250,000 infusions. Instead of the cardiothoracic signal increasing at 7 days, the signal had decreased by 9% in the CB.17 SCID line, and 20% in the SHO line. Signal decreases were also observed in the groin region, with the CB.17 SCID strain exhibiting a 33% decrease in signal, whereas only a 16% decrease was observed in the SHO strain. At the end-point, no signal was detectable in the cardiothoracic region, whilst the groin signals remained constant. Parasitaemias were consistent with those of the 250,000 mf infusions (Figure 5.3.E), however in this experiment the fluorescent signals did not complement the parasite enumerations. No differences in fluorescent signals were observed in either mouse strains and thus it was concluded that either strain could be used for subsequent studies, however using the higher parasite density. Due to the CB.17 SCID mice already validated as a filarial drug model, this strain was selected.

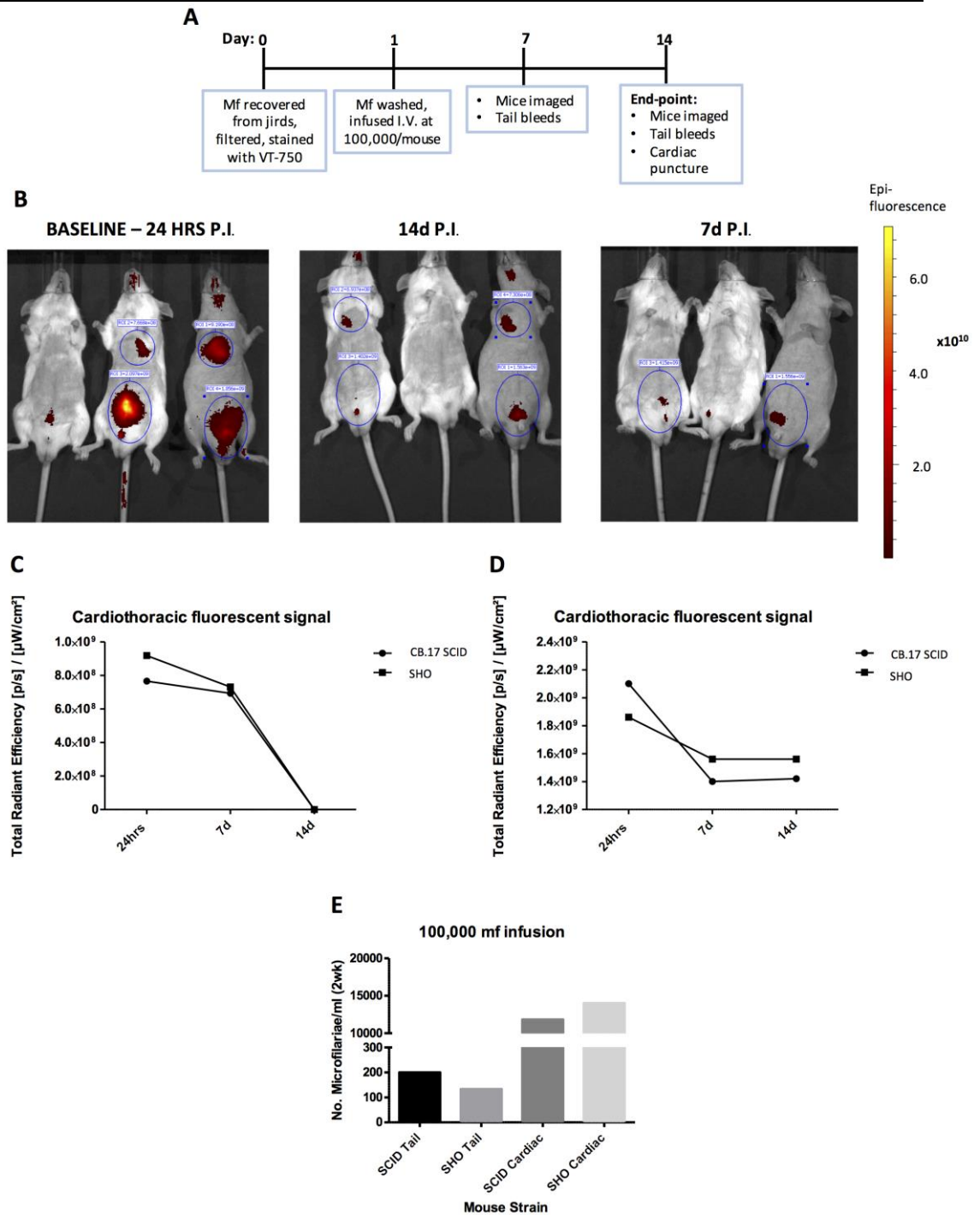


Figure 5.3. *In vivo* IVIS imaging optimisation with low yield parasitaemia (100,000 mf infused/mouse)

Experimental design schematic; mf fluorescently stained *in vitro*, infused i.v. into mice at 100,000/mouse, imaged 24h, 7d and 14d later with corresponding blood sampling for mf enumeration (A), fluorescent IVIS images at baseline, d14 and 7d p.i. Baseline from left to right = control, SCID, SHO. 14d + 21d from left to right = SCID, control, SHO (B), cardiothoracic fluorescent signal (C), groin fluorescent signal (D), cardiac and mf parasitaemias at d14 (E).

5.5.3. *B. malayi* microfilaraemic CB.17 SCID mouse ivermectin drug response pilot imaging study

An initial ivermectin microfilaricidal drug treatment response study was undertaken in CB.17 SCID mice (Figure 5.4). Mice were imaged 48-hours post-infection with 250,000 VivoTag-750 labelled mf to establish a baseline signal with corresponding peripheral parasitaemias. At this point, quantifiable signals were present in the cardiothoracic and groin regions (Figure 5.4.B). Mice in the vehicle control group displayed an average signal of $1.76 \times 10^9 \pm 3.0 \times 10^7$, whilst mice to be treated with IVM displayed an average cardiothoracic signal of $2.08 \times 10^9 \pm 1.75 \times 10^8$, 15% higher than the vehicle control mice (Figure 5.4.C). An 8% difference in signal intensity was observed in the groin region (vehicle control average = $5.82 \times 10^8 \pm 5.40 \times 10^7$; IVM average = $5.38 \times 10^8 \pm 5.00 \times 10^6$). 48-hours post-treatment, IVM treated mice displayed a more widespread anatomical fluorescent signal than the vehicle control mice, with a 22% increase in signal in the cardiothoracic region compared to baseline (IVM average cardiothoracic signal = $2.66 \times 10^9 \pm 1.60 \times 10^8$). This was 25% higher than the cardiothoracic signal quantified at 48hrs post-dosing in the vehicle control group (vehicle control average cardiothoracic signal = $2.00 \times 10^9 \pm 5.50 \times 10^7$), which was 11% higher than that at baseline. The groin signal intensity had increased by 10% in the IVM group (average = $6.02 \times 10^8 \pm 6.00 \times 10^6$), whereas only a 2% increase from baseline was observed in the vehicle control group (average = $5.95 \times 10^8 \pm 6.30 \times 10^7$) (Figure 5.4.D). This equated to only a 1% difference between groups. By day 7, cardiothoracic signals had decreased by 22% and 16% in IVM and vehicle control groups, respectively (IVM average = $2.18 \times 10^9 \pm 7.00 \times 10^7$; vehicle control average = $1.71 \times 10^9 \pm 2.00 \times 10^7$), equating to a 21% difference between groups. A decrease in signal intensity was also observed in the groin region, with decreases of 11% and 12% for IVM and vehicle control groups, respectively (IVM average = $5.42 \times 10^8 \pm 2.90 \times 10^7$; vehicle control average = $5.31 \times 10^8 \pm 1.90 \times 10^7$), equating to a 2% difference between groups.

Peripheral parasitaemias had decreased by 79% at 48-hours post treatment in the IVM group (baseline average = 400 ± 200 ; 48hrs post-dose average = 83.33 ± 16.67), before declining by a further 60% by end-point (average = 33.33 ± 33.33) (Figure 5.4.F). In contrast, peripheral parasitaemias in the vehicle control group has increased by 42% in comparison to baseline (baseline average = 100 ± 0 ; 48hrs post-dose average = 175 ± 75), and then increased by a further 43% by the end-point (average = 311.1 ± 88.89) (Figure 5.4.E).

Cardiopulmonary parasitaemias at end-point were 85% higher in the vehicle control group than IVM group (vehicle control average = 44175 ± 11375 ; IVM average = 6500 ± 450) (Figure 5.4.G). This confirmed the expected level of microfilaricidal drug efficacy.

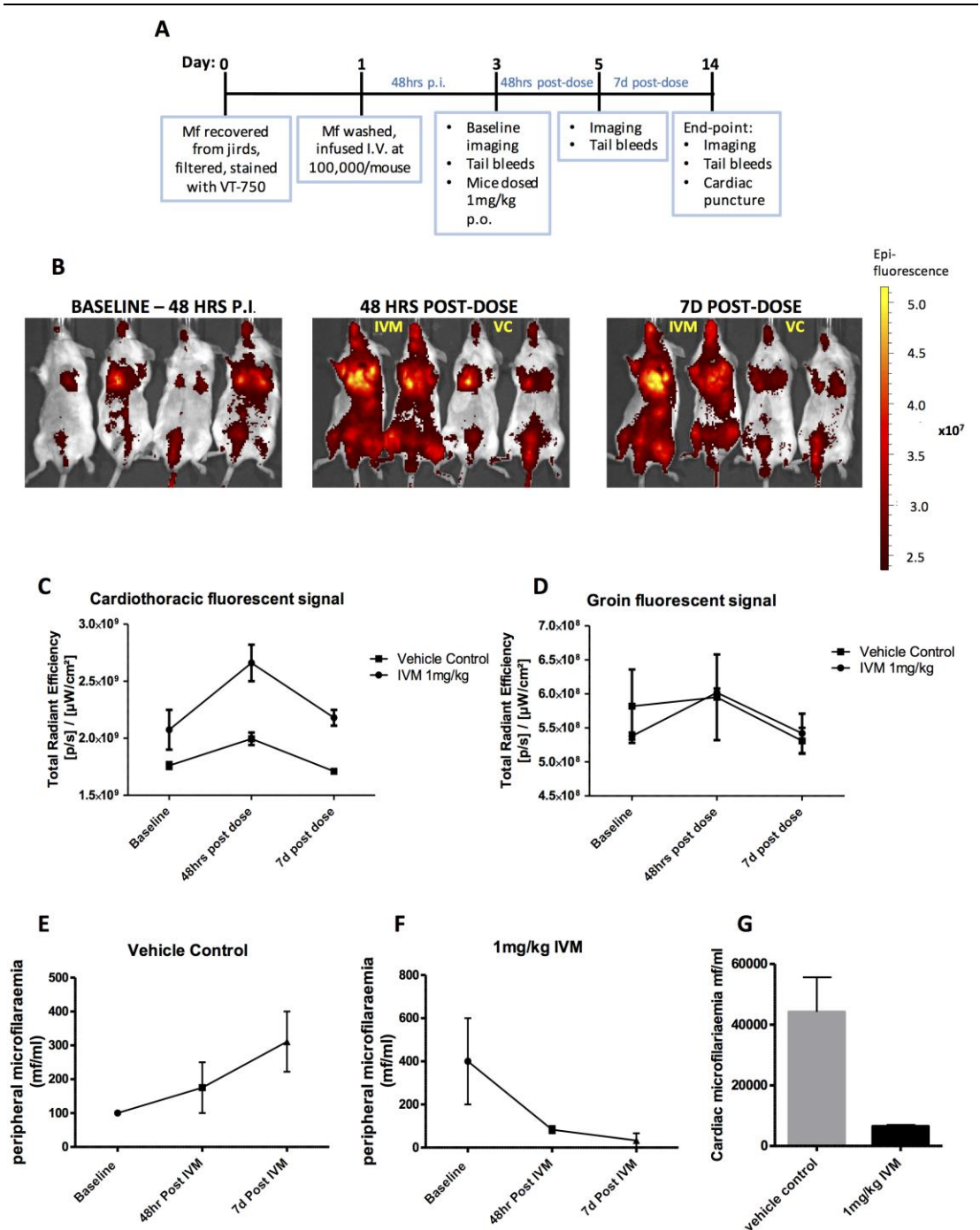


Figure 5.4. Pilot IVM drug challenge

Experimental set-up schematic; fluorescent mf infused i.v. at 250,000/mouse, imaged 48hrs later (baseline), dosed with 1mg/kg IVM and imaged 48hrs and 7d (end-point cardiac puncture) with corresponding blood sampling (A), baseline fluorescent imaging, Imaging at 48 hours post-dosing of vehicle control (right 2 mice) and IVM-treated (left 2 mice) (B), quantified cardiothoracic signal (C), quantified groin signal (D), peripheral microfilaraemias of IVM-treated mice (E), peripheral microfilaraemias of vehicle control mice (F), end-point cardiac parasitaemias (G)

CHAPTER 5

The pilot SCID IVM drug response imaging study was repeated with a larger sample size ($n=5$) for statistical testing (Figure 5.5). At baseline, a widespread fluorescent signal was observed which was quantified in the cardiac and groin regions (vehicle control cardiac mean = $1.13 \times 10^9 \pm 3.84 \times 10^7$, vehicle control groin mean = $1.19 \times 10^9 \pm 5.25 \times 10^7$; IVM cardiac mean = $1.23 \times 10^9 \pm 5.30 \times 10^7$, IVM groin mean = $7.73 \times 10^8 \pm 3.69 \times 10^7$) (Figure 5.5.B-D). Signals in the cardiothoracic region were comparable between groups, however signals quantified from the groin region were significantly higher in vehicle control mice (Student's T-test, $P < 0.001$). This was most-likely due to the differences in success rates of parasite infusions.

The intensity of the groin signal had significantly decreased in the vehicle control group by 48 hours post-treatment (mean = $7.04 \times 10^8 \pm 1.54 \times 10^8$, $P < 0.001$), which then continued to decrease until the end of the study (mean = $5.58 \times 10^8 \pm 5.25 \times 10^7$). In contrast, the groin signal remained fairly consistent in the IVM treated group, with a slight increase at the 48-hour post-treatment time-point (mean = $8.18 \times 10^8 \pm 3.46 \times 10^7$), followed by a slight decline back to approximate baseline signal levels (mean = $7.13 \times 10^8 \pm 1.61 \times 10^8$). At the 48 hour post-treatment time-point, cardiac fluorescent signals had significantly increased in the vehicle control group (vehicle control mean = $1.37 \times 10^9 \pm 3.03 \times 10^7$; IVM mean = $1.39 \times 10^9 \pm 3.70 \times 10^7$, Student's T-test, $P < 0.001$), followed by a significant decrease towards the end of the study whereby the signal was significantly lower in the vehicle control group (vehicle control mean = $9.24 \times 10^8 \pm 1.71 \times 10^7$; IVM mean = $1.18 \times 10^9 \pm 7.17 \times 10^7$, Student's T-test, $P < 0.05$). Peripheral microfilaraemias exhibited a significant decrease from baseline (vehicle control mean = 283.2 ± 89.13 ; IVM mean = 283.3 ± 117.4) to 48 hours post-treatment in both groups (vehicle control mean = 162.5 ± 74.65 ; IVM mean = 12.5 ± 12.5 , Student's T-test, $P < 0.05$), with no mf detected by end-point in the IVM group (Figure 5.5.F). Vehicle control microfilaraemias continued to decline until the end-point (mean = 87.5 ± 59.07) (Figure 5.5.E).

CHAPTER 5

Cardiopulmonary microfilaraemias were evaluated at end-point (Figure 5.5.F), which confirmed a significant decrease in the number of mf from the IVM treated group, signifying efficacy (vehicle control mean = 12438 ± 6312 ; IVM mean = 1081 ± 341.8 , Student's T-test, $P < 0.05$).

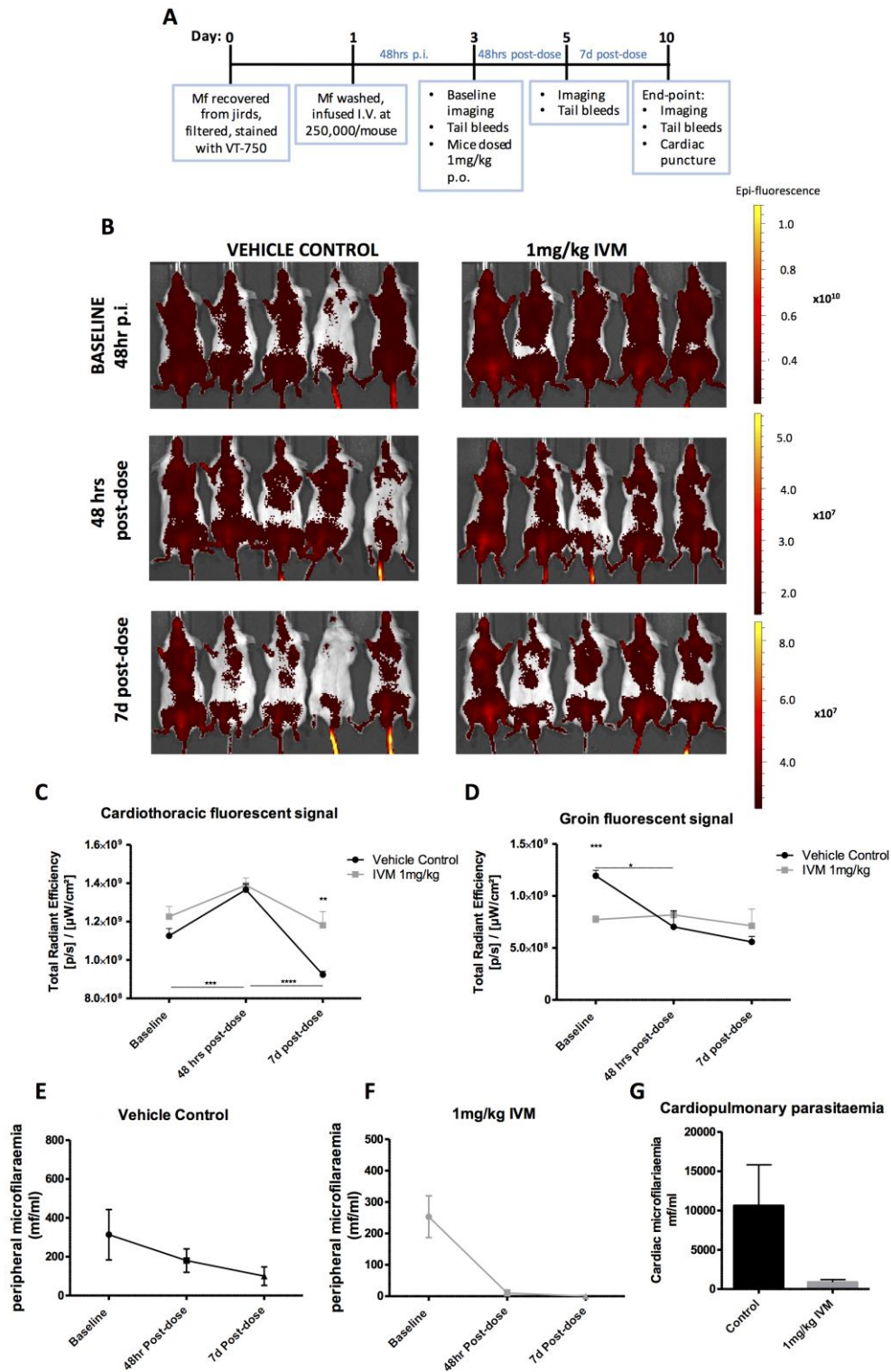


Figure 5.5. CB.17 SCID mouse IVM drug response imaging study A

Experimental set-up schematic; fluorescent mf infused i.v. at 250,000/mouse, imaged 48hrs later (baseline), dosed with 1mg/kg IVM and imaged 48hrs and 7d (end-point cardiac puncture) with corresponding blood sampling (A), fluorescent imaging at baseline, 48 hours post-IVM treatment, and 7 day end-point (B), quantified cardiothoracic signal (C), quantified groin signal (D), control mice peripheral microfilaraemias (E), IVM-treated mice peripheral microfilaraemias (F), end-point cardiac parasitaemias (G). Symbols represent mean values, error bars indicated SEM. ****P<0.0001, ***P<0.001, P<0.05.

5.5.4. *B. malayi* microfilaraemic CB.17 SCID mouse ivermectin drug response imaging study B

Due to differences in data between pilot and study A, a further repeat was undertaken in SCID mice with the addition of a heat-killed mf group to determine whether any changes in fluorescence post-IVM treatment were reflective of a “death signature signal” of VivoTag-750 labelled mf (Figure 5.6). At the baseline imaging time-point, no signal was determined in the cardiothoracic region of mice injected with heat-killed mf (Figure 5.6.B). However, a low signal was observed in the groin region (mean = $2.6 \times 10^9 \pm 1.62 \times 10^9$). Cardiothoracic signals were observed in the vehicle control (average = $6.52 \times 10^8 \pm 1.24 \times 10^7$) and IVM groups (average = $5.63 \times 10^8 \pm 1.46 \times 10^8$), in addition to groin signals (vehicle control average = $1.09 \times 10^9 \pm 2.99 \times 10^7$; IVM average = $1.52 \times 10^9 \pm 1.93 \times 10^8$), as observed in previous studies (Figure 5.6.B-D). By the 48 hour time-point, groin signals had significantly decreased in both the vehicle control and IVM groups (vehicle average = $2.21 \times 10^8 \pm 3.85 \times 10^7$; IVM average = $3.30 \times 10^8 \pm 2.08 \times 10^6$, $P < 0.001$), and had also decreased in the group injected with heat-killed mf (mean = $3.43 \times 10^8 \pm 1.42 \times 10^8$, $P < 0.001$). Cardiothoracic signals had also significantly declined in both IVM-treated and vehicle control mice (Figure 5.6.C) (IVM average = 0 ± 0 ; vehicle control average = $7.44 \times 10^7 \pm 7.44 \times 10^7$), whilst no signal could be detected in mice injected with heat-killed mf. By the 7-day end-point, the groin signal had increased slightly in the vehicle control group, which was significant compared with the 48 hour signal (average = $4.76 \times 10^8 \pm 8.71 \times 10^6$, Student’s T- test $P < 0.001$). No detectable signal was apparent in the groin ROI of the heat-killed mf group (average = 0 ± 0) (Figure 5.6.D), whilst the groin signal in the IVM group remained consistent with the 48-hour time-point (average = $2.86 \times 10^8 \pm 6.36 \times 10^6$). End-point cardiothoracic signals in the vehicle control (Figure 5.6.C) and IVM groups were determined to be significantly higher than the heat-killed mf group,

however no significant differences were determined between the IVM and vehicle control groups (one-way anova with Tukey's multiple comparisons test $P < 0.001$).

In terms of parasitology, peripheral parasitaemias were comparable between the vehicle control and IVM groups at baseline, prior to IVM administration (vehicle control average = 370 ± 100.7 ; IVM average = 478 ± 231), whilst no circulating mf were detected in the heat-killed group (Figure 5.6.E). Microfilaraemic levels in the IVM group sharply decreased to 0 by 48 hours, and a decrease was also observed in the vehicle control group (average = 110 ± 50.99) which then plateaued until the end of the study (average = 93.33 ± 47.9). Post-mortem cardiac parasitology analyses confirmed the significant reduction of mf in the IVM group in comparison to the vehicle control group (Figure 5.6.F) (vehicle control average = 17965 ± 2741 ; IVM average = 80 ± 80 , $P < 0.0001$), with no mf recovered from the heat-killed group).

Ex vivo imaging was conducted on selected organs to establish whether any fluorescent signals could be detected on this level (Figure 5.7). Upon imaging the heart, signals were observed in all hearts excised from the vehicle control group (average = $2.86 \times 10^7 \pm 4.27 \times 10^6$, $P < 0.0001$), whereas no signals were detected in the remaining two groups (Figure 5.7.A-B). Signals were also quantified in lungs from vehicle control mice (average = $5.28 \times 10^8 \pm 1.87 \times 10^7$, $P < 0.0001$), whilst no signals were present in the remaining groups. Splenic signals were observed in all mice across all groups, however the signal strength was significantly lower in the heat-killed group (vehicle control average = $2.88 \times 10^8 \pm 2.43 \times 10^6$; IVM average = $2.97 \times 10^8 \pm 3.38 \times 10^6$; heat-killed average = $1.69 \times 10^8 \pm 1.44 \times 10^6$, one-way anova with Tukey's multiple comparisons test, $P < 0.01$).

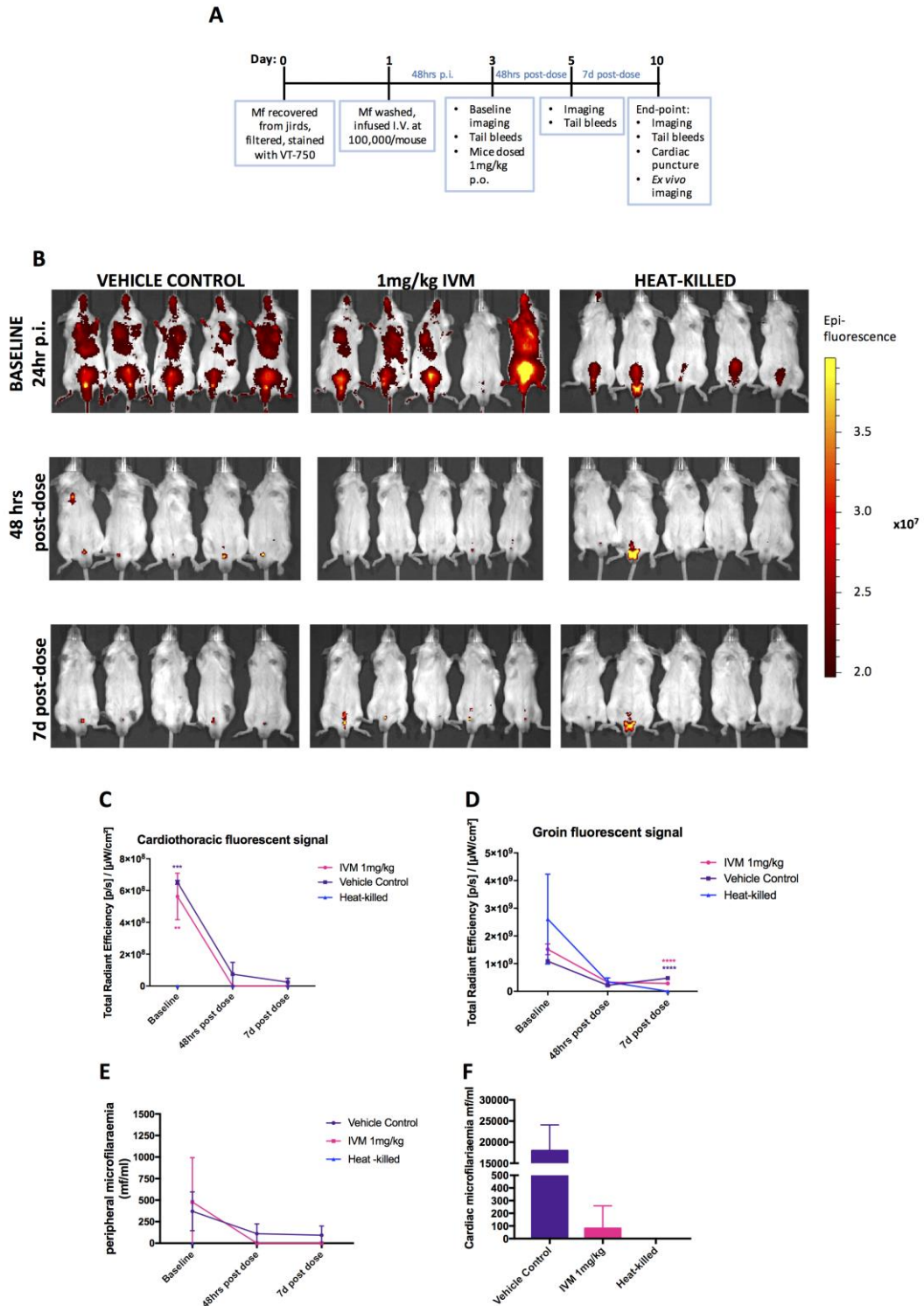


Figure 5.6a CB.17 SCID IVM treatment response imaging experiment B

Experimental set-up schematic; Experimental set-up schematic; fluorescent live or dead mf infused i.v. at 250,000/mouse, imaged 48hrs later (baseline), dosed with 1mg/kg IVM and imaged 48hrs and 7d (end-point cardiac puncture) with corresponding blood sampling and end-point ex vivo imaging (A), fluorescent imaging at baseline, 48 hours post-IVM treatment, and 7 day end-point (B), quantified cardiothoracic signal (C), quantified groin signal (D), peripheral microfilaraemias (E), end-point cardiac parasitaemias (F). Symbols represent mean values, error bars indicated SEM. ***P<0.001, P<0.05.

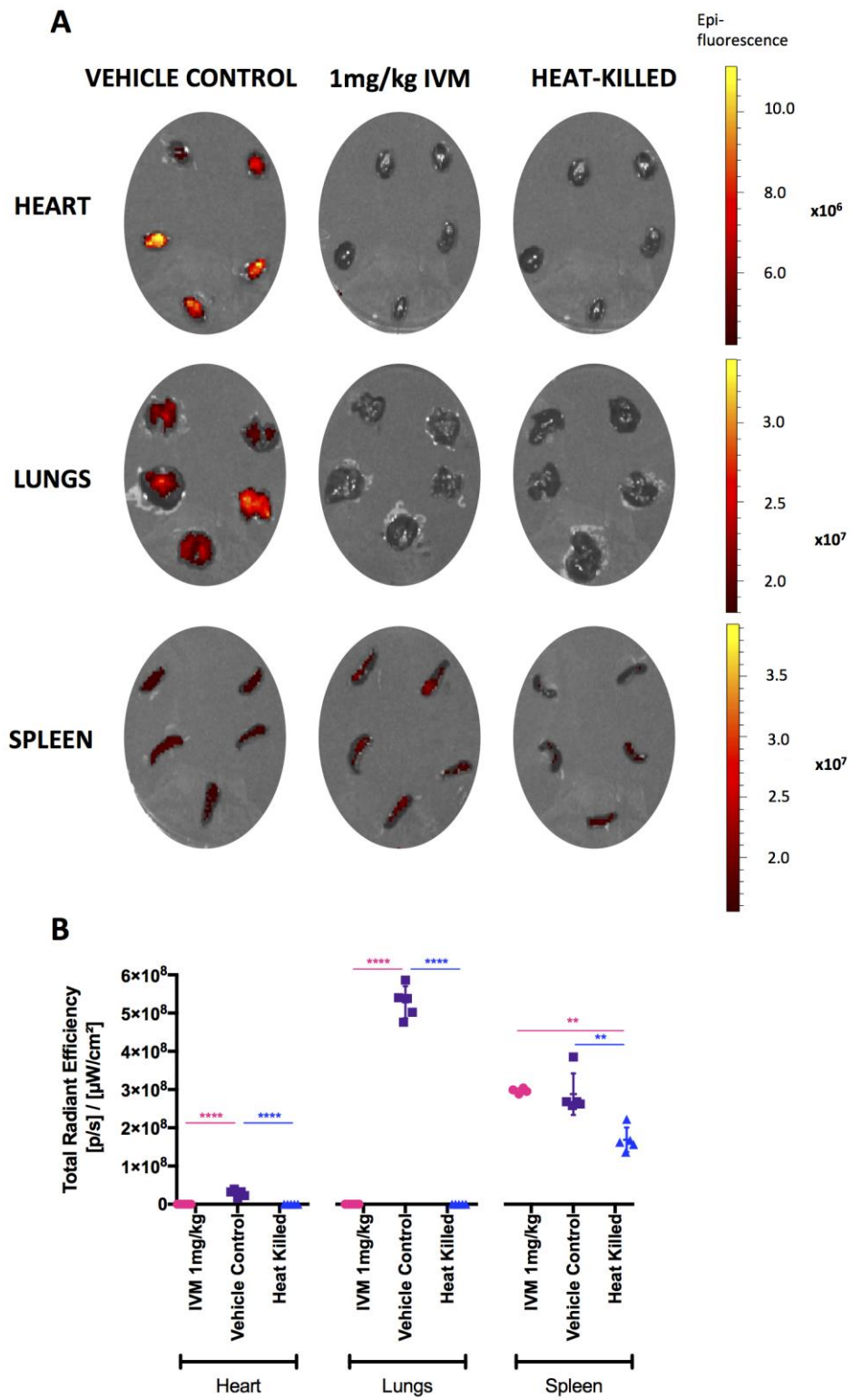


Figure 5.6b CB.17 SCID IVM treatment response imaging experiment B – *ex vivo* imaging

ex vivo imaging of heart, lungs and spleen from vehicle control mice infused with live fluorescent mf, IVM-treated mice infused with live fluorescent mf, and mice infused with heat-killed mf (A), quantification of *ex vivo* fluorescent signal (B). Horizontal bars represent the mean. Error bars represent the SEM ***P<0.001, P<0.05.

5.5.5. CB.17 SCID mouse *B. malayi* adult implant flubendazole drug treatment imaging experiment

An adult imaging model was trialled to determine whether macrofilaricidal efficacy could be detected *in vivo* using fluorescent imaging modalities (Figure 5.7). Adult *B. malayi* were stained with VivoTag-750 and surgically implanted into the peritoneal cavities of CB.17 SCID mice, prior to dosing with the known macrofilaricide, flubendazole (FBZ).

A strong fluorescent signal was located at the site of implantation in the peritoneal cavity at baseline (vehicle control average = $9.033 \times 10^9 \pm 1.975 \times 10^9$; FBZ average = $8.583 \times 10^9 \pm 2.474 \times 10^9$). FBZ dosing commenced 2 hours post-surgery. Imaging at 24 hours after starting treatment (and implantation) indicated a significant decrease in fluorescent signal of the vehicle control group (Figure 5.7.B-D) (average = $2.635 \times 10^9 \pm 1.546 \times 10^8$, Student's T-test, $P < 0.01$), which was significantly lower than the signal quantified for the FBZ group (average = $4.930 \times 10^9 \pm 3.204 \times 10^8$, Student's T-test, $P < 0.001$). Signals in both groups declined further in both groups at 24 hours after the final FBZ dose (6 days post-implantation and initiation of dosing) (vehicle control average = $2.26 \times 10^9 \pm 3.53 \times 10^8$; FBZ mean = $1.81 \times 10^9 \pm 5.06 \times 10^8$) and remained low at the endpoint of the study at 10 days post-implantation (vehicle control average = $7.73 \times 10^8 \pm 2.54 \times 10^8$; FBZ average = $2.40 \times 10^9 \pm 8.08 \times 10^8$). No fluorescent signal was apparent in FBZ treated naïve mice at any time point, indicating the drug did not induce any auto-fluorescence *in vivo*.

Post-mortem parasitological analyses revealed a lower recovery in mice treated with FBS (Figure 5.7.E). MTT analysis on vehicle control versus FBZ treated parasites concluded a significant decrease in the metabolic activity of parasites retrieved from FBZ treated mice

(Figure 5.7.F) ($P < 0.001$, Mann Whitney test), and lower numbers of mf recovered ip (Figure 5.7.G).

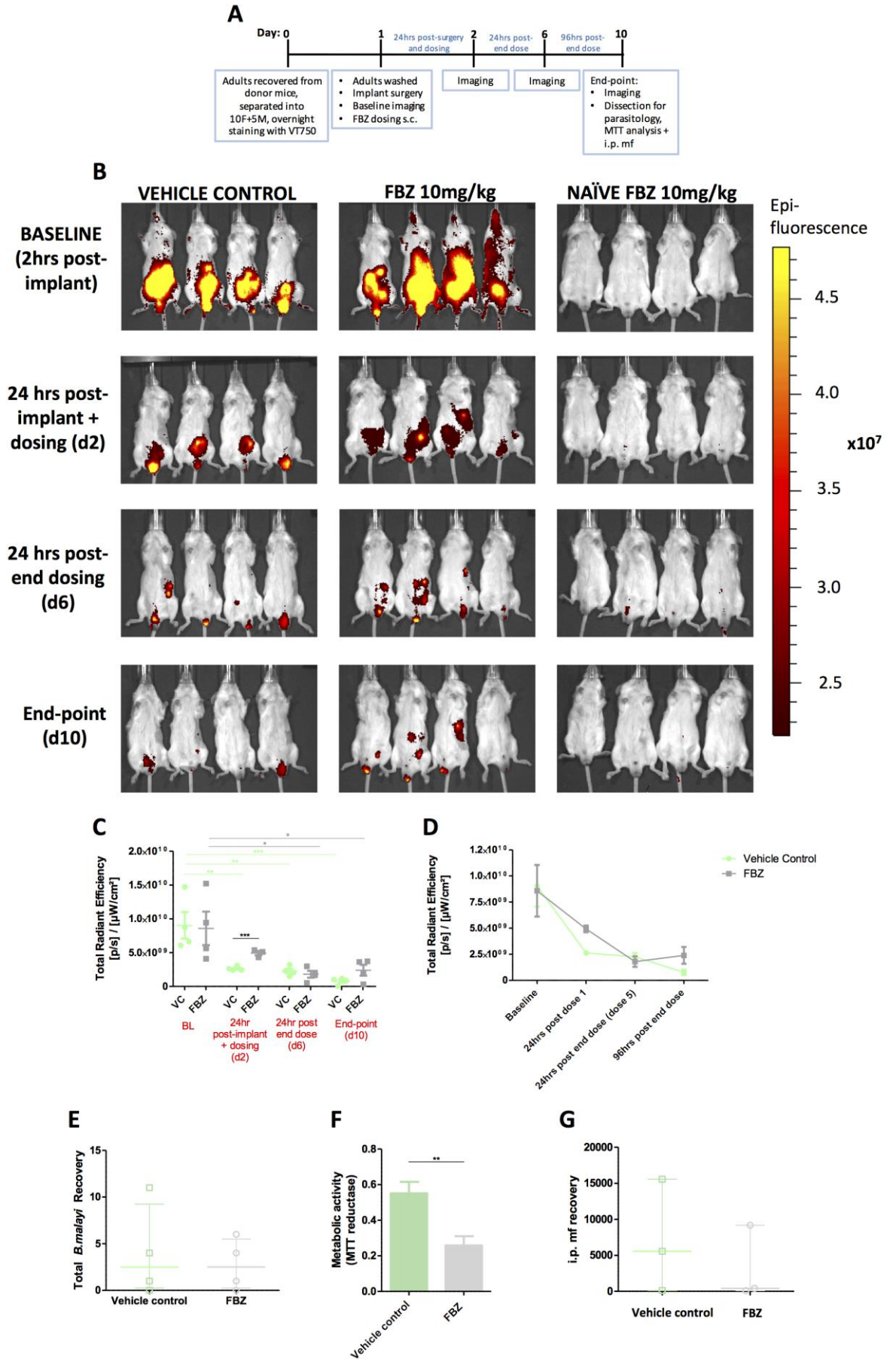


Figure 5.7. CB.17 SCID mouse *B. malayi* adult implant flubendazole drug challenge

Experimental set-up schematic; recovered adult *Bm* stained with fluorescent dye overnight, washed, and surgically implanted into mice peritonea, imaged 2hr post-surgery and dosed with 10mg/kg flubendazole. Imaging was conducted 24hr post first-dose, 24hr post final-dose and 96hr post final-dose (A), fluorescent IVIS imaging at baseline, 25 hours post initial FBZ dose, 24 hours post end FBZ dose and end-point (B) quantified fluorescent signal (C), end-point total *Bm* parasite recovery (D), end-point intraperitoneal mf recoveries (E), end-point optical density readings from MTT viability assay on recovered parasites (F), number of microfilariae recovered from the peritoneal cavity of mice treated with vehicle or flubendazole (G). Symbols represent mean values, error bars indicated SEM. ***P<0.001, **P<0.01.

5.6. Discussion

The aim of this chapter was to optimise a model to fluorescently label and track microfilariae and adult stage parasites *in vivo* and determine whether the model could be applied to assess the efficacy of anti-filarial agents using the reference drugs, IVM and FBZ, for longitudinal imaging to reduce and refine the number of animals used for pre-clinical screening.

Following successful labelling and quantification of fluorescently stained mf *in vitro*, experiments proceeded to the *in vivo* stage for optimisation. It was established that mf sequester in the cardio-pulmonary tissues shortly after infection, as well as potentially sequestering in the groin area. However, it could not be established whether this signal in the groin was due to the liberation and excretion of free dye from mf or a general signal of labelled mf in the superficial blood vessels, due to these being close the skin surface in this region. It was also concluded that no benefits arose from using hairless SCID mice (SHO) in comparison to CB.17 SCID mice, and hence either could be used for imaging purposes. The SCID mouse was therefore selected for subsequent studies due to it being the standard drug screening model (Halliday et al., 2014).

The translation as a model to determine drug efficacy was somewhat challenging. In the pilot study, an increased signal was observed in IVM-treated mice, which was hypothesised to be either the release of dye due to drug-induced damage of mf cuticle integrity, migration of dying or dead mf away from cardiopulmonary tissues and entrapment in multiple capillary beds following treatment or absorption of dye-labelled parasite proteins into host tissues following their death and disintegration. After subsequent repeats in CB.17 SCID mice, these imaging phenomena were unreproducible, with no reproducibly significant difference in fluorescent signal observed between control and treated mice relating to the treatment efficacy of IVM determined by parasitological enumeration of mf. To further test whether a

rapid killing of mf *in vivo* would be related to a change in fluorescent patterns, fluorescently labelled and heat killed mf were perfused into mice. Mice infused with heat-killed mf produced a signal in the groin region only, which supported the hypothesis that dead mf proteins and unbound dye were excreted via the bladder, particularly as dead mf did not sequester in cardiac tissues, as confirmed via parasitological analysis.

Unfortunately, there was no way to determine whether viable individual mf had retained their stain at end-point due to the high NIR wavelength dye used, which was incompatible with standard fluorescent and confocal microscope lasers available. Further, signals in both drug-treated and control mice dissipated early into the study, despite high parasitaemias at end-point, with no increase in groin signal or widespread signal. *Ex vivo* imaging was then carried out to determine whether the lack of signal could be a limit of the IVIS technology. Signals were prevalent in the heart and lungs in control mice, indicating stained mf had sequestered. However, this could not be detected with whole-body IVIS imaging. Fluorescent signals were observed *ex vivo* in the spleen of all mice, suggesting mf may also be cleared by the spleen. This then arose speculation as to whether staining efficiency was dependent on the age of the mf, and perhaps some mf of an earlier age were not initially stained, which may have affected the whole-body imaging. The mf age could not be controlled for due to the requirement of invasive catheterisation of gerbils for mf production, which was dependent on the availability of gerbils and the requirements for other experimentation within the laboratory.

Strong fluorescent signals were observed in mice implanted with fluorescently labelled adults, however this signal depreciated quickly over the course of the study, potentially due to a rapid protein turnover in adult stage *B. malayi*. After the initial dose of FBZ, the fluorescent signal was significantly higher in FBZ treated mice compared to vehicle treated

mice. This was potentially due to the excess leakage of dye following drug-induced damage to parasites, however these differences were only evident at this time-point.

At present the infusion of fluorescently labelled mf to image drug responses *in vivo* is too variable with too low long-term signal intensity to be utilised as a robust model for whole animal bioimaging. Instead, the technique may be of future use in tracking and quantifying filarial mf migrations and tissue tropisms, applying *ex vivo* bioimaging of dissected tissues. However a more sensitive imaging system such as PET or SPECT, or the incorporation of multi-modal imaging technologies, may be more appropriate for this purpose *in vivo* as these can provide more precise information discerning specific locations, offer higher resolution images, and more observable anatomical changes.

The use of bioluminescent reagents to evaluate host-parasite interactions, immunopharmacology, and vaccine efficacy offer great potential. However success and sensitivity may be vastly improved with the use of immunocompetent mouse strains, whereby more components of the immune system can be imaged, which will give a more informed output on the mechanisms of how drugs and vaccines may be working, as opposed to immune-deficient strains whereby some information may be missed.

The most successful examples of fluorescent and bioluminescent imaging occur in studies utilising genetically manipulated parasites, bacteria, and cells, able to express fluorescent proteins, or luciferase (Sanz et al., 2008, Sjölander and Jonsson, 2007, Engelsman et al., 2009), genetic manipulation of helminths is very much in its naivety. However a new approach has been undertaken. A recent study describes a 'piggybac' technique, allowing the manipulation of the *B. malayi* genome to introduce a fluorescent gene into the system, however when allowed to develop *in vivo*, only a small percentage of the progeny displayed this genotype, further highlighting the difficulties in this area of research (Liu et al., 2018). This approach could significantly improve the fluorescent imaging of filarial parasites *in vivo*, although

further work needs to be conducted to improve the expression of these fluorescent/bioluminescent genes to enable the horizontal transfer of the constructs throughout the different lifecycle stages, for which CRISPR technology could be utilised.

Alternatively, tools have been developed in which transgenic parasites are not required. Substrates, such as luminol and lucigenin have been developed which target the oxygen species released neutrophils and macrophages, respectively. Upon binding, bioluminescence is emitted a by-product, allowing for components of the immune system to be imaged *in vivo*, or in-directly, parasites, whereby the immune system can be tracked in response to worms. This was demonstrated in the context of filarial infection by Myburg et al (Myburgh et al., 2016), albeit with limited success due to issues with inflammation post-surgery. This technology could be applied to L3 infections to track immune responses *in vivo*, and also to allow development to adult stages for re-imaging which would negate the issues with surgical inflammation. This could then be used to elucidate the immune response to parasites in greater detail, and also gives the opportunity for the immune effects, and synergy with drugs (immunopharmacology) to be studied, having significant benefits on the reduction and refinement of animals.

Chapter 6: Concluding remarks, uptake and future work

The overall aims of this thesis were to develop novel and alternative methods of anti-filarial drug screening which reduce, refine and replace the use of animals in this area of research.

7.1. Replacement

As rodent, and canine models (in the context of veterinary filariae) are heavily relied upon for the generation of adult-stage parasites due to an inability to maintain the full life-cycle *in vitro*, Chapter 2 focused on the development of an *in vitro* model to support the whole life-cycle. More detailed analyses into evaluation of culture systems were incorporated to better inform the 'real' *in vitro* parasite fitness, which prior to this work were unknown. Unfortunately, parasites still failed to develop post 10 days, even on optimum cell layers, with *Wolbachia* titres comparable to those *in vivo*. This concludes that an *in vitro* system can not replace the full brugian life cycle. However further work trialling a fatty lymphatic composition with different immune cells could be trialled which may extend culture periods.

The related veterinary filariae, *Dirofilaria immitis*, displayed more promising results, whereby larval stages continued to grow, with high survival rates, for up to 38 days in culture. This work is only in its initial stages and would require more robust analyses, as conducted with *Brugia* larvae, to fully determine the success of this culture. If successful, it could allow for the screening of novel prophylactic treatments against heartworm, negating the need for testing on dogs for the purpose. Further, it could have great implications on the replacement of experimentally infected dogs to maintain the life cycle. Instead, mf could be collected from naturally-infected client-owned dogs, developed to larvae through mosquitoes, and cultured through to adults stages which could then release their own progeny.

Although the *in vitro* model did not suffice to replace rodents for the life cycle, the model could be utilised to determine activity of anti-*Wolbachia* compounds against larval stages for periods of up to 10 days, hence reducing and replacing the need for rodents for this purpose. Currently, the level of *Wolbachia* depletion to prevent further development is currently

unknown. With the likeness to *in vivo* parasites confirmed, this system could thus be utilised to evaluate this, in addition to basic parasite biology in future works.

7.2. Reduction

Chapter 3 centred around the reduction of animals in anti-filarial drug screening. A meta-analysis of long-term infections in gerbils, CB.17 SCID and BALB/c IL4R $\alpha^{-/-}$ /IL5 $^{-/-}$ mice concluded that by using immunodeficient mouse strains, rodent usage can be reduced 2-fold, with 4-fold lower BmL3 inoculations. It has been noted during routine experiments that CB.17 SCID mice often run into welfare issues with increasing age, meaning longer-term infections can not always be possible. Using the knockout mouse strain governing 'Th2' adaptive immune processes, BALB/c IL4R $\alpha^{-/-}$ /IL5 $^{-/-}$, these issues are not encountered and consequently, animal welfare is improved and refined.

Leading on from this was the successful development of an adult stage-specific model, that demonstrated that parasite survival is more dependent on a host-specific cell line. This demonstrates one of the onward applications that the model could be used for; looking at the interplay between macrophages, lymphatic cells and parasites. The *in vitro* model provides an additional step in the drug development pipeline, allowing potential compounds to be thoroughly scrutinized against the appropriate stage, and therefore may stop the progression of sub-optimal candidates progressing into pre-clinical studies, thus reducing animals. *In vitro* maintained parasites have been robustly compared against those *in vivo*, with the health of *Wolbachia* further exemplified in that recrudescence is observed following sub-optimal dosing with doxycycline, as observed *in vitro*. Due to this, the model has been implemented within the laboratory as a model to assess autophagy, and autophagy post *in vitro* drug treatment. Prior to this model, this work would have had to be conducted *in vivo* – further showing how animal usage can be reduced. Lastly, as the model was also validated for use as a 'direct-acting' compound assay, two potential candidates may have been

identified which show activity against adult Bm females, although further efficacy testing will be required.

7.3. Refinement

The lack of prognostic indicators of drug efficacy in both micro- and macrofilaricidal experimental drug efficacy tests *in vivo* make it difficult to predict end-points where efficacy should be assessed. As a result, multiple animal test groups are required to assess efficacy at different time-points post-treatment, and several repeat experiments with varying, or prolonged time courses are often required. The only method available to give any indication on efficacy is through repetitive, invasive blood sampling of microfilariae to establish whether compounds have exerted any sterility effects on adult female *B. malayi*.

To refine, and reduce, animal usage, ultrasonographic imaging of parasites in the peritoneal cavity was evaluated in Chapter 4, followed by the confirmation that ultrasound can be applied to assess direct-acting drug activity longitudinally. It was concluded that ultrasound can in fact detect and delineate approximate parasite yields *in vivo* with a sensitivity of >81%. This has a remarkable effect on the number of animals enrolled into pre-clinical studies and improve the quality of pre-clinical screen data. For example, ultrasound can detect high, low, and negative infections and can henceforth be implemented to randomise mice into drug testing experiments, ultimately reducing intra- and inter-group variability. Further, negatively infected animals can be eliminated from studies – refining the need for unnecessary, invasive dosing. The fact that drug efficacy can also accurately be evaluated longitudinally means that the need for multiple treatment groups to assess different drug washout times can be somewhat negated, and also obviate the need for re-implantation surgeries for extended washout periods – both refining animal usage and reducing animal use by as much as 40%. The ultrasonographic imaging has since been implemented into pre-clinical drug screens, whereby animals were imaged prior to treatment group allocation to

reduce bias and variability, and obviate the need for un-infected animals to undergo unnecessary dosing (Taylor et al., 2019).

Chapter 5 applied the use of bio-imaging tools to longitudinally study *in vivo* microfilarial drug efficacy using fluorescently stained mf and IVIS technology. Whilst mf could be visualised *in vivo* in the cardiothoracic and groin regions, with consistent parasitologies to previous mf infusion trajectories within the laboratory, the use as a drug model was unreproducible. Further work is required to allow for this system to be utilised as a fully functioning model to assess parasite tropisms and drug efficacy. One option would be to trial the new genetically modified fluorescent *B. malayi* within this system to evaluate whether signals persist longer and are capable of showing differences in response to drug treatment (Liu et al., 2018), potentially using different imaging systems with better depth perception. Another option is to use bioluminescent substrates able to indirectly label macrophages and neutrophils (Myburgh et al., 2016), amongst other immune/inflammatory components, to evaluate immune responses to parasites, look deeper into the immunopharmacology of novel and existing drugs, and try to predict/better understand the mechanisms of severe adverse drug reactions.

References

- ABRAHAM, D., LANGE, A. M., YUTANAWIBOONCHAI, W., TRPIS, M., DICKERSON, J. W., SWENSON, B. & EBERHARD, M. L. 1993. Survival and development of larval *Onchocerca volvulus* in diffusion chambers implanted in primate and rodent hosts. *The Journal of parasitology*, 79, 571-582.
- ABRAHAM, D., MOK, M., MIKA-GRIEVE, M. & GRIEVE, R. B. 1987. In vitro culture of *Dirofilaria immitis* third- and fourth-stage larvae under defined conditions. *J Parasitol*, 73, 377-83.
- AHMED, S. S. 1967. Studies on the laboratory transmission of sub-periodic *Brugia malayi* and *B. pahangi*. *Annals of Tropical Medicine & Parasitology*, 61, 432-436.
- ALJAYYOUSI, G., TYRER, H. E., FORD, L., SJOBERG, H., PIONNIER, N., WATERHOUSE, D., DAVIES, J., GAMBLE, J., METUGENE, H., COOK, D. A., STEVEN, A., SHARMA, R., GUIMARAES, A. F., CLARE, R. H., CASSIDY, A., JOHNSTON, K. L., MYHILL, L., HAYWARD, L., WANJI, S., TURNER, J. D., TAYLOR, M. J. & WARD, S. A. 2017. Short-Course, High-Dose Rifampicin Achieves Wolbachia Depletion Predictive of Curative Outcomes in Preclinical Models of Lymphatic Filariasis and Onchocerciasis. *Sci Rep*, 7, 210.
- AMARAL, F., DREYER, G., FIGUEREDO-SILVA, J., NOROES, J., CAVALCANTI, A., SAMICO, S. C., SANTOS, A. & COUTINHO, A. 1994. Live adult worms detected by ultrasonography in human Bancroftian filariasis. *Am J Trop Med Hyg*, 50.
- AMINO, R., MENARD, R. & FRISCHKNECHT, F. 2005. In vivo imaging of malaria parasites--recent advances and future directions. *Curr Opin Microbiol*, 8, 407-14.
- ANDREU, N., ZELMER, A. & WILES, S. 2011. Noninvasive biophotonic imaging for studies of infectious disease. *FEMS Microbiol Rev*, 35, 360-94.
- ASH, L. R. 1973. Chronic *Brugia pahangi* and *Brugia malayi* infections in *Meriones unguiculatus*. *J Parasitol*, 59.
- ASH, L. R. & RILEY, J. M. 1970. Development of Subperiodic *Brugia malayi* in the Jird, *Meriones unguiculatus*, with Notes on Infections in Other Rodents. *The Journal of Parasitology*, 56, 969-973.
- AWADZI, K. 2003. Clinical picture and outcome of serious adverse events in the treatment of Onchocerciasis. *Filaria J*, 2.
- AWADZI, K., OPOKU, N. O., ATTAH, S. K., LAZDINS-HELDS, J. & KUESEL, A. C. 2014. A randomized, single-ascending-dose, ivermectin-controlled, double-blind study of moxidectin in *Onchocerca volvulus* infection. *PLoS Negl Trop Dis*, 8.
- AZIZ, M. A., DIALLO, S., DIOP, I. M., LARIVIERE, M. & PORTA, M. 1982. Efficacy and tolerance of ivermectin in human onchocerciasis. *Lancet*, 2, 171-3.
- BABU, S. & NUTMAN, T. B. 2012. Immunopathogenesis of lymphatic filarial disease. *Seminars in immunopathology*, 34, 847-861.
- BAKOWSKI, M. A. & MCNAMARA, C. W. 2019. Advances in Antiwolbachial Drug Discovery for Treatment of Parasitic Filarial Worm Infections. *Trop Med Infect Dis*, 4.
- BALLESTEROS, C., TRITTEN, L., O'NEILL, M., BURKMAN, E., ZAKY, W. I., XIA, J., MOORHEAD, A., WILLIAMS, S. A. & GEARY, T. G. 2016. The Effect of In Vitro Cultivation on the Transcriptome of Adult *Brugia malayi*. *PLOS Neglected Tropical Diseases*, 10, e0004311.
- BANDI, C., ANDERSON, T. J., GENCHI, C. & BLAXTER, M. L. 1998. Phylogeny of Wolbachia in filarial nematodes. *Proceedings. Biological sciences*, 265, 2407-2413.
- BASANEZ, M. G., PION, S. D., BOAKES, E., FILIPE, J. A., CHURCHER, T. S. & BOUSSINESQ, M. 2008. Effect of single-dose ivermectin on *Onchocerca volvulus*: a systematic review and meta-analysis. *Lancet Infect Dis*, 8.

REFERENCES

- BAZZOCCHI, C., MORTARINO, M., GRANDI, G., KRAMER, L. H., GENCHI, C., BANDI, C., GENCHI, M., SACCHI, L. & MCCALL, J. W. 2008. Combined ivermectin and doxycycline treatment has microfilaricidal and adulticidal activity against *Dirofilaria immitis* in experimentally infected dogs. *Int J Parasitol*, 38, 1401-10.
- BÉLARD, S., TAMAROZZI, F., BUSTINDUY, A. L., WALLRAUCH, C., GROBUSCH, M. P., KUHN, W., BRUNETTI, E., JOEKES, E. & HELLER, T. 2016. Point-of-Care Ultrasound Assessment of Tropical Infectious Diseases—A Review of Applications and Perspectives. *The American Journal of Tropical Medicine and Hygiene*, 94, 8-21.
- BENNURU, S. & NUTMAN, T. B. 2009. Lymphangiogenesis and Lymphatic Remodeling Induced by Filarial Parasites: Implications for Pathogenesis. *PLOS Pathogens*, 5, e1000688.
- BIRD, A. C., EL-SHEIKH, H., ANDERSON, J. & FUGLSANG, H. 1979. Visual loss during oral diethylcarbamazine treatment for onchocerciasis. *Lancet*, 2.
- BIRD, A. C., EL-SHEIKH, H., ANDERSON, J. & FUGLSANG, H. 1980. Changes in visual function and in the posterior segment of the eye during treatment of onchocerciasis with diethylcarbamazine citrate. *Br J Ophthalmol*, 64, 191-200.
- BOATIN, B. 2008. The Onchocerciasis Control Programme in West Africa (OCP). *Annals of Tropical Medicine & Parasitology*, 102, 13-17.
- BOSSHARDT, S. C., MCCALL, J. W., COLEMAN, S. U., JONES, K. L., PETIT, T. A. & KLEI, T. R. 1993. Prophylactic activity of tetracycline against *Brugia pahangi* infection in jirds (*Meriones unguiculatus*). *The Journal of parasitology*, 79, 775-777.
- BOTTO, C., BASAÑEZ, M.-G., ESCALONA, M., VILLAMIZAR, N. J., NOYA-ALARCÓN, O., CORTEZ, J., VIVAS-MARTÍNEZ, S., CORONEL, P., FRONTADO, H., FLORES, J., GRATEROL, B., CAMACHO, O., TOVAR, Y., BORGES, D., MORALES, A. L., RÍOS, D., GUERRA, F., MARGELI, H., RODRIGUEZ, M. A., UNNASCH, T. R. & GRILLET, M. E. 2016. Evidence of suppression of onchocerciasis transmission in the Venezuelan Amazonian focus. *Parasites & Vectors*, 9, 40.
- BOUCHERY, T., LEFOULON, E., KARADJIAN, G., NIEGUISILA, A. & MARTIN, C. 2013. The symbiotic role of *Wolbachia* in Onchocercidae and its impact on filariasis. *Clin Microbiol Infect*, 19, 131-40.
- BOURGUINAT, C., KELLER, K., XIA, J., LEPAGE, P., MCTIER, T. L., WOODS, D. J. & PRICHARD, R. K. 2017. Genetic profiles of ten *Dirofilaria immitis* isolates susceptible or resistant to macrocyclic lactone heartworm preventives. *Parasites & vectors*, 10, 504-504.
- BOUSSINESQ, M., FOBI, G. & KUESEL, A. C. 2018. Alternative treatment strategies to accelerate the elimination of onchocerciasis. *International Health*, 10, i40-i48.
- BOUSSINESQ, M., GARDON, J., GARDON-WENDEL, N. & CHIPPAUX, J.-P. 2003. Clinical picture, epidemiology and outcome of Loa-associated serious adverse events related to mass ivermectin treatment of onchocerciasis in Cameroon. *Filaria journal*, 2 Suppl 1, S4-S4.
- BROWN, K. R., RICCI, F. M. & OTTESEN, E. A. 2000. Ivermectin: effectiveness in lymphatic filariasis. *Parasitology*, 121 Suppl, S133-46.
- BUCKINGHAM, S. D., PARTRIDGE, F. A. & SATTELLE, D. B. 2014. Automated, high-throughput, motility analysis in *Caenorhabditis elegans* and parasitic nematodes: Applications in the search for new anthelmintics. *International journal for parasitology. Drugs and drug resistance*, 4, 226-232.
- BULMAN, C. A., BIDLOW, C. M., LUSTIGMAN, S., CHO-NGWA, F., WILLIAMS, D., RASCON, A. A., JR., TRICOCHÉ, N., SAMJE, M., BELL, A., SUZUKI, B., LIM, K. C., SUPAKORNDEJ, N., SUPAKORNDEJ, P., WOLFE, A. R., KNUDSEN, G. M., CHEN, S., WILSON, C., ANG, K. H., ARKIN, M., GUT, J., FRANKLIN, C., MARCELLINO, C., MCKERROW, J. H., DEBNATH, A. & SAKANARI, J. A. 2015. Repurposing auranofin as a lead candidate for treatment of lymphatic filariasis and onchocerciasis. *PLoS Negl Trop Dis*, 9, e0003534.

REFERENCES

- BÜTTNER, D. W., WANJI, S., BAZZOCCHI, C., BAIN, O. & FISCHER, P. 2003. Obligatory symbiotic Wolbachia endobacteria are absent from Loa loa. *Filaria Journal*, 2, 10.
- CAMPBELL, W. C. 1982. Efficacy of the avermectins against filarial parasites: a short review. *Vet Res Commun*, 5, 251-62.
- CASIRAGHI, M., FAVIA, G., CANCRINI, G., BARTOLONI, A. & BANDI, C. 2001. Molecular identification of Wolbachia from the filarial nematode Mansonella ozzardi. *Parasitology Research*, 87, 417-420.
- CHAUBAL, N. G., PRADHAN, G. M., CHAUBAL, J. N. & RAMANI, S. K. 2003. Dance of live adult filarial worms is a reliable sign of scrotal filarial infection. *J Ultrasound Med*, 22, 765-9; quiz 770-2.
- CLARE, R. H., CLARK, R., BARDELLE, C., HARPER, P., COLLIER, M., JOHNSTON, K. L., PLANT, H., PLANT, D., MCCALL, E., SLATKO, B. E., CANTIN, L., WU, B., FORD, L., MURRAY, D., RICH, K., WIGGLESWORTH, M., TAYLOR, M. J. & WARD, S. A. 2019. Development of a High-Throughput Cytometric Screen to Identify Anti-Wolbachia Compounds: The Power of Public-Private Partnership. *SLAS DISCOVERY: Advancing Life Sciences R&D*, 24, 537-547.
- CLARE, R. H., COOK, D. A., JOHNSTON, K. L., FORD, L., WARD, S. A. & TAYLOR, M. J. 2015. Development and validation of a high-throughput anti-Wolbachia whole-cell screen: a route to macrofilaricidal drugs against onchocerciasis and lymphatic filariasis. *J Biomol Screen*, 20, 64-9.
- CLARK, M. E., VENETI, Z., BOURTZIS, K. & KARR, T. L. 2003. Wolbachia distribution and cytoplasmic incompatibility during sperm development: the cyst as the basic cellular unit of CI expression. *Mechanisms of Development*, 120, 185-198.
- COHLAN, S. Q., BEVELANDER, G. & TIAMSIC, T. 1963. Growth Inhibition of Prematures Receiving Tetracycline: A Clinical and Laboratory Investigation of Tetracycline-Induced Bone Fluorescence. *American Journal of Diseases of Children*, 105, 453-461.
- COMLEY, J. C., REES, M. J., TURNER, C. H. & JENKINS, D. C. 1989. Colorimetric quantitation of filarial viability. *Int J Parasitol*, 19, 77-83.
- COULIBALY, Y. I., DEMBELE, B., DIALLO, A. A., LIPNER, E. M., DOUMBIA, S. S., COULIBALY, S. Y., KONATE, S., DIALLO, D. A., YALCOUYE, D., KUBOFCIK, J., DOUMBO, O. K., TRAORE, A. K., KEITA, A. D., FAY, M. P., TRAORE, S. F., NUTMAN, T. B. & KLION, A. D. 2009. A randomized trial of doxycycline for Mansonella perstans infection. *N Engl J Med*, 361, 1448-58.
- CRANDALL, R. B., CRANDALL, C. A., HINES, S. A., DOYLE, T. J. & NAYAR, J. K. 1987. Peripheral Lymphedema in Ferrets Infected with Brugia malayi. *The American Journal of Tropical Medicine and Hygiene*, 37, 138-142.
- CRANDALL, R. B., MCGREEVY, P. B., CONNOR, D. H., CRANDALL, C. A., NEILSON, J. T. & MCCALL, J. W. 1982. The Ferret (Mustela Putorius Furo) as an Experimental Host for Brugia Malayi and Brugia Pahangi*. *The American Journal of Tropical Medicine and Hygiene*, 31, 752-759.
- CZEIZEL, A. E. & ROCKENBAUER, M. 2000. A population-based case-control teratologic study of oral oxytetracycline treatment during pregnancy. *European Journal of Obstetrics & Gynecology and Reproductive Biology*, 88, 27-33.
- DARGE, K., TROEGER, J., ENGELKE, C., LEICHSENTRING, M., NELLE, M., AWADZI, K. & BUETTNER, D. W. 1994. Evaluation of ultrasonography for the detection of drug-induced changes in onchocercal nodules. *Am J Trop Med Hyg*, 51.
- DEBRAH, A. Y., MAND, S., MARFO-DEBREKYEI, Y., BATSA, L., PFARR, K., BUTTNER, M., ADJEI, O., BUTTNER, D. & HOERAUF, A. 2007. Macrofilaricidal effect of 4 weeks of treatment with doxycycline on Wuchereria bancrofti. *Trop Med Int Health*, 12, 1433-41.
- DENHAM, D. A. & FLETCHER, C. 1987. The cat infected with Brugia pahangi as a model of human filariasis. *Ciba Found Symp*, 127, 225-35.

REFERENCES

- DEVANEY, E. 1985. *Dirofilaria immitis*: the moulting of the infective larva in vitro. *J Helminthol*, 59, 47-50.
- DREYER, G., ADDISS, D. & NOROES, J. 2005. Does longevity of adult *Wuchereria bancrofti* increase with decreasing intensity of parasite transmission? Insights from clinical observations. *Trans R Soc Trop Med Hyg*, 99, 883-92.
- DREYER, G., ADDISS, D., NOROES, J., AMARAL, F., ROCHA, A. & COUTINHO, A. 1996. Ultrasonographic assessment of the adulticidal efficacy of repeat high-dose ivermectin in bancroftian filariasis. *Tropical Medicine & International Health*, 1, 427-432.
- DREYER, G., AMARAL, F., NOROES, J., MEDEIROS, Z. & ADDISS, D. 1995. A new tool to assess the adulticidal efficacy in vivo of antifilarial drugs for bancroftian filariasis. *Trans R Soc Trop Med Hyg*, 89, 225-6.
- DREYER, G., NOROES, J., FIGUEREDO-SILVA, J. & PIESSENS, W. F. 2000. Pathogenesis of lymphatic disease in bancroftian filariasis: a clinical perspective. *Parasitol Today*, 16, 544-8.
- DREYER, G., SANTOS, A., NOROES, J., AMARAL, F. & ADDISS, D. 1998. Ultrasonographic detection of living adult *Wuchereria bancrofti* using a 3.5-MHz transducer. *Am J Trop Med Hyg*, 59.
- DUKE, B. O. 1980. Observations on *Onchocerca volvulus* in experimentally infected chimpanzees. *Tropenmed Parasitol*, 31, 41-54.
- EBERHARD, M. L., DICKERSON, J. W., TSANG, V. C. W., WALKER, E. M., OTTESEN, E. A., CHANDRASHEKAR, R., WEIL, G. J., TRPIS, M., STROBERT, E., CONSTANTINIDIS, I. & SWENSON, R. B. 1995. *Onchocerca volvulus*: Parasitological and Serologic Responses in Experimentally Infected Chimpanzees and Mangabey Monkeys. *Experimental Parasitology*, 80, 454-462.
- EDESON, J. F., WILSON, T., WHARTON, R. H. & LAING, A. B. 1960. Experimental transmission of *Brugia malayi* and *B. pahangi* to man. *Trans R Soc Trop Med Hyg*, 54, 229-34.
- ENGELSMAN, A. F., VAN DER MEI, H. C., FRANCIS, K. P., BUSSCHER, H. J., PLOEG, R. J. & VAN DAM, G. M. 2009. Real time noninvasive monitoring of contaminating bacteria in a soft tissue implant infection model. *Journal of Biomedical Materials Research Part B: Applied Biomaterials*, 88B, 123-129.
- EVANS, C. C., MOORHEAD, A. R., STOREY, B. E., WOLSTENHOLME, A. J. & KAPLAN, R. M. 2013. Development of an in vitro bioassay for measuring susceptibility to macrocyclic lactone anthelmintics in *Dirofilaria immitis*. *Int J Parasitol Drugs Drug Resist*, 3, 102-8.
- EVANS, H., FLYNN, A. F. & MITRE, E. 2016. Endothelial cells release soluble factors that support the long-term survival of filarial worms in vitro. *Exp Parasitol*, 170, 50-58.
- FALCONE, F., SCHLAAK, M. & HAAS, H. 1995. [*In vitro* cultivation of *Brugia malayi*, a parasitic nematode that causes human lymphatic filariasis].
- FALCONE, F., ZAHNER, H., SCHLAAK, M. & HAAS, H. 1996. *In vitro* cultivation of third-stage larvae of *Brugia malayi* to the young adult stage.
- FARIS, R., HUSSAIN, O., EL SETOUHY, M., RAMZY, R. M. & WEIL, G. J. 1998. Bancroftian filariasis in Egypt: visualization of adult worms and subclinical lymphatic pathology by scrotal ultrasound. *Am J Trop Med Hyg*, 59, 864-7.
- FERREE, P. M. & SULLIVAN, W. 2006. A Genetic Test of the Role of the Maternal Pronucleus in Wolbachia-Induced Cytoplasmic Incompatibility in *Drosophila melanogaster*. *Genetics*, 173, 839.
- FISCHER, C., IBIRICU URRIZA, I., BULMAN, C. A., LIM, K. C., GUT, J., LACHAU-DURAND, S., ENGELEN, M., QUIRYNEN, L., TEKLE, F., BAETEN, B., BEERNTSEN, B., LUSTIGMAN, S. & SAKANARI, J. 2019. Efficacy of subcutaneous doses and a new oral amorphous solid dispersion formulation of flubendazole on male jirds (*Meriones unguiculatus*)

REFERENCES

- infected with the filarial nematode *Brugia pahangi*. *PLOS Neglected Tropical Diseases*, 13, e0006787.
- FISCHER, K., BEATTY, W. L., JIANG, D., WEIL, G. J. & FISCHER, P. U. 2011. Tissue and Stage-Specific Distribution of *Wolbachia* in *Brugia malayi*. *PLOS Neglected Tropical Diseases*, 5, e1174.
- FOSTER, J., GANATRA, M., KAMAL, I., WARE, J., MAKAROVA, K., IVANOVA, N., BHATTACHARYYA, A., KAPATRAL, V., KUMAR, S., POSFAI, J., VINCZE, T., INGRAM, J., MORAN, L., LAPIDUS, A., OMELCHENKO, M., KYRPIDES, N., GHEDIN, E., WANG, S., GOLTSMAN, E., JOUKOV, V., OSTROVSKAYA, O., TSUKERMAN, K., MAZUR, M., COMB, D., KOONIN, E. & SLATKO, B. 2005. The *Wolbachia* Genome of *Brugia malayi*: Endosymbiont Evolution within a Human Pathogenic Nematode. *PLOS Biology*, 3, e121.
- FRANKE-FAYARD, B., WATERS, A. P. & JANSE, C. J. 2006. Real-time in vivo imaging of transgenic bioluminescent blood stages of rodent malaria parasites in mice. *Nat Protoc*, 1, 476-85.
- GARDON, J., GARDON-WENDEL, N., DEMANGA, N., KAMGNO, J., CHIPPAUX, J. P. & BOUSSINESQ, M. 1997. Serious reactions after mass treatment of onchocerciasis with ivermectin in an area endemic for *Loa loa* infection. *Lancet*, 350.
- GAUSE, W. C., WYNN, T. A. & ALLEN, J. E. 2013. Type 2 immunity and wound healing: evolutionary refinement of adaptive immunity by helminths. *Nature reviews. Immunology*, 13, 607-614.
- GEARY, T. G., MACKENZIE, C. D. & SILBER, S. A. 2019. Flubendazole as a macrofilaricide: History and background. *PLOS Neglected Tropical Diseases*, 13, e0006436.
- GLOECKNER, C., GARNER, A. L., MERSHA, F., OKSOV, Y., TRICOCHÉ, N., EUBANKS, L. M., LUSTIGMAN, S., KAUFMANN, G. F. & JANDA, K. D. 2010. Repositioning of an existing drug for the neglected tropical disease Onchocerciasis. *Proc Natl Acad Sci U S A*, 107, 3424-9.
- GROBUSCH, M. P., KOMBILA, M., AUTENRIETH, I., MEHLHORN, H. & KREMSNER, P. G. 2003. No evidence of *Wolbachia* endosymbiosis with *Loa loa* and *Mansonella perstans*. *Parasitol Res*, 90, 405-8.
- GUDERIAN, R. H., ANSELMINI, M., SEMPERTEGUI, R. & COOPER, P. J. 1991. Adverse reactions to ivermectin in reactive onchodermatitis. *Lancet*, 337, 188.
- HALL, L. R. & PEARLMAN, E. 1999. Pathogenesis of onchocercal keratitis (River blindness). *Clin Microbiol Rev*, 12, 445-53.
- HALLIDAY, A., GUIMARAES, A. F., TYRER, H. E., METUGE, H. M., PATRICK, C. N. W., ARNAUD, K.-O. J., KWENTI, T. D. B., FORSBROOK, G., STEVEN, A., COOK, D., ENYONG, P., WANJI, S., TAYLOR, M. J. & TURNER, J. D. 2014. A murine macrofilaricide pre-clinical screening model for onchocerciasis and lymphatic filariasis. *Parasites & Vectors*, 7, 472.
- HEWITSON, J. P., RÜCKERL, D., HARCUS, Y., MURRAY, J., WEBB, L. M., BABAYAN, S. A., ALLEN, J. E., KURNIAWAN, A. & MAIZELS, R. M. 2014. The secreted triose phosphate isomerase of *Brugia malayi* is required to sustain microfilaria production in vivo. *PLoS pathogens*, 10, e1003930-e1003930.
- HIRA, P. R. 1977. *Wuchereria bancrofti*: the staining of the microfilarial sheath in giemsa and haematoxylin for diagnosis. *Med J Zambia*, 11, 93-6.
- HOERAUF, A., NISSEN-PAHLE, K., SCHMETZ, C., HENKLE-DUHRSEN, K., BLAXTER, M. L., BUTTNER, D. W., GALLIN, M. Y., AL-QAOU, K. M., LUCIUS, R. & FLEISCHER, B. 1999. Tetracycline therapy targets intracellular bacteria in the filarial nematode *Litomosoides sigmodontis* and results in filarial infertility. *J Clin Invest*, 103, 11-8.
- HOMEIDA, M. A., MACKENZIE, C. D., WILLIAMS, J. F. & GHALIB, H. W. 1986. The detection of onchocercal nodules by ultrasound technique. *Trans R Soc Trop Med Hyg*, 80.

REFERENCES

- HONG, W. D., BENAYOUD, F., NIXON, G. L., FORD, L., JOHNSTON, K. L., CLARE, R. H., CASSIDY, A., COOK, D. A. N., SIU, A., SHIOTANI, M., WEBBORN, P. J. H., KAVANAGH, S., ALJAYOUSSI, G., MURPHY, E., STEVEN, A., ARCHER, J., STRUEVER, D., FROHBERGER, S. J., EHRENS, A., HÜBNER, M. P., HOERAUF, A., ROBERTS, A. P., HUBBARD, A. T. M., TATE, E. W., SERWA, R. A., LEUNG, S. C., QIE, L., BERRY, N. G., GUSOVSKY, F., HEMINGWAY, J., TURNER, J. D., TAYLOR, M. J., WARD, S. A. & O'NEILL, P. M. 2019. AWZ1066S, a highly specific anti-*Wolbachia* drug candidate for a short-course treatment of filariasis. *Proceedings of the National Academy of Sciences*, 116, 1414.
- HOOPER, P. J., CHU, B. K., MIKHAILOV, A., OTTESEN, E. A. & BRADLEY, M. 2014. Assessing Progress in Reducing the At-Risk Population after 13 Years of the Global Programme to Eliminate Lymphatic Filariasis. *PLOS Neglected Tropical Diseases*, 8, e3333.
- HOTEZ, P. 2007a. Measuring neglect. *PLoS neglected tropical diseases*, 1, e118-e118.
- HOTEZ, P. 2007b. A New Voice for the Poor. *PLOS Neglected Tropical Diseases*, 1, e77.
- HOTEZ, P. 2011. A handful of 'antipoverty' vaccines exist for neglected diseases, but the world's poorest billion people need more. *Health Aff (Millwood)*, 30, 1080-7.
- HÜBNER, M. P., KOSCHEL, M., STRUEVER, D., NIKOLOV, V., FROHBERGER, S. J., EHRENS, A., FENDLER, M., JOHANNES, I., VON GELDERN, T. W., MARSH, K., TURNER, J. D., TAYLOR, M. J., WARD, S. A., PFARR, K., KEMPF, D. J. & HOERAUF, A. 2019. In vivo kinetics of *Wolbachia* depletion by ABBV-4083 in *L. sigmodontis* adult worms and microfilariae. *PLOS Neglected Tropical Diseases*, 13, e0007636.
- HYLAND, K. V., ASFAW, S. H., OLSON, C. L., DANIELS, M. D. & ENGMAN, D. M. 2008. Bioluminescent imaging of *Trypanosoma cruzi* infection. *International journal for parasitology*, 38, 1391-1400.
- JACKSON-THOMPSON, B. M., KIM, S. Y., JAISWAL, S., SCOTT, J. R., JONES, S. R., MORRIS, C. P., FITE, J. J., LAURIE, K., HOY, A. R., DARDZINSKI, B. J. & MITRE, E. 2018. *Brugia malayi* infection in ferrets – A small mammal model of lymphatic filariasis. *PLOS Neglected Tropical Diseases*, 12, e0006334.
- JAMES, S. L., ABATE, D., ABATE, K. H., ABAY, S. M., ABBAFATI, C., ABBASI, N., ABBASTABAR, H., ABD-ALLAH, F., ABDELA, J., ABDELALIM, A., ABDOLLAHPOUR, I., ABDULKADER, R. S., ABEBE, Z., ABERA, S. F., ABIL, O. Z., ABRAHA, H. N., ABU-RADDAD, L. J., ABURMEILEH, N. M. E., ACCROMBESSI, M. M. K., ACHARYA, D., ACHARYA, P., ACKERMAN, I. N., ADAMU, A. A., ADEBAYO, O. M., ADEKANMBI, V., ADETOKUNBOH, O. O., ADIB, M. G., ADSUAR, J. C., AFANVI, K. A., AFARIDEH, M., AFSHIN, A., AGARWAL, G., AGESA, K. M., AGGARWAL, R., AGHAYAN, S. A., AGRAWAL, S., AHMADI, A., AHMADI, M., AHMADIEH, H., AHMED, M. B., AICHOUR, A. N., AICHOUR, I., AICHOUR, M. T. E., AKINYEMIJU, T., AKSEER, N., AL-ALY, Z., AL-EYADHY, A., AL-MEKHLAFI, H. M., AL-RADDADI, R. M., ALAHDAB, F., ALAM, K., ALAM, T., ALASHI, A., ALAVIAN, S. M., ALENE, K. A., ALIJANZADEH, M., ALIZADEH-NAVAEI, R., ALJUNID, S. M., ALKERWI, A. A., ALLA, F., ALLEBECK, P., ALOUANI, M. M. L., ALTIRKAWI, K., ALVIS-GUZMAN, N., AMARE, A. T., AMINDE, L. N., AMMAR, W., AMOAKO, Y. A., ANBER, N. H., ANDREI, C. L., ANDROUDI, S., ANIMUT, M. D., ANJOMSHOA, M., ANSHA, M. G., ANTONIO, C. A. T., ANWARI, P., ARABLOO, J., ARAUZ, A., AREMU, O., ARIANI, F., ARMOON, B., ÄRNLÖV, J., ARORA, A., ARTAMAN, A., ARYAL, K. K., ASAYESH, H., ASGHAR, R. J., ATARO, Z., ATRE, S. R., AUSLOOS, M., AVILA-BURGOS, L., AVOKPAHO, E. F. G. A., AWASTHI, A., AYALA QUINTANILLA, B. P., AYER, R., AZZOPARDI, P. S., BABAZADEH, A., BADALI, H., BADAWI, A., BALI, A. G., et al. 2018. Global, regional, and national incidence, prevalence, and years lived with disability for 354 diseases and injuries for 195 countries and territories, 1990–2017: a systematic analysis for the Global Burden of Disease Study 2017. *The Lancet*, 392, 1789-1858.

REFERENCES

- JELINEK, T., SCHULTE-HILLEN, J. & LOSCHER, T. 1996. Human dirofilariasis. *Int J Dermatol*, 35, 872-5.
- JICK, H., HOLMES, L. B., HUNTER, J. R., MADSEN, S. & STERGACHIS, A. 1981. First-Trimester Drug Use and Congenital Disorders. *JAMA*, 246, 343-346.
- JOHNSTON, K. L., COOK, D. A. N., BERRY, N. G., DAVID HONG, W., CLARE, R. H., GODDARD, M., FORD, L., NIXON, G. L., O'NEILL, P. M., WARD, S. A. & TAYLOR, M. J. 2017. Identification and prioritization of novel anti-Wolbachia chemotypes from screening a 10,000-compound diversity library. *Science Advances*, 3.
- JOHNSTON, K. L., FORD, L., UMAREDDY, I., TOWNSON, S., SPECHT, S., PFARR, K., HOERAUF, A., ALTMAYER, R. & TAYLOR, M. J. 2014. Repurposing of approved drugs from the human pharmacopoeia to target Wolbachia endosymbionts of onchocerciasis and lymphatic filariasis. *Int J Parasitol Drugs Drug Resist*, 4, 278-86.
- JOSEPH D. TURNER^{1*}, R. S., GHAITH AL JAYOUSSI¹, HAYLEY E. TYRER¹, JOANNE GAMBLE¹, LAURA HAYWARD¹, RICHARD PRIESTLEY¹, EMMA MURPHY¹, JILL DAVIES¹, DAVID WATERHOUSE¹, DARREN A. N. COOK¹, RACHEL H. CLARE¹, ANDREW CASSIDY¹, ANDREW STEVEN¹, KELLY L. JOHNSTON¹, JOHN MCCALL², LOUISE FORD¹, JANET HEMINGWAY¹, STEPHEN A. WARD¹ & MARK J. TAYLOR^{1‡} 2017. Albendazole and antibiotics synergise to deliver short-course anti-Wolbachia curative treatments in preclinical models of filariasis
Proc Natl Acad Sci U S A, in press.
- KEISER, P. B., COULIBALY, Y., KUBOFCIK, J., DIALLO, A. A., KLION, A. D., TRAORE, S. F. & NUTMAN, T. B. 2008. Molecular identification of Wolbachia from the filarial nematode *Mansonella perstans*. *Mol Biochem Parasitol*, 160, 123-8.
- KIM, J.-J., LEE, H.-M., SHIN, D.-M., KIM, W., YUK, J.-M., JIN, HYO S., LEE, S.-H., CHA, G.-H., KIM, J.-M., LEE, Z.-W., SHIN, SUNG J., YOO, H., PARK, YOUNG K., PARK, JIN B., CHUNG, J., YOSHIMORI, T. & JO, E.-K. 2012. Host Cell Autophagy Activated by Antibiotics Is Required for Their Effective Antimycobacterial Drug Action. *Cell Host & Microbe*, 11, 457-468.
- KIM, Y. E., REMME, J. H. F., STEINMANN, P., STOLK, W. A., ROUNGOU, J.-B. & TEDIOSI, F. 2015. Control, elimination, and eradication of river blindness: scenarios, timelines, and ivermectin treatment needs in Africa. *PLoS neglected tropical diseases*, 9, e0003664-e0003664.
- KING, C. H. 2002. Ultrasound monitoring of structural urinary tract disease in *Schistosoma haematobium* infection. *Memórias do Instituto Oswaldo Cruz*, 97, 149-152.
- KOZEK, W. J. 1977. Transovarially-transmitted intracellular microorganisms in adult and larval stages of *Brugia malayi*. *J Parasitol*, 63, 992-1000.
- KOZEK, W. J. & MARROQUIN, H. F. 1977. Intracytoplasmic Bacteria in *Onchocerca volvulus**. *The American Journal of Tropical Medicine and Hygiene*, 26, 663-678.
- KRAMER, L., CROSARA, S., GNUDI, G., GENCHI, M., MANGIA, C., VIGLIETTI, A. & QUINTAVALLA, C. 2018. Wolbachia, doxycycline and macrocyclic lactones: New prospects in the treatment of canine heartworm disease. *Veterinary Parasitology*, 254, 95-97.
- KRAUTZ-PETERSON, G., NDEGWA, D., VASQUEZ, K., KORIDECK, H., ZHANG, J., PETERSON, J. D. & SKELLY, P. J. 2009. Imaging schistosomes in vivo. *Faseb j*, 23, 2673-80.
- KWARTENG, A., AHUNO, S. T. & AKOTO, F. O. 2016. Killing filarial nematode parasites: role of treatment options and host immune response. *Infectious diseases of poverty*, 5, 86-86.
- LANDMANN, F., BAIN, O., MARTIN, C., UNI, S., TAYLOR, M. J. & SULLIVAN, W. 2012. Both asymmetric mitotic segregation and cell-to-cell invasion are required for stable germline transmission of Wolbachia in filarial nematodes. *Biol Open*, 1, 536-47.

REFERENCES

- LANG, T., GOYARD, S., LEBASTARD, M. & MILON, G. 2005. Bioluminescent *Leishmania* expressing luciferase for rapid and high throughput screening of drugs acting on amastigote-harboring macrophages and for quantitative real-time monitoring of parasitism features in living mice. *Cell Microbiol*, 7, 383-92.
- LANGWORTHY, N. G., RENZ, A., MACKENSTEDT, U., HENKLE-DUHRSEN, K., DE BRONSVOORT, M. B., TANYA, V. N., DONNELLY, M. J. & TREES, A. J. 2000. Macroparasiticide activity of tetracycline against the filarial nematode *Onchocerca ochengi*: elimination of *Wolbachia* precedes worm death and suggests a dependent relationship. *Proc Biol Sci*, 267, 1063-9.
- LEFOULON, E., BAIN, O., BOURRET, J., JUNKER, K., GUERRERO, R., CAÑIZALES, I., KUZMIN, Y., SATOTO, T. B. T., CARDENAS-CALLIRGOS, J. M., DE SOUZA LIMA, S., RACCURT, C., MUTAFCHIEV, Y., GAVOTTE, L. & MARTIN, C. 2015. Shaking the Tree: Multi-locus Sequence Typing Usurps Current Onchocercid (Filarial Nematode) Phylogeny. *PLOS Neglected Tropical Diseases*, 9, e0004233.
- LEFOULON, E., BAIN, O., MAKEPEACE, B. L., D'HAESE, C., UNI, S., MARTIN, C. & GAVOTTE, L. 2016. Breakdown of coevolution between symbiotic bacteria *Wolbachia* and their filarial hosts. *PeerJ*, 4, e1840-e1840.
- LEICHSENDRING, M., TROGER, J., NELLE, M., BUTTNER, D. W., DARGE, K. & DOEHRING-SCHWERDTFEGGER, E. 1990. Ultrasonographical investigations of onchocerciasis in Liberia. *Am J Trop Med Hyg*, 43.
- LI, Z. & CARLOW, C. K. S. 2012. Characterization of Transcription Factors That Regulate the Type IV Secretion System and Riboflavin Biosynthesis in *Wolbachia* of *Brugia malayi*. *PLOS ONE*, 7, e51597.
- LITT, E., BAKER, M. C. & MOLYNEUX, D. 2012. Neglected tropical diseases and mental health: a perspective on comorbidity. *Trends Parasitol*, 28, 195-201.
- LIU, C., MHASHILKAR, A. S., CHABANON, J., XU, S., LUSTIGMAN, S., ADAMS, J. H. & UNNASCH, T. R. 2018. Development of a toolkit for piggyBac-mediated integrative transfection of the human filarial parasite *Brugia malayi*. *PLOS Neglected Tropical Diseases*, 12, e0006509.
- LOK, J. B., MIKA-GRIEVE, M., GRIEVE, R. B. & CHIN, T. K. 1984a. In vitro development of third- and fourth-stage larvae of *Dirofilaria immitis*: comparison of basal culture media, serum levels and possible serum substitutes. *Acta Trop*, 41, 145-54.
- LOK, J. B., POLLACK, R. J., CUPP, E. W., BERNARDO, M. J., DONNELLY, J. J. & ALBIEZ, E. J. 1984b. Development of *onchocerca lienalis* and *O. volvulus* from the third to fourth larval stage in vitro. *Tropenmed Parasitol*, 35, 209-11.
- LU, I. M., KASSIS, T., ROGERS, A. M., SCHUDEL, A., WEIL, J., EVANS, C. C., MOORHEAD, A. R., THOMAS, S. N. & DIXON, J. B. 2018. Optimization of culture and analysis methods for enhancing long-term *Brugia malayi* survival, molting and motility in vitro. *Parasitology Open*, 4, e3.
- MACKENZIE, C. D. & GEARY, T. G. 2011. Flubendazole: a candidate macrofilaricide for lymphatic filariasis and onchocerciasis field programs. *Expert Rev Anti Infect Ther*, 9.
- MACKENZIE, C. D., GEARY, T. G. & GERLACH, J. A. 2003. Possible pathogenic pathways in the adverse clinical events seen following ivermectin administration to onchocerciasis patients. *Filaria J*, 2 Suppl 1, S5.
- MAIZELS, R. M. & DENHAM, D. A. 1992. Diethylcarbamazine (DEC): immunopharmacological interactions of an anti-filarial drug. *Parasitol*, 105.
- MAK, J. W., LIM, P. K., SIM, B. K. & LIEW, L. M. 1983. *Brugia malayi* and *B. pahangi*: cultivation in vitro of infective larvae to the fourth and fifth stages. *Exp Parasitol*, 55, 243-8.
- MAKEPEACE, B. L., RODGERS, L. & TREES, A. J. 2006. Rate of Elimination of *Wolbachia pipientis* by Doxycycline In Vitro Increases following Drug Withdrawal. *Antimicrobial Agents and Chemotherapy*, 50, 922.

REFERENCES

- MALONE, J. B. & THOMPSON, P. E. 1975. *Brugia pahangi*: Susceptibility and macroscopic pathology of golden hamsters. *Experimental Parasitology*, 38, 279-290.
- MAND, S., DEBRAH, A. Y., KLARMANN, U., BATSA, L., MARFO-DEBREKEYEI, Y., KWARTENG, A., SPECHT, S., BELDA-DOMENE, A., FIMMERS, R., TAYLOR, M., ADJEI, O. & HOERAUF, A. 2012. Doxycycline Improves Filarial Lymphedema Independent of Active Filarial Infection: A Randomized Controlled Trial. *Clinical Infectious Diseases*, 55, 621-630.
- MAND, S., MARFO-DEBREKEYEI, Y., DITTRICH, M., FISCHER, K., ADJEI, O. & HOERAUF, A. 2003. Animated documentation of the filaria dance sign (FDS) in bancroftian filariasis. *Filaria J*, 2.
- MAND, S., SUPALI, T., DJUARDI, J., KAR, S., RAVINDRAN, B. & HOERAUF, A. 2006. Detection of adult *Brugia malayi* filariae by ultrasonography in humans in India and Indonesia. *Trop Med Int Health*, 11, 1375-81.
- MARCELLINO, C., GUT, J., LIM, K. C., SINGH, R., MCKERROW, J. & SAKANARI, J. 2012. WormAssay: a novel computer application for whole-plate motion-based screening of macroscopic parasites. *PLoS Negl Trop Dis*, 6.
- MCCALL, J. W., MALONE, J. B., HYONG-SUN, A. & THOMPSON, P. E. 1973. Mongolian jirds (*Meriones unguiculatus*) infected with *Brugia pahangi* by the intraperitoneal route: a rich source of developing larvae, adult filariae, and microfilariae. *J Parasitol*, 59, 436.
- MCGARRY, H. F., EGERTON, G. L. & TAYLOR, M. J. 2004a. Population dynamics of *Wolbachia* bacterial endosymbionts in *Brugia malayi*. *Mol Biochem Parasitol*, 135.
- MCGARRY, H. F., EGERTON, G. L. & TAYLOR, M. J. 2004b. Population dynamics of *Wolbachia* bacterial endosymbionts in *Brugia malayi*. *Molecular and Biochemical Parasitology*, 135, 57-67.
- MCGARRY, H. F., PFARR, K., EGERTON, G., HOERAUF, A., AKUE, J.-P., ENYONG, P., WANJI, S., KLÄGER, S. L., BIANCO, A. E., BEECHING, N. J. & TAYLOR, M. J. 2003. Evidence against *Wolbachia* symbiosis in *Loa loa*. *Filaria journal*, 2, 9-9.
- MCNULTY, S. N., MITREVA, M., WEIL, G. J. & FISCHER, P. U. 2013. Inter and intra-specific diversity of parasites that cause lymphatic filariasis. *Infect Genet Evol*, 14, 137-46.
- MICHAEL, E. & BUNDY, D. A. 1997. Global mapping of lymphatic filariasis. *Parasitol Today*, 13, 472-6.
- MILLINGTON, O. R., MYBURGH, E., MOTTRAM, J. C. & ALEXANDER, J. 2010. Imaging of the host/parasite interplay in cutaneous leishmaniasis. *Experimental parasitology*, 126, 310-317.
- MILLS, B., BRADLEY, M. & DHALIWAL, K. 2016. Optical imaging of bacterial infections. *Clinical and translational imaging*, 4, 163-174.
- MOLYNEUX, D. H. 2004. "Neglected" diseases but unrecognised successes—challenges and opportunities for infectious disease control. *The Lancet*, 364, 380-383.
- MOLYNEUX, D. H., BRADLEY, M., HOERAUF, A., KYELEM, D. & TAYLOR, M. J. 2003. Mass drug treatment for lymphatic filariasis and onchocerciasis. *Trends Parasitol*, 19, 516-22.
- MOLYNEUX, D. H., DEAN, L., ADEKEYE, O., STOTHARD, J. R. & THEOBALD, S. 2018. The changing global landscape of health and disease: addressing challenges and opportunities for sustaining progress towards control and elimination of neglected tropical diseases (NTDs). *Parasitology*, 145, 1647-1654.
- MORCHÓN, R., CARRETÓN, E., GONZÁLEZ-MIGUEL, J. & MELLADO-HERNÁNDEZ, I. 2012. Heartworm Disease (*Dirofilaria immitis*) and Their Vectors in Europe - New Distribution Trends. *Frontiers in physiology*, 3, 196-196.
- MORENO, Y., NABHAN, J. F., SOLOMON, J., MACKENZIE, C. D. & GEARY, T. G. 2010. Ivermectin disrupts the function of the excretory-secretory apparatus in microfilariae of *Brugia malayi*. *Proc Natl Acad Sci U S A*, 107.

REFERENCES

- MORRIS, C. P., EVANS, H., LARSEN, S. E. & MITRE, E. 2013. A Comprehensive, Model-Based Review of Vaccine and Repeat Infection Trials for Filariasis. *Clinical Microbiology Reviews*, 26, 381.
- MURDOCH, M. E. 2010. Onchodermatitis. *Curr Opin Infect Dis*, 23, 124-31.
- MURDOCH, M. E. 2018. Onchodermatitis: Where Are We Now? *Tropical medicine and infectious disease*, 3, 94.
- MUTAFCHIEV, Y., BAIN, O., WILLIAMS, Z., MCCALL, J. W. & MICHALSKI, M. L. 2014. Intraperitoneal development of the filarial nematode *Brugia malayi* in the Mongolian jird (*Meriones unguiculatus*). *Parasitology research*, 113, 1827-1835.
- MYBURGH, E., RITCHIE, R., GOUNDRY, A., O'NEILL, K., MARCHESI, F. & DEVANEY, E. 2016. Attempts to Image the Early Inflammatory Response during Infection with the Lymphatic Filarial Nematode *Brugia pahangi* in a Mouse Model. *PLOS ONE*, 11, e0168602.
- NANDURI, J. & KAZURA, J. W. 1989. Clinical and laboratory aspects of filariasis. *Clinical microbiology reviews*, 2, 39-50.
- NELSON, F. K., GREINER, D. L., SHULTZ, L. D. & RAJAN, T. V. 1991a. The immunodeficient scid mouse as a model for human lymphatic filariasis. *J Exp Med*, 173.
- NELSON, F. K., GREINER, D. L., SHULTZ, L. D. & RAJAN, T. V. 1991b. The immunodeficient scid mouse as a model for human lymphatic filariasis. *The Journal of Experimental Medicine*, 173, 659.
- NJOUENDOU, A. J., RITTER, M., NDONGMO, W. P. C., KIEN, C. A., NARCISSE, G. T. V., FOMBAD, F. F., TAYONG, D. B., PFARR, K., LAYLAND, L. E., HOERAUF, A. & WANJI, S. 2017. Successful long-term maintenance of *Mansonella perstans* in an in vitro culture system. *Parasites & Vectors*, 10, 563.
- NOLAN, T. J. & LOK, J. B. 2012. Macrocyclic lactones in the treatment and control of parasitism in small companion animals. *Curr Pharm Biotechnol*, 13, 1078-94.
- NOROES, J., ADDISS, D., AMARAL, F., COUTINHO, A., MEDEIROS, Z. & DREYER, G. 1996. Occurrence of living adult *Wuchereria bancrofti* in the scrotal area of men with microfilaraemia. *Trans R Soc Trop Med Hyg*, 90, 55-6.
- NUTMAN, T. B. 2013. Insights into the pathogenesis of disease in human lymphatic filariasis. *Lymphatic research and biology*, 11, 144-148.
- O'CONNELL, E. M., BENNURU, S., STEEL, C., DOLAN, M. A. & NUTMAN, T. B. 2015. Targeting Filarial Abl-like Kinases: Orally Available, Food and Drug Administration-Approved Tyrosine Kinase Inhibitors Are Microfilaricidal and Macrophilicidal. *J Infect Dis*, 212, 684-93.
- O'NEILL, M., MANSOUR, A., DICOSTY, U., GEARY, J., DZIMIANSKI, M., MCCALL, S. D., MCCALL, J. W., MACKENZIE, C. D. & GEARY, T. G. 2016. An In Vitro/In Vivo Model to Analyze the Effects of Flubendazole Exposure on Adult Female *Brugia malayi*. *PLOS Neglected Tropical Diseases*, 10, e0004698.
- OPOKU, N. O., BAKAJIKA, D. K., KANZA, E. M., HOWARD, H., MAMBANDU, G. L., NYATHIROMBO, A., NIGO, M. M., KASONIA, K., MASEMBE, S. L., MUMBERE, M., KATALIKO, K., LARBELEE, J. P., KPAWOR, M., BOLAY, K. M., BOLAY, F., ASARE, S., ATTAH, S. K., OLIPOH, G., VAILLANT, M., HALLEUX, C. M. & KUESEL, A. C. 2018. Single dose moxidectin versus ivermectin for *Onchocerca volvulus* infection in Ghana, Liberia, and the Democratic Republic of the Congo: a randomised, controlled, double-blind phase 3 trial. *Lancet*, 392, 1207-1216.
- ORIHIL, T. C. & EBERHARD, M. L. 1985. Loa loa: development and course of patency in experimentally-infected primates. *Trop Med Parasitol*, 36.
- OTTESEN, E. A. 1998. The global programme to eliminate lymphatic filariasis. *Parasitology International*, 47, 46.

REFERENCES

- OTTO, G. F. 1969. Geographical distribution, vectors, and life cycle of *Dirofilaria immitis*. *J Am Vet Med Assoc*, 154, 370-3.
- PAMPIGLIONE, S., CANESTRI TROTTI, G. & RIVASI, F. 1995. Human dirofilariasis due to *Dirofilaria* (*Nochtiella*) *repens*: a review of world literature. *Parassitologia*, 37, 149-93.
- PARTRIDGE, F. A., BROWN, A. E., BUCKINGHAM, S. D., WILLIS, N. J., WYNNE, G. M., FORMAN, R., ELSE, K. J., MORRISON, A. A., MATTHEWS, J. B., RUSSELL, A. J., LOMAS, D. A. & SATTELLE, D. B. 2018. An automated high-throughput system for phenotypic screening of chemical libraries on *C. elegans* and parasitic nematodes. *International journal for parasitology. Drugs and drug resistance*, 8, 8-21.
- PARTRIDGE, F. A., MURPHY, E. A., WILLIS, N. J., BATAILLE, C. J., FORMAN, R., HEYER-CHAUHAN, N., MARINIC, B., SOWOOD, D. J., WYNNE, G. M., ELSE, K. J., RUSSELL, A. J. & SATTELLE, D. B. 2017. Dihydrobenz[e][1,4]oxazepin-2(3H)-ones, a new anthelmintic chemotype immobilising whipworm and reducing infectivity in vivo. *PLoS Negl Trop Dis*, 11, e0005359.
- PEARLMAN, E. 1997. Immunopathology of onchocerciasis: a role for eosinophils in onchocercal dermatitis and keratitis. *Chem Immunol*, 66, 26-40.
- PEARLMAN, E. & HALL, L. R. 2000. Immune mechanisms in *Onchocerca volvulus*-mediated corneal disease (river blindness). *Parasite Immunol*, 22, 625-31.
- PERERA, M., WHITEHEAD, M., MOLYNEUX, D., WEERASOORIYA, M. & GUNATILLEKE, G. 2007. Neglected Patients with a Neglected Disease? A Qualitative Study of Lymphatic Filariasis. *PLOS Neglected Tropical Diseases*, 1, e128.
- PFARR, K. M., DEBRAH, A. Y., SPECHT, S. & HOERAUF, A. 2009. Filariasis and lymphoedema. *Parasite Immunol*, 31, 664-72.
- PHILIPP, M., WORMS, M. J., MAIZELS, R. M. & OGILVIE, B. M. 1984. Rodent Models of Filariasis. In: MARCHALONIS, J. J. (ed.) *Immunobiology of Parasites and Parasitic Infections*. Boston, MA: Springer US.
- PION, S. D. S., CHESNAIS, C. B., WEIL, G. J., FISCHER, P. U., MISSAMOU, F. & BOUSSINESQ, M. 2017. Effect of 3 years of biannual mass drug administration with albendazole on lymphatic filariasis and soil-transmitted helminth infections: a community-based study in Republic of the Congo. *Lancet Infect Dis*, 17, 763-769.
- PIONNIER, N. P., SJOBERG, H., CHUNDA, V. C., FOMBAD, F. F., CHOUNNA, P. W., NJOUENDOU, A. J., METUGE, H. M., NDZESHANG, B. L., GANDJUI, N. V., AKUMTOH, D. N., TAYONG, D. B., TAYLOR, M. J., WANJI, S. & TURNER, J. D. 2019. Mouse models of *Loa loa*. *Nature Communications*, 10, 1429.
- POLTERA, A. A., REYNA, O., ZEA-FLORES, G., BELTRANENA, F., NOWELL DE AREVALO, A. & ZAK, F. 1991. Use of an ophthalmologic ultrasound scanner in human onchocercal skin nodules for non-invasive sequential assessment during a macrofilaricidal trial with amocarzine in Guatemala. The first experiences. *Trop Med Parasitol*, 42.
- POLTERA, A. A., REYNA, O., ZEA FLORES, G., NOWELL DE AREVALO, A. M. & BELTRANENA, F. 1987. Detection of skin nodules in onchocerciasis by ultrasound scans. *Lancet*, 1.
- POLTERA, A. A. & ZAK, F. 1988. The in vitro determination of the visual resolution in onchocercal nodules of bovine and human origin by a portable ophthalmologic ultrasound scanner. *Trop Med Parasitol*, 39 Suppl 4, 349-55.
- POROT, C., KNAPP, J., WANG, J., GERMAIN, S., CAMPORESE, D., SEIMBILLE, Y., BOULAHDOUR, H., VUITTON, D. A., GOTTSTEIN, B. & BLAGOSKLONOV, O. 2014. Development of a specific tracer for metabolic imaging of alveolar echinococcosis: A preclinical study. *Conf Proc IEEE Eng Med Biol Soc*, 2014, 5587-90.
- RAMACHANDRAN, C. P. & PACHECO, G. 1965. American cotton rat (*Sigmodon hispidus*) as an experimental host for *Brugia pahangi*. *J Parasitol*, 51, 722-6.

REFERENCES

- RAMAIAH, K. D. & OTTESEN, E. A. 2014. Progress and Impact of 13 Years of the Global Programme to Eliminate Lymphatic Filariasis on Reducing the Burden of Filarial Disease. *PLOS Neglected Tropical Diseases*, 8, e3319.
- RAO, R. & WELL, G. J. 2002. In vitro effects of antibiotics on *Brugia malayi* worm survival and reproduction. *J Parasitol*, 88, 605-11.
- RAO, R. U., MOUSSA, H. & WEIL, G. J. 2002. *Brugia malayi*: effects of antibacterial agents on larval viability and development in vitro. *Exp Parasitol*, 101, 77-81.
- REDDY, M. V. 2013. Human dirofilariasis: An emerging zoonosis. *Tropical parasitology*, 3, 2-3.
- RIBERU, W. A., ATMOSOEDJONO, S., PURNOMO, TIRTOKUSUMO, S., BANGS, M. J. & BAIRD, J. K. 1990. Cultivation of sexually mature *Brugia malayi* in vitro. *Am J Trop Med Hyg*, 43, 3-5.
- SALEM, N., BALKMAN, J. D., WANG, J., WILSON, D. L., LEE, Z., KING, C. L. & BASILION, J. P. 2010. In Vivo Imaging of Schistosomes to Assess Disease Burden Using Positron Emission Tomography (PET). *PLOS Neglected Tropical Diseases*, 4, e827.
- SÄNGER, I., LÄMMLER, G. & KIMMIG, P. 1981. Filarial infections of *Mastomys natalensis* and their relevance for experimental chemotherapy. *Acta tropica*, 38, 277-288.
- SANPRASERT, V., SUJARIYAKUL, A. & NUCHPRAYOON, S. 2010. A single dose of doxycycline in combination with diethylcarbamazine for treatment of bancroftian filariasis. *Southeast Asian J Trop Med Public Health*, 41, 800-12.
- SANZ, P., TEEL, L. D., ALEM, F., CARVALHO, H. M., DARNELL, S. C. & O'BRIEN, A. D. 2008. Detection of *Bacillus anthracis* spore germination in vivo by bioluminescence imaging. *Infection and immunity*, 76, 1036-1047.
- SARMA, R. V., VALLISHAYEE, R. S., RAO, R. S., PRABHAKAR, R. & TRIPATHY, S. P. 1988. Use of mebendazole in combination with DEC in bancroftian filariasis. *The Indian journal of medical research*, 87, 579-583.
- SCHNEIDER, C. R., BLAIR, L. S., SCHARDEIN, J. L., BOCHE, L. K. & THOMPSON, P. E. 1968. Comparison of Early *Litomosoides carinii* Infections in Cotton Rats and Gerbils. *The Journal of Parasitology*, 54, 1099-1105.
- SHARMA, R., AL JAYOUSSI, G., TYRER, H. E., GAMBLE, J., HAYWARD, L., GUIMARAES, A. F., DAVIES, J., WATERHOUSE, D., COOK, D. A., MYHILL, L. J., CLARE, R. H., CASSIDY, A., STEVEN, A., JOHNSTON, K. L., FORD, L., TURNER, J. D., WARD, S. A. & TAYLOR, M. J. 2016. Minocycline as a re-purposed anti-*Wolbachia* macrofilaricide: superiority compared with doxycycline regimens in a murine infection model of human lymphatic filariasis. *Sci Rep*, 6, 23458.
- SHENOY, R. K., JOHN, A., HAMEED, S., SUMA, T. K. & KUMARASWAMI, V. 2016. Apparent failure of ultrasonography to detect adult worms of *Brugia malayi*. *Annals of Tropical Medicine & Parasitology*, 94, 77-82.
- SIMON, F., LOPEZ-BELMONTE, J., MARCOS-ATXUTEGI, C., MORCHON, R. & MARTIN-PACHO, J. R. 2005. What is happening outside North America regarding human dirofilariasis? *Vet Parasitol*, 133, 181-9.
- SIMON, F., SILES-LUCAS, M., MORCHON, R., GONZALEZ-MIGUEL, J., MELLADO, I., CARRETON, E. & MONTOYA-ALONSO, J. A. 2012. Human and animal dirofilariasis: the emergence of a zoonotic mosaic. *Clin Microbiol Rev*, 25, 507-44.
- SJOBERG, H. T., PIONNIER, N., ALJAYOUSSI, G., METUGE, H. M., NJOUENDOU, A. J., CHUNDA, V. C., FOMBAD, F. F., TAYONG, D. B., GANDJUI, N. V. T., AKUMTOH, D. N., CHOUNNA, P. W. N., NDZESHANG, B. L., LACHAUD, S., TEKLE, F., QUIRYNEN, L., ENGELEN, M., BAETEN, B., STEVEN, A., WARD, S. A., TAYLOR, M. J., WANJI, S. & TURNER, J. D. 2019. Short-course, oral flubendazole does not mediate significant efficacy against *Onchocerca* adult male worms or *Brugia microfilariae* in murine infection models. *PLoS Negl Trop Dis*, 13, e0006356.

REFERENCES

- SJÖLINDER, H. & JONSSON, A.-B. 2007. Imaging of Disease Dynamics during Meningococcal Sepsis. *PLOS ONE*, 2, e241.
- SMILLIE, C. L., VICKERY, A. C., KWA, B. H., NAYAR, J. K. & RAO, U. R. 1994. Evaluation of different medium supplements for in vitro cultivation of *Brugia malayi* third-stage larvae. *J Parasitol*, 80, 380-3.
- STOREY, B., MARCELLINO, C., MILLER, M., MACLEAN, M., MOSTAFA, E., HOWELL, S., SAKANARI, J., WOLSTENHOLME, A. & KAPLAN, R. 2014. Utilization of computer processed high definition video imaging for measuring motility of microscopic nematode stages on a quantitative scale: "The Worminator". *Int J Parasitol Drugs Drug Resist*, 4, 233-43.
- TAMAROZZI, F., HALLIDAY, A., GENTIL, K., HOERAUF, A., PEARLMAN, E. & TAYLOR, M. J. 2011. Onchocerciasis: the Role of Wolbachia Bacterial Endosymbionts in Parasite Biology, Disease Pathogenesis, and Treatment. *Clinical Microbiology Reviews*, 24, 459-468.
- TAYLOR, M. J., BANDI, C. & HOERAUF, A. 2005a. Wolbachia bacterial endosymbionts of filarial nematodes. *Adv Parasitol*, 60, 245-84.
- TAYLOR, M. J., HOERAUF, A. & BOCKARIE, M. 2010a. Lymphatic filariasis and onchocerciasis. *Lancet*, 376.
- TAYLOR, M. J., HOERAUF, A. & BOCKARIE, M. 2010b. Lymphatic filariasis and onchocerciasis. *Lancet*, 376, 1175-85.
- TAYLOR, M. J., MAKUNDE, W. H., MCGARRY, H. F., TURNER, J. D., MAND, S. & HOERAUF, A. 2005b. Macrofilaricidal activity after doxycycline treatment of *Wuchereria bancrofti*: a double-blind, randomised placebo-controlled trial. *Lancet*, 365, 2116-21.
- TAYLOR, M. J., VAN ES, R. P., SHAY, K., FOLKARD, S. G., TOWNSON, S. & BIANCO, A. E. 1994. Protective immunity against *Onchocerca volvulus* and *O. lienalis* infective larvae in mice. *Trop Med Parasitol*, 45.
- TAYLOR, M. J., VON GELDERN, T. W., FORD, L., HUBNER, M. P., MARSH, K., JOHNSTON, K. L., SJOBERG, H. T., SPECHT, S., PIONNIER, N., TYRER, H. E., CLARE, R. H., COOK, D. A. N., MURPHY, E., STEVEN, A., ARCHER, J., BLOEMKER, D., LENZ, F., KOSCHEL, M., EHRENS, A., METUGE, H. M., CHUNDA, V. C., NDONGMO CHOUNNA, P. W., NJOUENDOU, A. J., FOMBAD, F. F., CARR, R., MORTON, H. E., ALJAYYOUSI, G., HOERAUF, A., WANJI, S., KEMPF, D. J., TURNER, J. D. & WARD, S. A. 2019. Preclinical development of an oral anti-Wolbachia macrolide drug for the treatment of lymphatic filariasis and onchocerciasis. *Sci Transl Med*, 11.
- TIPPAWANGKOSOL, P., CHOOCHOTE, W., RIYONG, D., JITPAKDI, A. & PITASAWAT, B. 2002. A simple technique for the in vitro cultivation of nocturnally subperiodic *Brugia malayi* infective larvae. *Southeast Asian J Trop Med Public Health*, 33 Suppl 3, 16-22.
- TISCH, D. J., MICHAEL, E. & KAZURA, J. W. 2005. Mass chemotherapy options to control lymphatic filariasis: a systematic review. *Lancet Infect Dis*, 5, 514-23.
- TOWNSON, S. 1988. The development of a laboratory model for onchocerciasis using *Onchocerca gutturosa*: in vitro culture, collagenase effects, drug studies and cryopreservation. *Trop Med Parasitol*, 39.
- TOWNSON, S., CONNELLY, C., DOBINSON, A. & MULLER, R. 1987. Drug activity against *Onchocerca gutturosa* males in vitro: a model for chemotherapeutic research on onchocerciasis. *Journal of Helminthology*, 61, 271-281.
- TOWNSON, S., CONNELLY, C. & MULLER, R. 1986. Optimization of culture conditions for the maintenance of *Onchocerca gutturosa* adult worms in vitro. *Journal of Helminthology*, 60, 323-330.
- TREES, A. J., GRAHAM, S. P., RENZ, A., BIANCO, A. E. & TANYA, V. 2000. *Onchocerca ochengi* infections in cattle as a model for human onchocerciasis: recent developments. *Parasitology*, 120 Suppl, S133-42.

REFERENCES

- TURNER, J. D., MAND, S., DEBRAH, A. Y., MUEHLFELD, J., PFARR, K., MCGARRY, H. F., ADJEL, O., TAYLOR, M. J. & HOERAUF, A. 2006. A randomized, double-blind clinical trial of a 3-week course of doxycycline plus albendazole and ivermectin for the treatment of *Wuchereria bancrofti* infection. *Clin Infect Dis*, 42.
- TURNER, J. D., PIONNIER, N., FURLONG-SILVA, J., SJOBERG, H., CROSS, S., HALLIDAY, A., GUIMARAES, A. F., COOK, D. A. N., STEVEN, A., VAN ROOIJEN, N., ALLEN, J. E., JENKINS, S. J. & TAYLOR, M. J. 2018. Interleukin-4 activated macrophages mediate immunity to filarial helminth infection by sustaining CCR3-dependent eosinophilia. *PLOS Pathogens*, 14, e1006949.
- TURNER, J. D., TENDONGFOR, N., ESUM, M., JOHNSTON, K. L., LANGLEY, R. S., FORD, L., FARAGHER, B., SPECHT, S., MAND, S., HOERAUF, A., ENYONG, P., WANJI, S. & TAYLOR, M. J. 2010a. Macrofilaricidal Activity after Doxycycline Only Treatment of *Onchocerca volvulus* in an Area of *Loa loa* Co-Endemicity: A Randomized Controlled Trial. *PLOS Neglected Tropical Diseases*, 4, e660.
- TURNER, J. D., TENDONGFOR, N., ESUM, M., JOHNSTON, K. L., LANGLEY, R. S., FORD, L., FARAGHER, B., SPECHT, S., MAND, S., HOERAUF, A., ENYONG, P., WANJI, S. & TAYLOR, M. J. 2010b. Macrofilaricidal activity after doxycycline only treatment of *Onchocerca volvulus* in an area of *Loa loa* co-endemicity: a randomized controlled trial. *PLoS Negl Trop Dis*, 4.
- VAN HOEGAERDEN, M., IVANOFF, B., FLOCARD, F., SALLE, A. & CHABAUD, B. 1987. The use of mebendazole in the treatment of filariases due to *Loa loa* and *Mansonella perstans*. *Ann Trop Med Parasitol*, 81, 275-82.
- VENETI, Z., CLARK, M. E., ZABALOU, S., KARR, T. L., SAVAKIS, C. & BOURTZIS, K. 2003. Cytoplasmic Incompatibility and Sperm Cyst Infection in Different *Drosophila*-*Wolbachia* Associations. *Genetics*, 164, 545.
- VERVER, S., WALKER, M., KIM, Y. E., FOBI, G., TEKLE, A. H., ZOURE, H. G. M., WANJI, S., BOAKYE, D. A., KUESEL, A. C., DE VLAS, S. J., BOUSSINESQ, M., BASANEZ, M. G. & STOLK, W. A. 2018. How Can Onchocerciasis Elimination in Africa Be Accelerated? Modeling the Impact of Increased Ivermectin Treatment Frequency and Complementary Vector Control. *Clin Infect Dis*, 66, S267-s274.
- VON GELDERN, T. W., MORTON, H. E., CLARK, R. F., BROWN, B. S., JOHNSTON, K. L., FORD, L., SPECHT, S., CARR, R. A., STOLARIK, D. F., MA, J., RIESER, M. J., STRUEVER, D., FROHBERGER, S. J., KOSCHEL, M., EHRENS, A., TURNER, J. D., HUBNER, M. P., HOERAUF, A., TAYLOR, M. J., WARD, S. A., MARSH, K. & KEMPF, D. J. 2019. Discovery of ABBV-4083, a novel analog of Tylosin A that has potent anti-*Wolbachia* and anti-filarial activity. *PLoS Negl Trop Dis*, 13, e0007159.
- VORONIN, D., COOK, D. A. N., STEVEN, A. & TAYLOR, M. J. 2012. Autophagy regulates Wolbachia populations across diverse symbiotic associations. *Proceedings of the National Academy of Sciences*, 109, E1638.
- VORONIN, D., TRICOCHÉ, N., JAWAHAR, S., SHLOSSMAN, M., BULMAN, C. A., FISCHER, C., SUDERMAN, M. T., SAKANARI, J. A. & LUSTIGMAN, S. 2019. Development of a preliminary in vitro drug screening assay based on a newly established culturing system for pre-adult fifth-stage *Onchocerca volvulus* worms. *PLOS Neglected Tropical Diseases*, 13, e0007108.
- WALKER, M., SPECHT, S., CHURCHER, T. S., HOERAUF, A., TAYLOR, M. J. & BASÁÑEZ, M.-G. 2014. Therapeutic Efficacy and Macrofilaricidal Activity of Doxycycline for the Treatment of River Blindness. *Clinical Infectious Diseases*, 60, 1199-1207.
- WANG, L. V. & HU, S. 2012. Photoacoustic tomography: in vivo imaging from organelles to organs. *Science (New York, N.Y.)*, 335, 1458-1462.
- WANJI, S., ENYONG, E.-E., TENDONGFOR, N., NGWA, C., ESUKA, E., KENGNE-OUAFO, A., DATCHOUA-POUTCHEU, F., ENYONG, P., HOPKINS, A. & MACKENZIE, C. D. 2015.

REFERENCES

- Parasitological, Hematological and Biochemical Characteristics of a Model of Hyper-microfilariaemic Loiasis (*Loa loa*) in the Baboon (*Papio anubis*). *PLoS neglected tropical diseases*, 9, e0004202-e0004202.
- WANJI, S., EYONG, E.-E. J., TENDONGFOR, N., NGWA, C. J., ESUKA, E. N., KENGNE-OUAFO, A. J., DATCHOUA-POUTCHEU, F. R., ENYONG, P., AGNEW, D., EVERSOLE, R. R., HOPKINS, A. & MACKENZIE, C. D. 2017. Ivermectin treatment of *Loa loa* hyper-microfilaraemic baboons (*Papio anubis*): Assessment of microfilarial load reduction, haematological and biochemical parameters and histopathological changes following treatment. *PLoS neglected tropical diseases*, 11, e0005576-e0005576.
- WANJI, S., TENDONGFOR, N., NJI, T., ESUM, M., CHE, J. N., NKWESCHEU, A., ALASSA, F., KAMNANG, G., ENYONG, P. A., TAYLOR, M. J., HOERAUF, A. & TAYLOR, D. W. 2009. Community-directed delivery of doxycycline for the treatment of onchocerciasis in areas of co-endemicity with loiasis in Cameroon. *Parasit Vectors*, 2.
- WESSELS, J. T., BUSSE, A. C., MAHRT, J., DULLIN, C., GRABBE, E. & MUELLER, G. A. 2007. In vivo imaging in experimental preclinical tumor research--a review. *Cytometry A*, 71, 542-9.
- WOLSTENHOLME, A. J., EVANS, C. C., JIMENEZ, P. D. & MOORHEAD, A. R. 2015. The emergence of macrocyclic lactone resistance in the canine heartworm, *Dirofilaria immitis*. *Parasitology*, 142, 1249-59.
- WOLSTENHOLME, A. J., MACLEAN, M. J., COATES, R., MCCOY, C. J. & REAVES, B. J. 2016. How do the macrocyclic lactones kill filarial nematode larvae? *Invertebrate neuroscience : IN*, 16, 7-7.
- WU, B., NOVELLI, J., JIANG, D., DAILEY, H. A., LANDMANN, F., FORD, L., TAYLOR, M. J., CARLOW, C. K. S., KUMAR, S., FOSTER, J. M. & SLATKO, B. E. 2013. Interdomain lateral gene transfer of an essential ferrochelatase gene in human parasitic nematodes. *Proceedings of the National Academy of Sciences*, 110, 7748.
- ZAHNER, H. & SCHARES, G. 1993. Experimental chemotherapy of filariasis: comparative evaluation of the efficacy of filaricidal compounds in *Mastomys coucha* infected with *Litomosoides carinii*, *Acanthocheilonema viteae*, *Brugia malayi* and *B. pahangi*. *Acta Trop*, 52, 221-66.
- ZOFOU, D., FOMBAD, F. F., GANDJUI, N. V. T., NJOUENDOU, A. J., KENGNE-OUAFO, A. J., NDONGMO, P. W. C., DATCHOUA-POUTCHEU, F. R., ENYONG, P. A., BITA, D. T., TAYLOR, M. J., TURNER, J. D. & WANJI, S. 2018. Evaluation of in vitro culture systems for the maintenance of microfilariae and infective larvae of *Loa loa*. *Parasites & Vectors*, 11, 275.